Report No. K-TRAN: KSU-11-3 ▪ FINAL REPORT ▪ April 2013

LRFD Software for Design and Actual Ultimate Capacity of Confined Rectangular Columns

Ahmed Mohsen ABD El Fattah, Ph.D., LEED AP
Hayder Rasheed, Ph.D., P.E.
Asad Esmaeily, Ph.D., P.E.

Kansas State University Transportation Center

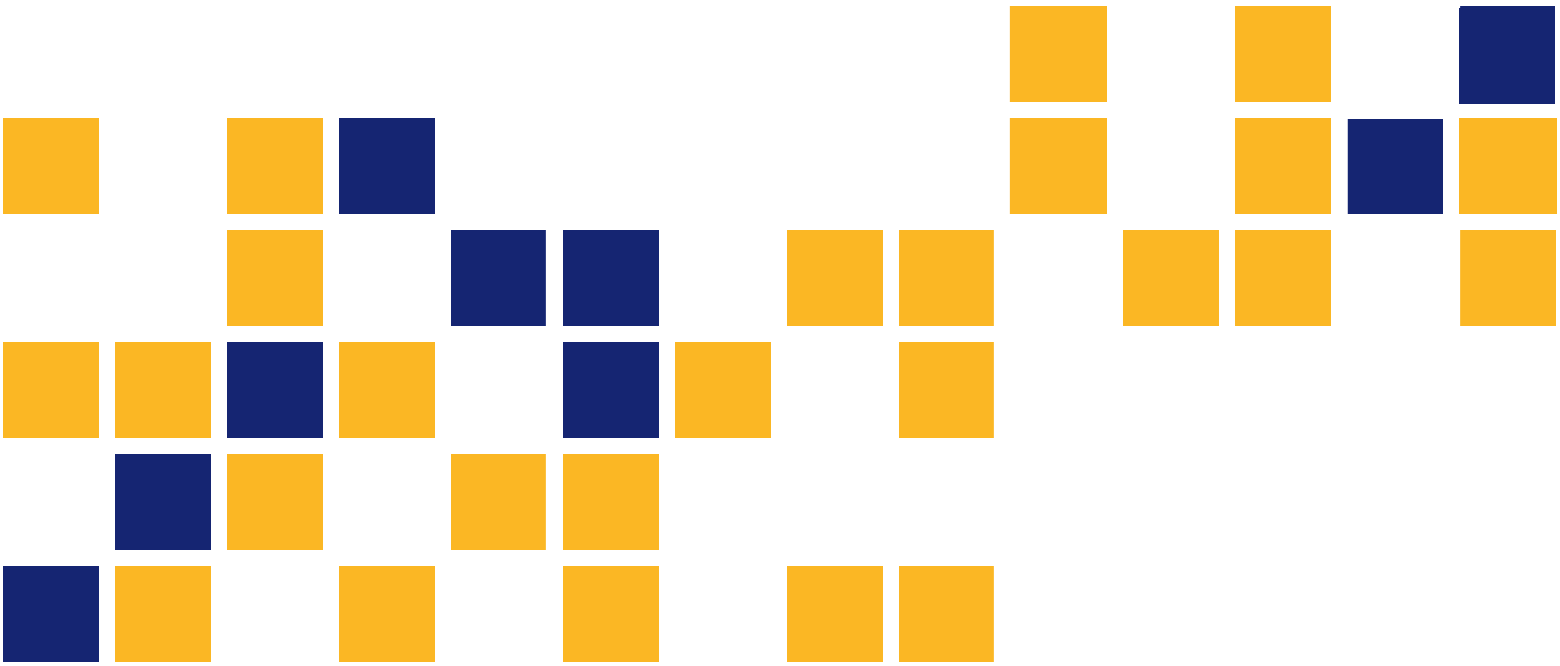

A cooperative transportation research program between
Kansas Department of Transportation,
Kansas State University Transportation Center, and
The University of Kansas

Kansas Department of Transportation

This page intentionally left blank.

1 Report No. K-TRAN: KSU-11-3	**2 Government Accession No.**	**3 Recipient Catalog No.**
4 Title and Subtitle LRFD Software for Design and Actual Ultimate Capacity of Confined Rectangular Columns		**5 Report Date** April 2013 **6 Performing Organization Code**
7 Author(s) Ahmed Mohsen ABD El Fattah, Ph.D., LEED AP; Hayder Rasheed, Ph.D., P.E.; Asad Esmaeily, Ph.D., P.E.		**8 Performing Organization Report No.**
9 Performing Organization Name and Address Department of Civil Engineering Kansas State University Transportation Center 2118 Fiedler Hall Manhattan, Kansas 66506		**10 Work Unit No. (TRAIS)** **11 Contract or Grant No.** C1880
12 Sponsoring Agency Name and Address Kansas Department of Transportation Bureau of Materials and Research 700 SW Harrison Street Topeka, Kansas 66603-3745		**13 Type of Report and Period Covered** Final Report October 2010–September 2012 **14 Sponsoring Agency Code** RE-0546-01
15 Supplementary Notes For more information write to address in block 9.		

The analysis of concrete columns using unconfined concrete models is a well established practice. On the other hand, prediction of the actual ultimate capacity of confined concrete columns requires specialized nonlinear analysis. Modern codes and standards are introducing the need to perform extreme event analysis. There has been a number of studies that focused on the analysis and testing of concentric columns or cylinders. This case has the highest confinement utilization since the entire section is under confined compression. On the other hand, the augmentation of compressive strength and ductility due to full axial confinement is not applicable to pure bending and combined bending and axial load cases simply because the area of effective confined concrete in compression is reduced. The higher eccentricity causes smaller confined concrete region in compression yielding smaller increase in strength and ductility of concrete. Accordingly, the ultimate confined strength is gradually reduced from the fully confined value f_{cc} (at zero eccentricity) to the unconfined value f'_c (at infinite eccentricity) as a function of the compression area to total area ratio. The higher the eccentricity, the smaller the confined concrete compression zone. This paradigm is used to implement adaptive eccentric model utilizing the well known Mander Model.

Generalization of the moment of area approach is utilized based on proportional loading, finite layer procedure and the secant stiffness approach, in an iterative incremental numerical model to achieve equilibrium points of P-ε and M-φ response up to failure. This numerical analysis is adapted to assess the confining effect in rectangular columns confined with conventional lateral steel. This model is validated against experimental data found in literature. The comparison shows good correlation. Finally computer software is developed based on the non-linear numerical analysis. The software is equipped with an elegant graphics interface that assimilates input data, detail drawings, capacity diagrams and demand point mapping in a single sheet. Options for preliminary design, section and reinforcement selection are seamlessly integrated as well. The software generates 3D failure surface for rectangular columns and allows the user to determine the 2D interaction diagrams for any angle α between the x-axis and the resultant moment. Improvements to KDOT Bridge Design Manual using this software with reference to AASHTO LRFD are made. This study is limited to stub columns.

17 Key Words Software, Columns, Bridge, Certified Reinforced Concrete, LRFD, Load and Resistance Factor Design		**18 Distribution Statement** No restrictions. This document is available to the public through the National Technical Information Service www.ntis.gov.	
19 Security Classification (of this report) Unclassified	**20 Security Classification (of this page)** Unclassified	**21 No. of pages** 220	**22 Price**

Form DOT F 1700.7 (8-72)

LRFD Software for Design and Actual Ultimate Capacity of Confined Rectangular Columns

Final Report

Prepared by

Ahmed Mohsen ABD El Fattah, Ph.D., LEED AP

Hayder Rasheed, Ph.D., P.E.

Asad Esmaeily, Ph.D., P.E.

Kansas State University Transportation Center

A Report on Research Sponsored by

THE KANSAS DEPARTMENT OF TRANSPORTATION
TOPEKA, KANSAS

and

KANSAS STATE UNIVERSITY TRANSPORTATION CENTER
MANHATTAN, KANSAS

April 2013

PREFACE

The Kansas Department of Transportation's (KDOT) Kansas Transportation Research and New-Developments (K-TRAN) Research Program funded this research project. It is an ongoing, cooperative and comprehensive research program addressing transportation needs of the state of Kansas utilizing academic and research resources from KDOT, Kansas State University and the University of Kansas. Transportation professionals in KDOT and the universities jointly develop the projects included in the research program.

NOTICE

The authors and the state of Kansas do not endorse products or manufacturers. Trade and manufacturers names appear herein solely because they are considered essential to the object of this report.

This information is available in alternative accessible formats. To obtain an alternative format, contact the Office of Transportation Information, Kansas Department of Transportation, 700 SW Harrison, Topeka, Kansas 66603-3754 or phone (785) 296-3585 (Voice) (TDD).

DISCLAIMER

The contents of this report reflect the views of the authors who are responsible for the facts and accuracy of the data presented herein. The contents do not necessarily reflect the views or the policies of the state of Kansas. This report does not constitute a standard, specification or regulation.

Abstract

The analysis of concrete columns using unconfined concrete models is a well established practice. On the other hand, prediction of the actual ultimate capacity of confined concrete columns requires specialized nonlinear analysis. Modern codes and standards are introducing the need to perform extreme event analysis. There has been a number of studies that focused on the analysis and testing of concentric columns or cylinders. This case has the highest confinement utilization since the entire section is under confined compression. On the other hand, the augmentation of compressive strength and ductility due to full axial confinement is not applicable to pure bending and combined bending and axial load cases simply because the area of effective confined concrete in compression is reduced. The higher eccentricity causes smaller confined concrete region in compression yielding smaller increase in strength and ductility of concrete. Accordingly, the ultimate confined strength is gradually reduced from the fully confined value f_{cc} (at zero eccentricity) to the unconfined value f'_c (at infinite eccentricity) as a function of the compression area to total area ratio. The higher the eccentricity, the smaller the confined concrete compression zone. This paradigm is used to implement adaptive eccentric model utilizing the well known Mander Model.

Generalization of the moment of area approach is utilized based on proportional loading, finite layer procedure and the secant stiffness approach, in an iterative incremental numerical model to achieve equilibrium points of P-ε and M-φ response up to failure. This numerical analysis is adapted to assess the confining effect in rectangular columns confined with conventional lateral steel. This model is validated against experimental data found in literature. The comparison shows good correlation. Finally computer software is developed based on the non-linear numerical analysis. The software is equipped with an elegant graphics interface that assimilates input data, detail drawings, capacity diagrams and demand point mapping in a single sheet. Options for preliminary design, section and reinforcement selection are seamlessly integrated as well. The software generates 3D failure surface for rectangular columns and allows the user to determine the 2D interaction diagrams for any angle α between the x-axis and the resultant moment. Improvements to KDOT Bridge Design Manual using this software with reference to AASHTO LRFD are made. This study is limited to stub columns.

Table of Contents

List of Figures

List of Tables

Acknowledgements

This research was made possible by funding from KDOT. Special thanks are extended to John Jones, Loren Risch, and Ken Hurst of KDOT, for their interest in the project and their continuous support and feedback that made it possible to arrive at such important findings

Chapter 1: Introduction

1.1 Background

Columns are considered the most critical elements in structures. The unconfined analysis for columns is well established in the literature. Structural design codes dictate reduction factors for safety. It wasn't until very recently that design specifications and codes of practice, like AASHTO LRFD, started realizing the importance of introducing extreme event load cases that necessitates accounting for advanced behavioral aspects like confinement. Confinement adds another dimension to columns analysis as it increases the column's capacity and ductility. Accordingly, confinement needs special non linear analysis to yield accurate predictions. Nevertheless the literature is still lacking specialized analysis tools that take into account confinement despite the availability of all kinds of confinement models. In addition the literature has focused on axially loaded members with less attention to eccentric loading. Although the latter is more likely to occur, at least with misalignment tolerances, the eccentricity effect is not considered in any confinement model available in the literature.

It is widely known that code Specifications involve very detailed design procedures that need to be checked for a number of limit states making the task of the designer very tedious. Accordingly, it is important to develop software that guide through the design process and facilitate the preparation of reliable analysis/design documents.

1.2 Objectives

This study is intended to determine the actual capacity of confined reinforced concrete columns subjected to eccentric loading and to generate the failure envelope at three different levels. First, the well-known ultimate capacity analysis of unconfined concrete is developed as a benchmarking step. Secondly, the unconfined ultimate interaction diagram is scaled down based on the reduction factors of the AASHTO LRFD to the design interaction diagram. Finally, the actual confined concrete ultimate analysis is developed based on a new eccentricity model accounting for partial confinement effect under eccentric loading. The analyses are conducted for rectangular columns confined with conventional transverse steel. It is important to note that the

present analysis procedure will be benchmarked against a wide range of experimental and analytical studies to establish its accuracy and reliability.

It is also the objective of this study to furnish interactive software with a user-friendly interface having analysis and design features that will facilitate the preliminary design of circular columns based on the actual demand. The overall objectives behind this research are summarized in the following points:

- Introduce the eccentricity effect in the stress-strain modeling
- Implement non-linear analysis for considering the confinement effects on column's actual capacity
- Test the analysis for rectangular columns confined with conventional transverse steel.
- Generate computer software that helps in designing and analyzing confined concrete columns through creating three levels of Moment-Force envelopes; unconfined curve, design curve based on AASHTO-LRFD and confined curve.

1.3 Scope

This study is composed of four chapters covering the development of material models, analysis procedures, benchmarking and practical applications.

- Chapter one introduces the objectives of the study and the content of the different chapters.
- Chapter two reviews the literature through two independent sections:
- Section 1: Reinforced concrete confinement models
- Section 2: Rectangular Columns subjected to biaxial bending and Axial Compression
- Chapter three presents rectangular columns analysis for both the unconfined and confined cases. Chapter three addresses the following subjects:
    - Finite Layer Approach (Fiber Model)
    - Present Confinement Model for Concentric Columns
    - Present Confinement Model for Eccentric Columns

    - Moment of Area Theorem
    - Numerical Formulation
    - Results and Discussion
- Chapter four states the conclusions and recommendations.

Chapter 2: Literature Review

This chapter reviews two different topics; lateral steel confinement models and rectangular columns subjected to biaxial bending and axial compression.

2.1 Steel Confinement Models

A comprehensive review of confined models for concrete columns under concentric axial compression that are available in the literature is conducted. The models reviewed are chronologically presented then compared by a set of criteria that assess consideration of different factors in developing the models such as effectively confined area, yielding strength and ductility.

2.1.1 Chronological Review of Models

The confinement models available are presented chronologically regardless of their comparative importance first. After that, discussion and categorization of the models are carried out and conclusions are made. Common notation is used for all the equations for the sake of consistency and comparison.

2.1.1.1 Notation

A_s: the cross sectional area of longitudinal steel reinforcement

A_{st}: the cross sectional area of transverse steel reinforcement

A_e: the area of effectively confined concrete

A_{cc}: the area of core within centerlines of perimeter spirals or hoops excluding area of longitudinal steel

b: the confined width (core) of the section

h: the confined height (core) of the section

c: center-to-center distance between longitudinal bars

d'_s: the diameter of longitudinal reinforcement

d'_{st}: the diameter of transverse reinforcement

D: the diameter of the column

d_s the core diameter of the column

f_{cc}: the maximum confined strength

f'_c: the peak unconfined strength

f_l: the lateral confined pressure

f'_l: the effective lateral confined pressure

f_{yh}: the yield strength of the transverse steel

f_s: the stress in the lateral confining steel

k_e: the effective lateral confinement coefficient

q: the effectiveness of the transverse reinforcement

s: tie spacing

s_o: the vertical spacing at which transverse reinforcement is not effective in concrete confinement

ε_{co}: the strain corresponding to the peak unconfined strength f'_c

ε_{cc}: the strain corresponding to the peak confined strength f_{cc}

ε_y: the strain at yielding for the transverse reinforcement

ε_{cu}: the ultimate strain of confined concrete

ρ_s: the volumetric ratio of lateral steel to concrete core

ρ_l: the ratio of longitudinal steel to the gross sectional area

ρ: the volumetric ratio of lateral + longitudinal steel to concrete core

Richart, Brandtzaeg, and Brown (1929)

Richart et al.'s (1929) model was the first to capture the proportional relationship between the lateral confined pressure and the ultimate compressive strength of confined concrete.

$$f_{cc} = f_c^{'} + k_1 f_l \qquad \textbf{Equation 2.1}$$

The average value for the coefficient k_1, which was derived from a series of short column specimen tests, came out to be (4.1). The strain corresponding to the peak strength ε_{cc} (see Mander et al. 1988) is obtained using the following function:

$$\varepsilon_{cc} = \varepsilon_{co}\left[1 + k_2\left(\frac{f_l}{f_c'}\right)\right] \qquad k_2 = 5k_1 \qquad \textbf{Equation 2.2}$$

where ε_{co} is the strain corresponding to $f'c$, k_2 is the strain coefficient of the effective lateral confinement pressure. No stress-strain curve graph was proposed by Richart et al. (1929).

Chan (1955)

A tri-linear curve describing the stress-strain relationship was suggested by Chan (1955) based on experimental work. The ratio of the volume of steel ties to concrete core volume and concrete strength were the only variables in the experimental work done. Chan assumed that OA approximates the elastic stage and ABC approximates the plastic stage (Figure 2.1). The positions of A, B and C may vary with different concrete variables. Chan assumed three different slopes E_c, $\lambda_1 E_c$, $\lambda_2 E_c$ for lines OA, AB and BC respectively. However no information about λ_1 and λ_2 was provided.

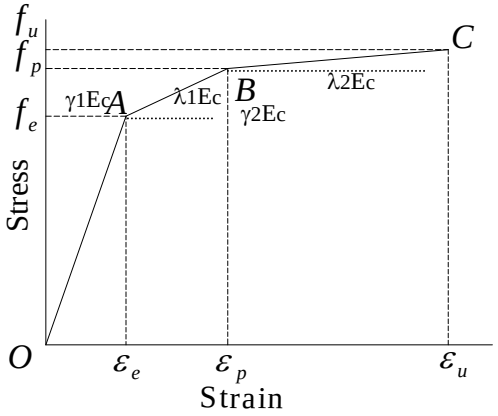

FIGURE 2.1
General Stress-Strain Curve by Chan (1955)

Blume, Newmark, and Corning (1961)

Blume et al. (1961) were the first to impose the effect of the yield strength for the transverse steel f_{yh} in different equations defining the model. The model generated, Figure 2.2, has ascending straight line with steep slope starting from the origin till the plain concrete peak strength f'_c and the corresponding strain ε_{co}, then a less slope straight line connect the latter point and the confined concrete peak strength f_{cc} and ε_{cc}. Then the curve flatten till ε_{cu}

$$f_{cc} = 0.85 f_c^{'} + 4.1 \frac{A_{st} f_{yh}}{sh} \qquad \text{for rectangular columns} \qquad \textbf{Equation 2.3}$$

$$\varepsilon_{co} = \frac{0.22 f_c^{'} + 400 psi}{10^6 psi} \qquad \textbf{Equation 2.4}$$

$$\varepsilon_{cc} = 5\varepsilon_y \qquad \textbf{Equation 2.5}$$

$$\varepsilon_{cu} = 5\varepsilon_{su} \qquad \textbf{Equation 2.6}$$

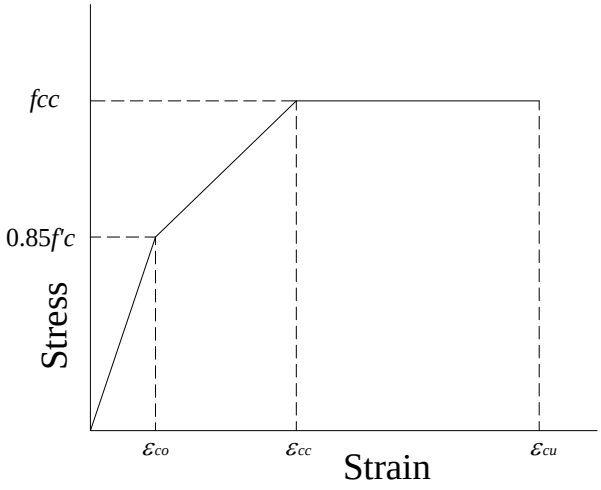

FIGURE 2.2
General Stress-Strain Curve by Blume et al. (1961)

where ε_y is the strain at yielding for the transverse reinforcement, A_{st} is the cross sectional area of transverse steel reinforcement, h is the confined cross sectional height, ε_{su} is the strain of transverse spiral reinforcement at maximum stress and ε_{cu} is the ultimate concrete strain.

Roy and Sozen (1965)

Based on their experimental results, which were controlled by two variables; ties spacing and amount of longitudinal reinforcement, Roy and Sozen (1965) concluded that there is no enhancement in the concrete capacity by using rectilinear ties. On the other hand there was significant increase in ductility. They proposed a bilinear ascending-descending stress strain curve that has a peak of the maximum strength of plain concrete f'_c and corresponding strain ε_{co} with a value of 0.002. The second line goes through the point defined by ε_{50} till it intersects with the strain axis. The strain ε_{50} was suggested to be a function of the volumetric ratio of ties to concrete core ρ_s, tie spacing s and the shorter side dimension b' (see Sheikh 1982).

$$\varepsilon_{50} = \frac{3\rho_s b'}{4s} \qquad \textbf{Equation 2.7}$$

Soliman and Yu (1967)

Soliman and Yu (1967) proposed another model that emerged from experimental results. The main parameters involved in the work done were tie spacing s, a new term represents the effectiveness of ties s_o, the area of ties A_{st}, and finally section geometry, which has three different variables; A_{cc} the area of confined concrete under compression, A_c the area of concrete under compression and b. The model has three different portions as shown in Figure 2.3. The ascending portion which is represented by a curve till the peak point (f'_c, ε_{ce}). The flat straight-line portion with its length varying depending on the degree of confinement. The last portion is a descending straight line passing through (0.8 f'_c, ε_{cf}) then extending down till an ultimate strain.

$$q = \left(1.4\frac{A_{cc}}{A_c} - 0.45\right)\frac{A_{st}\left(s_o - s\right)}{A_{st}s + 0.0028Bs^2} \qquad \textbf{Equation 2.8}$$

$$f_{cc} = 0.9 f_c^{'}(1 + 0.05q)$$ **Equation 2.9**

$$\varepsilon_{ce} = 0.55 f_{cc} * 10^{-6}$$ **Equation 2.10**

$$\varepsilon_{cs} = 0.0025(1 + q)$$ **Equation 2.11**

$$\varepsilon_{cf} = 0.0045(1 + 0.85q)$$ **Equation 2.12**

where q refers to the effectiveness of the transverse reinforcement, s_o is the vertical spacing at which transverse reinforcement is not effective in concrete confinement and B is the greater of b and 0.7 h.

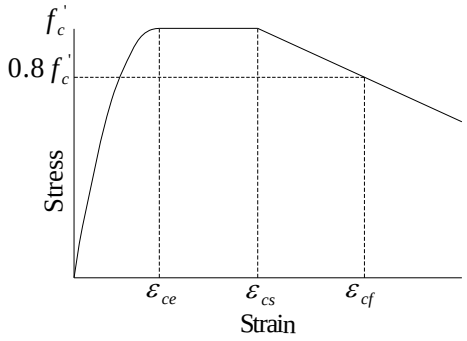

FIGURE 2.3
General Stress-Strain Curve by Soliman and Yu (1967)

Sargin (1971)

Sargin conducted experimental work on low and medium strength concrete with no longitudinal reinforcement. The transverse steel that was used had different size and different yield and ultimate strength. The main variables affecting the results were the volumetric ratio of lateral reinforcement to concrete core ρ_s, the strength of plain concrete f'_c, the ratio of tie spacing to the width of the concrete core and the yield strength of the transverse steel f_{yh}.

$$f_c = k_3 f_c^{'}\left[\frac{Ax+(m-1)x^2}{1+(A-2)x+mx^2}\right]$$ **Equation 2.13**

where *m* is a constant controlling the slope of the descending branch:

$$m = 0.8 - 0.05 f_c^{'}$$ **Equation 2.14**

$$x = \frac{\varepsilon_c}{\varepsilon_{cc}}$$ **Equation 2.15**

$$A = \frac{E_c \varepsilon_{cc}}{k_3 f_c^{'}}$$ **Equation 2.16**

$$k_3 = 1 + 0.0146\left[1 - 0.245\frac{s}{b}\right]\frac{\rho_s f_{yh}}{\sqrt{f_c^{'}}}$$ **Equation 2.17**

$$\varepsilon_{cc} = 0.0024 + 0.0374\left[1 - \frac{0.734s}{b}\right]\frac{\rho_s f_{yh}}{\sqrt{f_c^{'}}}$$ **Equation 2.18**

$$f_{cc} = k_3 f_c^{'}$$ **Equation 2.19**

where k_3 is concentric loading maximum stress ratio.

Kent and Park (1971)

As Roy and Sozen (1965) did, Kent and Park (1971) assumed that the maximum strength for confined and plain concrete is the same f'_c. The suggested curve, Figure 2.4, starts from the origin then increases parabolically (Hognestad's Parabola) till the peak at f'_c and the corresponding strain ε_{co} at 0.002. Then it descends with one of two different straight lines. For the confined concrete, which is more ductile, it descends till the point (0.5 $f'c$, ε_{50c}) and continues descending to 0.2$f'c$ followed by a flat plateau. For the plain concrete it descends till the point (0.5 $f'c$, ε_{50u}) and continue descending to 0.2f'_c as well without a flat plateau. Kent and Park assumed that confined concrete could sustain strain to infinity at a constant stress of 0.2 $f'c$:

$$f_c = f_c^{'}\left[\frac{2\varepsilon_c}{\varepsilon_{co}} - \left(\frac{\varepsilon_c}{\varepsilon_{co}}\right)^2\right] \qquad \text{for ascending branch}$$

$$f_c = f_c^{'}\left[1 - Z\left(\varepsilon_c - \varepsilon_{co}\right)\right] \qquad \text{for descending branch} \qquad \textbf{Equation 2.20}$$

$$\varepsilon_{50u} = \frac{3 + 0.002 f_c^{'}}{f_c^{'} - 1000} \qquad \textbf{Equation 2.21}$$

$$\rho_s = \frac{2(h+b)A_{st}}{hbs} \qquad \textbf{Equation 2.22}$$

$$\varepsilon_{50h} = \varepsilon_{50c} - \varepsilon_{50u} \qquad \textbf{Equation 2.23}$$

$$\varepsilon_{50h} = \frac{3}{4}\rho_s\sqrt{\frac{b}{s}} \qquad \textbf{Equation 2.24}$$

$$Z = \frac{0.5}{\varepsilon_{50h} + \varepsilon_{50u} - \varepsilon_{co}} \qquad \textbf{Equation 2.25}$$

where ρ_s is the ratio of lateral steel to the concrete core, Z is a constant controlling the slope of descending portion.

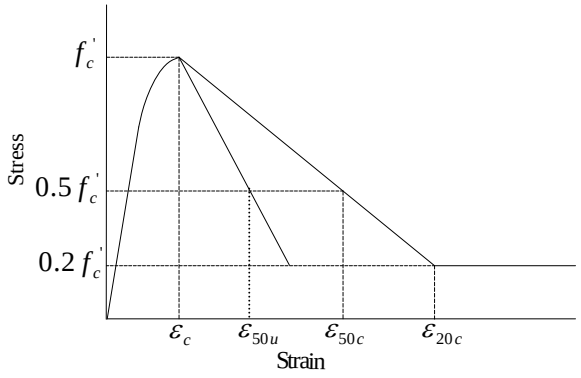

FIGURE 2.4
Stress-Strain Curve by Kent and Park (1971)

Popovics (1973)

Popovics pointed out that the stress-strain diagram is influenced by testing conditions and concrete age. The stress equation is:

$$f_c = f_{cc}\frac{\varepsilon_c}{\varepsilon_{cc}}\frac{n}{n-1+\left(\frac{\varepsilon_c}{\varepsilon_{cc}}\right)^n} \qquad \textbf{Equation 2.26}$$

$$n = 0.4*10^{-3} f_{cc} + 1.0 \qquad \textbf{Equation 2.27}$$

$$\varepsilon_{cc} = 2.7*10^{-4}\sqrt[4]{f_{cc}} \qquad \textbf{Equation 2.28}$$

Vallenas, Bertero, and Popov (1977)

The variables utilized in the experimental work conducted by Vallenas et al. (1977) were the volumetric ratio of lateral steel to concrete core ρ_s, ratio of longitudinal steel to the gross area of the section ρ_l, ties spacing s, effective width size, strength of ties and size of longitudinal bars. The model generated was similar to Kent and Park model with improvement in the peak strength for confined concrete (Figure 2.5). For the ascending branch:

$$\frac{f_c}{f_c^{'}} = k\left[1 - Z\varepsilon_{cc}(x-1)\right] \qquad \varepsilon_{cc} \le \varepsilon_c \le \varepsilon_{0.3k} \qquad \textbf{Equation 2.29}$$

$$\frac{f_c}{f_c^{'}} = 0.3k \qquad \varepsilon_{0.3k} \le \varepsilon_c \qquad \textbf{Equation 2.30}$$

$$x = \frac{\varepsilon_c}{\varepsilon_{cc}} \qquad \textbf{Equation 2.31}$$

$$f_{cc} = kf_c^{'} \qquad \textbf{Equation 2.32}$$

$$\frac{f_c}{f_c'} = \frac{\frac{E_c \varepsilon_{cc}}{f_c'} x - kx^2}{1 + \left(\frac{E_c \varepsilon_{cc}}{k f_c'} - 2 \right) x} \qquad \varepsilon_c \le \varepsilon_{cc}$$ **Equation 2.33**

For the descending branch:

$$k = 1 + 0.0091 \left[1 - 0.245 \frac{s}{h} \right] \frac{\left[\rho + \frac{d_{st}'}{d_s'} \rho_l \right] f_{yh}}{\sqrt{f_c'}}$$ **Equation 2.34**

$$\varepsilon_{cc} = 0.0024 + 0.005 \left[1 - \frac{0.734 s}{h} \right] \frac{\rho f_{yh}}{\sqrt{f_c'}}$$ **Equation 2.35**

$$Z = \frac{0.5}{\frac{3}{4} \rho_s \sqrt{\frac{h}{s}} + \left[\frac{3 + 0.002 f_c'}{f_c' - 1000} \right] - 0.002}$$ **Equation 2.36**

where k is coefficient of confined strength ratio, Z is the slope of descending portion, d'_s and d'_{st} are the diameter of longitudinal and transverse reinforcement, respectively.

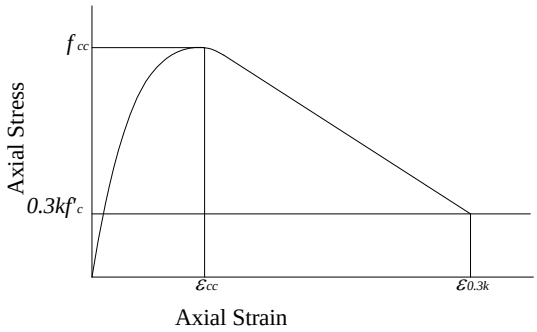

FIGURE 2.5
Stress-Strain Curve by Vallenas et al. (1977)

Wang, Shah, and Naaman (1978)

Wang et al. (1978) obtained experimentally another stress-strain curve describing the behavior of confined reinforced concrete under compression, Figure 2.6. The concrete tested was normal weight concrete ranging in strength from 3000 to 11000 psi (20.7 to 75.8 *MPa*) and light weight concrete with strength of 3000-8000 psi (20.7 to 55 *MPa*). Wang et al. utilized an equation, with four constants, similar to that of Sargin et al.

$$Y = \frac{AX + BX^2}{1 + CX + DX^2} \qquad \textbf{Equation 2.37}$$

where

$$Y = \frac{f_c}{f_{cc}} \qquad \textbf{Equation 2.38}$$

$$X = \frac{\varepsilon_c}{\varepsilon_{cc}} \qquad \textbf{Equation 2.39}$$

The four constant *A, B, C, D* were evaluated for the ascending part independently of the descending one. The four conditions used to evaluate the constants for the ascending part were

$dY/dX = E_{0.45}/E_{sec}$ at X=0 $E_{sec} = f_{cc}/\varepsilon_{cc}$

Y = 0.45 for $X = 0.45/(E_{0.45}/E_{sec})$

Y=1 for X=1

dY/dX = 0 at X=1

whereas for the descending branch:

Y=1 for X=1

dY/dX = 0 at X=1

$Y = f_i/f_{cc}$ for $X = \varepsilon_i/\varepsilon_{cc}$

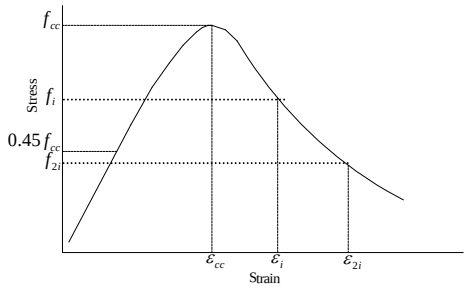

FIGURE 2.6
Proposed Stress-Strain Curve by Wang et al. (1978)

where f_i and ε_i are the stress and strain at the inflection point, f_{2i} and ε_{2i} refer to a point such that $\varepsilon_{2i} - \varepsilon_i = \varepsilon_i - \varepsilon_{cc}$ and $E_{0.45}$ represents the secant modulus of elasticity at 0.45 f_{cc}

$Y = f_{2i}/f_{cc}$ for $X = \varepsilon_{2i}/\varepsilon_{cc}$

Muguruma, Watanabe , Katsuta, and Tanaka (1980)

Muguruma et al. (1980) obtained their stress-strain model based on experimental work conducted by the model authors, Figure 2.7. The stress-strain model is defined by three zones; Zone 1 from 0-A:

$$f_c = E_i \varepsilon_c + \frac{f_c^{'} - E_i \varepsilon_{co}}{\varepsilon_{co}^{\ 2}} \varepsilon_c^{\ 2} \qquad (\text{kgf/cm}^2) \qquad 0 \le \varepsilon_c \le \varepsilon_{co} \qquad \textbf{Equation 2.40}$$

Zone 2 from A-D

$$f_c = f_{cc} + \frac{\left(\varepsilon_c - \varepsilon_{cc}\right)^2}{\left(\varepsilon_{co} - \varepsilon_{cc}\right)^2}\left(f_c^{'} - f_{cc}\right) (\text{kgf/cm}^2) \qquad \varepsilon_{co} < \varepsilon_c \le \varepsilon_{cc} \qquad \textbf{Equation 2.41}$$

Zone 3 from D-E

$$f_c = f_{cc} + \frac{f_u - f_{cc}}{\varepsilon_{cu} - \varepsilon_{cc}}\left(\varepsilon_c - \varepsilon_{cc}\right) \quad (\text{kgf/cm}^2) \quad \varepsilon_{cc} < \varepsilon_c \le \varepsilon_{cu} \qquad \textbf{Equation 2.42}$$

$$f_u = \frac{2\left(\overline{S} - f_{cc}\varepsilon_{cc}\right)}{\varepsilon_{cc} + \varepsilon_{cu}} \quad (\text{kgf/cm}^2) \qquad \textbf{Equation 2.43}$$

$$\varepsilon_u = 0.00413\left(1 - f_c^{'}/2000\right) \quad (\text{kgf/cm}^2) \qquad \textbf{Equation 2.44}$$

$$Cc = \rho_s \frac{\sqrt{f_{yh}}}{f_c^{'}}\left(1 - 0.5\frac{s}{W}\right) \qquad \textbf{Equation 2.45}$$

where $\overline{S}$ is the area surrounded by the idealized stress-strain curve up to the peak stress and W is the minimum side length or diameter of confined concrete

For circular columns confined with circular hoops:

$$f_{cc} = \left(1 + 150Cc\right) f_c^{'} \quad (\text{kgf/cm}^2) \qquad \textbf{Equation 2.46}$$

$$\varepsilon_{cc} = \left(1 + 1460Cc\right)\varepsilon_{co} \qquad \textbf{Equation 2.47}$$

$$\varepsilon_{cu} = \left(1 + 990Cc\right)\varepsilon_u \qquad \textbf{Equation 2.48}$$

whereas for square columns confined with square hoops:

$$f_{cc} = \left(1 + 50Cc\right) f_c^{'} \quad (\text{kgf/cm}^2) \qquad \textbf{Equation 2.49}$$

$$\varepsilon_{cc} = \left(1 + 450Cc\right)\varepsilon_{co} \qquad \textbf{Equation 2.50}$$

$$\varepsilon_{cu} = \left(1 + 450Cc\right)\varepsilon_u \qquad \textbf{Equation 2.51}$$

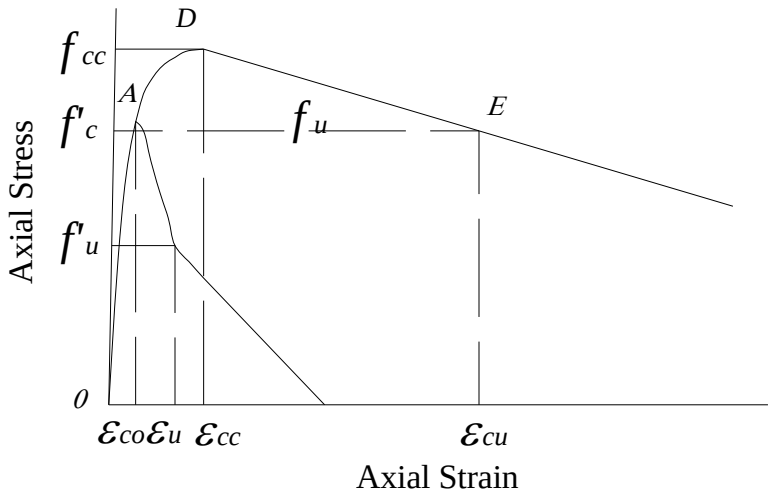

FIGURE 2.7
Proposed Stress-Strain Curve by Muguruma et al. (1980)

Scott, Park, Priestly (1982)

Scott et al. (1982) examined specimens by loading at high strain rate to correlate with the seismic loading. They presented the results including the effect of eccentric loading, strain rate, amount and distribution of longitudinal steel and amount and distribution of transverse steel. For low strain rate Kent and Park equations were modified to fit the experimental data

$$f_c = kf_c^{'}\left[\frac{2\varepsilon_c}{0.002k} - \left(\frac{\varepsilon_c}{0.002k}\right)^2\right] \qquad \varepsilon_c \le 0.002k \qquad \textbf{Equation 2.52}$$

$$f_c = kf_c^{'}\left[1 - Z_m(\varepsilon_c - 0.002k)\right] \quad \varepsilon_c > 0.002k \qquad \textbf{Equation 2.53}$$

where

$$k = 1 + \frac{\rho_s f_{yh}}{f_c^{'}} \qquad \textbf{Equation 2.54}$$

$$Z_m = \frac{0.5}{\frac{3 + 0.29 f_c^{'}}{145 f_c^{'} - 1000} + \frac{3}{4}\rho_s\sqrt{\frac{b''}{s}} - 0.002k} \qquad f'_c \text{ is in } MPa \qquad \textbf{Equation 2.55}$$

where *b"* is the width of concrete core measured to outside of the hoops. For the high strain rate, the k and Z_m were adapted to

$$k = 1.25(1 + \frac{\rho_s f_{yh}}{f_c^{'}}) \qquad \textbf{Equation 2.56}$$

$$Z_m = \frac{0.625}{\frac{3 + 0.29 f_c^{'}}{145 f_c^{'} - 1000} + \frac{3}{4}\rho_s \sqrt{\frac{b}{s}} - 0.002k} \quad f'_c \text{ is in } MPa \qquad \textbf{Equation 2.57}$$

and the maximum strain was suggested to be:

$$\varepsilon_{cu} = 0.004 + 0.9\rho_s \left(\frac{f_{yh}}{300} \right) \qquad \textbf{Equation 2.58}$$

It was concluded that increasing the spacing while maintaining the same ratio of lateral reinforcement by increasing the diameter of spirals, reduce the efficiency of concrete confinement. In addition, increasing the number of longitudinal bars will improve the concrete confinement due to decreasing the spacing between the longitudinal bars.

Sheikh and Uzumeri (1982)

Sheikh and Uzumeri (1982) introduced the effectively confined area as a new term in determining the maximum confined strength (Soliman and Yu (1967) had trial in effective area introduction). In addition to that they, in their experimental work, utilized the volumetric ratio of lateral steel to concrete core, longitudinal steel distribution, strength of plain concrete, and ties strength, configuration and spacing. The stress-strain curve, Figure 2.8, was presented parabolically up to (f_{cc}, ε_{cc}), then it flattens horizontally till $\varepsilon_{cs,}$ and finally it drops linearly passing by ($0.85f_{cc}$, ε_{85}) till $0.3\ f_{cc}$, In that sense, it is conceptually similar to the earlier model of Soliman and Yu (1967).

f_{cc} and ε_{cc} can be determined from the following equations:

$$f_{cc} = k_s f_{cp} \qquad f_{cp} = k_p f_c^{'} \qquad k_p = 0.85$$ **Equation 2.59**

$$k_s = 1 + \frac{2.73b^2}{P_{occ}}\left[\left(1 - \frac{nc^2}{5.5b^2}\right)\left(1 - \frac{s}{2b}\right)^2\right]\sqrt{\rho_s f_{st}^{'}}$$ **Equation 2.60**

$$\varepsilon_{cc} = 0.55 k_s f_c^{'} * 10^{-6}$$ **Equation 2.61**

$$\varepsilon_{cs} = \varepsilon_{co}\left(1 + \frac{0.81}{c}\left(1 - 5\left(\frac{s}{b}\right)^2\right)\frac{\rho_s f_{st}^{'}}{\sqrt{f_c^{'}}}\right)$$ **Equation 2.62**

$$\varepsilon_{85} = 0.225\rho_s\sqrt{\frac{b}{s}} + \varepsilon_{cs}$$ **Equation 2.63**

$$Z = \frac{0.5}{\frac{3}{4}\rho_s\sqrt{\frac{b}{s}}}$$ **Equation 2.64**

where *b* is the confined width of the cross section, f'_{st} is the stress in the lateral confining bar, c is center-to-center distance between longitudinal bars, ε_{s85} is the value of strain corresponding to 85% of the maximum stress on the unloading branch, *n* is the number of laterally supported longitudinal bars, *Z* is the slope for the unloading part, f_{cp} is the equivalent strength of unconfined concrete in the column, and $P_{occ} = K_p f'_c(A_{cc} - A_s)$

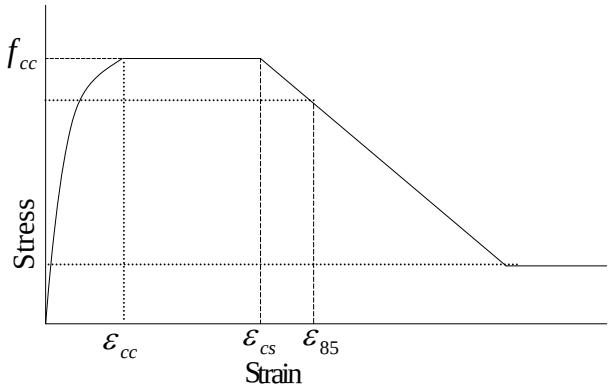

FIGURE 2.8
Proposed General Stress-Strain Curve by Sheikh and Uzumeri (1982)

Ahmad and Shah (1982)

Ahmad and Shah (1982) developed a model based on the properties of hoop reinforcement and the constitutive relationship of plain concrete. Normal weight concrete and lightweight concrete were used in tests that were conducted with one rate of loading. No longitudinal reinforcement was provided and the main two parameters varied were spacing and yield strength of transverse reinforcement. Ahmed and Shah observed that the spirals become ineffective when the spacing exceeds 1.25 the diameter of the confined concrete column. They concluded also that the effectiveness of the spiral is inversely proportional with compressive strength of unconfined concrete.

Ahmad and Shah adapted Sargin model counting on the octahedral failure theory, the three stress invariants and the experimental results:

$$Y = \frac{A_i X + (D_i - 1)X^2}{1 + (A_i - 2)X + D_i X^2} \qquad \textbf{Equation 2.65}$$

$$Y = \frac{f_{pcs}}{f_{pcn}} \qquad \textbf{Equation 2.66}$$

$$X = \frac{\varepsilon_i}{\varepsilon_{ip}}$$ **Equation 2.67**

where f_{pcs} is the most principal compressive stress, f_{pcn} is the most principal compressive strength, ε_i is the strain in the i-th principal direction and ε_{ip} is the strain at the peak in the *i-th* direction.

$$A_i = \frac{E_i}{E_{ip}} \qquad E_{ip} = \frac{f_{pcn}}{\varepsilon_{ip}}$$

E_i is the initial slope of the stress strain curve, D_i is a parameter that governs the descending branch. When the axial compression is considered to be the main loading, which is typically the case in concentric confined concrete columns, Equations 2.65, 2.66, and 2.67 become:

$$Y = \frac{AX + (D-1)X^2}{1 + (A-2)X + DX^2}$$ **Equation 2.68**

$$Y = \frac{f_c}{f_{cc}}$$ **Equation 2.69**

$$X = \frac{\varepsilon_c}{\varepsilon_{cc}}$$ **Equation 2.70**

$$A = \frac{E_c}{E_{\sec}}$$ **Equation 2.71**

Park, Priestly, and Gill (1982)

Park et al. (1982) modified Kent and Park (1971) equations to account for the strength improvement due to confinement based on experimental work conducted for four square full scaled columns (21.7 in^2 (14 000 mm^2) cross sectional area and 10.8 ft (3292 mm) high (Figure 2.9). The proposed equations are as follow:

$$f_c = kf_c^{'}\left[\frac{2\varepsilon_c}{0.002k} - \left(\frac{\varepsilon_c}{0.002k}\right)^2\right] \quad \text{for ascending branch} \qquad \textbf{Equation 2.72}$$

$$f_c = kf_c^{'}\left[1 - Z_m\left(\varepsilon_c - \varepsilon_{co}\right)\right] \geq 0.2kf'c \quad \text{for descending branch} \qquad \textbf{Equation 2.73}$$

$$Z_m = \frac{0.5}{\frac{3 + 0.29f_c^{'}}{145f_c^{'} - 1000} + \frac{3}{4}\rho_s\sqrt{\frac{b}{s}} - 0.002k} \qquad \textbf{Equation 2.74}$$

$$k = 1 + \frac{\rho_s f_{yh}}{f_c^{'}} \qquad \textbf{Equation 2.75}$$

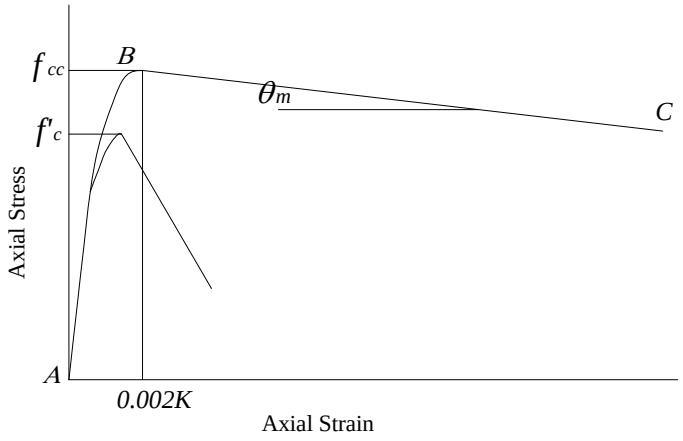

FIGURE 2.9
Proposed General Stress-Strain Curve by Park et al. (1982)

Martinez, Nilson, and Slate (1984)

Experimental investigation was conducted to propose equations to define the stress strain curve for spirally reinforced high strength concrete under compressive loading. The main parameters used were compressive strength for unconfined concrete, amount of confinement and specimen size. Two types of concrete where used; normal weight concrete with strength to about

12000 *psi. (82.75 MPa)* and light weight concrete with strength to about 9000 *psi (62 MPa)*. Martinez et al. (1984) concluded that the design specification for low strength concrete might be unsafe if applied to high strength concrete. For normal weight concrete:

$$\left(f_{cc} - f_c^{'}\right) = 4 f_l \left(1 - \frac{s}{d_{st}^{'}}\right) \qquad \textbf{Equation 2.76}$$

and for light weight concrete:

$$\left(f_{cc} - f_c^{'}\right) = 1.8 f_l \left(1 - \frac{s}{d_{st}^{'}}\right) \qquad \textbf{Equation 2.77}$$

where d'_{st} is the diameter of the lateral reinforcement.

Fafitis and Shah (1985)

Fafitis and Shah (1985) assumed that the maximum capacity of confined concrete occurs when the cover starts to spall off. The experimental work was done on high strength concrete with varying the confinement pressure and the concrete strength. Two equations are proposed to express the ascending and the descending branches of the model. For the ascending branch:

$$f_c = f_{cc}\left[1 - \left(1 - \frac{\varepsilon_c}{\varepsilon_{cc}}\right)^A\right] \qquad 0 \le \varepsilon_c \le \varepsilon_{cc} \qquad \textbf{Equation 2.78}$$

and for the descending branch:

$$f_c = f_{cc} \exp\left[-k\left(\varepsilon_c - \varepsilon_{cc}\right)^{1.15}\right] \qquad \varepsilon_{cc} \le \varepsilon_c \qquad \textbf{Equation 2.79}$$

The equations for the constant *A* and *k*:

$$A = \frac{E_c \varepsilon_{cc}}{f_{cc}} \qquad \textbf{Equation 2.80}$$

$$k = 0.17 f_{cc} \exp(-0.01 f_l)$$ **Equation 2.81**

f_{cc} and ε_{cc} can be found using the following equations:

$$f_{cc} = f_c^{'} + \left(1.15 + \frac{3048}{f_c^{'}}\right) f_l$$ **Equation 2.82**

$$\varepsilon_{cc} = 1.027 * 10^{-7} f_c^{'} + 0.0296 \frac{f_l}{f_{cc}} + 0.00195$$ **Equation 2.83**

f_l represents the confinement pressure and is given by the following equations:

$$f_l = \frac{2A_{st} f_{yh}}{s d_s}$$ for circular columns **Equation 2.84**

$$f_l = \frac{2A_{st} f_{yh}}{d_e s}$$ for square columns **Equation 2.85**

d_s is the core diameter of the column and d_e is the equivalent diameter.

Yong, Nour, and Nawy (1988)

The model suggested by Yong et al. (1988) was based on experimental work done for rectangular columns with rectangular ties (Figure 2.10).

$$f_{cc} = K f_c^{'}$$ **Equation 2.86**

$$\varepsilon_{cc} = 0.00265 + \frac{0.0035\left(1 - \frac{0.734s}{h}\right)\left(\rho_s f_{yh}\right)^{2/3}}{\sqrt{f_c^{'}}}$$ **Equation 2.87**

$$K = 1 + 0.0091\left(1 - \frac{0.245s}{h}\right)\left(\rho_s + \frac{nd_{st}^{'}}{8sd_s^{'}}\rho_l\right)\frac{f_{yh}}{\sqrt{f_c^{'}}} \qquad \textbf{Equation 2.88}$$

$$f_i = f_{cc}\left[0.25\left(\frac{f_c^{'}}{f_{cc}}\right) + 0.4\right] \qquad \textbf{Equation 2.89}$$

$$\varepsilon_i = K\left[1.4\left(\frac{\varepsilon_{cc}}{K}\right) + 0.0003\right] \qquad \textbf{Equation 2.90}$$

$$f_{2i} = f_c^{'}\left[0.025\left(\frac{f_{cc}}{1000}\right) - 0.065\right] \geq 0.3 f_{cc} \qquad \textbf{Equation 2.91}$$

Mander, Priestly and Park (1988)

Using the same concept of effective lateral confinement pressure introduced by Sheikh and Uzumeri, Mander et al. (1988) developed a new confined model for circular spiral and hoops or rectangular ties (Figure 2.11). In addition Mander et al. (1988) was the second group after Bazant et al. (1972) to investigate the effect of the cyclic load side by side with monotonic one.

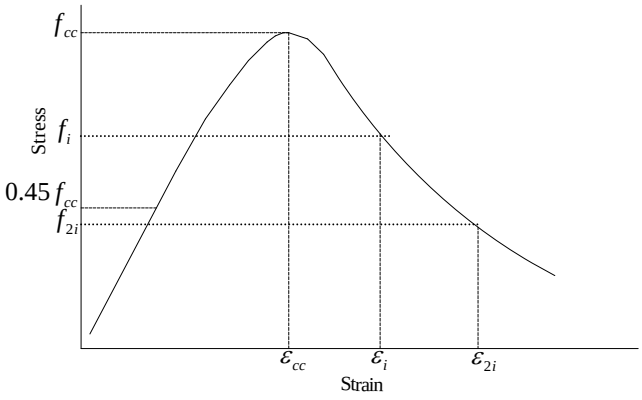

FIGURE 2.10
Proposed General Stress-Strain Curve by Yong et al. (1988)

$$f_{cc} = f_c^{'}\left(-1.254 + 2.254\sqrt{1+\frac{7.94 f_l^{'}}{f_c^{'}}} - 2\frac{f_l^{'}}{f_c^{'}}\right)$$ **Equation 2.92**

$$\varepsilon_{cc} = \varepsilon_{co}\left[1+5\left(\frac{f_{cc}^{'}}{f_c^{'}}-1\right)\right]$$ **Equation 2.93**

$$f_l^{'} = \frac{1}{2}k_e \rho_s f_{yh} = k_e f_l$$ **Equation 2.94**

$$f_c = \frac{f_{cc} xr}{r-1+x^r}$$ **Equation 2.95**

$$r = \frac{E_c}{E_c - E_{\sec}}$$ **Equation 2.96**

$$x = \frac{\varepsilon_c}{\varepsilon_{cc}}$$ **Equation 2.97**

where k_e is the effective lateral confinement coefficient:

$$k_e = \frac{A_e}{A_{cc}}$$ **Equation 2.98**

A_e is the area of effectively confined concrete, $E_{sec} = f_{cc}/\varepsilon_{cc}$ and A_{cc} is area of core within centerlines of perimeter spirals or hoops excluding area of longitudinal steel.

$$k_e = \frac{\left(1-\frac{s^{'}}{2d_s}\right)^2}{1-\rho_{cc}}$$ For circular hoops **Equation 2.99**

$$k_e = \frac{1 - \frac{s'}{2d_s}}{1 - \rho_{cc}}$$ For circular spirals

Equation 2.100

$$k_e = \frac{\left(1 - \sum_{i=1}^{n} \frac{(w_i')^2}{6b\ h}\right)\left(1 - \frac{s'}{2b}\right)\left(1 - \frac{s'}{2h}\right)}{(1 - \rho_{cc})}$$ For rectangular ties

Equation 2.101

where *s'* is the clear spacing, ρ_{cc} is the the ratio of longitudinal reinforcement to the core area $\sum w_i^2$ is the sum of the squares of all the clear spacing between adjacent longitudinal steel bars in a rectangular section. Mander et al. (1988) proposed calculation for the ultimate confined concrete strain ε_{cu} based on the strain energy of confined concrete.

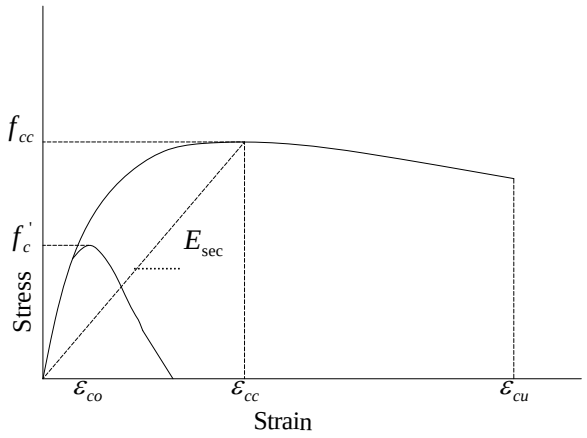

FIGURE 2.11
Stress-Strain Model Proposed by Mander et al. (1988)

Fujii, Kobayashi, Miyagawa, Inoue, and Matsumoto (1988)

Fujii et al. (1988) developed a stress strain relation by uniaxial testing of circular and square specimen of 150 mm wide and 300 mm tall (Figure 2.12). The tested specimen did not have longitudinal bars and no cover. The proposed stress strain model has four regions;

Region 1 from 0-*A*

$$f_c = E_i \varepsilon_c + \frac{f_c^{'} - E_i \varepsilon_{co}}{\varepsilon_{co}^{\,2}} \varepsilon_c^{\,2} \qquad 0 \le \varepsilon_c \le \varepsilon_{co} \qquad \textbf{Equation 2.102}$$

Region 2 from *A*-*B*

$$f_c = f_{cc} + \frac{\left(\varepsilon_c - \varepsilon_{cc}\right)^3}{\left(\varepsilon_{co} - \varepsilon_{cc}\right)^3}\left(f_c^{'} - f_{cc}\right) \qquad \varepsilon_{co} < \varepsilon_c \le \varepsilon_{cc} \qquad \textbf{Equation 2.103}$$

Region 3 from *B*-*C*

$$f_c = f_{cc} - \theta\left(\varepsilon_c - \varepsilon_{cc}\right) \qquad \varepsilon_{cc} < \varepsilon_c \le \varepsilon_{c20} \qquad \textbf{Equation 2.104}$$

Region 4 from *C*-*end*

$$f_c = 0.2 f_{cc} \qquad \varepsilon_{c20} < \varepsilon_c \qquad \textbf{Equation 2.105}$$

Fujii et al. (1988) defined three confinement coefficients for maximum stress C_{cf}, corresponding strain $C_{c\varepsilon u}$ and stress degradation gradient C_θ. For circular specimens, the peak strength and corresponding strain are as follow:

$$\frac{f_{cc}}{f_c^{'}} = 1.75 C_{cf} + 1.02 \qquad \textbf{Equation 2.106}$$

$$\frac{\varepsilon_{cc}}{\varepsilon_{co}} = 50\, C_{c\varepsilon u} + 1.25 \qquad \textbf{Equation 2.107}$$

$$\theta = 417 C_\theta - 574 \qquad \textbf{Equation 2.108}$$

$$C_{cf} = \rho_s \left(1 - \frac{s}{0.51 d_s}\right) \frac{\sqrt{f_{yh}}}{f_c^{'}} \qquad \textbf{Equation 2.109}$$

$$C_{cu} = \rho_s \left(1 - \frac{s}{0.95 d_s}\right) \frac{\sqrt{f_{yh}}}{\left(f_c^{'}\right)^2} \qquad \textbf{Equation 2.110}$$

$$\theta = 1240 C_\theta - 2720 \qquad \textbf{Equation 2.111}$$

$$C_{cf} = \rho_s \left(1 - \frac{s}{h}\right) \qquad \textbf{Equation 2.112}$$

$$C_{cu} = \rho_s \left(1 - \frac{s}{h}\right) \frac{\sqrt{f_{yh}}}{\left(f_c^{'}\right)^2} \qquad \textbf{Equation 2.113}$$

$$C_\theta = 1 / \rho_s \left(f_c^{'}\right)^2 / f_{yh} \qquad \textbf{Equation 2.114}$$

They showed that the proposed model has higher accuracy than Park et al. (1982) model compared to the experimental work done by Fujii et al. (1988).

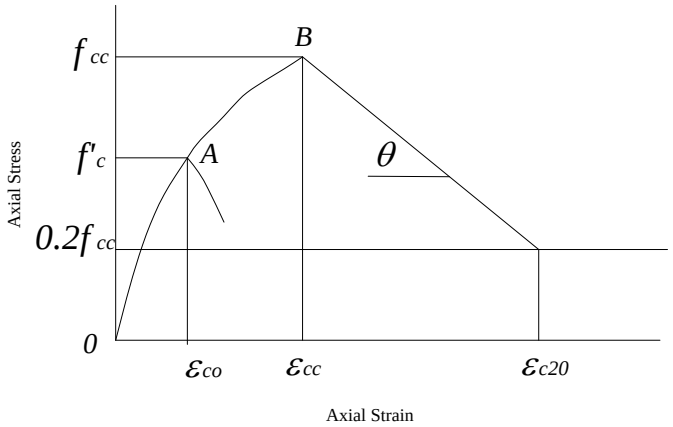

FIGURE 2.12
Proposed General Stress-Strain Curve by Fujii et al. (1988)

Saatcioglu and Razvi (1992)

Saatcioglu and Razvi (1992) concluded that the passive lateral pressure generated by laterally expanding concrete and restraining transverse reinforcement is not always uniform. Based on tests on normal and high strength concrete ranging from 30 to 130 *MPa*, Saatcioglu and Razvi proposed a new model (Figure 2.13) that has exponential relationship between the lateral confinement pressure and the peak confinement strength. They ran tests by varying volumetric ratio, spacing, yield strength, arrangement of transverse reinforcement, concrete strength and section geometry. In addition, the significance of imposing the tie arrangement as a parameter in determining the peak confined strength was highlighted

$$f_{cc} = f_c^{'} + k_1 f_l$$ for circular cross section **Equation 2.115**

$$k_1 = 6.7(f_l)^{-0.17}$$ **Equation 2.116**

$$f_l = \frac{2A_s f_{yh}}{d_s s}$$ for circular cross section **Equation 2.117**

$$f_{cc} = f_c^{'} + k_1 f_{le}$$ for rectangular cross section **Equation 2.118**

$$f_{le} = k_2 f_l$$ **Equation 2.119**

$$f_l = \frac{\sum A_s f_{yh} \sin\alpha}{sh}$$ for square columns **Equation 2.120**

$$k_2 = 0.15\sqrt{\left(\frac{h}{s}\right)\left(\frac{h}{c}\right)\left(\frac{1}{f_l}\right)} \le 1$$ **Equation 2.121**

$$f_{le} = \frac{f_{lex} b + f_{ley} h}{b + h}$$ for rectangular columns **Equation 2.122**

$$\varepsilon_{cc} = \varepsilon_{co}\left(1 + 5\frac{k_1 f_{le}}{f_c^{'}}\right)$$ **Equation 2.123**

For the stress strain curve

$$\varepsilon_{85} = 260\frac{\sum A_s}{s(b+h)}\varepsilon_{cc} + \varepsilon_{085}$$ **Equation 2.124**

where ε_{085} is the strain at $0.85\,f'c$ for the unconfined concrete

$$f_c = f_{cc}\left[2\left(\frac{\varepsilon_c}{\varepsilon_{cc}}\right) - \left(\frac{\varepsilon_c}{\varepsilon_{cc}}\right)^2\right]^{1/\left(1+2\frac{k_1 f_{le}}{f_c^{'}}\right)}$$ **Equation 2.125**

where c is spacing of longitudinal reinforcement and α is the angle between the transverse reinforcement and b.

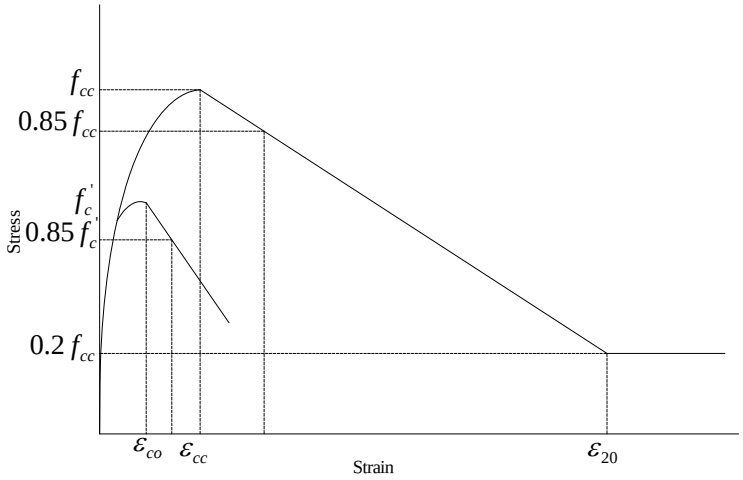

FIGURE 2.13
Proposed Stress-Strain Curve by Saatcioglu and Razvi (1992-1999)

Sheikh and Toklucu (1993)

Sheikh and Toklucu (1993) studied the ductility and strength for confined concrete and they concluded that ductility is more sensitive, than the strength, to amount of transverse steel, and the increase in concrete strength due to confinement was observed to be between 2.1 and 4 times the lateral pressure.

Karabinis and Kiousis (1994)

Karabinis and Kiousis (1994) utilized the theory of plasticity in evaluating the development of lateral confinement in concrete columns. However, no stress-strain equations were proposed

Hsu and Hsu (1994)

Hsu and Hsu (1994) modified Carreira and Chu (1985) equation that was developed for unconfined concrete, to propose an empirical stress strain equations for high strength concrete. The concrete strength equation is:

$$f_c = f_{cc}\left(\frac{\xi\omega x}{\xi\omega - 1 + x^{\xi\omega}}\right) \quad \text{for} \quad 0 \le x \le x_d \qquad \textbf{Equation 2.126}$$

$$x = \frac{\varepsilon_c}{\varepsilon_{cc}} \qquad \textbf{Equation 2.127}$$

$$\omega = \frac{1}{1 - \frac{f_c^{'}}{\varepsilon_{cc} E_{ic}}} \quad \text{for} \quad \omega \ge 1 \qquad \textbf{Equation 2.128}$$

where ω and ζ are material properties. ω depends on the shape of the stress strain curve and ζ depends on material strength and it is taken equal to 1.0 and x_d is the strain at 0.6 $f'_{c.}$ in the descending portion of the curve.

Rasheed and Dinno (1994)

Rasheed and Dinno (1994) introduced a fourth degree polynomial to express the stress strain curve of concrete under compression.

$$f_c = a_o + a_1\varepsilon_c + a_2\varepsilon_c^2 + a_3\varepsilon_c^3 + a_4\varepsilon_c^4 \qquad \textbf{Equation 2.129}$$

They evaluated the constants a_o-a_4 using the boundary conditions of the stress strain curve. Similar to Kent and Park, they assumed no difference between the unconfined and confined peak strength.

$$f_{cc} = k_c f_c^{'} \qquad \textbf{Equation 2.130}$$

where

$$k_c = 1$$

They used expression taken from Kent and Park model to evaluate the slope of the descending branch starting at strain of 0.003. A flat straight line was proposed when the stress reaches $0.2\ f_{cc}$ up to $C_c\varepsilon_{cc.}$ where C_c is the ratio of maximum confined compressive strain to $\varepsilon_{cc.}$
The five boundary conditions used are:

$f_c = 0$ at ε_c=0

$d\ f_c / d\ \varepsilon_c = E_c$ at ε_c=0

$f_c = f'_c$ at $\varepsilon_c = \varepsilon_{co}$

$d\ f_c / d\ \varepsilon_c = 0$ at $\varepsilon_c = \varepsilon_{co}$

$d\ f_c / d\ \varepsilon_c = -Z\ f_c$ at $\varepsilon_c = 0.003$

El-Dash and Ahmad (1995)

El-Dash and Ahmad (1995) used Sargin et al. model to predict analytically the behavior of spirally confined normal and high strength concrete in one series of equations. They used the internal force equilibrium, properties of materials, and the geometry of the section to predict the pressure. The parameters imposed in the analytical prediction where plain concrete strength, confining reinforcement diameter and yield strength, the volumetric ratio of lateral reinforcement to the core, the dimension of the column and spacing.

$$Y = \frac{AX + (B-1)X^2}{1 + (A-2)X + BX^2}$$ **Equation 2.131**

where

$$Y = \frac{f_c}{f_{cc}}$$ **Equation 2.132**

$$X = \frac{\varepsilon_c}{\varepsilon_{cc}}$$ **Equation 2.133**

$$f_{cc} = f_c^{'} + k_1 f_l$$ **Equation 2.134**

$$\varepsilon_{cc} = \varepsilon_{co} + k_2 \frac{f_l}{f_c^{'}}$$ **Equation 2.135**

The values of A, B, k_1, k_2 and f_l are defined by the following equations

$$A = \frac{E_c \varepsilon_{cc}}{f_{cc}} = \frac{E_c}{E_{\sec}}$$ **Equation 2.136**

$$B = \frac{16.5}{\sqrt{f_c^{'}}} \left(\frac{f_l}{\frac{s}{d_{st}^{'}}} \right)^{0.33}$$ **Equation 2.137**

$$k_1 = 5.1 \left(\frac{f_c^{'}}{f_{yh}} \right)^{0.5} \left(\frac{d_{st}^{'}}{\rho_s} \right)^{0.25}$$ **Equation 2.138**

$$k_2 = \frac{66}{\left(\frac{s}{d_{st}^{'}} \right) f_c^{'1.7}}$$ **Equation 2.139**

$$f_l = 0.5 \rho_s f_{yh} (1 - \sqrt{\frac{s}{1.25 d_s}})$$ **Equation 2.140**

where d_s is the core diameter.

Cusson and Paultre (1995)

Unlike all the previous work, Cusson and Paultre (1995) built their model based on the actual stress in the stirrups upon failure and they did not consider the yield strength, as the experimental work have shown that the yield strength for the transverse steel is reached in case of well confined columns. The ascending and the descending branches in the model curve are expressed by two different equations (Figure 2.14). For the ascending portion:

$$f_c = f_{cc} \left(\frac{k \left(\frac{\varepsilon_c}{\varepsilon_{cc}} \right)}{k + 1 + \left(\frac{\varepsilon_c}{\varepsilon_{cc}} \right)^k} \right) \qquad \varepsilon_c \le \varepsilon_{cc}$$ **Equation 2.141**

$$k = \frac{E_c}{E_c - \left(\frac{f_{cc}}{\varepsilon_{cc}} \right)}$$ **Equation 2.142**

For descending one:

$$f_c = f_{cc} \exp\left(k_1 \left(\varepsilon_{c50c} - \varepsilon_{cc}\right)^{k_2}\right) \qquad \varepsilon_c \geq \varepsilon_{cc}$$ **Equation 2.143**

$$k_1 = \frac{\ln 0.5}{\left(\varepsilon_{c50c} - \varepsilon_{cc}\right)^{k_2}}$$ **Equation 2.144**

$$k_2 = 0.58 + 16\left(\frac{f_l^{'}}{f_c^{'}}\right)^{1.4}$$ **Equation 2.145**

where ε_{c50c} is axial strain in confined concrete when stress drops to 0.5 fcc. It is observed that equation (2.144) proposed by Cusson and Paultre is identical to equation (2.95) suggested by Mander et al. (1988).

Following the same methodology of Sheikh and Uzumeri (1982) and Mander et al. (1988) Cusson and Paultre considered the lateral confinement pressure f_l.

$$f_l = \frac{f_{hcc}}{s}\left(\frac{A_{sx} + A_{sy}}{b + h}\right)$$ **Equation 2.146**

where A_{sx} and A_{sy} are the lateral cross sectional area of the lateral steel perpendicular to x and y axes respectively and f_{hcc} is the stress in the transverse reinforcement at the maximum strength of confined concrete.

$$k_e = \frac{\left(1 - \frac{\sum w_i^2}{6bh}\right)\left(1 - \frac{s'}{2b}\right)\left(1 - \frac{s'}{2h}\right)}{1 - \rho_{cc}}$$ **Equation 2.147**

$$f_l^{'} = k_e f_l$$ **Equation 2.148**

where $\sum w_i^2$ is the sum of the squares of all the clear spacing between adjacent longitudinal steel bars in a rectangular section. f_{cc} and ε_{cc} can be found by the following equations

$$f_{cc} = f_c^{'}\left[1 + 2.1\left(\frac{f_l^{'}}{f_c^{'}}\right)^{0.7}\right]$$ **Equation 2.149**

$$\varepsilon_{cc} = \varepsilon_{co} + 0.21\left(\frac{f_l^{'}}{f_c^{'}}\right)^{1.7}$$ **Equation 2.150**

$$\varepsilon_{c50c} = 0.004 + 0.15\left(\frac{f_l^{'}}{f_c^{'}}\right)^{1.1}$$ **Equation 2.151**

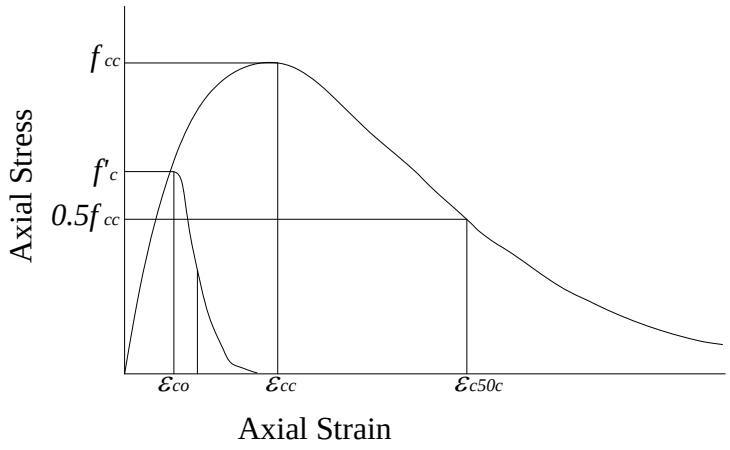

FIGURE 2.14
Proposed Stress-Strain Curve by Cusson and Paultre (1995)

Attard and Setunge (1996)

Attard and Setunge (1996) experimentally determined full stress-strain curve for concrete with compressive strength of 60 –130 *MPa* and with confining pressure of 1-20 *MPa*, Figure 2.15. The main parameters used were peak stress; strain at peak stress, modulus of elasticity, and the stress and strain at point of inflection. Attard and Setunge followed the same equation used by Wang et al. (1978). and Sargin (1971):

$$Y = \frac{AX + BX^2}{1 + CX + DX^2}$$ **Equation 2.152**

where

$$Y = \frac{f_c}{f_{cc}}$$ **Equation 2.153**

$$X = \frac{\varepsilon_c}{\varepsilon_{cc}}$$ **Equation 2.154**

For the ascending branch, the four constant are determined by setting four conditions:

1- at $f_c = 0$, $\frac{df_c}{d\varepsilon_c} = E_c$

2- at $f_c = f_{cc}, \frac{df_c}{d\varepsilon_c} = 0$

3- at $f_c = f_{cc}, \varepsilon_c = \varepsilon_{cc}$

4- at $f_c = 0.45 f'_c, \varepsilon_c = \frac{f_c}{E_{0.45}}$

The constants are given by:

$$A = \frac{E_c \varepsilon_{cc}}{f_{cc}} = \frac{E_c}{E_{\text{sec}}}$$ **Equation 2.155**

$$B = \frac{(A-1)^2}{\frac{E_c}{E_{0.45}}\left(1 - \frac{0.45 f_c^{'}}{f_{cc}}\right)} + \frac{A^2 (1 - \frac{E_c}{E_{0.45}})}{\left(\frac{E_c}{E_{0.45}}\right)^2 \frac{0.45 f_c^{'}}{f_{cc}}\left(1 - \frac{0.45 f_c^{'}}{f_{cc}}\right)} - 1$$ **Equation 2.156**

$$C = A - 2$$ **Equation 2.157**

$$D = B + 1$$ **Equation 2.158**

while for the descending curve the four boundary conditions were

1- at $f_c = f_{cc}, \frac{df_c}{d\varepsilon_c} = 0$

2- at $f_c = f_{cc}, \varepsilon_c = \varepsilon_{cc}$

3- at $f_c = f_i, \varepsilon_c = \varepsilon_i$

4- at $f_c = f_{2i}, \varepsilon_c = \varepsilon_{2i}$

where f_i and ε_i refer to the coordinate of the inflection point.

The four constants for the descending curve are

$$A = \left[\frac{\varepsilon_{2i} - \varepsilon_i}{\varepsilon_{cc}}\right]\left[\frac{\varepsilon_{2i} E_i}{(f_{cc} - f_i)} - \frac{4\varepsilon_i E_{2i}}{(f_{cc} - f_{2i})}\right] \quad \textbf{Equation 2.159}$$

$$B = (\varepsilon_{2i} - \varepsilon_i)\left[\frac{E_i}{(f_{cc} - f_i)} - \frac{E_{2i}}{(f_{cc} - f_{2i})}\right] \quad \textbf{Equation 2.160}$$

$$C = A - 2 \quad \textbf{Equation 2.161}$$

$$D = B + 1 \quad \textbf{Equation 2.162}$$

The f_{cc} came out to be a function of the confining pressure, the compressive and tensile strength of concrete f'_c, f_l, f_t, and a parameter k that reflects the effectiveness of confinement.

$$\frac{f_{cc}}{f_c^{'}} = \left(\frac{f_l}{f_t} + 1\right)^k \quad \textbf{Equation 2.163}$$

$$k = 1.25\left[1 + 0.062\frac{f_l}{f_c^{'}}\right]\left(f_c^{'}\right)^{-0.21} \quad \text{MPa} \quad \textbf{Equation 2.164}$$

$$\frac{\varepsilon_{cc}}{\varepsilon_{co}} = 1 + \left(17 - 0.06 f_c^{'}\right)\left(\frac{f_l}{f_c^{'}}\right) \quad \textbf{Equation 2.165}$$

No lateral pressure equation was provided

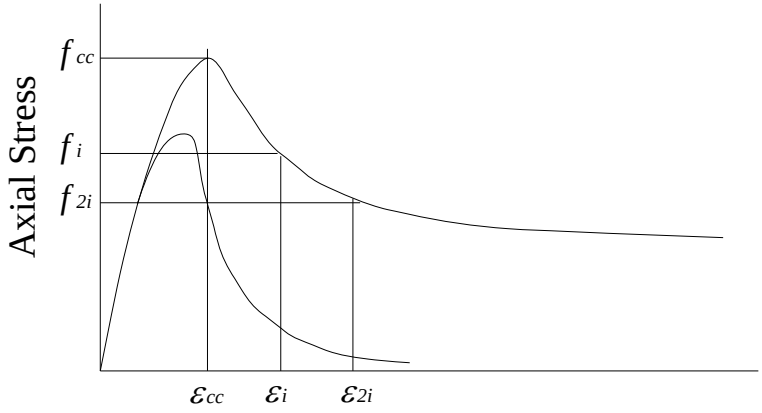

FIGURE 2.15
Proposed Stress-Strain Curve by Attard and Setunge (1996)

Mansur, Chin, and Wee (1996)

Mansur et al. (1996) introduced casting direction, if the member is cast in place(vertically) or pre-cast (horizontally), as a new term among the test parameters, for high strength concrete, which were tie diameter and spacing and concrete core area. They concluded that the vertically cast confined fiber concrete has higher strain at peak stress and higher ductility than the horizontally cast specimen. In addition, vertically cast confined non-fiber concrete has larger strain than that of horizontally cast concrete with no enhancement in ductility. Mansur et al. utilized the same equations found by Carreira and Chu for plain concrete with some modifications. For the ascending branch, they used the exact same equation

$$f_c = f_{cc}\left\{\frac{\beta\left(\frac{\varepsilon}{\varepsilon_{cc}}\right)}{\beta - 1 + \left(\frac{\varepsilon}{\varepsilon_{cc}}\right)^{\beta}}\right\} \qquad \textbf{Equation 2.166}$$

where β is a material parameter depending on the stress strain shape diagram and can be found by :

$$\beta = \frac{1}{1 - \frac{f_{cc}}{\varepsilon_{cc} E_c}}$$ **Equation 2.167**

k_1 and k_2 are two constants introduced in the equation describing the descending branch:

$$f_c = f_{cc} \left\{ \frac{k_1 \beta \left(\frac{\varepsilon_c}{\varepsilon_{cc}} \right)}{k_1 \beta - 1 + \left(\frac{\varepsilon_c}{\varepsilon_{cc}} \right)^{k_2 \beta}} \right\}$$ **Equation 2.168**

for confined horizontally and vertically cast non-fiber concrete:

$$k_1 = 2.77 \left(\frac{\rho_s f_{yh}}{f_c^{'}} \right)$$ **Equation 2.169**

$$k_2 = 2.19 \left(\frac{\rho_s f_{yh}}{f_c^{'}} \right) + 0.17$$ **Equation 2.170**

for horizontally cast confined fiber concrete

$$k_1 = 3.33 \left(\frac{\rho_s f_{yh}}{f_c^{'}} \right) + 0.12$$ **Equation 2.171**

$$k_2 = 1.62 \left(\frac{\rho_s f_{yh}}{f_c^{'}} \right) + 0.35$$ **Equation 2.172**

and the values of f_{cc} and ε_{cc} can be obtained from the following equations for confined non-fiber concrete:

$$\frac{f_{cc}}{f_c^{'}} = 1 + 0.6\left(\frac{\rho_s f_{yh}}{f_c^{'}}\right)^{1.23}$$ **Equation 2.173**

for confined fiber concrete:

$$\frac{f_{cc}}{f_c^{'}} = 1 + 11.63\left(\frac{\rho_s f_{yh}}{f_c^{'}}\right)^{1.23}$$ **Equation 2.174**

for vertically cast fiber concrete

$$\frac{\varepsilon_{cc}}{\varepsilon_{co}} = 1 + 62.2\left(\frac{\rho_s f_{yh}}{f_c^{'}}\right)^{2}$$ **Equation 2.175**

for horizontally cast fiber concrete and vertically cast non-fiber concrete

$$\frac{\varepsilon_{cc}}{\varepsilon_{co}} = 1 + 2.6\left(\frac{\rho_s f_{yh}}{f_c^{'}}\right)^{0.8}$$ **Equation 2.176**

and for horizontally cast non-fiber concrete

$$\frac{\varepsilon_{cc}}{\varepsilon_{co}} = 1 + 5.9\left(\frac{\rho_s f_{yh}}{f_c^{'}}\right)^{1.5}$$ **Equation 2.177**

Hoshikuma, Kawashima, Nagaya, and Taylor (1997)

Hoshikuma et al. (1997) developed their models to satisfy bridge column section design in Japan. The model was based on series of compression loading tests of reinforced concrete column specimens that have circular, square and wall type cross sections. The variables that varied in the experimental wok were hoop volumetric ratio, spacing, configuration of the hook in the hoop reinforcement and tie arrangement.

Hoshikuma et al. (1997) asserted that the ascending branch represented in second degree parabola is not accurate to satisfy four boundary conditions:

1. Initial condition $f_c = 0$, $\varepsilon_c = 0$.

2. Initial stiffness condition $df_c/d\,\varepsilon_c = E_c$ at $\varepsilon_c = 0$.

3. Peak condition $f_c = f_{cc}$ at $\varepsilon_c = \varepsilon_{cc}$

4. Peak stiffness condition $df_c/d\varepsilon_c = 0$ at $\varepsilon_c = \varepsilon_{cc}$

The function that defines the ascending branch is:

$$f_c = E_c \varepsilon_c \left[1 - \frac{1}{\beta} \left(\frac{\varepsilon_c}{\varepsilon_{cc}} \right)^{\beta - 1} \right] \qquad \textbf{Equation 2.178}$$

$$\beta = \frac{E_c \varepsilon_{cc}}{E_c \varepsilon_{cc} - f_{cc}} \qquad \textbf{Equation 2.179}$$

For the descending branch:

$$f_c = f_{cc} - E_{des} \left(\varepsilon_c - \varepsilon_{cc} \right) \qquad \textbf{Equation 2.180}$$

where E_{des} is the deterioration rate that controls slope of the descending line and can be found using the following equation

$$E_{des} = \frac{11.2}{\dfrac{\rho_s f_{yh}}{f_c^{'2}}} \qquad \textbf{Equation 2.181}$$

The peak stress and the corresponding strain for the circular section

$$\frac{f_{cc}}{f_c^{'}} = 1 + 3.83 \frac{\rho_s f_{yh}}{f_c^{'}} \qquad \textbf{Equation 2.182}$$

$$\varepsilon_{cc} = 0.00218 + 0.0332\frac{\rho_s f_{yh}}{f_c^{'}}$$ **Equation 2.183**

while for the square section

$$\frac{f_{cc}}{f_c^{'}} = 1 + 0.73\frac{\rho_s f_{yh}}{f_c^{'}}$$ **Equation 2.184**

$$\varepsilon_{cc} = 0.00245 + 0.0122\frac{\rho_s f_{yh}}{f_c^{'}}$$ **Equation 2.185**

Razvi and Saatcioglu (1999)

Razvi and Saatcioglu modified their model of Saatcioglu and Razvi (1992) to fit the high strength concrete (30 – 130 MPa). The ascending zone is defined by Popovics equation as follow:

$$f_c = \frac{f_{cc}\frac{\varepsilon_c}{\varepsilon_{cc}} r}{r - 1 + \left(\frac{\varepsilon_c}{\varepsilon_{cc}}\right)^r}$$ **Equation 2.186**

and for the descending branch:

$$\varepsilon_{cc} = \varepsilon_{co}\left(1 + 5k_3 K\right)$$ **Equation 2.187**

$$\varepsilon_{85} = 260K_3\frac{\sum A_s}{S(B+h)}\varepsilon_{cc}\left[1 + 0.5k_2\left(k_4 - 1\right)\right] + \varepsilon_{085}$$ **Equation 2.188**

$$k_3 = \frac{40}{f_c^{'}} \le 1.0 \qquad k_4 = \frac{f_{yh}}{500} \ge 1.0 \qquad K = \frac{k_1 f_{le}}{f_c^{'}}$$ **Equation 2.189**

Razvi and Saatcioglu (1999) showed the good agreement of the model with some experimental work available in the literature.

Mendis, Pendyala, and Setunge (2000)

Mendis et al. (2000) modified Scott et al. (1982) equations to fit high strength concrete. They empirically adjusted Scott et al. (1982) equations to the following ones:

$$f_c = kf_c^{'}\left[\frac{2\varepsilon_c}{\varepsilon_{cc}} - \left(\frac{\varepsilon_c}{\varepsilon_{cc}}\right)^2\right] \quad \text{for} \quad \varepsilon_c \le \varepsilon_{cc} \qquad \textbf{Equation 2.190}$$

$$f_c = kf_c^{'}\left[1 - Z_m(\varepsilon_c - \varepsilon_{cc})\right] \ge f_{res} \quad \text{for} \quad \varepsilon_c > \varepsilon_{cc} \qquad \textbf{Equation 2.191}$$

$$f_{res} = RKf_c^{'} \qquad \textbf{Equation 2.192}$$

$$K = 1 + 3\frac{f_l}{f_c^{'}} \qquad \textbf{Equation 2.193}$$

$$Z_m = \frac{0.5}{\frac{3 + 0.29f_c^{'}}{145f_c^{'} - 1000} + \frac{3}{4}\rho_s\sqrt{\frac{b''}{s}} - \varepsilon_{cc}} \ge 0 \qquad f'_c \text{ in } MPa \qquad \textbf{Equation 2.194}$$

$$\varepsilon_{cc} = \left(0.24K^3 + 0.76\right)\varepsilon_{co} \qquad \textbf{Equation 2.195}$$

$$R = 0.28 - 0.0032f_c^{'} \qquad R \ge 0 \qquad \textbf{Equation 2.196}$$

$$Z = 0.018f_c^{'} + 0.55 \qquad \textbf{Equation 2.197}$$

f_l is calculated according to Mander equations.

Assa, Nishiyama, and Watanabe (2001)

A new model was proposed for concrete confined by spiral reinforcement based on concrete-transverse steel interaction. The two main parameters were concrete strength and lateral stress-lateral strain relationship that represents the response characteristics of the transverse steel to the lateral expansion of concrete. Assa et al. (2001) modeled a confinement mechanism and

limited the lateral expansion of the confined concrete with the maximum lateral expansion capacity. Assa et al. (2001) reached some relationships expressed in the following equations:

$$\frac{f_{cc}}{f_c^{'}} = 1 + 3.36\frac{f_l}{f_c^{'}} \qquad \textbf{Equation 2.198}$$

$$\frac{\varepsilon_{cc}}{\varepsilon_{co}} = 1 + 21.5\frac{f_l}{f_c^{'}} \qquad \textbf{Equations 2.199}$$

$$\varepsilon_{lcu} = 0.0021 + 0.016\frac{f_l}{f_c^{'}} \qquad \textbf{Equation 2.200}$$

where ε_{lcu} is the maximum lateral concrete strain. The proposed stress-strain curve has one equation:

$$f_c = f_{cc}\left(\frac{\gamma X + (\delta - 1)X^2}{1 + (\gamma - 2)X + \delta X^2}\right) \qquad \textbf{Equation 2.201}$$

$$X = \frac{\varepsilon_c}{\varepsilon_{cc}} \qquad \textbf{Equation 2.202}$$

where γ controls the stiffness of ascending branch and δ controls the slope of the descending branch:

$$\gamma = \frac{E_c \varepsilon_{cc}}{f_{cc}} = \frac{E_c}{E_{\sec}} \qquad \textbf{Equation 2.203}$$

$$\delta = \left(\frac{\left(\frac{\varepsilon_{80}}{\varepsilon_{cc}}\right)^2 - (0.2\gamma + 1.6)\frac{\varepsilon_{80}}{\varepsilon_{cc}} + 0.8}{0.2\left(\frac{\varepsilon_{80}}{\varepsilon_{cc}}\right)^2}\right) \qquad \textbf{Equation 2.204}$$

where ε_{80} is the strain at $0.8f_{cc}$.

Lokuge, Sanjayan, and Setunge (2005)

A simple stress-strain model was proposed based on shear failure. The model was based on the experimental results taken from Candappa (2000). Lokuge et al. (2005) proposed a relationship between axial and lateral strain:

$$\frac{\varepsilon_l}{\varepsilon_{lcc}} = v\left(\frac{\varepsilon}{\varepsilon_{cc}}\right) \qquad \varepsilon \le \varepsilon' \qquad \textbf{Equation 2.205}$$

$$\frac{\varepsilon_l}{\varepsilon_{lcc}} = \left(\frac{\varepsilon}{\varepsilon_{cc}}\right)^a \qquad \varepsilon > \varepsilon' \qquad \textbf{Equation 2.206}$$

where ε' is a strain at a point where axial strain and lateral strain curves deviate, v is the initial Poisson's ratio, and a is a material parameter which depends on the uniaxial concrete strength

$$v = 8*10^{-6}\left(f_c'\right)^2 + 0.0002 f_c' + 0.138 \qquad \textbf{Equation 2.207}$$

$$a = 0.0177 f_c' + 1.2818 \qquad \textbf{Equation 2.208}$$

where f'_c is in MPa.

Binici (2005)

Binici (2005) introduced a generalized formulas describing concrete under triaxial compression. The proposed stress strain curve is defined by elastic region then non linear curve. The axial compression is expressed using Leon-Paramono criterion as follow

$$f_c = f_c^{'}\left(k\sqrt{c+m\phi}-(1-k)\phi^2+\phi\right) \qquad \textbf{Equation 2.209}$$

$$\phi = \frac{f_l}{f_c^{'}} \qquad m = \frac{f_c^{'2}-f_t^{'2}}{f_c^{'}f_t^{'}} \qquad \textbf{Equation 2.210}$$

where f'_t is the uniaxial tensile strength, c is the softening parameter and is equal to one in hardening region and zero for residual strength and k is the hardening parameter and is equal to one at ultimate strength and softening region and is equal to 0.1 at the elastic limit. Binici (2005) defined three equations for determining the stress in the elastic, hardening and softening zones as follow:

For elastic zone:

$$f_c = E_c\varepsilon_c \qquad \varepsilon_c \le \varepsilon_{1e} \qquad \textbf{Equation 2.211}$$

For the hardening zone:

$$f_c = f_{1e}+\left(f_{cc}-f_{1e}\right)\left(\frac{\varepsilon_c-\varepsilon_{1e}}{\varepsilon_{cc}-\varepsilon_{1e}}\right)\frac{r}{r-1+\left(\frac{\varepsilon_c-\varepsilon_{1e}}{\varepsilon_{cc}-\varepsilon_{1e}}\right)^r} \quad \varepsilon_{1e} \le \varepsilon_c \le \varepsilon_{cc} \qquad \textbf{Equation 2.212}$$

$$r = \frac{E_c}{E_c-E_{\sec}} \qquad \varepsilon_{1e} = \frac{f_{1e}}{E_c} \qquad \varepsilon_{cc} = 5\varepsilon_{co}\left(\frac{f_{cc}}{f_c^{'}}-0.8\right) \qquad \textbf{Equation 2.213}$$

For the softening zone:

$$\alpha = \frac{1}{\sqrt{\pi}\left(f_{cc} - f_{1r}\right)}\left(\frac{2G_{fc}}{l_c} - \frac{\left(f_{cc} - f_{1r}\right)^2}{E_c}\right) \qquad \textbf{Equation 2.214}$$

where l_c is the length of the specimen and G_{fc} is the compressive failure energy and is calculated as follow:

$$G_{fc} = l_c\left[\int_{\varepsilon_{cc}}^{\infty}\left(f_{cc} - f_{1r}\right)\exp\left[-\left(\frac{\varepsilon_c - \varepsilon_{cc}}{\alpha}\right)^2\right]d\varepsilon_c + \frac{\left(f_{cc} - f_{1r}\right)^2}{2E_c}\right] \qquad \textbf{Equation 2.215}$$

To fully define the stress strain curve for constant pressure, Equation 2.212 is used to define the limit stresses. These stresses are imposed in Equations 2.215 and 2.217 to fully define the stress strain curve. The lateral pressure is calculated using the lateral strain ε_l found by:

$$\varepsilon_l = -\nu_s\varepsilon_c \qquad \textbf{Equation 2.216}$$

$$\nu_s = \nu_o \qquad \text{for} \qquad \varepsilon_c \le \varepsilon_{1e} \qquad \textbf{Equation 2.217}$$

$$\nu_s = \nu_1 - \left(\nu_1 - \nu_o\right)\exp\left[-\left(\frac{\varepsilon_c - \varepsilon_{cc}}{\left(\frac{\varepsilon_{cc} - \varepsilon_{1e}}{\sqrt{-\ln\beta}}\right)}\right)^2\right] \quad \text{for} \quad \varepsilon_{1e} \le \varepsilon_c \qquad \beta = \frac{\nu_1 - \nu_p}{\nu_1 - \nu_o} \qquad \textbf{Equation 2.218}$$

where ν_s is the secant Poisson's ratio

$$\nu_1 = \nu_p + \frac{1}{\left(\phi + 0.85\right)^4} \qquad \varepsilon_1 \le \varepsilon_{1e} \qquad \textbf{Equation 2.219}$$

whereas in case of changing lateral pressure, the lateral pressure is solved by equating the lateral strain in jacket to the lateral strain of concrete:

$$\varepsilon_1 \nu_s(f_l) - \frac{2 f_l}{E_j \rho_j} = 0 \qquad \textbf{Equation 2.220}$$

where E_j and ρ_j is the modulus of elasticity and volumetric ratio of the jacket respectively.

2.1.2 Discussion

As stated by many research studies, like Mander et al. (1988), Scott et al. (1982), Sheikh and Uzumeri (1980) and Shuhaib and Mallare (1993), the spirals or circular hoops are more efficient than the rectangular hoops. The uniform pressure generated by the circular hoop is one of the reasons of circular spirals advantage.

According to Eid and Dancygier (2005), there are four main approaches for the modeling of confined concrete by lateral ties

1. The empirical approach: in which the stress-strain curve is generated based on the experimental results. Fafitis and Shah (1985) and Hoshikuma et al. (1997) followed that approach.
2. Physical engineering model based approach: the lateral pressure causing the confined behavior of the concrete core, is provided by the arch action between the lateral reinforcement ties. This approach was adopted by Sheikh and Uzumeri (1980), and was followed by Mander et al. (1988).
3. The third approach is based either on the first approach or the second one, but it does not assume the lateral ties yielding. Instead, It include computation of the steel stress at concrete peak stress, either by introducing compatibility conditions, solved by iterative process as Cusson and Paultre (1995) did, or by introducing empirical expressions as Saatcigolu and Razvi (1992) followed.
4. A plasticity model for confined concrete core introduced by Karabinis and Kiousis (1994). The shape of the confined core is based on the arching action.

Based on the reviewed models, around 50% followed the empirical approach, whereas 10% used the physical engineering approach, and the rest combined between the empirical and physical engineering approach.

According to Lokuge et al. (2005), the stress strain models can be classified as three categories:

1. Sargin (1971) based models: Martinez et al. (1984), Ahmad and Shah (1982), Eldash and Ahmad (1995) Assa et al. (2001).
2. Kent and Park (1971) based models: Sheikh and Uzumeri (1982), Saatcigolu and Razvi (1992).
3. Popovics (1973) based models: Mander et al. (1988), Cusson and Paultre (1995) and Hoshikuma et al. (1997).

Most of the confined models were developed by testing small specimens that did not simulate the real cases for the actual column, and small portion used real columns to verify their works such as Mander et al. (1988).

TABLE 2.1
Lateral Steel Confinement Models Comparison

	Long. steel	spacing	Lateral steel size	Lateral steel config.	Effective area	Section geometry	Lateral pressure	Lateral steel stress
Richart							*	
Chan	*							
Blume			*			*	*	*
Roy	*	*						
Soliman		*			*			
Sargin		*	*				*	*

	Long. steel	spacing	Lateral steel size	Lateral steel config.	Effective area	Section geometry	Lateral pressure	Lateral steel stress
Kent		*	*				*	
Vallenas	*	*	*				*	
Muguruma		*	*			*		
Scott	*	*	*				*	
Sheikh	*	*	*	*		*	*	
Ahmed		*						*
Park		*	*				*	
Martinez		*	*				*	
Fafitis		*	*			*	*	
Young	*	*	*				*	
Mander	*	*	*	*	*	*	*	*
Fujii		*	*			*	*	*
Saatcioglu	*	*	*	*	*	*	*	*
El-Dash		*	*				*	*
Cusson	*	*	*	*	*		*	*
Attard		*					*	*
Mansur		*					*	*
Fujii		*				*	*	*
Razvi	*	*	*	*	*	*	*	*
Mendis	*	*	*	*	*		*	*

	Long. steel	spacing	Lateral steel size	Lateral steel config.	Effective area	Section geometry	Lateral pressure	Lateral steel stress
Assa							*	*
Binici							*	*

Table 2.1 shows that the most successful models considering the lateral pressure determination parameters are Mander et al. (1988) that lies in the third group according to Lokuge et al. (2005) comparison and Saatcioglu and Razvi (1992), second group (Razvi and Saatcioglu (1999) was developed for high strength concrete). For the sake of comparing three models, one from each group, with the experimental results, El-Dash and Ahmad Model (1995) is selected from the first group as the model that considered most of the contributing factors, Table 2.1, compared to Attard and Setunge (1996), Mansur et al. (1997), Martinez et al. (1984) and Sargin (1971) models. However El-Dash and Ahmad model was developed for spirally confined concrete, hence, it was eliminated from Rectangular column comparison. The model selected from group 2 is Mander et al. (1988) and that chosen from group 3 is Saatcioglu and Razvi (1992) as mentioned above.

TABLE 2.2
Experimental Cases Properties

	Length (in.)	Width (in.)	Cover (in.)	Fc (ksi)	Fy (ksi)	Bars #	Bars diameter (in.)	Lateral steel diameter (in.)	Spacing (in.)	Fyh (ksi.)
Case1	19.69	Circular	0.98	4.06	42.8	12	0.63	0.47	1.61	49.3
Case2	19.69	Circular	0.98	4.2	42.8	12	0.63	0.63	3.66	44.5
Case3	17.7	17.7	0.787	3.65	57.13	8	0.945	0.394	2.83	44.8

The three models are compared with two experimental results, case 1 and case 2 for circular cross section columns, Table 2.2. All the three models are successfully capturing the ascending branch. However, Mander model is the best in expressing the descending one, Figure 2.16 and 2.17.

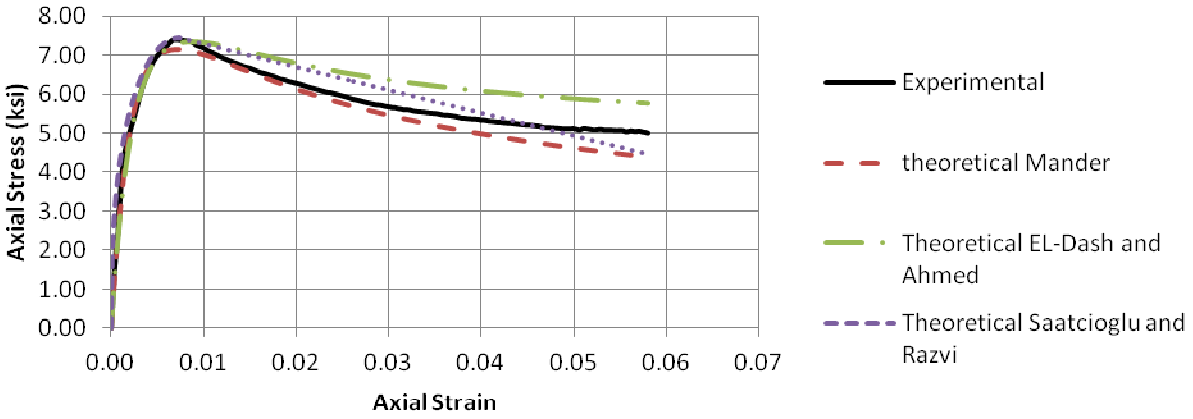

FIGURE 2.16
Mander et al. (1988), Saatcioglu and Razvi (1992) and El-Dash and Ahmad (1995) Models Compared to Case 1

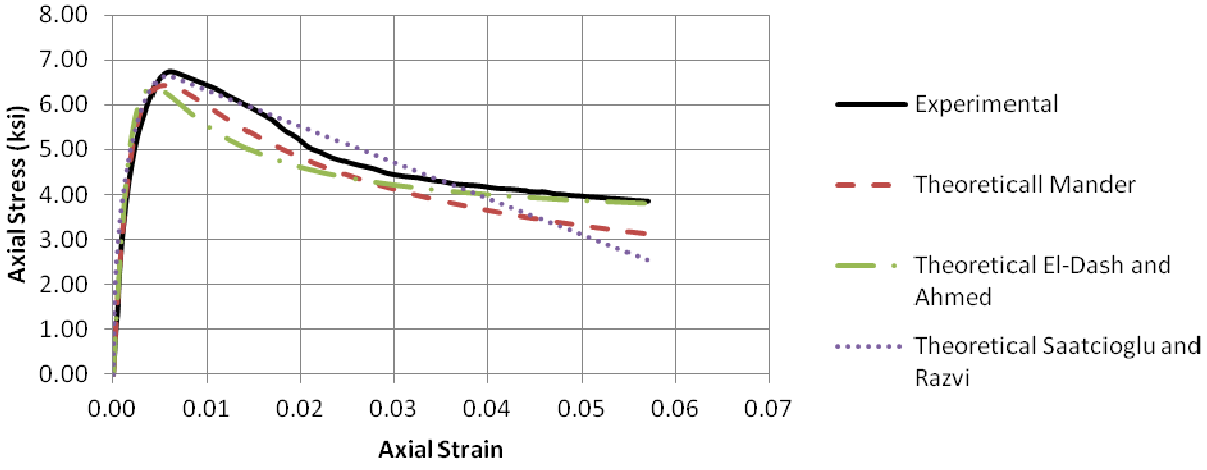

FIGURE 2.17
Mander et al. (1988), Saatcioglu and Razvi (1992) and El-Dash and Ahmad (1995) Models Compared to Case 2

For the case of rectangular column comparison, Figure 2.18, Saatcioglu and Razvi (1992) is better in capturing the ultimate compressive strength. Whereas Mander describes the softening zone better than Saatcioglu and Razvi model. Based on Table 2.1 and Figures 2.16, 2.17, and 2.18, Mander model is seen to be the best in expressing the stress strain response for circular and rectangular columns.

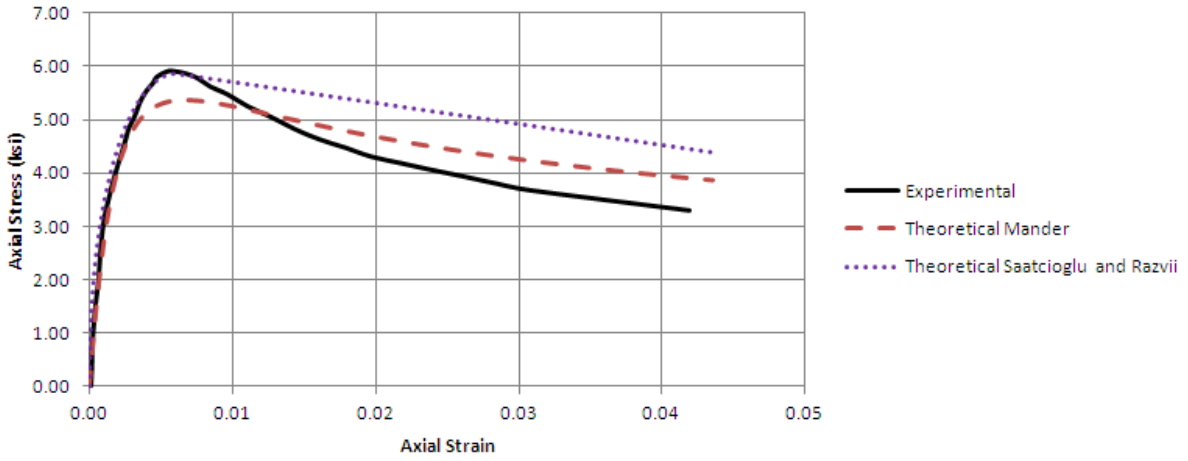

FIGURE 2.18
Mander et al. (1988), Saatcioglu and Razvi (1992) and El-Dash and Ahmad (1995) Models Compared to Case 3

2.2 Rectangular Columns Subjected to Biaxial Bending and Axial Compression

Rectangular reinforced concrete columns can be subjected to biaxial bending moments plus axial force. When the load acts on one of the cross section bending axes the problem becomes uniaxial bending. However when the load is applied eccentrically on a point that is not along any of the bending axes the case becomes biaxial bending. The biaxial bending case can be found in many structures nowadays. This case is visited extensively in the literature disregarding the confinement effect. The failure surface of rectangular columns is 3D surface consisted of many 2D interaction diagrams. Each of the 2D interaction diagrams represents one angle between the bending moment about x-axis and the resultant moment. Many simplifications are introduced to justify the compressive trapezoidal shape of concrete, due to the two bending axes existence. This section reviews the previous work concerns rectangular columns subjected to biaxial bending and axial load chronologically. Hence, the review is classified according to its author/s.

2.2.1 Past Work Review

2.2.1.1 A Study of Combined Bending and Axial Load in Reinforced Concrete Members (Hogenstad 1930)

Hogenstad classified concrete failure subjected to flexure with or without axial load to five modes

1. Failure by excessive compressive strain in the concrete with no yield in tensioned steel (compression failure).
2. Tension failure where the tensioned steel yield cause excessive strain in the concrete.
3. Balanced failure where tensioned steel yield at the same time compressive concrete fail.
4. Compression failure where the tensioned steel pass the yield stress.
5. Brittle failure caused by tensioned steel rupture after the cracks developed in the compressive concrete.
6. Hogenstad (1930) suggested designing by the ultimate failure theory in his report as opposed to the linear elastic theory (standard theory) that was widely applicable up to nearly fifty years. He discussed some of the available inelastic theories that were limited to uniaxial stress according to him. The theories discussed were E. Suenson (1912), L. Mensch (1914), H. Dyson (1922), F. Stussi (1932). C. Schreyer (1933). S. Steuermann (1933). G. Kazinczy (1933). F. Gebauer (1934) O. Baunmann (1934). E. Bittner (1935). A. Brandtzxg (1935). F. Emperger (1936). R. Saliger (1936). C. Witney (1937), USSR specifications OST 90003, (1938). V. Jensen1943. R. Chambaud (1949). Also Hognestad (1930) introduced his new theory of inelastic flexural failure. He sat equations for tension failure and compression one.

2.2.1.2 A Simple Analysis for Eccentrically Loaded Concrete Sections (Parker and Scanlon 1940)

Parker and Scanlon (1940) used elastic theory.

$$\sigma = \frac{P}{A} \pm \frac{M_x c}{I_x} \pm \frac{M_y c}{I_y}$$

Equation 2.221

They developed a procedure by first calculating stresses at the four corners, then checking if all stresses are positive, no further steps are needed, otherwise, calculating center of gravity and recalculating moment of inertia then recalculating stress and determining the new position of the neutral axis. These steps are repeated till the internal forces converge with the applied one.

2.2.1.3 Reinforced Concrete Columns Subjected to Bending about Both Principal Axes (Troxell 1941)

Troxell (1941) Suggested that portion of the applied axial load can be used with the bending moment about one axis to find the maximum compressive and tensile strength in the cross section. Then the remaining load along with the other bending moment about the other axis can be used the same way, using the method of superposition. The summation stresses are the stresses generated from the section. He also suggested taking equivalent steel area in each side to facilitate the calculation procedure.

2.2.1.4 Design Diagram for Square Concrete Columns Eccentrically Loaded in Two Directions (Anderesen 1941)

Andersen (1941) implemented a new procedure for determining maximum compressive and tensile stresses on cross sections without determining the location of the neutral axis. The limitation of this procedure that it is just applied on square cross sections and the steel has to be symmetric. Based on the linear elastic theory and the perpendicularity of the neutral axis to the plane of bending which was proven in a previous study, Andersen derived stresses coefficients equations basically for cross sections reinforced with four bars, and then represented them graphically. This derivation was set after classifying the problem into three different cases based on the neutral axis location.

$$C = \frac{c_1 + 3np(2k - \cos\theta)\cos 2\theta}{6k\cos 2\theta}$$ **Equation 2.222**

$$T = \left(1 - \frac{d}{D}\right)\frac{\cos\theta}{k} - 1$$ **Equation 2.223**

c_1 = is a coefficient that is fully determined in his paper for each case of the three cases

n = modular ratio

P = steel ratio

k = distance from apex of compression area to neutral axis divided by diagonal length θ

D= diagonal length

d = distance from corner to reinforcing bar

These two values can be substituted in the following equations to determine the maximum compressive strength and tensile strength respectively

$$f_c = \frac{P}{Ca^2}$$ **Equation 2.224**

$$f_s = nTf_c$$ **Equation 2.225**

where a is the side length of cross section and P is force magnitude.

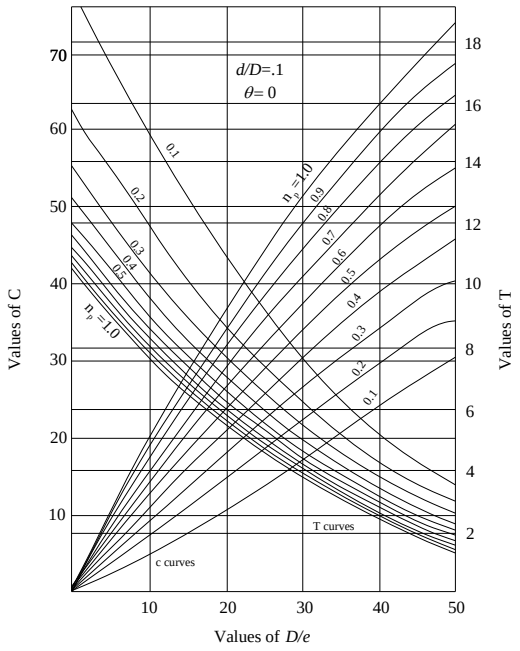

FIGURE 2.19
Relation between T and C by Andersen (1941)

Anderesen (1941) plotted graphs relating T and C; Figure 2.19. It should be noted that the graphs differ with angle θ and the ratio *d/D* variations. Andersen adapted his procedure to fit the 8 bar reinforcement, as well as 16 bar one. That was done by finding the location of the equivalent four bars in the same cross section that yields the same internal moment and moment of inertia.

2.2.1.5 Reinforced Concrete Columns under Combined Compression and Bending (Wessman 1946)

Wessman (1946) introduced algebraic method under a condition of the plane of the bending coincides with the axis of symmetry. Based on the elastic theory, Wessman (1946) found that the distance between the applied load and the neutral axis a:

$$a = \frac{I_p}{Q_p}$$

Equation 2.226

I_p = moment of inertia of the effective area with respect to the load axis

Q_p = the first moment of the effective area.

The procedure proposed has very limited applicability since it required the applied load lies on the axis of symmetry, which consider a very special case. In addition it relies on the elastic theory.

2.2.1.6 Analysis of Normal Stresses in Reinforced Concrete Section under Symmetrical Bending (Bakhoum 1948)

Using the elastic theory and equating the internal forces and moments to the applied one, Bakhoum (1948) developed procedure in locating the neutral axis. This procedure was set for uniaxial bending. He also intensified the importance of taking the tensioned concrete into account while analyzing.

$$H' = \frac{i + \alpha_1}{s + \beta_1}$$ **Equation 2.227**

$$H' = \frac{H}{t}$$ **Equation 2.228**

$$i = \frac{nI_{ps}}{bt^3}$$ **Equation 2.229**

$$s = \frac{nS_{ps}}{bt^2}$$ **Equation 2.230**

H = distance between the load and the neutral axis

N= modular ratio

b= section width

t = section height

I_{ps} = Moment of inertia of the total reinforcement steel about the line parallel to the neutral axis through the point of application of the external force.

S_{ps} = Statical moment of the total reinforcement steel about the line parallel to the neutral axis through the point of application of the external force.

The relation between α and β is plotted graphically; Figure 2.20.

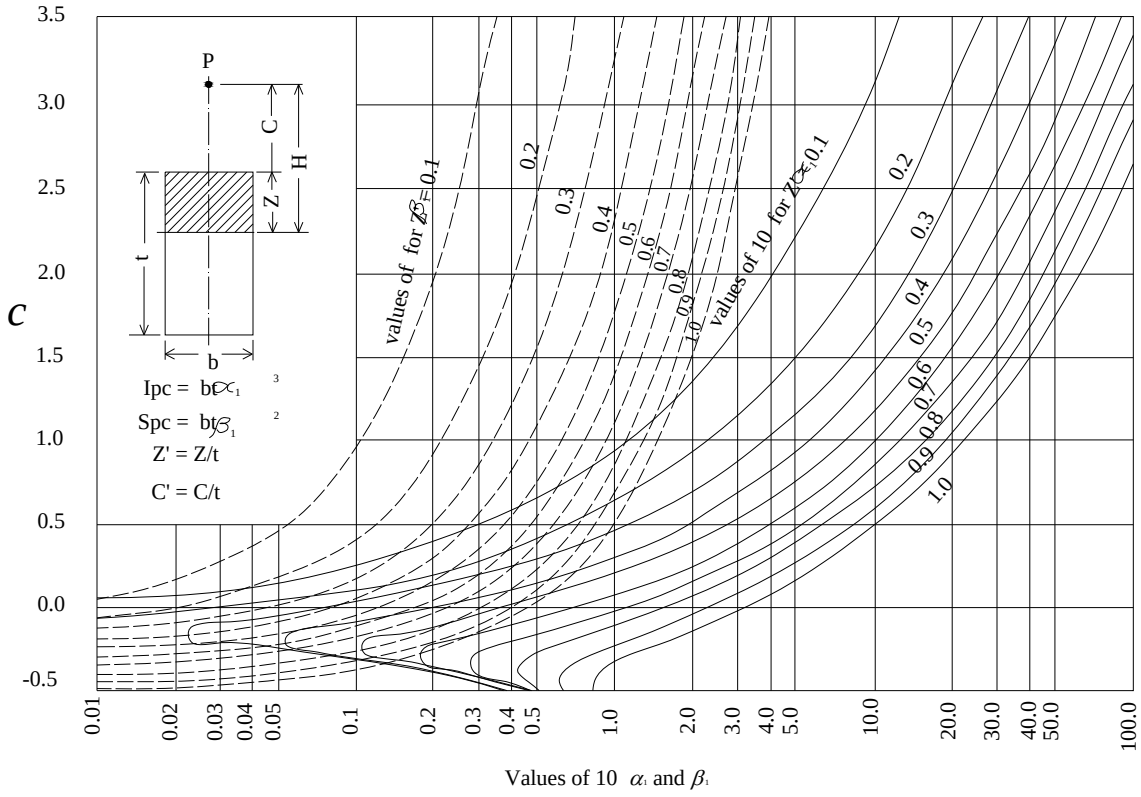

FIGURE 2.20
Relation between c and α by Bakhoum (1948)

For the case of unsymmetrical bending, Bakhoum (1948) suggested three solutions; methods of center of action of steel and concrete, product of inertia method and method of mathematical successful trial. It is noted that the first two methods are trial and error methods, and all the three methods were built on the elastic linear theory.

2.2.1.7 Design of Rectangular Tied Columns Subjected to Bending with Steel in All Faces (Cervin 1948)

The Portland cement association published “continuity in concrete frames” (third edition) that has an equation that relates the maximum load to the actual applied load and moment. It can be applied on a cross section:

$$P = N + CD\frac{M}{t}$$ **Equation 2.231**

P = total allowable axial load on column section

N= actual axial load on column section

M = moment

T = section height

$$C = \frac{f_a}{0.45 f_c^{'}}$$ **Equation 2.232**

f_a = the average allowable stress on axially loaded reinforced concrete column

$$D = \frac{t^2}{2R^2}$$ **Equation 2.233**

R = radius of gyration

This equation is limited to reinforcement on the end faces. Crevin (1948) redefined the term D in the equation to fit reinforcement in the four faces as follow

$$D = \frac{1 + (n-1)p}{0.167 + (x + yz^2)(n-1)pg^2}$$ **Equation 2.234**

$$n = \frac{E_s}{E_c}$$ **Equation 2.235**

p = reinforcement ratio

g = ratio between extremities of column steel and overall column depth

x = ratio of total column steel at one end

y = ratio of total column steel between centroid and one end

z = arm from cetroid of steel ratio y to centroid of column

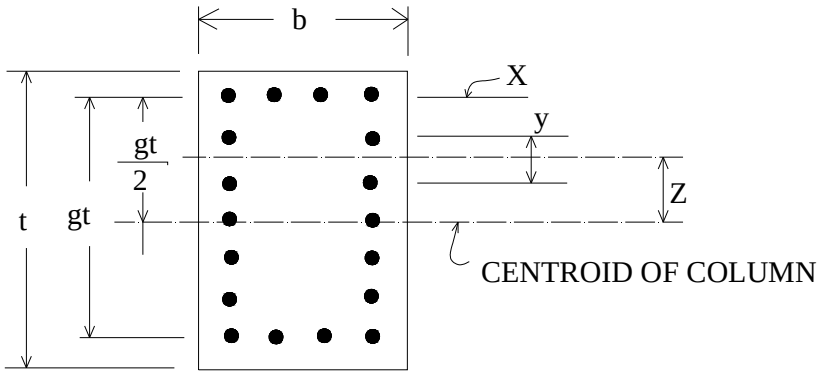

FIGURE 2.21
Geometric Dimensions in Crevin Analysis (1948)

He showed that $x+yz^2$ vary from 0.25 to 0.5. The limitation of this equation applicability is that the ratio e/t has to be less than one.

2.2.1.8 The Strength of Reinforced Concrete Members Subjected to Compression and Unsymmetrical Bending (Mikhalkin 1952)

Mikhalkin (1952) performed studies on determination of the allowable load and ultimate load of biaxially loaded rectangular members. He developed design and analysis procedure for tension and compression failure according to ultimate theory, as he generated charts for design simplification based on the elastic theory using simple compatibility equations Figure 2.22 and 2.23. These charts locate the concrete and steel centers of pressure with respect to the neutral axis.

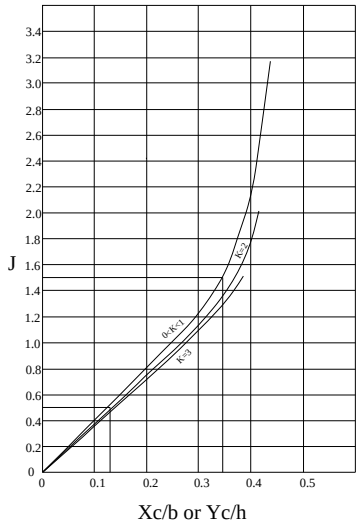

FIGURE 2.22
Concrete Center of Pressure versus Neutral Axis Location, Mikhalkin 1952

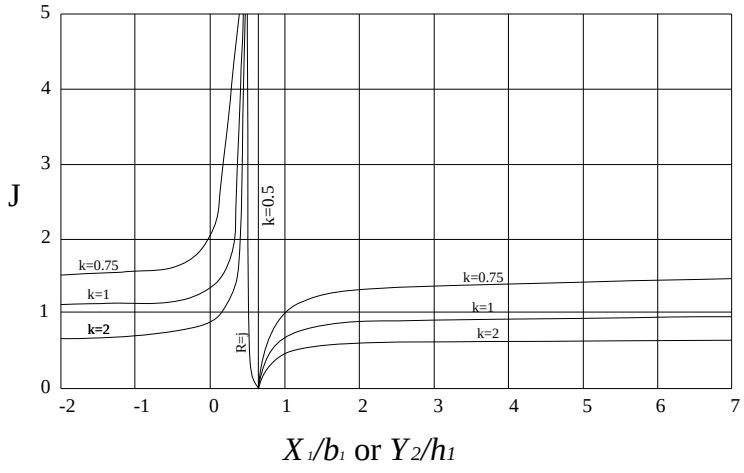

FIGURE 2.23
Steel Center of Pressure versus Neutral Axis Location, Mikhalkin 1952

2.2.1.9 Eccentric Bending in Two Directions of Rectangular Concrete Columns (Hu 1955)

Hu (1955) followed the elastic assumption in building his analysis. He showed numerically that the slope of the neutral axis for non homogeneous section can be replaced by that of homogeneous one with small error percentage. He found algebraically the equilibrium equations

$$\frac{N}{bdf_c} = \frac{chk}{6} - np\left(\frac{1}{2h} + \frac{1}{2k} - 1\right)$$ **Equation 2.236**

$$f_s = nf_c\left(1 - \frac{1-a_x}{h} - \frac{1-a_y}{k}\right)$$ **Equation 2.237**

$$\frac{N}{bdf_c} e_y\left(1+m^2\right) = \frac{chk}{6}\left[m\left(\frac{1}{2} - c_b\right) + \left(\frac{1}{2} - c_d\right)\right] + \frac{Qnp}{12k}$$ **Equation 2.238**

$$Q = \left(m^2 nq_x + nq_y\right)/(np)$$ **Equation 2.239**

N = the normal compressive force

b = section width

d = section height

f_c = maximum concrete strength

h and k define the position of the neutral axis

c, c_b, c_d coefficients (functions of h)

A_x = cover in x direction coefficient

A_b = cover in y direction coefficient

e_x = load eccentricity from the geometric centroid (in x-direction)

e_y= load eccentricity from the geometric centroid (in y-direction)

$$n = \frac{E_s}{E_c}$$ **Equation 2.240**

$$p = \frac{A_s}{A_c}$$

Equation 2.241

$$q_x = \frac{I_{sx}}{I_{cx}} \qquad q_y = \frac{I_{sy}}{I_{cy}}$$

Equation 2.242

$$m = \frac{e_x}{e_y}$$

Equation 2.243

The previous equations are plotted graphically to obtain the unkown values *k*, n/bdf'_c, Figure 2.24.

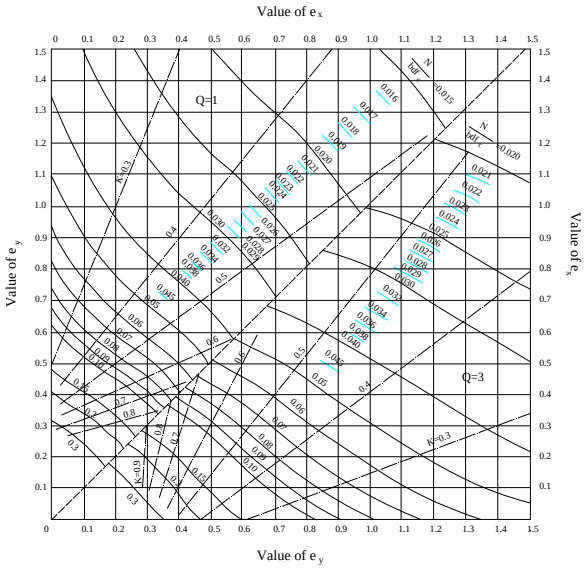

FIGURE 2.24
Bending with Normal Compressive Force Chart *np* = 0.03, Hu (1955). In His Paper the Graphs Were Plotted with Different Values of *np* 0.03,0.1 ,0.3

The first obvious interest in the ultimate strength of the structural members appeared in the first half of the past century. Prior to that, there were some designations to the importance of designing with ultimate strength. While Thullies's flexural theory (1897) and Ritter's introduction of the parabolic distribution of concrete stresses (1899) were introduced prior to the

straight line theory of Coignet and Tedesco (1900). The straight line theory became accepted due to its simplicity and the agreement with the tests' requirements that time. Coignet's theory grew widely till it was contradicted by some experimental work done on beams by Lyse, Slatter and Zipprodt in 1920's, and on columns by McMillan (1921), as the concrete's construction applicability was spreading out (ACI-ASCE committee 327(1956)). After 1950 there was a call to start working with the ultimate strength design as it was adopted in several countries in Europe and others, as the reinforced concrete design has advanced. This led the ACI-ASCE committee 327 to propose the first report on ultimate strength design in 1956 (ACI-ASCE committee 327(1956)). The committee members showed in their studies that the ultimate strength design load can be found accurately.

They defined the maximum load capacity for concentric load

$$P_o = 0.85 f_c^{'}(A_g - A_{st}) + A_{st} f_y \qquad \textbf{Equation 2.244}$$

A_g = the gross area of the section.

A_{st} = steel bars area

The committee considered minimum eccentricity value to design with. For tied columns the value was 0.1 times the section's depth.

For combined axial load and bending moment

$$P_u = 0.85 f_c^{'} b d k_u k_1 + A_s^{'} f_y - A_s f_s \qquad \textbf{Equation 2.245}$$

$$P_u e = 0.85 f_c^{'} b d^2 k_u k_1 \left(1 - \frac{k_2}{k_1} k_u k_1\right) + A_s^{'} f_y d \left(1 - \frac{d^{'}}{d}\right) \qquad \textbf{Equation 2.246}$$

P_u = axial load on the section

e = eccentricity of the axial load measured from the centroid of tensile reinforcement.

f_s = stress in the tensile reinforcement.

dk_u = distance from extreme fiber to neutral axis, where k_u is less than one

k_1 = ratio of the average compressive stress to 0.85 $f_c^{'}$, where k_1 is not greater than 0.85 and is to be reduced at the rate of 0.5 per 1000 psi for concrete strength over 5000 psi.

k_2 = ratio of distance between extreme fiber and resultant of compressive stresses to distance between extreme fiber and the neutral axis.

$\frac{k_2}{k_1}$ should not be taken less than 0.5.

After ultimate strength design was released, the ACI committee 318 in their "Building code requirements for reinforced concrete (ACI 318-56)" approved the usage of the ultimate strength method for designing reinforced concrete members along with the standard method in 1956. They conditioned that:

$$\frac{f_a}{F_a}+\frac{f_{bz}}{F_b}+\frac{f_{by}}{F_b}\le 1$$ **Equation 2.247**

Given that the ratio *e/t* does not exceed 2/3 where

f_{by} = the bending moment about y-axis divided by section modulus of the transformed section relative to y-axis.

f_{bz} = the bending moment about y-axis divided by section modulus of the transformed section relative to y-axis.

e = eccentricity of the load measured from the geometric centroid

t = overall depth of the column

f_a = nominal axial unit stress.

f_b = allowable bending unit stress = $0.8*\left(0.225 f_c^{'} + f_s p_g\right)$

p_g = steel ratio to the gross area.

f_s = nominal allowable stress in reinforcement.

2.2.1.10 Guide for Ultimate Strength Design of Reinforced Concrete (Whitney and Cohen 1957)

Following this massive change in paradigm, Charles Whitney and Edward Cohen released their paper " guide for ultimate strength design of reinforced concrete" which served as

a supplement to the ACI building code (318-56). They suggested a linear relationship between the case of the pure bending and that of concentric load in the following equation

$$\frac{M_u}{M_o} = \frac{P_o - P_u}{P_o}$$ **Equation 2.248**

M_u = total moment of the plastic centroid of the section.

P_o = ultimate direct load capacity for a concentrically loaded short column.

P_u = ultimate direct load capacity for an eccentrically loaded short column.

M_o = the moment capacity without thrust as controlled by compressin assuming enough tensile steel to develop it in full and it is equal to

$$M_o = 0.333bd^2 f_c^{'} + A_s^{'} f_y^{'}\left(d - d^{'}\right)$$ **Equation 2.249**

They limited the maximum moment allowed for design to M_u using the following equation

$$\frac{M_u}{bd^2} = 0.306 f_c^{'} + p^{'} f_y^{'}\left(1 - \frac{d^{'}}{d}\right)$$ **Equation 2.250**

$$f_y^{'} = f_y - 0.85 f_c^{'}$$ **Equation 2.251**

$$p^{'} = A_s^{'} / bd$$ **Equation 2.252**

$A_s^{'}$ = compressive steel area.

d = distance from extreme compressive fiber to centroid of tension force in tensile reinforcement.

d' = distance from extreme compressive fiber to centroid of tension force in compressive reinforcement.

b = column width.

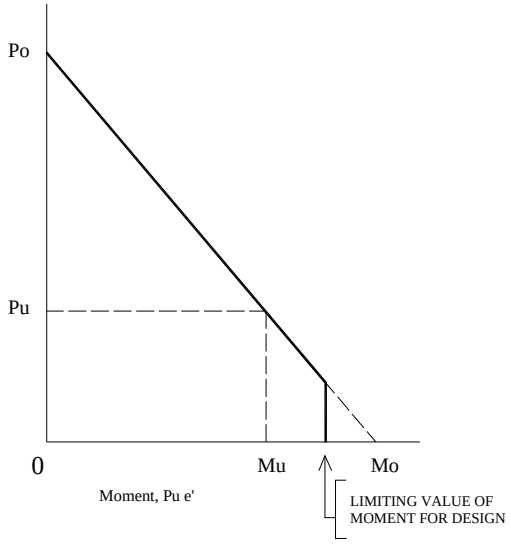

FIGURE 2.25
Linear Relationship between Axial Load and Moment for Compression Failure Whitney and Cohen 1957

2.2.1.11 Ultimate Strength Design of Rectangular Concrete Members Subjected to Unsymmetrical Bending (Au 1958)

Au (1958) generated charts to calculate the equivalent compressive depth of the stress block based on assumed values of section's dimensions and bars arrangements. The design equations were created complying with the ACI-ASCE assumptions.

He showed that when a member is subjected to compressive force as well as bending, the section can be controlled either by tension or compression failure depending on the magnitude of eccentricities.

His procedure is to first approximate the location of the neutral axis that can be made by observing that the applied load, the resultant of the tensile force in steel and the resultant of the compressive forces in compressive steel and concrete must all lie in the same plane. This classifies the problem as one of the three cases:

1. Neutral axis intersects with two opposite sides
2. Neutral axis intersects with two adjacent sides forming a compression zone bigger than half of the cross sectional area

3. Neutral axis intersects with two adjacent sides forming a compression zone smaller than half of the cross sectional area

Equilibrium equations plus compatibility equations are needed when the section is controlled by compression (concrete crush). Whereas, equilibrium equations are sufficient in tension controlled cases. Tung specified two conditions based on ACI-ASCE report, that are the average stress f_s is assigned to each tensioned bar and the resultant tensile force is considered the tensile bar group centroid. Based on that, the bars close to the neutral axis are ignored in computations. Having equilibrium equations, Tung denoted six dimensionless variables, two for each case of the three cases mentioned above and plotted charts relating each two associated variables Figures 2.26, 2.27, and 2.28. The charts generated have an output of determining the neutral axis position. The dimensionless variables utilized are:

$$c_1 = \left(\frac{t}{d_y}\right)^2 \left[- p' m' \left(\frac{d_y}{t} - \frac{d'_y}{t}\right) + \frac{P_u}{0.85 f'_c bt} \left(\frac{r_y}{t} + \frac{e'_y}{t}\right)\right] \quad \textbf{Equation 2.253}$$

$$c_2 = \left(\frac{t}{d_y}\right) \left[- p' m' \left(\frac{d_x}{b} - \frac{d'_x}{b}\right) + \frac{P_u}{0.85 f'_c bt} \left(\frac{r_x}{b} + \frac{e'_x}{b}\right)\right] \quad \textbf{Equation 2.254}$$

$$Q_1 = \left(\frac{2bt^2}{d_x d_y^2}\right) \left[p' m' \left(\frac{d_y}{t} - \frac{d'_y}{t}\right) - \frac{P_u}{0.85 f'_c bt} \left(\frac{r_y}{t} + \frac{e'_y}{t}\right)\right] \quad \textbf{Equation 2.255}$$

$$Q_2 = \left(\frac{2b^2 t}{d_x^2 d_y}\right) \left[p' m' \left(\frac{d_x}{b} - \frac{d'_x}{b}\right) - \frac{P_u}{0.85 f'_c bt} \left(\frac{r_x}{b} + \frac{e'_x}{b}\right)\right] \quad \textbf{Equation 2.256}$$

$$U_1 = \frac{r_y}{t} - p' m' \left(\frac{d_y}{t} - \frac{d'_y}{t}\right) + \frac{P_u}{0.85 f'_c bt} \left(\frac{r_y}{t} + \frac{e'_y}{t}\right) \quad \textbf{Equation 2.257}$$

$$U_2 = \frac{r_x}{b} - p' m' \left(\frac{d_x}{b} - \frac{d'_x}{b}\right) + \frac{P_u}{0.85 f'_c bt} \left(\frac{r_x}{b} + \frac{e'_x}{b}\right) \quad \textbf{Equation 2.258}$$

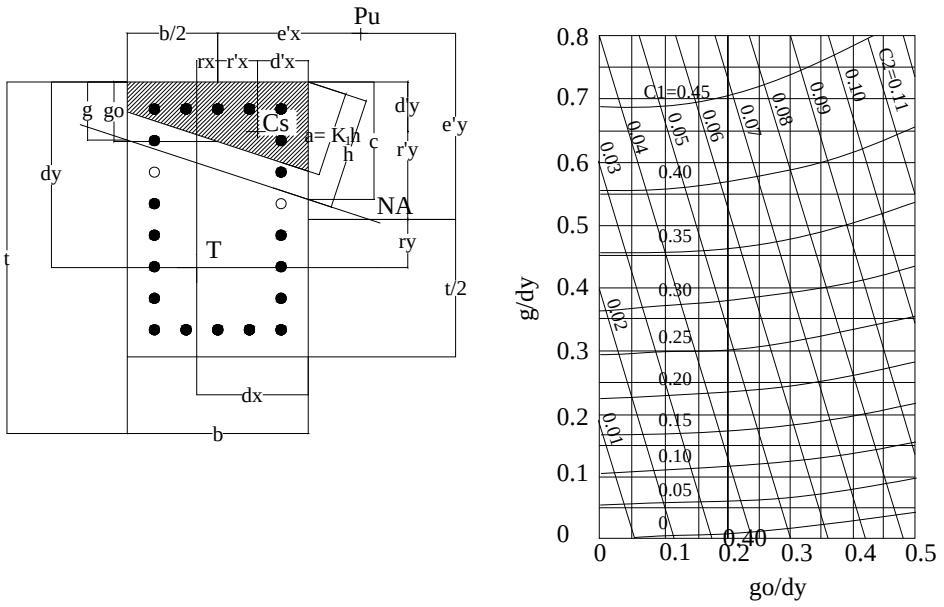

FIGURE 2.26
Section and Design Chart for Case 1(rx/b = 0.005), Au (1958)

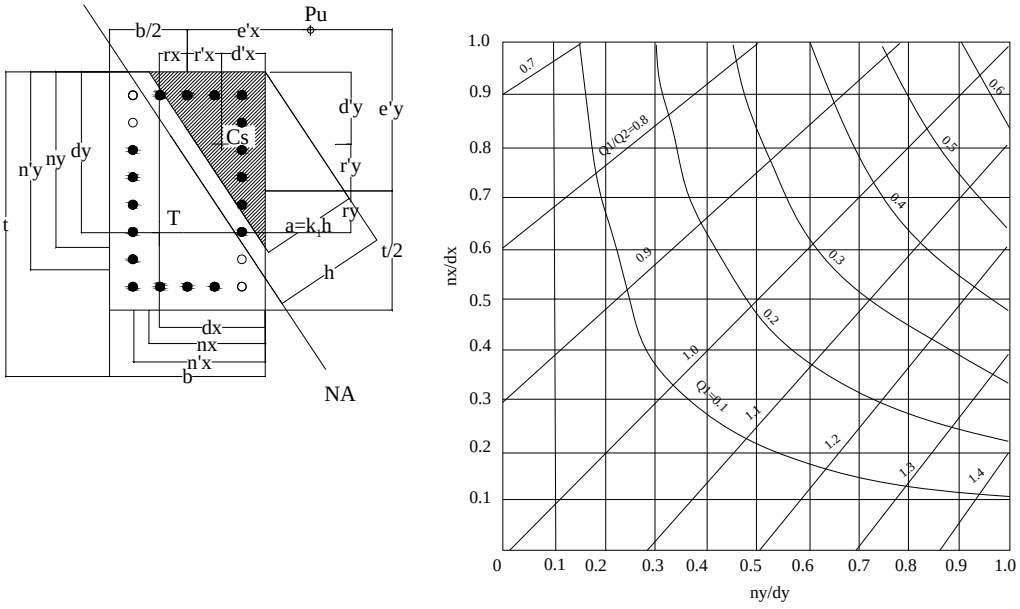

FIGURE 2.27
Section and Design Chart for Case 2, Au (1958)

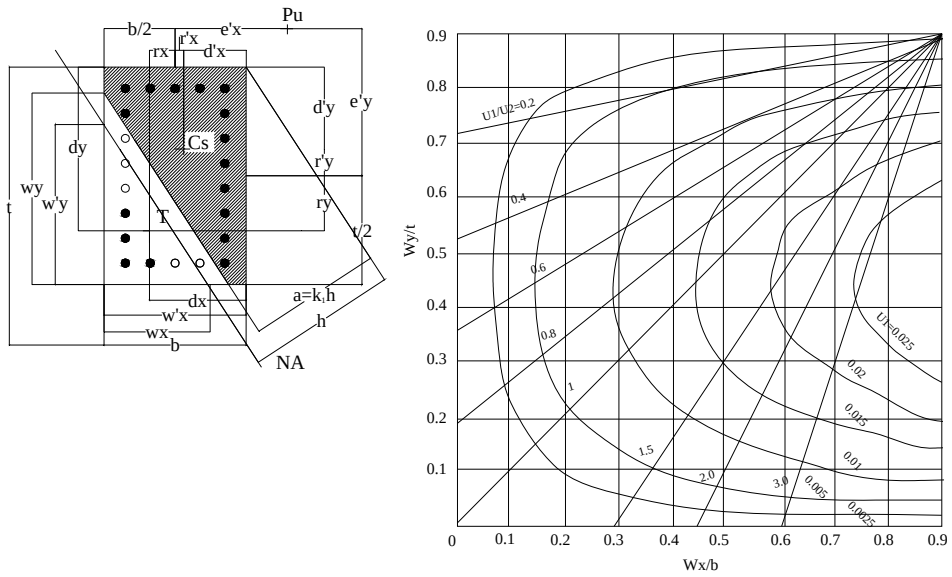

FIGURE 2.28
Section and Design Chart for Case 3(d_x/b = 0.7, d_y/t = 0. 7), Au (1958)

t = total depth of rectangular section

d_y = distance from extreme compressive corner to centroid of tensile reinforcement measured in the direction of y-axis

$p' = A'_s/bt$

b = width of rectangular section

$m' = m-1$, $m = f_y/0.85f'_c$

d'_y = distance from extreme compressive corner to centroid of compressive reinforcement measured in the direction of y-axis.

P_u = ultimate direct load capacity for the member subject to bending in two directions

r_y = distance from centroid of tensile reinforcement to x'-axis.

r_x = distance from centroid of tensile reinforcement to y'-axis.

e'_y = eccentricity of ultimate direct load measured from centroid of rectangular section in the direction of y-axis

d'_x = distance from extreme compressive corner to centroid of compressive reinforcement measured in the direction of x-axis

d_x = distance from extreme compressive corner to centroid of tensile reinforcement measured in the direction of x-axis

e'_x = eccentricity of ultimate direct load measured from centroid of rectangular section in the direction of x-axis.

2.2.1.12 Design of Symmetrical Columns with Small Eccentricities in One or Two Directions (Wiesinger 1958)

Using the section moment of inertia and the section modulus, Wiesinger (1957) introduced a new designing equation for the gross sectional area required by design for columns subjected to small eccentricities in one direction or two. Wiesinger (1957) proposed gross section equation:

$$A_g = \frac{N}{Q\left[0.225 f_c^{'} + f_s p_g\right]} + \frac{Ne^{'}/t}{F_b\left[\alpha_g + \alpha_s (n-1) g^2 p_g\right]}$$

Equation 2.259

and the capacity of a given column is calculated using the following equation

$$N = \frac{1}{\frac{1}{Q\left[0.225 f_c^{'} + f_s p_g\right]} + \frac{e^{'}/t}{F_b\left[\alpha_g + \alpha_s (n-1) g^2 p_g\right]}}$$

Equation 2.260

$$\alpha_g = \frac{2I_g}{t^2 A_g}$$

Equation 2.261

$$\alpha_s = \frac{2I_s}{(gt)^2 A_s}$$

Equation 2.262

A_g = gross area

A_s= Steel area

t = column length in the direction of bending

I_g= gross moment of inertia in the bending direction

I_s= moment of inertia of steel in the bending direction

e' = eccentricity of the resultant load measured to center of gravity

N= applied axial load

Q= reduction factor = 0.8 for short tied column

$p_g = A_s/A_g$

F_b= allowable bending unit stress that is permitted if bending stress existed = 0.45 f'_c

G = center to center steel in the direction of bending divided by column length in the direction of bending

2.2.1.13 Biaxially Loaded Reinforced Concrete Columns (Chu and Pabarcius 1958)

In 1958 Chu and Pabarcius introduced a new numerical procedure to determine the actual stresses for a give section. Their procedure was based on the inelastic theory showed earlier by Hogenstad. Initially, they assumed the cross section is in the elastic range, and assumed a location for the neutral axis. Then used the following formula that was found by Hardy Cross (1930), to solve for stresses

$$f = \frac{P''}{A_E} + \frac{M''_{oy} - M''_{ox}\frac{I_{oxy}}{I_{ox}}}{I_{oy} - \frac{I_{oxy}^2}{I_{ox}}} X + \frac{M''_{ox} - M''_{oy}\frac{I_{oxy}}{I_{ox}}}{I_{ox} - \frac{I_{oxy}^2}{I_{oy}}} Y$$

Equation 2.263

f = stress

A_e = Area of the elastic portion.

I_{ox} = moment of inertia about x-axis

I_{oy} = moment of inertia about y axis

I_{oxy} = product of inertia

M''_{oy} =moment of the elastic portion about the y axis

M''_{ox} =moment of the elastic portion about the x axis

P'' = axial force taken by the elastic portion.

If the concrete and steel stresses lie in the elastic range, the above equation was used to locate a new position for the neutral axis, and comparing it with the assumed one. The whole process is repeated till the position of the calculated neutral axis coincides with the assumed one. On the other hand if any of the concrete or steel are beyond the elastic range, the plastic load and moments are calculating, then deducted from the total load and moments. The reminder is used, as the elastic portion of the load, to locate the neutral axis.

2.2.1.14 Design Criteria for Reinforced Columns under Axial Load and Biaxial Bending (Bresler 1960)

Bresler (1960) proposed a new approach of approximations of the failure surface in two different forms. He showed the magnitude of the failure load is a function of primary factors; column dimensions, steel reinforcement, stress-strain curves and secondary factors; concrete cover, lateral ties arrangement. He introduced two different methods. The first method named reciprocal load method

$$\frac{1}{P_i} = \frac{1}{P_x} + \frac{1}{P_y} - \frac{1}{P_o}$$

Equation 2.264

P_i =approximation of P_u

P_x = load carrying capacity in compression with uniaxial eccentricity x.

P_y = load carrying capacity in compression with uniaxial eccentricity y.

P_u = load carrying capacity under pure axial compression

The second method is the load contour

$$\left(\frac{M_x}{M_{xo}}\right)^{\alpha} + \left(\frac{M_y}{M_{yo}}\right)^{\beta} = 1$$

Equation 2.265

and this can be simplified to

$$\left(\frac{y}{y_o}\right)^{\alpha}+\left(\frac{x}{x_o}\right)^{\beta}=1$$

Equation 2.266

By equating α and β for more simplification the interaction diagram can be plotted as shown in Figure 2.31 Bresler (1960) well correlated Equation 2.270 to experimental studies formed from eight columns, and analytically showed the strength criteria can be approximated by

$$\left(\frac{y}{y_o}\right)^{\alpha}+\left(\frac{x}{x_o}\right)^{\alpha}=1$$

Equation 2.267

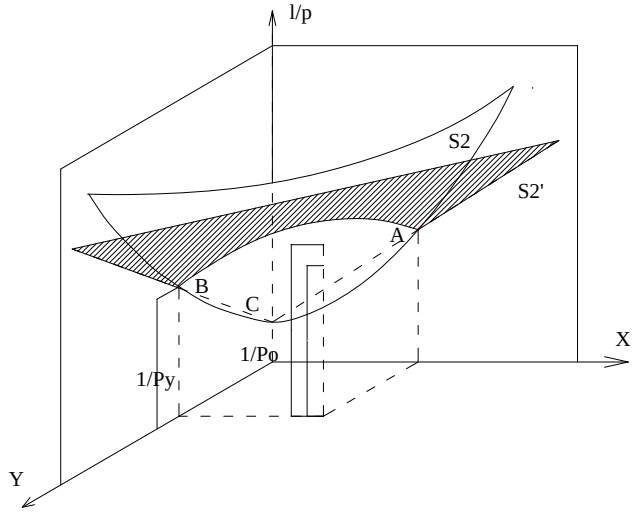

FIGURE 2.29
Graphical Representation of Method One by Bresler (1960)

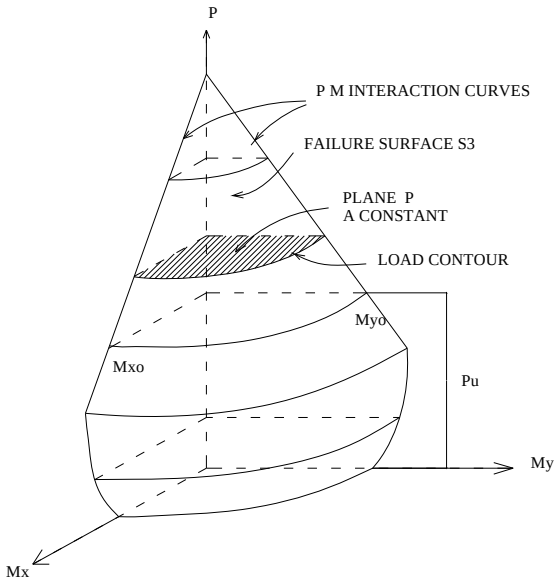

FIGURE 2.30
Graphical Representation of Method Two by Bresler (1960)

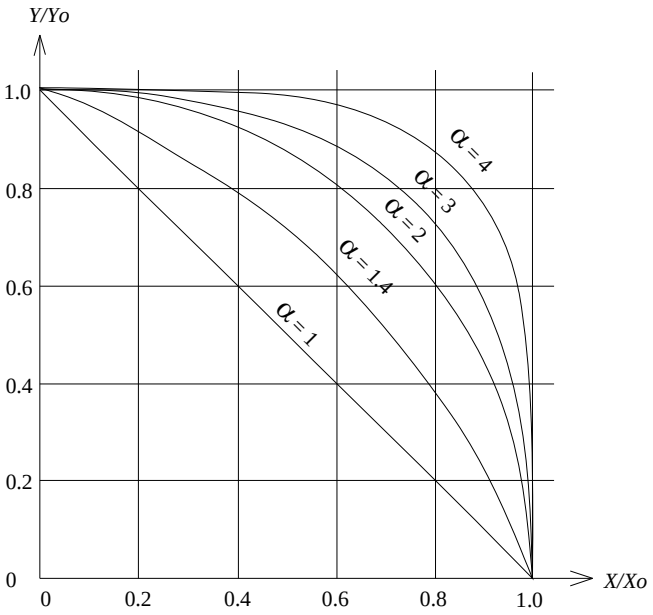

FIGURE 2.31
Interaction Curves Generated from Equating α and by Bresler (1960)

2.2.1.15 Rectangular Concrete Stress Distribution in Ultimate Strength Design (Mattock and Kritz 1961)

Mattock and Kritz (1961) determined five cases for the position of the neutral axis with respect to the rectangular cross section; when the neutral axis cut through two adjacent sides with small and big compression zone, the neutral axis intersect with the section length or width and when it lies outside the cross section. They implemented formulas for calculating the position of the neutral axis based on the load and moment equilibrium and the geometry of the compression zone.

2.2.1.16 Square Columns with Double Eccentricities Solved by Numerical Methods (Ang 1961)

Ang (1961) introduced a numerical method to solve the problem. He proposed iterative process to find equilibrium between internal forces and applied ones, by assuming a position for the neutral axis. The location of the neutral axis kept changing till equilibrium. However, he calculated stresses based on Bernoulli's plane theorem which was built upon straight line theory (elastic theory). The stress of the extreme compression fiber was approximately calculated according to the specification of AASHTO 1957 "Standard specifications for highway bridges".

2.2.1.17 Ultimate Strength of Square Columns under Biaxially Eccentric Load (Furlong 1961)

Furlong (1961) analyzed square columns that have equal reinforcement in the four sides and reinforcement in two sides only, to visualize the behavior of rectangular columns that has unsymmetrical bending axis. He used a series of parallel neutral axis with the crushing ultimate strain of 0.003 at one of the section corners to develop a full interaction diagram at one angle. And by using different angles and locations of the neutral axis a full 3D interaction surface can be developed. He was the first to introduce this procedure. Furlong (1961) concluded that the minimum capacity of a square column, having equal amount of steel in all sides, exists when the load causes bending about an axis of 45 degree from a major axis. He also concluded that

$$\left(\frac{m_x}{M_x}\right)^2+\left(\frac{m_y}{M_y}\right)^2<1$$

Equation 2.268

M_x = moment component in direction of major axis.

M_y = moment component in direction of minor axis.

M_x = moment capacity when the load acts along the major axis.

M_y= moment capacity when the load acts along the minor axis.

2.2.1.18 Tie Requirements for Reinforced Concrete Columns (Bresler and Gilbert 1961)

Bresler (1961) introduced the importance of the tie confinement in columns as objects to hold the longitudinal bars in place and prevent them from buckling after the cover spalling off. No concrete strength improvement was discussed.

2.2.1.19 Analytical Approach to Biaxial Eccentricity (Czerniak 1962)

Czerniak (1962) proved that the slope of the neutral axis is depending on the relative magnitude of moment about the *X* axis to the moment about the *Y* axis and the geometry of the sections and it is independent of the magnitude of bending moment and the applied force for the elastic range. According to the effective compressive concrete, Czerniak (1962) determined five cases based on the location of the neutral axis, Figure 2.44.

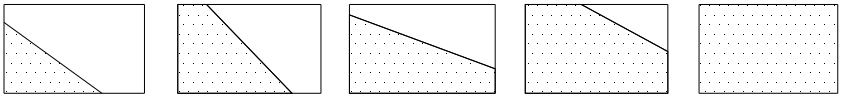

FIGURE 2.32
Five Cases for the Compression Zone Based on the Neutral Axis Location Czerniak (1962)

He developed an iterative procedure for locating the neutral axis position for a given cross section, by using equations 2.272 and 2.273 to determine the initial position of the neutral axis

$$a = \frac{\left(I_{xy} - Y_p Q_{oy}\right)\left(I_{xy} - X_p Q_{ox}\right) - \left(I_{ox} - Y_p Q_{ox}\right)\left(I_{oy} - X_p Q_{oy}\right)}{\left(Q_{ox} - Y_p A\right)\left(I_{xy} - X_p Q_{ox}\right) - \left(Q_{oy} - X_p A\right)\left(I_{ox} - Y_p Q_{ox}\right)} \qquad \textbf{Equation 2.269}$$

$$b = \frac{\left(I_{xy} - Y_p Q_{oy}\right)\left(I_{xy} - X_p Q_{ox}\right) - \left(I_{ox} - Y_p Q_{ox}\right)\left(I_{oy} - X_p Q_{oy}\right)}{\left(Q_{ox} - X_p A\right)\left(I_{xy} - Y_p Q_{oy}\right) - \left(Q_{ox} - Y_p A\right)\left(I_{oy} - X_p Q_{oy}\right)}$$

Equation 2.270

a = x-intercept of the neutral axis line

b = y-intercept of the neutral axis line

I_{xy} = elastic product of inertia of the area about the origin

I_{ox} =elastic moment of inertia of the area about the x-axis

I_{oy} =elastic moment of inertia of the area about the y-axis

Q_{ox} = moment area about x-axis (within elastic region)

Q_{oy} = moment area about y-axis (within elastic region)

A = area of transformed section (within elastic regions)

Y_p = y-coordinate of the applied eccentric load

X_p = x-coordinate of the applied eccentric load

then calculating the new section properties, effective concrete and transformed steel, and finding the new values of X_p and Y_p.

$$Y_p = \frac{\left(\bar{y} - \frac{r_{xy}^2}{a} - \frac{r_{ox}^2}{b}\right)}{\left(1 - \frac{\bar{x}}{a} - \frac{\bar{y}}{b}\right)}$$

Equation 2.271

$$X_p = \frac{\left(\bar{x} - \frac{r_{oy}^2}{a} - \frac{r_{xy}^2}{b}\right)}{\left(1 - \frac{\bar{x}}{a} - \frac{\bar{y}}{b}\right)}$$

Equation 2.272

and solving for a, b again and repeat the procedure up till convergence.

As for ultimate strength design, Czerniak (1962) proved with some simplification that the neutral axis is parallel to concrete plastic compression line and steel plastic tension and

compression line, so they can be found by multiplying the location of the neutral axis by some values. The ultimate eccentric load and its moment about x and y axis can be found from:

$$P_u = f_o\left[A_u^{'} - \frac{Q_{oy}}{a} - \frac{Q_{ox}}{b}\right]$$ **Equation 2.273**

$$M_{ux} = f_o\left[Q_{ux}^{'} - \frac{I_{xy}}{a} - \frac{I_{ox}}{b}\right] = P_u Y_p$$ **Equation 2.274**

$$M_{uy} = f_o\left[Q_{uy}^{'} - \frac{I_{oy}}{a} - \frac{I_{xy}}{b}\right] = P_u X_p$$ **Equation 2.275**

$$Q_{ux}^{'} = Q_{ox} + \alpha\left[Q_{xc} + (m-1)Q_{xs}^{'} - mQ_{xs}\right]$$ **Equation 2.276**

$$Q_{uy}^{'} = Q_{oy} + \alpha\left[Q_{yc} + (m-1)Q_{ys}^{'} - mQ_{ys}\right]$$ **Equation 2.277**

f_o = stress intensity at the origin

and the x-axis and y-axis intercept of the neutral axis are found:

$$a = \frac{\left(I_{xy} - Y_p Q_{oy}\right)\left(I_{xy} - X_p Q_{ox}\right) - \left(I_{ox} - Y_p Q_{ox}\right)\left(I_{oy} - X_p Q_{oy}\right)}{\left(Q_{ux}^{'} - Y_p A_u^{'}\right)\left(I_{xy} - X_p P_{ox}\right) - \left(Q_{uy}^{'} - X_p A_u^{'}\right)\left(I_{ox} - Y_p Q_{ox}\right)}$$ **Equation 2.278**

$$b = \frac{\left(I_{xy} - Y_p Q_{oy}\right)\left(I_{xy} - X_p Q_{ox}\right) - \left(I_{ox} - Y_p Q_{ox}\right)\left(I_{oy} - X_p Q_{oy}\right)}{\left(Q_{uy}^{'} - X_p A_u\right)\left(I_{xy} - Y_p Q_{oy}\right) - \left(Q_{ux}^{'} - Y_p A_u^{'}\right)\left(I_{oy} - X_p Q_{oy}\right)}$$ **Equation 2.279**

where

$$A_u^{'} = A + \frac{f_c^{''}}{f_o}\left[A_{uc} + (m-1)A_{us}^{'} - mA_{us}\right]$$ **Equation 2.280**

$$Q'_{ux} = Q_{ox} + \frac{f''_c}{f_o}\left[Q_{xc} + (m-1)Q'_{xs} - mQ_{xs}\right]$$

Equation 2.281

$$Q'_{uy} = Q_{oy} + \frac{f''_c}{f_o}\left[Q_{yc} + (m-1)Q'_{ys} - mQ_{ys}\right]$$

Equation 2.282

Q_{xc} = moment of area about x-axis of the plastic portion of the concrete effective section

Q_{yc} = moment of area about y-axis of the plastic portion of the concrete effective section

Q_{xs} = moment of area about x-axis of the plastic portion of the yielded tensile reinforcement

Q_{ys} = moment of area about y-axis of the plastic portion of the yielded tensile reinforcement

Q'_{xs} = moment of area about x-axis of the plastic portion of the yielded compressive reinforcement

Q'_{ys} = moment of area about y-axis of the plastic portion of the yielded compressive reinforcement

A'_u = equivalent plastic transformed area.

A_{uc} = area of concrete under plastic compression

A_{us} = area of yielded tensile reinforcement

A'_{us} = area of yielded compressive reinforcement.

P_u = ultimate strength of eccentrically loaded cross section

M_{ux} = moment of the ultimate load about x-Axis

M_{uy} = moment of the ultimate load about y-Axis

f''_c = maximum concrete stress at ultimate loads (assumed as 0.85 f'_c)

$m = \frac{f_y}{f''_c}$

2.2.1.20 Failure Surfaces for Members in Compression and Biaxial Bending (Pannell 1963)

Pannell implemented a relation between the failure moment about y-axis for a given load and the *y* component of radial moment with the same load. The formula was found based on deviation study between the actual load contour curve and an imaginary curve found from the revolution of the failure point about y axis, with the same load, about the z axis. The equation found for sections that have equal steel in each face:

$$M_{fy} = \frac{M_y}{1 - N \sin^2 2\theta}$$

Equation 2.283

$$N = 1 - \frac{M_d}{M_{fy}}$$

Equation 2.284

M_{fy} = failure moment for some load in plane y

θ = angle between y and the transformed failure plane

He showed that his formula is more accurate and conservative than that of Bresler. He also developed a chart for N for unequal steel distribution; Figure 2.33.

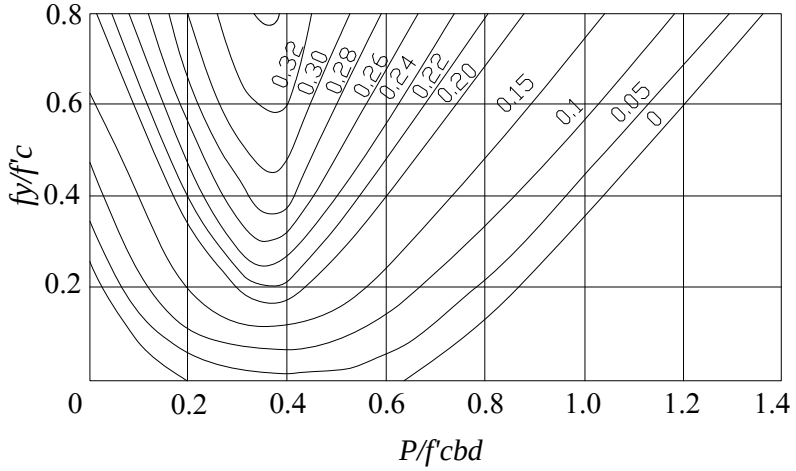

FIGURE 2.33
Values for N for Unequal Steel Distribution by Pannell (1963)

2.2.1.21 Ultimate Strength of Column with Biaxially Eccentric Load (Meek 1963)

Meek (1963) assumed constant ratio of moment about the x-axis and the y-axis. Consequently, increasing the force will increase the moment proportionally.

$$\frac{M_y}{M_x} = \frac{e_x}{e_y} = \alpha = const.$$

Equation 2.285

Using the above relation a location of the neutral axis is selected. Then this location is adjusted until the following relation is satisfied

$$P_u = \sum A_c f_c + \sum A_{sc} f_{sc} - \sum A_{st} f_{st}$$

Equation 2.286

He also showed set of experimental points correlated well to the theoritical interaction diagram developed.

2.2.1.22 Biaxial Eccentricities in Ultimate Load Design (Aas-Jakobsen 1964)

To comply with local design code, Aas-jakbosen (1964) replaced biaxially eccentric load acts on a regtangular cross section with an equivelant load acts on the main axis of symmetry with an equivelant moment. He showed , using moment and force equilibrium, that the eqivelant moment M_e:

$$M_e = \left(Pe_x + cM_1\right)m$$

Equation 2.287

$$c = \frac{e_y t_x}{e_x t_y}$$

Equation 2.288

$$m = \sqrt{1 + c^2}$$

Equation 2.289

The moment M_1 is small additional moment depends on failure mode and some other factors. And in most cases it is equal to zero.

2.2.1.23 Design of Columns Subjected to Biaxial Bending (Fleming and Werner 1965)

Fleming and Werner (1965) utilized the formulas found by Mattock (1961) for locating the neutral axis in the different cases of the compression zone shape along with Furlong (1961) method, by varying the location and inclination angle of the neutral axis, to plot the interaction diagram. Fleming and Werner (1965) plotted dimensionless interaction diagram for a square cross section for fourteen cases using parameters that is commonly used.

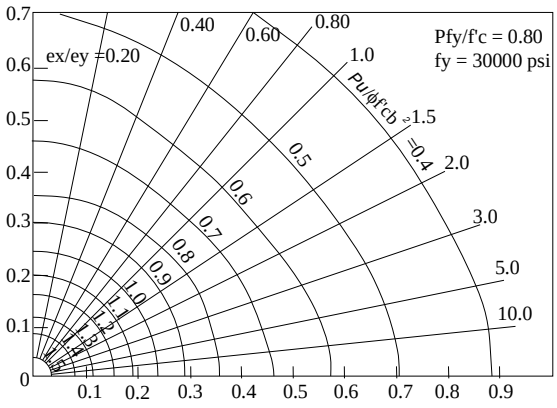

FIGURE 2.34
Design Curve by Fleming et al. (1961)

2.2.1.24 Investigation of the Ultimate Strength of Square and Rectangular Column under Biaxially Eccentric Loads (Ramamurthy 1966)

Ramamurthy (1966) proposed a new method for defining the load contour for sections having eight or more bars distributed evenly. He mentioned that the available methods of design of biaxially loaded column are trial and error procedure and determination of ultimate load from failure surface. He showed that columns containing four bars behave differently than those containing eight or more bars with the same reinforcement ratio. He found theoretically for square columns that the neutral axis inclination angle and the angle formed between the load ray

and y-axis are almost equal. And the relation between the moment and the moment about x-axis in any load contour level is equal to

$$M_{ux} = M_{uxo}\left(1-\sin^3\theta\right)$$ **Equation 2.290**

M_{ux} =ultimate moment about x-Axis

M_{uxo} = uniaxial moment on the same load contour of M_{ux}

θ = inclination of the neutral axis to x-axis angle

Equation 2.293 can be simplified to

$$M_u = M_{uxo}\left(1-\sin^3\alpha\right)\sec\alpha$$ **Equation 2.291**

M_u =ultimate radial load about z axis

and with plotting the previous equation against some actual load contour he found the following relation is more accurate especially for small angle (α)

$$M_u = M_{uxo}\left(1-0.1\frac{\alpha}{45}\right)$$ **Equation 2.292**

Similarly for rectangular columns, by finding the transformed shape of the rectangular interaction diagram to the square ones using some similar triangles calculations

$$M_u = M_{uxo}\left(1-0.1\frac{\beta}{45}\right)\sqrt{\cos^2\beta+\frac{\sin^2\beta}{K^2}}$$ **Equation 2.293**

β = transformed equivalent angle of α

K = transformation factor equal to $= \dfrac{M_{uxo}}{M_{uyo}}$

Also he showed that the upper equation is in good comparison with experimental actual load contour. He plotted the relation between θ and α for different ratios of length to width for rectangular columns.

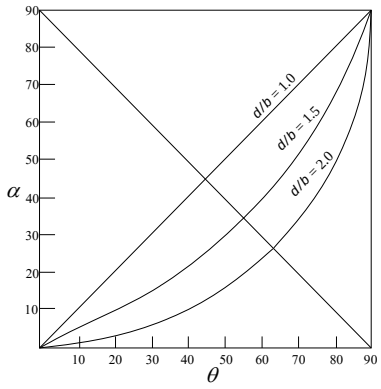

FIGURE 2.35
Relation between α and θ
by Ramamurthy (1966)

2.2.1.25 Capacity of Reinforced Rectangular Columns Subjected to Biaxial Bending (Parme, Nieves, and Gouwens 1966)

Parme *et.al* (1966). suggested relating the biaxial bending to the uniaxial resistance. They restated Bresler equation

$$\left(\frac{M_x}{M_{ux}}\right)^{\frac{\log 0.5}{\log \beta}} + \left(\frac{M_y}{M_{uy}}\right)^{\frac{\log 0.5}{\log \beta}} = 1$$

Equation 2.294

M_x = uniaxial ultimate moment capacity about x-axis

M_{uy} = uniaxial ultimate moment capacity about y-axis

M_x= biaxial bending capacity component about x-axis.

M_y= biaxial bending capacity component about y-axis.

β is a function of reinforcement position, column dimension and the materialistic properties of steel and concrete. Parme *et.al* (1966) used a computer program to obtain values for β. Then β was represented graphically in four charts, Figure 2.37, 2.38, 2.39, 2.40.

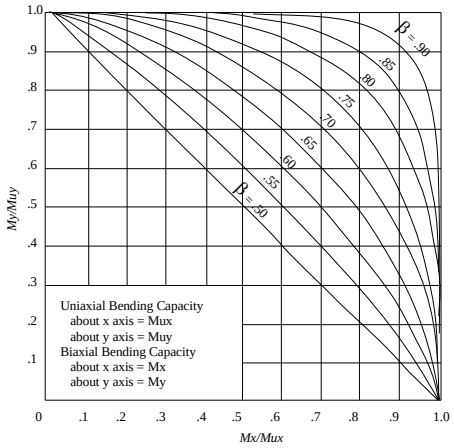

FIGURE 2.36
Biaxial Moment Relationship by Parme et al. (1966)

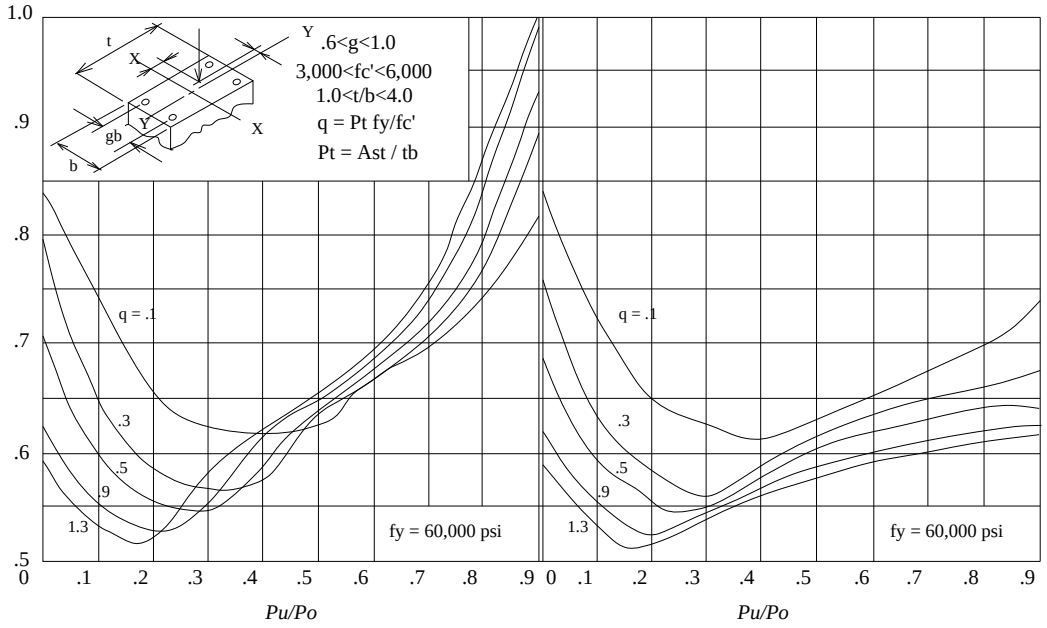

FIGURE 2.37
Biaxial Bending Design Constant (Four Bars Arrangement) by Parme et al. (1966)

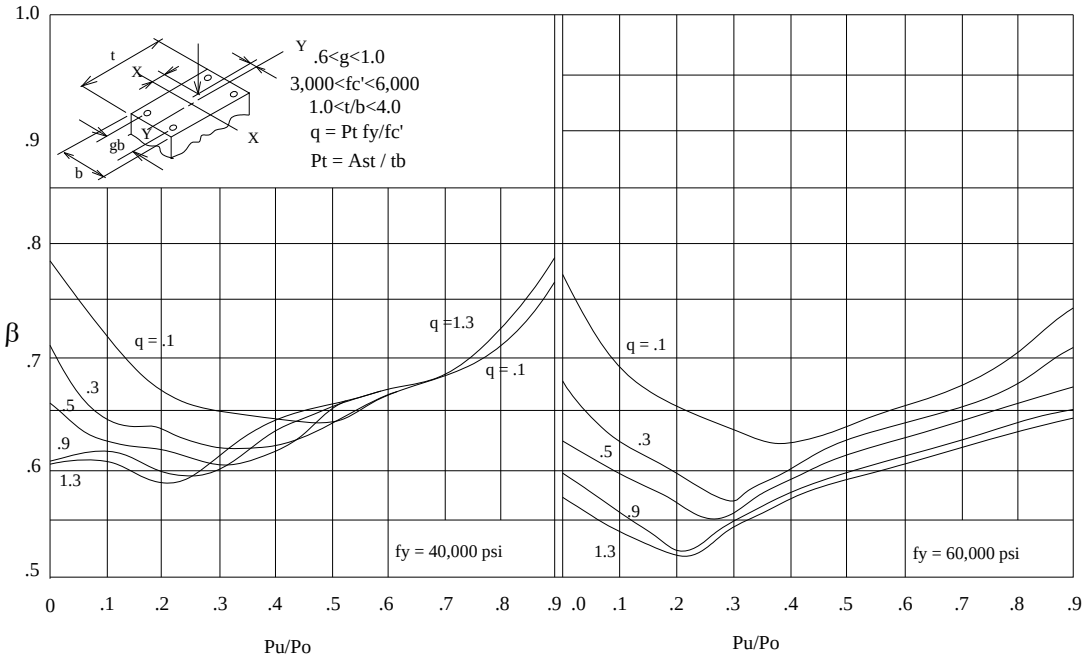

FIGURE 2.38
Biaxial Bending Design Constant (Eight Bars Arrangement) by Parme et al. (1966)

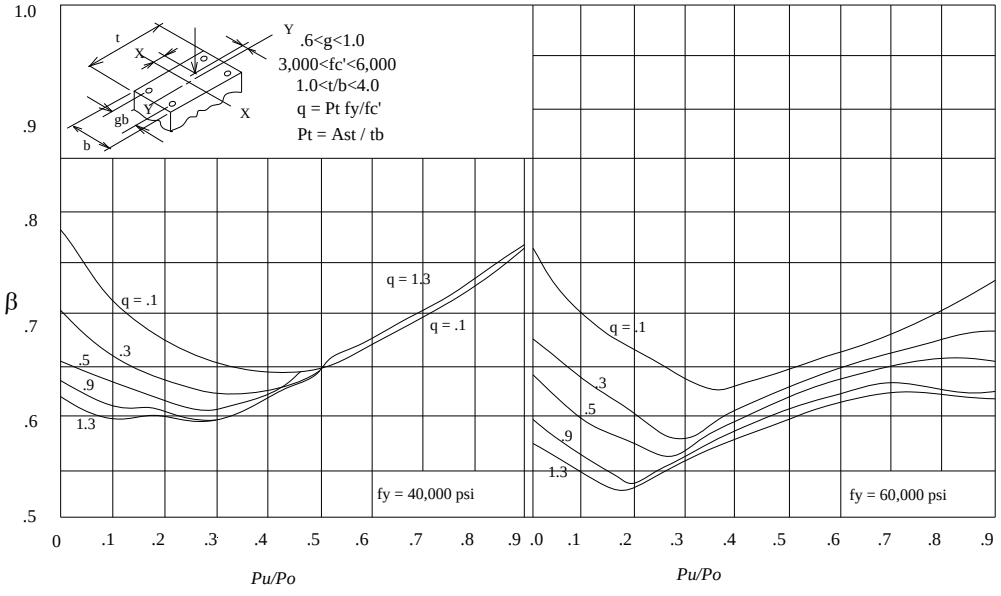

FIGURE 2.39
Biaxial Bending Design Constant (Twelve Bars Arrangement) by Parme et al. (1966)

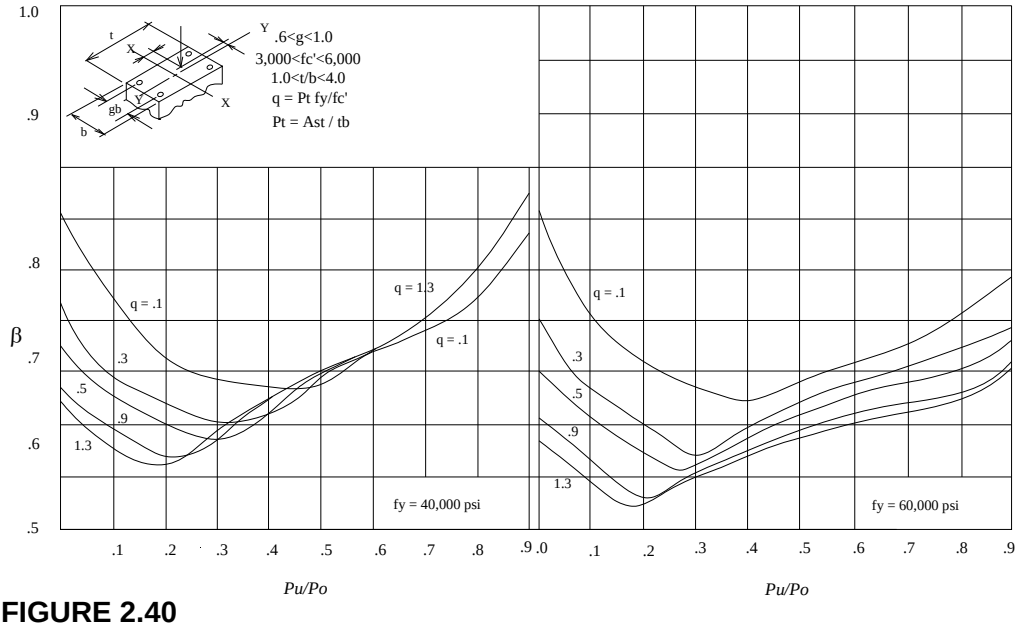

FIGURE 2.40
Biaxial Bending Design Constant (6-8-10 Bars Arrangement) by Parme et al. (1966)

Parme et al. (1966) showed agreement between the suggested Equation 2.297 and the theoretical one calculated with equilibrium equations. Furthermore, they simplified the exponential representation of the upper equation by introducing two equations for two straight line starting from My/Muy =1 and Mx/ Mux =1 intersecting at the point of equal relative moment Figure 2.41. The equations of the two straight lines are as follow:

$$M_y + M_x \frac{M_{uy}}{M_{ux}} \frac{(1-\beta)}{\beta} = M_{uy}$$

Equation 2.295

$$M_x + M_y \frac{M_{ux}}{M_{uy}} \frac{(1-\beta)}{\beta} = M_{ux}$$

Equation 2.296

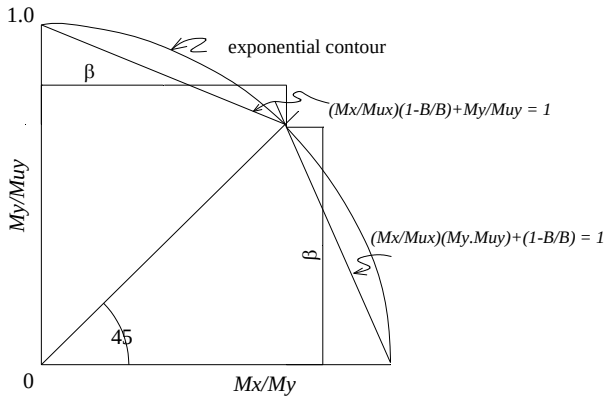

FIGURE 2.41
Simplified Interaction Curve by Parme et al. (1966)

2.2.1.26 Ultimate Strength Design Charts for Columns with Biaxial Bending (Weber1966)

Based on Furlong conclusion that the most critical bending axes is the 45 degree ones after the major and minor axes in the case of biaxial bending. Weber (1966) generated sixteen chart for the 45 degree interaction diagrams for square columns. the columns are having symmetrical reinforcement with different amount of steel bars. Design aids in the 1970 ACI SP-17A Handbookl2 and the 1972 CRSI Handbookl3 were based on interaction diagrams developed be Weber (1966).

2.2.1.27 Working Stress Column Design Using Interaction Diagrams (Mylonas 1967)

Mylonas (1967) adapted the interaction diagrams charts generated in the ACI Design handbook (1965), that were mainly for columns subjected to axial load and uniaxial bending and the steel is distributed on two faces parallel to the bending axis, to fit cases of biaxial bending and steel distributed along the four faces. Two reduction factors were introduced , one for each zone (Figure 2.42).

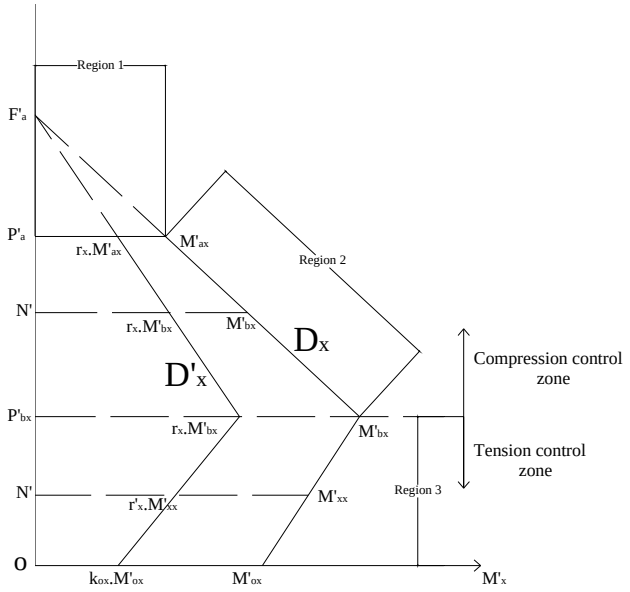

FIGURE 2.42
Working Stress Interaction Diagram for Bending about X-Axis by Mylonas (1967)

for zone 2:

$$r_x = \frac{1 + k_x w_x}{1 + w_x}$$

Equation 2.297

k_x is the moment of the steel distributed on two faces and is equal to

$$k_x = \frac{\sum a_s \lambda_x^2}{\sum a_s (0.5)^2}$$

Equation 2.298

$$w_x = 3(2n-1) g_x^2 p_g$$

Equation 2.299

g_x =bars center

p_g = steel ratio

a_s = section area of arbitrary bar

λ_x = bar distance from x-axis divided by gx t(section height)

For zone 3

$$r_x^{'} = k_{ox} + \frac{N^{'}}{P_{bx}^{'}}\left(r_x - k_{ox}\right)$$

Equation 2.300

K_{ox} is the moment reduction factor for pure bending about x-axis

$$k_{ox} = \frac{\sum a_s \lambda_x}{\sum a_s (0.5)}$$

Equation 2.301

P'_{bx} = load at balance failure

N' = normalized axial load

Mylonas (1967) also suggested that the applied bending moment should be compared to the reduced moment capacity, the moment capacity found from uniaxial bending interaction chart, of the section in form

$$\frac{M_x^{'}}{r_x M_{xx}^{'}} + \frac{M_y^{'}}{r_y M_{yy}^{'}} \leq 1$$

Equation 2.302

M'_x ,M'_y are the applied moment

M'_{xx} ,M'_{yy} moment capacity

2.2.1.28 Comparison of Experimental Results with Ultimate Strength Theory for Reinforced Concrete Columns in Biaxial Bending (Brettle and Taylor 1968)

Brettle and Taylor (1968) suggested partitioning the cross section into small size area, and using the limiting strain and the neutral axis position in calculating stresses in each filament using curvilinear stress distribution or rectangular stress distribution or trapezoidal stress

distribution for concrete. They generated ultimate strength design charts relating P_u/P_o to e_r/b for different t/b ratios and different inclination angle beween the line conecting the load to the centroid and the x-axis.

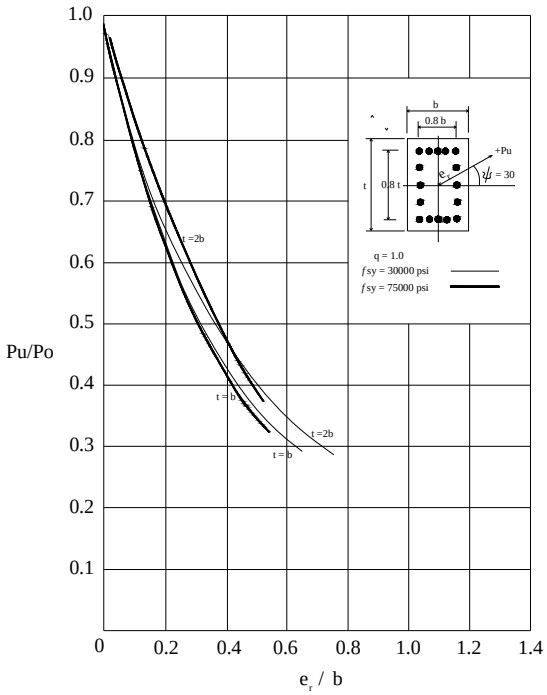

FIGURE 2.43
Comparison of Steel Stress Variation for Biaxial Vending When ψ = 30 and q = 1.0

Brettle and Taylor (1968)

er = resultant eccentricityed

t = section height

b = section width

Po = theoretical ultimate load with no eccentricities

Pu= theoretical ultimate load with eccentricities

2.2.1.29 Biaxial Flexure and Axial Load Interaction in Short Rectangular Reinforced Concrete Columns (Row and Paulay 1973)

Row and Paulay (1974) introduced six charts relating the m_ϕ to $P_u/f'_c bh$ to facilitate the design process. However these charts are applicable to limited cases only based on the material properties required for design

$$m_\theta = \frac{M_{ux}\sqrt{1+k^2}}{f_c' bh^2}$$ **Equation 2.303**

$$k = \frac{M_y}{M_x}$$ **Equation 2.304**

2.2.1.30 Biaxial Bending Simplified (Gouwens 1975)

Gouwens (1975) proposed simplified analytical equations for design column subjected to biaxial bending. He utilized Parme et al. (1966) simplified moment Equations 2.298 and 2.299. He found that β approaches 1 for 0.25 f'_c bh by examining 67 column cases. Based on that he proposed β equations as follow:

For $P \geq 0.25\ C_c$

$$\beta = \beta_{25} + 0.2\frac{P/C_c - 0.25}{0.85 + C_s/C_c}$$ **Equation 2.305**

For $P < 0.25\ C_c$

$$\beta = \beta_{25} + 0.2\left(0.25 - P/C_c\right)^2\left(0.85 + C_s/2C_c\right)$$ **Equation 2.306**

$$C_c = f_c' bh \qquad C_s = A_s f_y$$ **Equation 2.307**

$$\beta_{25} = 0.485 + 0.03\frac{C_c}{C_s} \qquad \frac{C_c}{C_s} \geq 0.5$$ **Equation 2.308**

$$\beta_{25} = 0.545 + 0.35\left(0.5 - \frac{C_c}{C_s}\right)^2 \qquad \frac{C_c}{C_s} < 0.5$$ **Equation 2.309**

2.2.1.31 Analysis of Short Rectangular Reinforced Concrete Columns Subjected to Biaxial Moments (Sallah 1983)

Sallah (1983) evaluated the Parameter β, found by Parme et al. (1966) and found that it was most affected by f_y, f'_c, r, P_u/P_{uo} and less affected by the number of bars. Sallah (1983) introduced number of charts similar to Parme et al.'s (1966) for finding β.

2.2.1.32 Design Contour Charts for Biaxial Bending of Rectangular Reinforced Concrete Columns Using Bresler Method (Taylor and Ho 1984)

Taylor and Ho (1984) developed a computer program to generate the two main interaction diagrams (with uniaxial bending-one for each axis). These two charts were used to generate the whole biaxial failure surface (and the failure contours)using Bresler equations. Different positions of parallel neutral axis and crushing strain of concrete were used to generate strain profile. The stresses were generated by stress block or other accepted formulas. And forces and moments were calculated. They plotted chart showing the load tracing on the cross section.

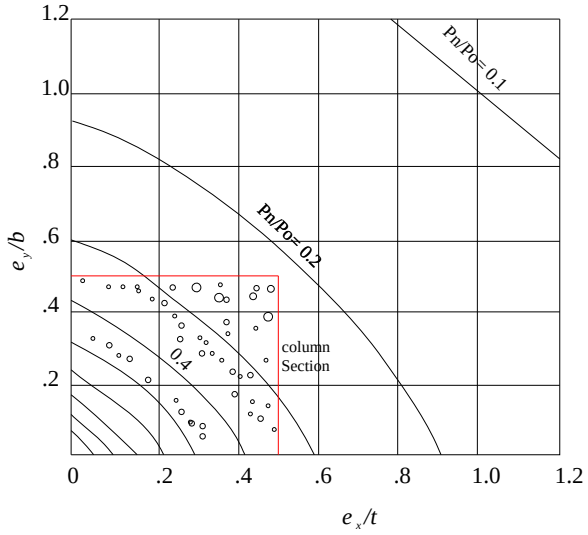

FIGURE 2.44
Non Dimensional Biaxial Contour on Quarter Column by Taylor and Ho (1984)

2.2.1.33 Radial Contour Method of Biaxial Short Column Design (Hartley 1985)

Hartley (1985) proposed two design procedure, one for finding the cross sectional length and the other to calculate the steel reinforcement, given all other desin parametes. He showed an optimum point to exist on the *3 D.* interaction diagram that relates to the smallest area of the cross section. Initially, he showed the relation between the load and eccentricity in the form:

$$\ln\left(\frac{P_u}{P_o}\right) = C\left(\frac{e}{b}\right)$$

Equation 2.310

where *c* is a curve constant,*b* is section length and *e* is force eccentricity the initial value of the cross section length can be found by

$$3.58b^2 - \left[3.26 + \ln\left(\frac{P_u}{P_o / A_g} * \frac{b}{t}\right)\right]b + c\left(\frac{M_x}{P_u}\right) = 0$$

Equation 2.311

Hartley (1985), using computer program, plotted graphically the relation between the cross sectional area and the ratio of P_u/P_o. These charts can be used to determine the suitable length in design.

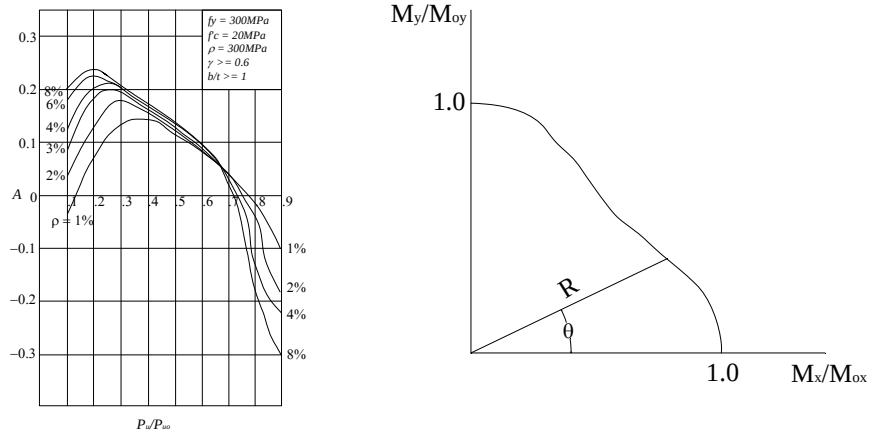

FIGURE 2.45
***P_u/P_{uo}* to A Relation for 4bars Arrangement by Hartley (1985) (left)**
Non-Dimensional Load Contour (Right)

Hartley (1985) also showed the relation between the R and θ in the load contour by

$$R = 1 - A\sin^n 2\theta$$ **Equation 2.312**

where R and θ are showen in Figure 2.45 (right).

2.2.1.34 Expert Interactive Design of R/C Columns under Biaxial Bending (Sacks snd Buyukozturk 1986)

Sacks and Buyukozturk (1986) developed computer software EIDOCC (Expert interactive design of concrete columns) to analyse and design columns subjected to biaxial bending. The procedure as follow

1. Finding the neutral axis location, according to Ramamurthy procedure, such that

$$\tan\left(\frac{e_{uy}}{e_{ux}}\right) = \tan\left(\frac{e_y}{e_x}\right)$$ **Equation 2.313**

e_{ux} = ultimate eccentricity measured parallel to x-axis

e_{uy} = ultimate eccentricity measured parallel to y-axis

e_x = eccentricity measured parallel to x-axis

e_y = eccentricity measured parallel to y-axis

2. Using the neutral axis depth,c, for the balanced failure as initial value
3. Calculating P_u and iterating for c using modified secant numerical method till the load is very close to P_u
4. Calculating e_{uy}, e_{ux} and comparing them to e_y, e_x to check section adequacy.

2.2.1.35 Interactive Design of Reinforced Concrete Columns with Biaxial Bending (Ross and Yen 1986)

Ross and Yen (1986) developed a computer program to analyze and design rectangular columns subjected to biaxial bending. The procedure is to change the inclination angle of the neutral axis to find adequate relation between M_{nx}, M_{ny}, and then change the position of the neutral axis to solve for the axial load. The section capacity is calculated using a predifined postion of the neutral axis and crushing strain equal to 0.003 for concrete. They suggested using four bars initially in the design process and keep increasing according to the applied loads with limiting the number of bars as stated by ACI code.

2.2.1.36 Design of Columns Subjected to Biaxial Bending (Horowitz 1989)

Horowitz (1989) developed a computer program for columns with any cross section subjected to biaxial bending. He relied on finding the least possible location of steel bars that make the section capacity more than the applied load.

2.2.1.37 Strength of Reinforced Concrete Column in Biaxial Bending (Amirthandan 1991)

Amirthandan *et.al (1991)* showed good corelation between the experimental work done before and the method propsed in the austrailian standard for concrete structures AS 3600 for short columns. The load contour in the standard is approximated by bresler equation. They adopted the beta value from the British standard

$$\beta = 0.7 + 1.7\left(N / 0.6Nuo\right)$$ **Equation 2.314**

N = design axial force

N_{uo} = ultimate axial load.

2.2.1.38 Computer Analysis of Reinforced Concrete Sections under Biaxial Bending and Longitudinal Load (Zak 1993)

Zak (1993) proposed solving the equilibrium equation with the modification of the secant modulus method. The ultimate strain was not determined. However, it was found using maximization method.

2.2.1.39 Analysis and Design of Square and Rectangular Column by Equation of Failure Surface Hsu (1994)

Hsu (1994) proposed equation that covers columns subjected to biaxial bending and axial compression or tension. The proposed equation is as follow:

$$\left(\frac{P_n - P_{nb}}{P_o - P_{nb}}\right) + \left(\frac{M_{nx}}{M_{nbx}}\right)^{1.5} + \left(\frac{M_{ny}}{M_{nby}}\right)^{1.5} = 1.0$$

Equation 2.315

Pn = nominal axial compression or tension

Mnx, Mny= nominal bending moments about x and y axis

Po = maximum nominal axial compression or axial tension

Pnb = nominal axial compression at balanced strain condition

Mnbx, Mnby = nominal bending moments about x and y axis at balanced strain condition.

2.2.1.40 Biaxial Interaction Diagrams for Short RC Columns of Any Cross Section (Rodriguez and Ochoa 1999)

Rodriguez and Ochoa (1999) proposed a general method for analyzing any cross section subjected to biaxial bending. They developed closed form solution for nominal total axial force strength and nominal bending moment strengths about the global X and Y-axes. Quasi-Newton's method was used to solve these coupled nonlinear equations to locate the neutral axis position.

$$P_n = \sum_{i=1}^{m} P_{ci} + \sum_{i=1}^{n} A_{bi} f_{si} - \sum_{i=1}^{n_{bc}} A_{bi} f_{si}$$ **Equation 2.316**

$$M_{nx} = \sin\alpha \sum_{i=1}^{n_t} M_{ciy} + \cos\alpha \sum_{i=1}^{n_t} M_{cix} + Y_a \sum_{i=1}^{n_t} P_{ci} + \sum_{i=1}^{n_t} A_{bi} f_{si} Y_{bi} - \sum_{i=1}^{n_{bc}} A_{bi} f_{ci} Y_{bi}$$ **Equation 2.317**

$$M_{ny} = \cos\alpha \sum_{i=1}^{n_t} M_{ciy} - \sin\alpha \sum_{i=1}^{n_t} M_{cix} + X_a \sum_{i=1}^{n_t} P_{ci} + \sum_{i=1}^{n_t} A_{bi} f_{si} X_{bi} - \sum_{i=1}^{n_{bc}} A_{bi} f_{ci} X_{bi}$$ **Equation 2.318**

P_n= Nominal axial force strength.

M_{nx} = nominal bending moment strength about x axis

M_{ny} = nominal bending moment strength about x axis

X_a, Y_a = coordinates of origin with respect to global x, xaxes

α = angle of inclination of neutral axis with respect to Xaxis;

n = number of reinforcement bars;

n_{bc} = number of rebars located on compression side of cross section;

n_t = number of trapezoids used to approximate concrete under compression;

A_{bi} = area of steel rebar i;

f_{ci} = concrete stress at reinforcement bar i

f_{si} = steel stress at reinforcement bar i

P_{ci} = force for each trapazoid.

M_{ciy} = Moment of each trapazoid about y axis.

M_{cix} = Moment of each trapazoid about x axis.

2.2.1.41 Short Reinforced Concrete Column Capacity under Biaxial Bending and Axial Load (Hong 2000)

Hong (2000) did not assume any crushing strain limit. He proposed two equation from equating forces and moments:

$$\frac{M_y}{P_n} - e_{xL} = 0$$

Equation 2.319

$$\frac{M_x}{P_n} - e_{yL} = 0$$

Equation 2.320

where e_{xl} , e_{yl} is the load eccentricity to x and y axes respectively.The two equations has three unknows; the curvature, neutral axis inclination angle and the neutral axis intercipt with the y-axis. Hong (2000) used the sequential quadratic programming method to solve the case as a nonlinearly constrained optimization problem.

2.2.1.42 Reliability of Reinforced Concrete Columns under Axial Load and Biaxial Bending (Wang and Hong 2002)

Wang and Hong (2002) evaluated the parameter β (Parme et al. 1966) and fount that it is insensitive to the reinforced ratio, it is more sensitive to biaxial bending than uniaxial bending, it increases withload and concncrete compressive strength.

2.2.1.43 Analysis and Design of Concrete Columns for Biaxial Bending: Overview (Furlong, Hsu, and Mirza 2004)

Furlong et al. (2004) reviewed many of the proposed formulas for analysis. These formulas were compared to experimental work. They concluded that the equations of Bresler (1960), although simple, are not very conservative, while Hsu equation is much more conservative. As Hsu equation can be used in biaxial bending and tension as well. However, both Hsu equation and Bresler reciprocal load equation can not be used in selecting cross section, unlike Bresler load contour equation.

2.2.1.44 New Method to Evaluate the Biaxial Interaction Exponent for RC Columns (Bajaj and Mendis 2005)

Bajaj and Mendis (2005) suggested new equations to evaluate the biaxial interaction exponenet a found by Bresler (1960). The proposed equations are as follow

$$\beta = \frac{\frac{M_{nx}}{M_{nox}} + \frac{M_{ny}}{M_{noy}}}{2}$$ **Equation 2.321**

$$\alpha = K\frac{\log 0.5}{\log \beta}$$ **Equation 2.322**

Bajaj and Mendis (2005) benchmarked their equastion by comparing the results with experimental work done on 8 (150* 150 mm) columns.

2.2.1.45 Analysis of Reinforced Concrete Columns Subjected to Biaxial Loads (Demagh, Chabil, and Hamzaoui 2005)

Demagh et al. (2005) suggested solving for the three equations of equilibrium to find the nominal force P_n, the inclination angle of the neutral axis α and the depth of the neutral axis b. The three equation are:

$$P_n = \sum P_{ci} + \sum (f_{si} - f_{ci})A_{si}$$ **Equation 2.323**

$$M_{nx} = P_n e_y = \sin\alpha \sum M_{ci} y + \cos\alpha \sum M_{ci} x + Y \sum P_{ci} + \sum (f_{si} - f_{ci})A_{si} y_{si}$$ **Equation 2.324**

$$M_{ny} = P_n e_x = \cos\alpha \sum M_{ci} y + \sin\alpha \sum M_{ci} x + X \sum P_{ci} + \sum (f_{si} - f_{ci})A_{si} y_{si}$$ **Equation 2.325**

where the subscript i refers to a concrete layer or steel bar element.

2.2.1.46 Analytical Approach to Failure Surfaces in Reinforced Concrete Sections Subjected to Axial Loads and Biaxial Bending (Bonet, Miguel, Fernandez, and Romero 2006)

Bonet et al. (2006) developed a new method for the surface failure based on numerical simulation. The numerical simulation was generated using a computer program capable of analysing moment-curvature diagram for given axial load and moment ratio. The maximum value was used as a failure point for the given loads. The failure surface is defined by two

directrix curves and generatrix curves. The directrix curves are the curve corresponds to zero axial force and the one corresponds to balance failure.the generatix curves are defined in Muy/Mux plane, the first curve connects the pure tension axial load to balnce failure load. Whearas the second curve connects the balnce failure load to the pure compression load. The equations for the four curves are as follow

Directrix 1

$$\left[\frac{M_{d1}.\cos\beta}{M_{d1,x}}\right]^{\gamma 1}+\left[\frac{M_{d1}.\sin\beta}{M_{d1,y}}\right]^{\gamma 2}=1$$

Equation 2.326

Directrix 2

$$\left[\frac{M_{d2}.\cos\beta}{M_{d2,x}}\right]^{\eta 1}+\left[\frac{M_{d2}.\sin\beta}{M_{d2,y}}\right]^{\eta 2}=1$$

Equation 2.327

generatix 1

$$\left(\frac{M_u-M_{d1}\left(1-\frac{N_u}{n_{ut}}\right)}{M_{d2}-M_{d1}\left(1-\frac{N_{d2}}{N_{ut}}\right)}\right)-\left(\frac{N_u-N_{ut}}{N_{d2}-N_{ut}}\right)*\left(\frac{N_u}{N_{d2}}\right)=0$$

Equation 2.328

generatix 2

$$\left(\frac{M_u-M_{d1}\left(1-\frac{N_u}{n_{ut}}\right)}{M_{d2}-M_{d1}\left(1-\frac{N_{d2}}{N_{ut}}\right)}\right)-\left(\frac{N_u-N_u}{N_{uc}-N_{d2}}\right)^{\zeta}-\left(\frac{M_u}{M_{d2}}\right)=0$$

Equation 2.329

M_{d1}= absolute value of the nominal bending moment of the section in simple flexure corresponding to angle beta

$Md_{1,x}$, $Md_{1,y}$= nominal bending moments of the section in simple flexure for the x and y axes, respectively.

M_{d2} = absolute value of the nominal bending moment corresponding to the maximum bending capacity

of the section for a particular angle β

$Md_{2,x}$, $Md_{2,y}$ = nominal bending moments corresponding to the maximum flexure capacity of the section for the x and the y axes, respectively.

γ, η=exponents of the directrices.

$\gamma = 1.3\omega + 2$

$\eta = -0.22\omega + 1.15$

ω = steel reinforcement

N_u = axial load applied

N_{uc} = the ultimate axial load in pure compression

N_{d2} =balance failure load.

$$\zeta = \left(0.8 * \omega - 0.7\right)\left[\frac{N_{uc} - N_u}{N_{uc} - N_{\lim}}\right] + 0.95$$

Equation 2.330

N_{lim} = nominal axial compression at the balanced strain condition

2.2.1.47 Biaxial Bending of Concrete Columns: an Analytical Solution (Cedolin, Cusatis, Eccheli, Roveda 2006)

Cedolin et al. (2006) introduced analytical solution of the failure envelope of rectangular R/C cross sections subjected to biaxial bending and to an axial force by approximating the rectangle to equivalent square section. The analysis was for unconfined concrete and the solution outcome was dimensionless.

2.2.1.48 Comparative Study of Analytical and Numerical Algorithms for Designing Reinforced Concrete Sections under Biaxial Bending (Bonet, Barros, Romero 2006)

Bonet et al. (2006) introduced analytical and numerical methods for designing circular and rectangular cross sections subjected to bi-axial bending. The analytical method uses the heviside function (Barros et al. 2004) to define the failure strain, then integrate the stress based on that failure. The numerical method breaks the section into multi thick layers parallel to the nuteral axis. The internal forces are found by numerical integration of each layer using Gausss-Legendre quadrature (Barros et al. 2004). They concluded that the two method are effeicint for circular cross section's analysis and the modified thick layer integration is more efficient for the rectangular cross section's analysis.

2.2.1.49 Investigation of Biaxial Bending of Reinforced Concrete Columns through Fiber Method Modeling (Lejano 2007)

Lejano (2007) expanded the finite element method found by Kaba and Mahin (1984). To predict the behavior of unconfined rectangular columns subjected to biaxial bending. The analysis was limited to uniform semmetric square columns. Lejano (2007) utilized Bazant's Endochronic theory for concrete and Ciampi model for steel.

2.2.1.50 Variation of Ultimate Concrete Strain at RC Columns Subjected to Axial Loads with Bi-Directional Eccentricities (Yoo and Shin 2007)

Yoo and Shin (2007) introduced the modified rectangular stress block (MRSB) to account for non-rectangular compression zone induced by bi-axial bending. They showed experimentally that the ultimate strain of concrete exposed to bi-directional eccentricities can reach up to 0.0059. Based on this finding they introduced new equation for the unconfined ultimate strain as follow:

$$\varepsilon_{cu} = 0.003 + \frac{\varepsilon_{0.45} - 0.003}{0.45}\frac{P_n}{P_o} \qquad \frac{P_n}{P_o} \le 0.45 \qquad \textbf{Equation 2.331}$$

$$\varepsilon_{cu} = 0.003 + \frac{\varepsilon_{0.45} - 0.003}{0.55}\left(1 - \frac{P_n}{P_o}\right) \qquad \frac{P_n}{P_o} \geq 0.45 \qquad \textbf{Equation 2.332}$$

$$\varepsilon_{0.45} = 0.003 + \frac{0.0025}{\tan^{-1}\left(\frac{h}{b}\right)}\theta \qquad 0 \leq \theta \leq \tan^{-1}\left(\frac{h}{b}\right) \qquad \textbf{Equation 2.333}$$

$$\varepsilon_{0.45} = 0.003 + \frac{0.0025}{90 - \tan^{-1}\left(\frac{h}{b}\right)}(90 - \theta) \qquad \tan^{-1}\left(\frac{h}{b}\right) \leq \theta \leq 90 \qquad \textbf{Equation 2.334}$$

No definition for θ was provided.

2.2.1.51 Capacity of Rectangular Cross Sections under Biaxially Eccentric Loads (Cedolin, Cusatis, Eccheli, Roveda 2008)

Cedolin et al. (2008) utilized the work of Cedolin et al. 2006 to generate more accurate moment failure contour through creating one extra points on the contour. This point correspond to the load acting on rectangle diagonlas and was approximated by using equivelant square to benefit from symmetry. The developed moment contour was used for better evaluating the parameter α found by Bresler (1960).

2.2.1.52 Development of a Computer Program to Design Concrete Columns for Biaxial Moments and Normal Force (Helgason 2010)

Helgason 2010 developed a computer program using Matlab for designing unconfined rectangular hollow or solid columns subjected to axial force and bending moment. Helgason 2010 used the predefined strain profile to generate the interaction diagram and the equivelant stress block equal to 80% of the compression zone depth. The outcome was compared to Eurocode.

2.2.2 Discussion

According to the literature review, there are five different approaches that treated the columns under axial load and bending moment problem. These ways are summarized as follow:

1. Trial for locating the neutral axis position such as Parker and Scanlon (1941), Ang (1961) and Czerniak (1962) works.
2. Implementing closed form equations for special cases such as Andersen (1941), Wiesinger (1958), Cedolin et al. (2006) and Yoo and Shin (2007) works.
3. Generating charts that relate two or more variable to facilitate the design process, such as Mikhalkin, Au (1958), Fleming and Werner (1965) and Brettle and Taylor (1968) works.
4. Developing simplified Interaction diagrams by using coefficients for curve defining. This method was adopted by some researchers like Whitney and Cohen (1957), Bresler (1960), Furlong (1961), Parme (1966), Mylons (1967), Bonet et al. (2006).
5. Generating Sets of ready Interaction diagrams to be used directly by designers, Weber (1966) and others.

There are some conclusions that can be drawn as follow

- The finite layer approach is successful in analysis. This approach was adopted by some authors such as Brettle and Taylor (1968), Bonet et al. (2006) and Lejano (2007).
- The Bresler Method is one of the most well known and successful method in predicting the unconfined interaction diagrams and load contours. This method was utilized and refined by many such as Rammamurthy (1966), Parme et al. (1966), Gouwens (1975), Sallah (1983) Amirthandan (1991), Wang and Hong (2002) and Bajaj and Mendis (2005). However it is very conservative for some cases as shown by Furlong et al. (2004) and others.
- Software applications on columns spread and became popular in the beginning of 1980s.Taylor and Ho (1984) developed computer program

based on Bresler Method. Sacks and Bugukoztruck (1986) developed their program based on iterating for neutral axis and load converge. Ross and Yen (1986) used the predefined strain profile in their software. Horowitz (1989) incremented the steel bars till the column capacity exceeded the load applied. This transition in relying on machines for facilitates calculations. Hence more accurate and precise analysis is needed to define exactly the unconfined and confined capacity of different sections.

- The predefined strain profile is seen to be one of the most effective and fast procedure foe unconfined analysis. This method was suggested by Furlong (1961) and utilized by many, such as Ross and Yan (1986).
- There is lack of confinement effect analysis on columns capacity. Nowadays, there is a need in predicting columns extreme events as stated by some structural codes like AASHTO-LRFD.

Chapter 3: Rectangular Columns Subjected to Biaxial Bending and Axial Compression

3.1 Introduction

Rectangular reinforced concrete columns can be subjected to biaxial bending moments plus axial force. When the load acts directly on one of the cross section bending axes the problem becomes of uniaxial bending and axial force. However when the load is applied eccentrically on a point that is not along any of the bending axes the case is generally biaxial bending and axial force. The biaxial bending case can be found in many structures nowadays. This case is visited extensively in the literature aside from the confinement effect. The failure surface of rectangular columns is 3D surface consisted of many adjacent 2D interaction diagrams. Each of the 2D interaction diagrams represents one angle between the bending moment about x-axis and the resultant moment. Many simplifications are introduced to justify the compressive trapezoidal shape of the concrete compression zone, due to the existence of the two bending axes. Approximations also were presented to depict the 3D failure shape from the principal interaction diagrams, in the two axes of symmetry. The most effective procedure found in the literature is the predefined ultimate strain profile that determines a certain position of the neutral axis and assigns crushing ultimate strain (typically 0.003) in one of the column corners. With the advance in technology and the enormous speed of computations, analysis is needed to plot a more accurate failure interaction diagram for both the unconfined and confined cases.

The methodology in this study is based on two different approaches; the adjusted predefined ultimate strain profile and the moment of area generalization approaches described below. The two methods are compared to benchmark the moment of area generalization method that will be used in the actual capacity analysis (Confined analysis). This analysis is compared to experimental data from the literature.

3.2 Unconfined Rectangular Columns Analysis

3.2.1 Formulations

3.2.1.1 Finite Layer Approach (Fiber Method)

The column cross section is divided into finite small-area filaments (Figure 3.1a). The force and moment of each filament is calculated and stored. The rebars are treated as discrete objects in their actual locations. The advantage of that is to avoid inaccuracy generated from using the approximation of the stress block method, as a representative of the compression zone and to well treat cases that have compressive trapezoidal or triangular shapes generated from the neutral axis inclination (Figure 3.1b).

a) b)

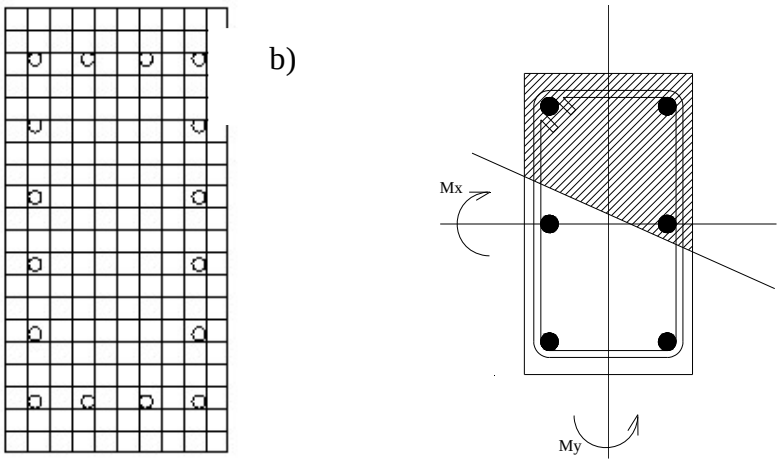

FIGURE 3.1
a) Using Finite Filaments in Analysis b)Trapezoidal Shape of Compression Zone

3.2.1.2 Concrete Model

Concrete is analyzed using the model proposed by Hognestad that was adopted from Ritter's Parabola 1899 (Hognestad 1951). Hognestad model is used extensively in numerous papers as it well explains concrete stress-strain behavior in compression. In addition, it was utilized by widely used concrete models such as Kent and Park model (1971). The stress-strain model is expressed using the following equation (Figure 3.2):

$$f_c = f_c^{'}\left(2\frac{\varepsilon_c}{\varepsilon_o} - \left(\frac{\varepsilon_c}{\varepsilon_o}\right)^2 \right)$$

Equation 3.1

f_c = stress in concrete in compression.

$f_c^{'}$ = maximum compressive strength of the concrete.

ε_c = strain at f_c

ε_o = strain at $f_c^{'}$

As shown in Figure 3.2a concrete carries tension up to cracking strength, then it is neglected in calculation beyond that.

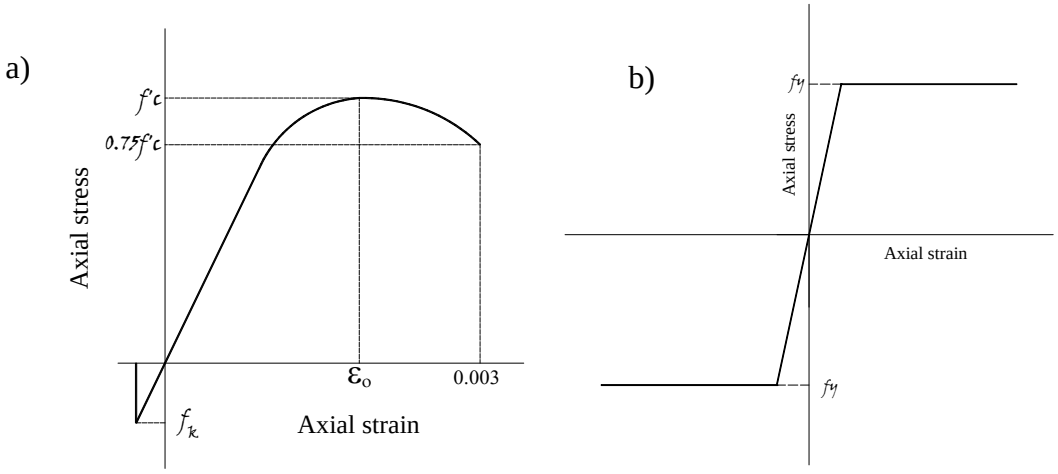

FIGURE 3.2
a) Stress-Strain Model for Concrete by Hognestad b) Steel Stress-Strain Model

3.2.1.3 Steel Model

Steel is assumed to be elastic up to the yield stress then perfectly plastic as shown in Figure 3.2b. It is assumed that there is perfect bond between the longitudinal steel bars and the concrete. According to Bernoulli's Hypothesis, strains along the depth of the column are assumed to be distributed linearly.

3.2.2 Analysis Approaches

The process of generalization of the moment-force interaction diagram is developed using two different approaches; the adjusted predefined ultimate strain profile and the generalized moment of area methods. The common features of the two approaches are described as follow:

3.2.2.1 Approach One: Adjusted Predefined Ultimate Strain Profile

The first approach is the well known method that was used by many researchers and practicing engineers. The procedure is to assign compressive failure strain at one of the column corners (0.003) and to vary the position and the inclination angle of the neutral axis that ranges from zero degree, parallel to the width of the column, to ninety degrees parallel to the height as shown in Figure 3.3.

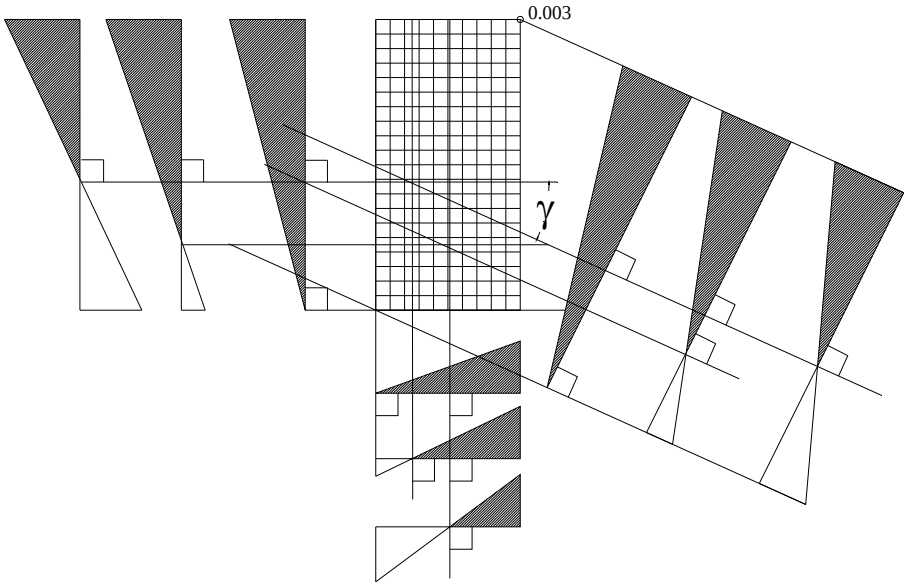

FIGURE 3.3
Different Strain Profiles Due to Different Neutral Axis Positions

Each set of the parallel neutral axes of a certain orientation represents approximately one 2D interaction diagram, and all of the sets from zero to ninety degrees represent the 3D failure surface in one quadrant, which is identical to the other three quadrants due to the existence of

two axis of symmetry with respect of concrete and steel. The procedure is described in the following steps:

1. Defining the strain profile for each neutral axis position and corner ultimate strain applied.
2. Calculating strain and the corresponding stress in each filament of concrete and doing the same for each steel bar Figure 3.4.

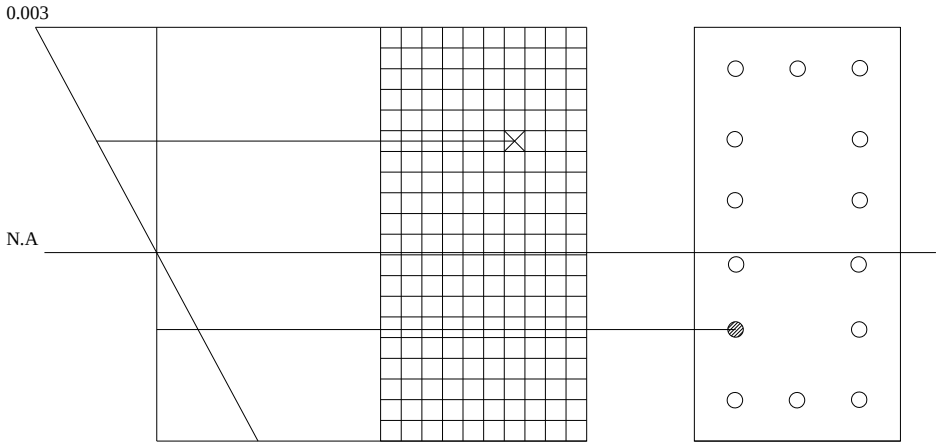

FIGURE 3.4
Defining Strain for Concrete Filaments and Steel Rebars from Strain Profile

3. Calculating the force and the moment about the geometric centroid for each filament and steel bar Figure 3.5.

for concrete: for steel

$$P_{ci} = f_{ci} w_i t_i \qquad P_{si} = f_{si} A_{si} \qquad \textbf{Equation 3.2}$$

$$Mx_{ci} = P_{ci} * Y\_i \qquad Mx_{si} = P_{si} * Y\_si \qquad \textbf{Equation 3.3}$$

$$My_{ci} = P_{ci} * X\_i \qquad My_{si} = P_{si} * X\_si \qquad \textbf{Equation 3.4}$$

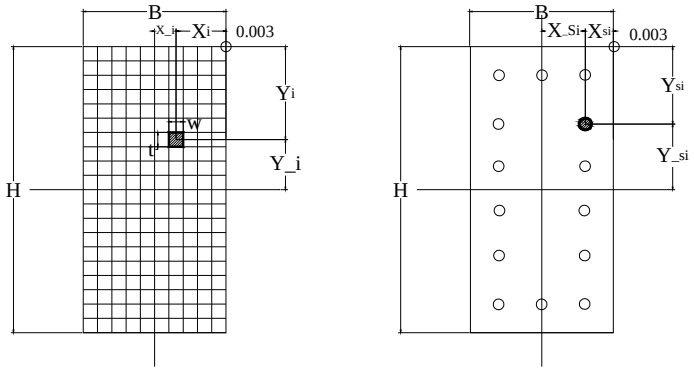

FIGURE 3.5
Filaments and Steel Rebars Geometric Properties with Respect to Crushing Strain Point and Geometric Centroid

Summing up the forces and moments, from steel bars and concrete filaments, to get the internal force and moment about x-axis and y-axis. The resultant force and moments represent one point on the unconfined interaction diagram (Figure 3.6).

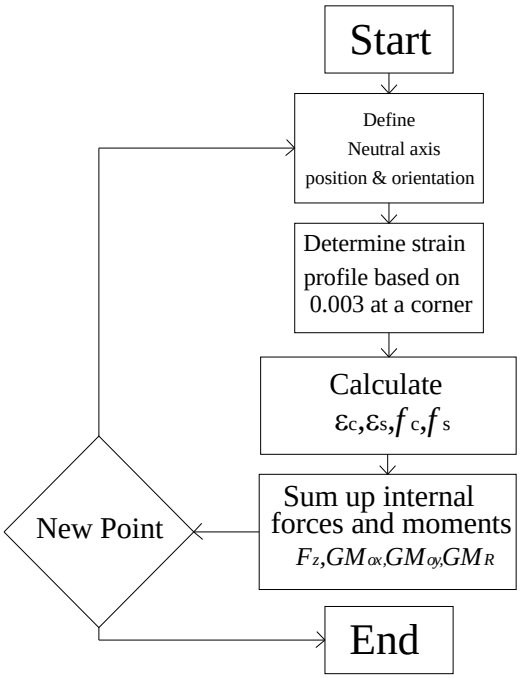

FIGURE 3.6
Method One Flowchart for the Predefined Ultimate Strain Profile Method

The problem arising from this procedure is that the points developed from one set of parallel neutral axes are close to but not lined up in one plane. However, they are scattered tightly near that plane (Figure 3.7). To correct for that, an average angle of $\overline{\alpha} = \cos^{-1}(M_x / M_R)$ is calculated and another run is established by slightly changing the inclination angle γ of the neutral axis of the section with respect to the y-axis and iterating till the angle determined for each point converges to the average angle $\overline{\alpha}$. The average angle $\overline{\alpha}$ is taken as the average of all α angles obtained for a certain γ angle orientation of the neutral axis (Figure 3.3 and Figure 3.7).

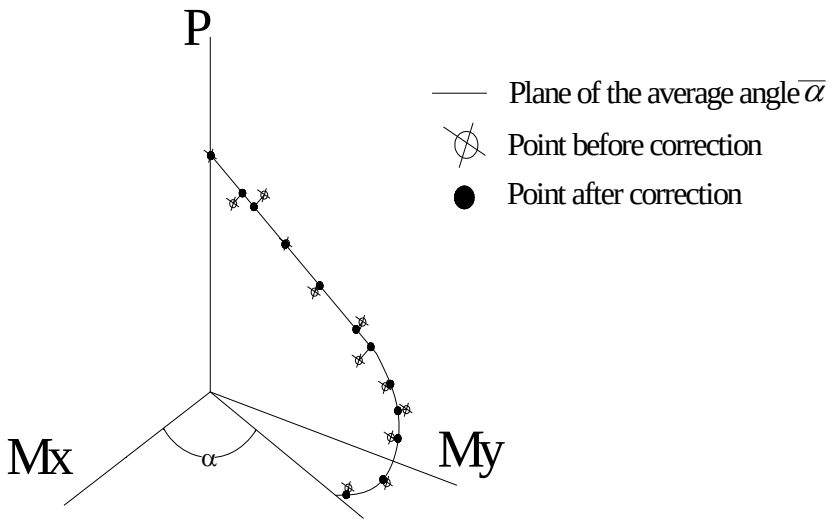

Figure 3.7
2D Interaction Diagram from Approach One Before and After Correction

The iterations mentioned above converge fast in all cases. This approach yields a very fast computation since it directly evaluates the ultimate unconfined strain profile. However, no moment curvature or load-strain history response is available with this approach.

3.2.2.2 Approach Two: Generalized Moment of Area Theorem

Moment of Area Theorem

The very general axial stress equation in an unsymmetrical section subjected to axial force *P* and biaxial bending M_x and M_y (Hardy Cross 1930):

$$\sigma_z = \frac{P}{A} + \frac{M_x I_y - M_y I_{xy}}{I_x I_y - I_{xy}^2} y + \frac{M_y I_x - M_x I_{xy}}{I_x I_y - I_{xy}^2} x$$

Equation 3.5

σ_z = normal stress at any point (a) in cross section

P = applied load.

A = cross sectional area.

M_x = bending moment about the geometric x-axis

M_y = bending moment about the geometric y-axis

x = distance between the point (a) and y-axis

y = distance between the point (a) and x-axis

I_x = moment of inertia about the geometric x-axis

I_y = moment of inertia about the geometric y-axis

I_{xy} = product moment of inertia in xy plane

Rewriting Equation 3.5 to determine the strain at any point in the cross section:

$$\varepsilon_z = \frac{P}{EA} + \frac{M_x EI_y - M_y EI_{xy}}{EI_x EI_y - EI_{xy}^2} y + \frac{M_y EI_x - M_x EI_{xy}}{EI_x EI_y - EI_{xy}^2} x$$

Equation 3.6

In case of linear elastic analysis, E in EA or EI expressions is constant ($E=E_c$). However, if the section has linear strain but nonlinear stress profile, it will amount to variable E profile (per layer or filament) in nonlinear analysis. Accordingly, the section parameters must include $\sum_i E_i A_i$, $\sum_i E_i I_i$ for a more generalized theory (Rasheed and Dinno 1994). Note that the linear strain profile of the section from Equation 3.6 yields two distinct constant curvatures:

$$\phi_x = \frac{M_x EI_y - M_y EI_{xy}}{\beta^2}$$

Equation 3.7

$$\phi_y = \frac{M_y EI_x - M_x EI_{xy}}{\beta^2}$$

Equation 3.8

ϕ_x = curvature about the x-axis

ϕ_y = curvature about the y-axis

$\beta^2 = EI_x EI_y - EI_{xy}^2$

To prove Equations 3.7 and 3.8 above, invoke the coupled equations of moments about the actual or current centroid (Bickford 1998).

$$M_x = EI_x\phi_x + EI_{xy}\phi_y \qquad \textbf{Equation 3.9}$$

$$M_y = EI_{xy}\phi_x + EI_y\phi_y \qquad \textbf{Equation 3.10}$$

In a matrix form:

$$\begin{bmatrix} M_x \\ M_y \end{bmatrix} = \begin{bmatrix} EI_x & EI_{xy} \\ EI_{xy} & EI_y \end{bmatrix} \begin{bmatrix} \phi_x \\ \phi_y \end{bmatrix} \qquad \textbf{Equation 3.11}$$

Inverting Equation 3.11

$$\begin{bmatrix} \phi_x \\ \phi_y \end{bmatrix} = \frac{1}{\beta^2} \begin{bmatrix} EI_y & -EI_{xy} \\ -EI_{xy} & EI_x \end{bmatrix} \begin{bmatrix} M_x \\ M_y \end{bmatrix} \qquad \textbf{Equation 3.12}$$

which reproduces Equations 3.7 and 3.8. Rewriting Equation 3.6 in terms of ϕ_x and ϕ_y

$$\varepsilon_z = \frac{P}{EA} + \phi_x y + \phi_y x \qquad \textbf{Equation 3.13}$$

Finding ε_z at the actual or current centroid, since $x = y = 0$.

$$\varepsilon_o = \frac{P}{EA} \qquad \textbf{Equation 3.14}$$

Finding ε_z at the geometric centroid, $y = \bar{y}$

$$\overline{\varepsilon_o} = \frac{P}{EA} + \phi_x \bar{y} + \phi_y \bar{x}$$ **Equation 3.15**

Solving for *P* at the geometric centroid;

$$P = EA\overline{\varepsilon_o} - EA\bar{y}\phi_x - EA\bar{x}\phi_y$$ **Equation 3.16**

But

$$EAM_x = EA\bar{y} \qquad \bar{y} = Y_G - Y_c$$

$$EAM_y = EA\bar{x} \qquad \bar{x} = X_G - X_c$$

Y_G is the vertical distance to the geometric centroid measured from bottom, X_G is the distance to the geometric centroid measured from the cross section's left side, Y_c is the vertical distance to the inelastic centroid measured from the bottom and X_c is the horizontal distance to the inelastic centroid measured from the cross section's left side (Figure 3.8).

Thus,

$$P = EA\overline{\varepsilon_o} - EAM_x\phi_x - EAM_y\phi_y$$ **Equation 3.17**

The general formula of the moments about the geometric x-axis and the geometric y-axis is derived as follows:

when the moment is transferred from the centroid to the geometric centroid (Figure 5.8a)

$$\overline{M_x} = M_x - P\bar{y}$$ **Equation 3.18**

Substituting Equations 3.9 and 3.16 in 3.17 yields:

$$\overline{M_x} = EI_x\phi_x + EI_{xy}\phi_y - EA\overline{\varepsilon_o}\bar{y} + EAM_x\phi_x\bar{y} + EAM_y\phi_y\bar{y}$$ **Equation 3.19**

$$\overline{M_x} = -EAM_x\overline{\varepsilon_o} + \left(EI_x + EAM_x\bar{y}\right)\phi_x + \left(EI_{xy} + EAM_y\bar{y}\right)\phi_y \qquad \textbf{Equation 3.20}$$

Similarly (Figure 3.8b):

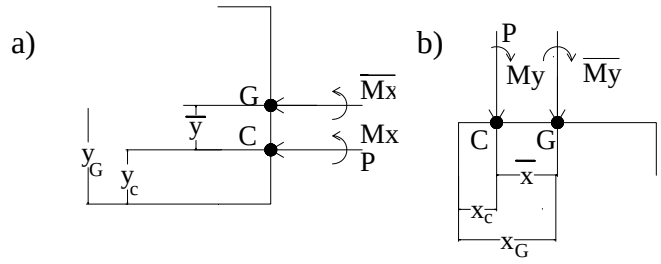

FIGURE 3.8
Transferring Moment from Centroid to the Geometric Centroid

$$\overline{M_y} = M_y - P\bar{x} \qquad \textbf{Equation 3.21}$$

$$\overline{M_y} = EI_{xy}\phi_x + EI_y\phi_y - EA\overline{\varepsilon_o}\,\bar{x} + EAM_x\phi_x\bar{x} + EAM_y\phi_y\bar{x} \qquad \textbf{Equation 3.22}$$

$$\overline{M_y} = -EAM_y\overline{\varepsilon_o} + \left(EI_{xy} + EAM_x\bar{x}\right)\phi_x + \left(EI_y + EAM_y\bar{x}\right)\phi_y \qquad \textbf{Equation 3.23}$$

The terms $EI_x + EAM_x\bar{y}$ and $EI_y + EAM_y\bar{x}$ represent the $\overline{EI_x}$ and $\overline{EI_y}$ about the geometric centroid respectively using the parallel axis theorem. And the terms $EI_{xy} + EAM_x\bar{x}$ and $EI_{xy} + EAM_y\bar{y}$ are equal given that: $EAM_x\bar{x} = EA\bar{y}\bar{x}$ and $EAM_y\bar{y} = EA\bar{y}\bar{x}$. Using Equations 3.16, 3.19, and 3.22 yields the extended generalized moment of area equation:

$$\begin{bmatrix} P \\ \overline{Mx} \\ \overline{M_y} \end{bmatrix} = \begin{bmatrix} EA & -EAM_x & -EAM_y \\ -EAM_x & \overline{EI_x} & \overline{EI_{xy}} \\ -EAM_y & \overline{EI_{xy}} & \overline{EI_y} \end{bmatrix} \begin{bmatrix} \overline{\varepsilon_o} \\ \phi_x \\ \phi_y \end{bmatrix} \qquad \textbf{Equation 3.24}$$

Since the moment of area about the inelastic centroid vanishes (Rasheed and Dinno 1994), Equation 3.23 reduces to a partially uncoupled set when it is applied back at inelastic the centroid since EAM_x and EAM_y vanish about that centroid.

$$\begin{bmatrix} P \\ M_x \\ M_y \end{bmatrix} = \begin{bmatrix} EA & 0 & 0 \\ 0 & EI_x & EI_{xy} \\ 0 & EI_{xy} & EI_y \end{bmatrix} \begin{bmatrix} \varepsilon_o \\ \phi_x \\ \phi_y \end{bmatrix}$$

Equation 3.25

which is simply Equations 3.9, 3.10, and 3.14

3.2.2.3 Method Two

This approach simulates the radial loading of the force and moments by keeping the relative proportion between them constant during the loading. Accordingly, all the points comprising an interaction diagram of angle α will be exactly on that 2D interaction diagram. In addition to the ultimate points, the complete load deformation response is generated. The cross section analyzed is loaded incrementally by maintaining a certain eccentricity between the axial force P and the resultant moment M_R. Since M_R is generated as the resultant of M_x and M_y, the angle $\alpha = \tan^{-1}(M_y/M_x)$ is kept constant for a certain 2D interaction diagram. And since increasing the load and resultant moment proportionally causes the neutral axis to vary unpredictably, the generalized moment of area theorem is devised. This method is based on the general response of rectangular unsymmetrical section subjected to biaxial bending and axial compression. The asymmetry stems from the different behavior of concrete in compression and tension.

The method is developed using incremental iterative analysis algorithm, secant stiffness approach and proportional or radial loading. It is explained in the following steps. (Figure 3.12 presents a flowchart of the outlined procedure):

1. Calculating the initial section properties:
    - Elastic axial rigidity *EA*:

$$EA = \sum_i E_c w_i t_i + \sum_i (E_s - E_c) A_{si}$$ **Equation 3.26**

E_c = initial modulus of elasticity of the concrete

E_s = initial modulus of elasticity of the steel rebar

- The depth of the elastic centroid position from the bottom fiber of the section Y_c and from the left side of the section X_c

$$Y_c = \frac{\sum_i E_c w_i t_i (H - Y_i) + \sum_i (E_s - E_c) A_{si} (H - Y_{si})}{EA}$$ **Equation 3.27**

$$X_c = \frac{\sum_i E_c w_i t_i (B - X_i) + \sum_i (E_s - E_c) A_{si} (B - X_{si})}{EA}$$ **Equation 3.28**

where Y_i and Y_{si} are measured to the top extreme fiber, X_i and X_{si} are measured to the right most extreme fiber, see Figure 3.9.

- Elastic flexural rigidity about the elastic centroid *EI*:

$$EI_x = \sum_i E_c w_i t_i (H - Y_i - Y_c)^2 + \sum_i (E_s - E_c) A_{si} (H - Y_{si} - Y_c)^2$$ **Equation 3.29**

$$EI_y = \sum_i E_c w_i t_i (B - X_i - X_c)^2 + \sum_i (E_s - E_c) A_{si} (B - X_{si} - X_c)^2$$ **Equation 3.30**

$$EI_{xy} = \sum_i E_c w_i t_i (H - Y_i - Y_c)(B - X_i - X_c) + \sum_i (E_s - E_c) A_{si} (H - Y_{si} - Y_c)(B - X_{si} - X_c)$$ **Equation 3.31**

Typically the initial elastic Yc = *H/2*, X_c = *B/2* and EI_{xy} = 0

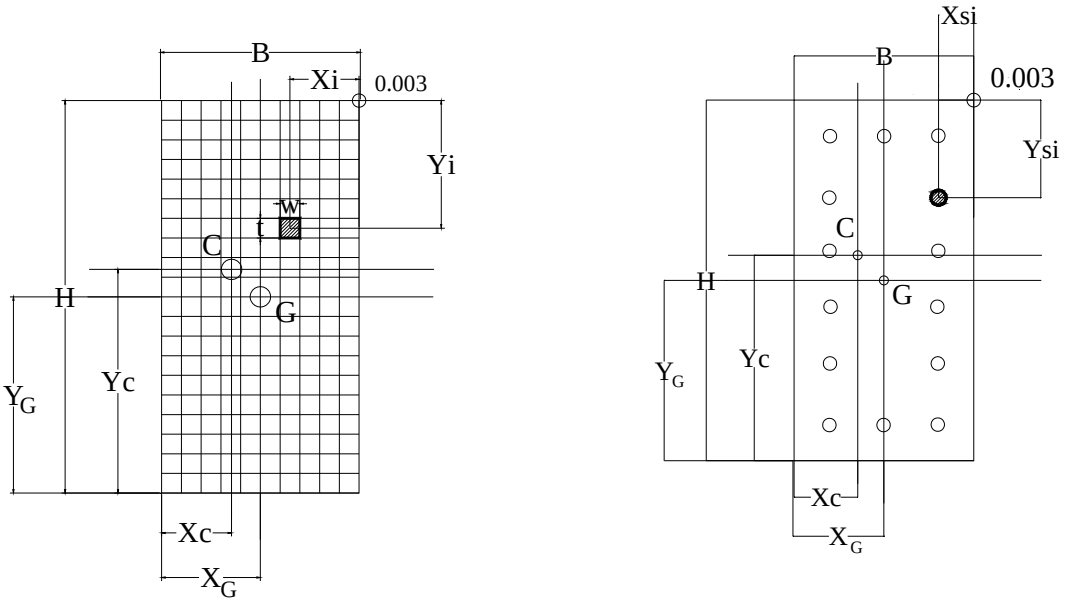

FIGURE 3.9
Geometric Properties of Concrete Filaments and Steel Rebars with Respect to Geometric Centroid and Inelastic Centroid

The depth of the geometric section centroid position from the bottom and left fibers of the section Y_G, $X_{G:}$

$$Y_G = \frac{H}{2}$$ **Equation 3.32**

$$X_G = \frac{B}{2}$$ **Equation 3.33**

2. Defining the eccentricity *e*, which specifies the radial path of loading on the interaction diagram. Also, defining the angle α in between the resultant moment GM_R and GM_X

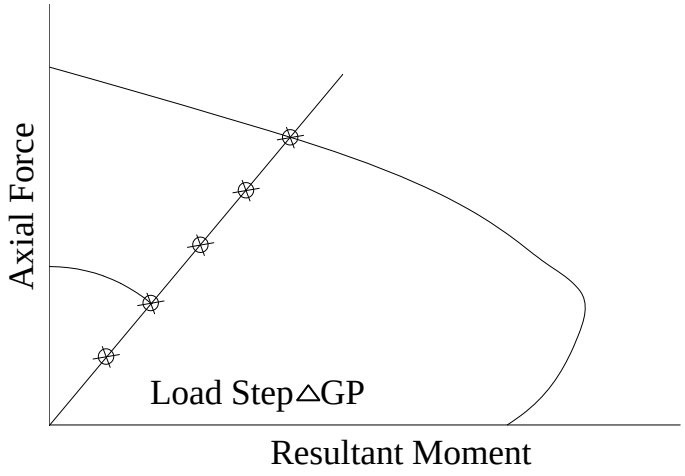

FIGURE 3.10
Radial Loading Concept

3. Defining the loading step ΔGP as a small portion of the maximum load, and computing the axial force at the geometric centroid.

$$GP_{new} = GP_{old} + \Delta GP \qquad \textbf{Equation 3.34}$$

4. Calculating the moment GM_R about the geometric centroid.

$$e = \frac{GM_R}{GP} \qquad GM_R = e * GP \qquad \textbf{Equation 3.35}$$

$$GM_X = GM_R \cos\alpha \qquad \textbf{Equation 3.36}$$

$$GM_Y = GM_X \tan\alpha \qquad \textbf{Equation 3.37}$$

5. Transferring the moments to the inelastic centroid and calculating the new transferred moments TM_X and TM_Y :

$$TM_X = GM_X + GP(Y_G - Y_c) \qquad \textbf{Equation 3.38}$$

$$TM_Y = GM_Y + GP(X_G - X_c)$$

Equation 3.39

The advantage of transferring the moment to the position of the inelastic centroid is to eliminate the coupling effect between the force and the two moments, since $EAM_x = EAM_y = 0$ about the inelastic centroid

$$\begin{bmatrix} P \\ TM_x \\ TM_y \end{bmatrix} = \begin{bmatrix} EA & 0 & 0 \\ 0 & EI_x & EI_{xy} \\ 0 & EI_{xy} & EI_y \end{bmatrix} \begin{bmatrix} \varepsilon_o \\ \phi_x \\ \phi_y \end{bmatrix}$$

Equation 3.40

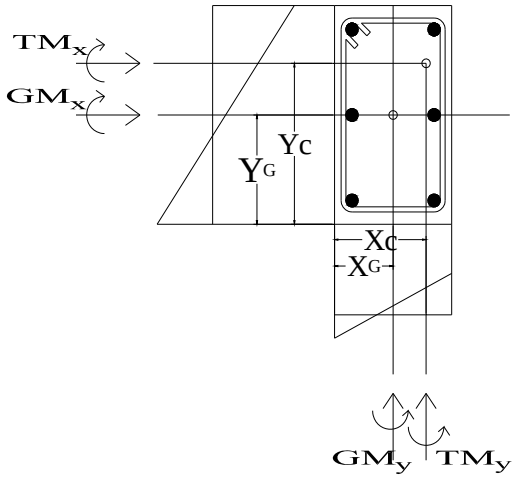

FIGURE 3.11
Moment Transferring from Geometric Centroid to Inelastic Centroid

6. Finding: Curvatures ϕ_X and ϕ_Y

$$\phi_X = \frac{TM_X}{\beta^2} * EI_Y - \frac{TM_Y}{\beta^2} * EI_{XY}$$

Equation 3.41

$$\phi_Y = \frac{TM_Y}{\beta^2} * EI_X - \frac{TM_X}{\beta^2} * EI_{XY}$$

Equation 3.42

$$\beta^2 = EI_X EI_Y - EI_{xy}^2$$ **Equation 3.43**

Strain at the inelastic centroid ε_o, the extreme compression fiber strain ε_{ec}, and strain at the extreme level of steel in tension ε_{es} are found as follow:

$$\varepsilon_o = \frac{GP}{EA}$$ **Equation 3.44**

$$\varepsilon_{ec} = \varepsilon_o + \phi_x (H - Y_c) + \phi_y (B - X_c)$$ **Equation 3.45**

$$\varepsilon_{es} = \varepsilon_o - \phi_x (Y_c - Cover) - \phi_y (X_c - Cover)$$ **Equation 3.46**

where cover is up to center of bars

1. Calculating strain ε_{ci} and corresponding stress f_{ci} in each filament of concrete section by using Hognestad's model (Equation 3.1) in case of unconfined analysis

$$\varepsilon_{ci} = \frac{GP}{EA} + \frac{TM_x (H - Y_c - Y_i)}{\beta^2} EI_y + \frac{TM_y (B - X_c - X_i)}{\beta^2} EI_x - \frac{TM_x (B - X_c - X_i)}{\beta^2} EI_{xy} - \frac{TM_y (H - Y_c - Y_i)}{\beta^2} EI_{xy}$$ **Equation 3.47**

2. Calculating strain ε_{si} and corresponding stress f_{si} in each bar in the given section by using the steel model shown in Figure 3.2b.

$$\varepsilon_{si} = \frac{GP}{EA} + \frac{TM_x (H - Y_c - Y_{si})}{\beta^2} EI_y + \frac{TM_y (B - X_c - X_{si})}{\beta^2} EI_x - \frac{TM_x (B - X_c - X_{si})}{\beta^2} EI_{xy} - \frac{TM_y (H - Y_c - Y_{si})}{\beta^2} EI_{xy}$$ **Equation 3.48**

1. Calculating the new section properties: axial rigidity EA, flexural rigidities about the inelastic centroid EI_x, EI_y, EI_{xy} moment of axial rigidity about inelastic centroid EAM_x, EAM_y, internal axial force F_z, internal bending moments about the inelastic centroid M_{ox} ,M_{oy}:

$$EA = \sum_i E_{ci} w_i t_i + \sum_i (E_{si} - E_{ci}) A_{si}$$ **Equation 3.49**

$$EAM_x = \sum_i E_{ci} w_i t_i (H - Y_c - Y_i) + \sum_i (E_{si} - E_{ci}) A_{si} (H - Y_c - Y_{si})$$ **Equation 3.50**

$$EAM_y = \sum_i E_{ci} w_i t_i (B - X_c - X_i) + \sum_i (E_{si} - E_{ci}) A_{si} (B - X_c - X_{si})$$ **Equation 3.51**

$$F_z = \sum f_{ci} w_i t_i + \sum (f_{si} - f_{ci}) A_{si}$$ **Equation 3.52**

$$EI_x = \sum_i E_{ci} w_i t_i (H - Y_c - Y_i)^2 + \sum_i (E_{si} - E_{ci}) A_{si} (H - Y_c - Y_{si})^2$$ **Equation 3.53**

$$EI_y = \sum_i E_{ci} w_i t_i (B - X_c - X_i)^2 + \sum_i (E_{si} - E_{ci}) A_{si} (H - X_c - X_{si})^2$$ **Equation 3.54**

$$EI_{xy} = \sum_i E_{ci} w_i t_i (H - Y_c - Y_i)\left(B - X_c - X_i\right) + \sum_i (E_{si} - E_{ci}) A_{si} (H - Y_c - Y_{si})\left(B - X_c - X_{si}\right)$$ **Equation 3.55**

$$M_{ox} = \sum_i f_{ci} w_i t_i (H - Y_c - Y_i) + \sum_i (f_{si} - f_{ci}) A_{si} \left(H - Y_c - Y_{si}\right)$$ **Equation 3.56**

$$M_{oy} = \sum_i f_{ci} w_i t_i (B - X_c - X_i) + \sum_i (f_{si} - f_{ci}) A_{si} \left(B - X_c - X_{si}\right)$$ **Equation 3.57**

where E_{ci} = secant modulus of elasticity of the concrete filament.

E_{si} = secant modulus of elasticity of the steel bar.

2. Transferring back the internal moment about the geometric centroid

$$GM_{ox} = M_{ox} - GP(Y_G - Y_c)$$ **Equation 3.58**

$$GM_{oy} = M_{oy} - GP(X_G - X_c)$$ **Equation 3.59**

3. Checking the convergence of the inelastic centroid

$$TOL_x = EAM_x / EA / Y_c \qquad \textbf{Equation 3.60}$$

$$TOL_y = EAM_y / EA / X_c \qquad \textbf{Equation 3.61}$$

4. Comparing the internal force to applied force, internal moments to applied moments, and making sure the moments are calculated about the geometric centroid :

$$\left|GP - F_z\right| \le 1*10^{-5} \qquad \textbf{Equation 3.62}$$

$$\left|GM_x - GM_{ox}\right| \le 1*10^{-5} \qquad \left|GM_y - GM_{oy}\right| \le 1*10^{-5} \qquad \textbf{Equation 3.63}$$

$$\left|TOL_x\right| \le 1*10^{-5} \qquad \left|TOL_y\right| \le 1*10^{-5} \qquad \textbf{Equation 3.64}$$

If Equations 3.61, 3.62, and 3.63 are not satisfied, the location of the inelastic centroid is Updated by EAM_x/EA and EAM_y/EA and steps 5 to 12 are repeated till Equations 3.61, 3.62 and 3.63 are satisfied.

$$Y_{c_{new}} = Y_{c_{old}} + \frac{EAM_x}{EA} \qquad \textbf{Equation 3.65}$$

$$X_{c_{new}} = X_{c_{old}} + \frac{EAM_y}{EA} \qquad \textbf{Equation 3.66}$$

Once equilibrium is reached, the algorithm checks for ultimate strain in concrete ε_{ec} and steel ε_{es} not to exceed 0.003 and 0.05 respectively, then it increases the loading by ΔGP and runs the analysis for the new load level using the latest section properties. Otherwise, if ε_{ec}

equals 0.003 or ε_{es} equals 0.05, the target force and resultant moment are reached as a point on the failure surface for the amount of eccentricity and angle α used.

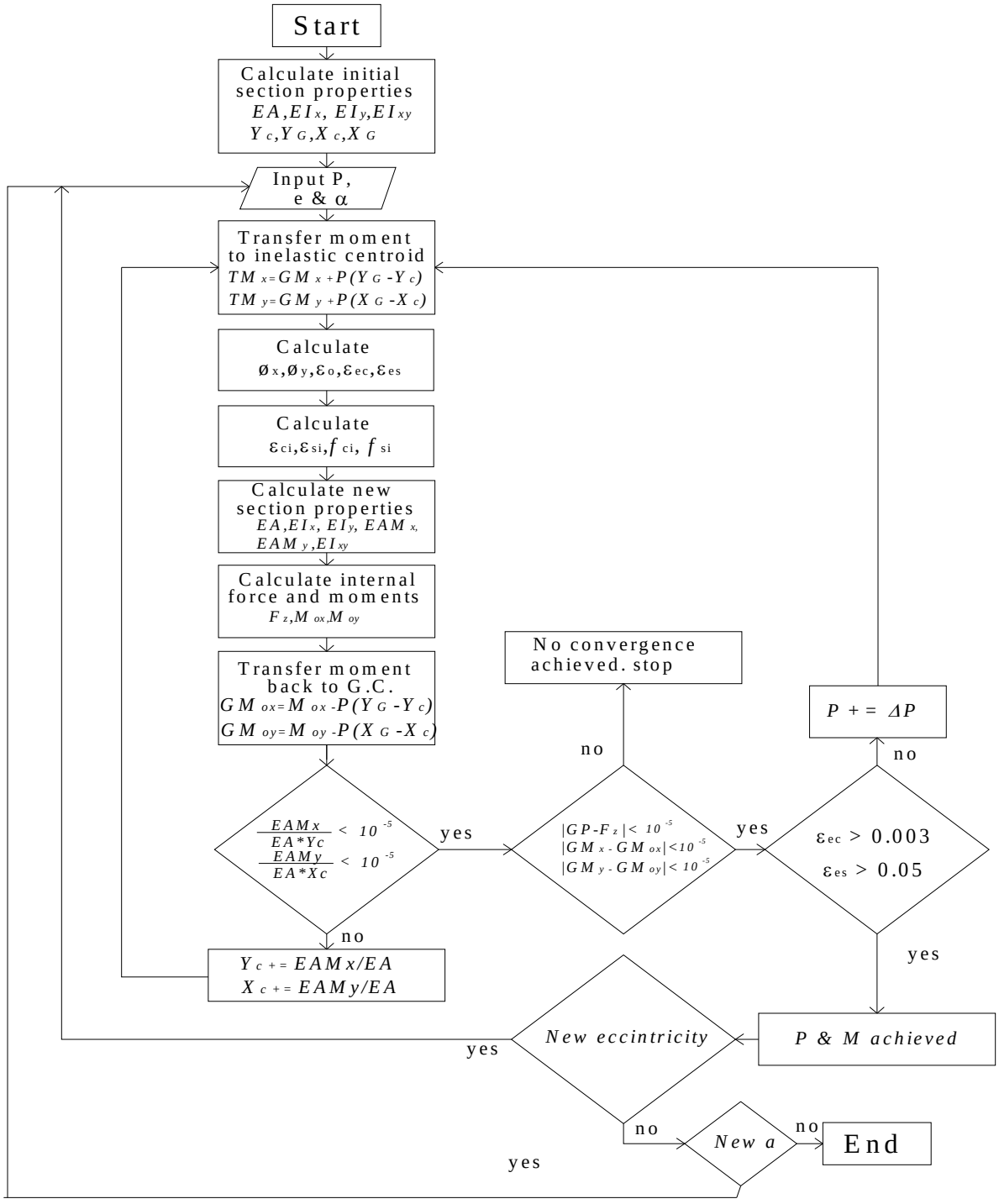

FIGURE 3.12
Flowchart of Generalized Moment of Area Method Used for Unconfined Analysis

3.2.3 Results and Discussion

3.2.3.1 Comparison between the Two Approaches

The two approaches are compared to each other in the following. The column used in comparison has the following properties:

Section Height = 20 inches

Section Width = 10 inches

Clear Cover = 2 inches

Steel Bars in x direction = 3 # 4

Steel Bars in x direction = 6 # 4

Hoop #3

f'_c = 4 ksi

f_y = 60 ksi.

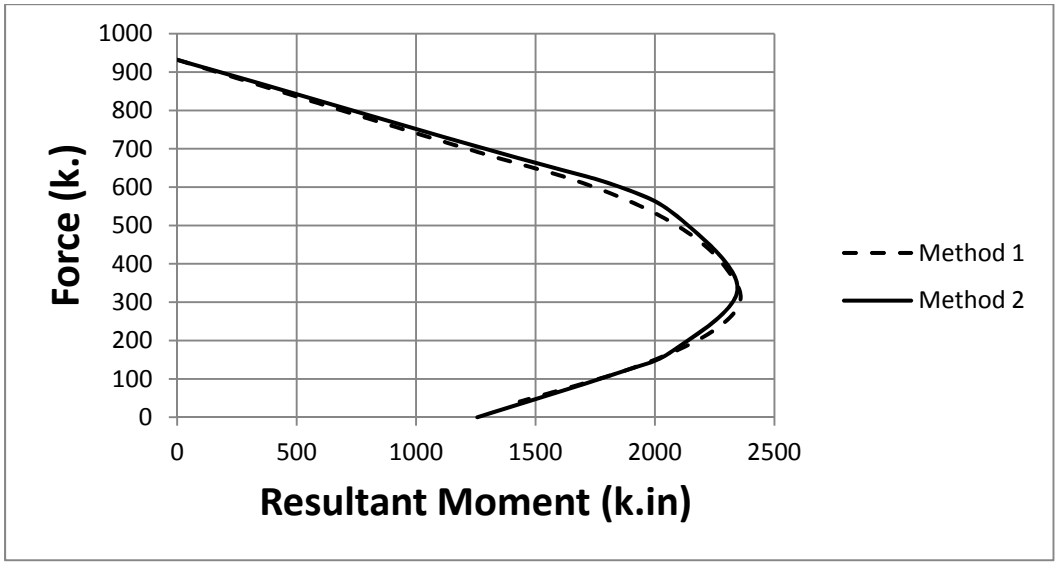

FIGURE 3.13
Comparison of Approach One and Two (α = 0)

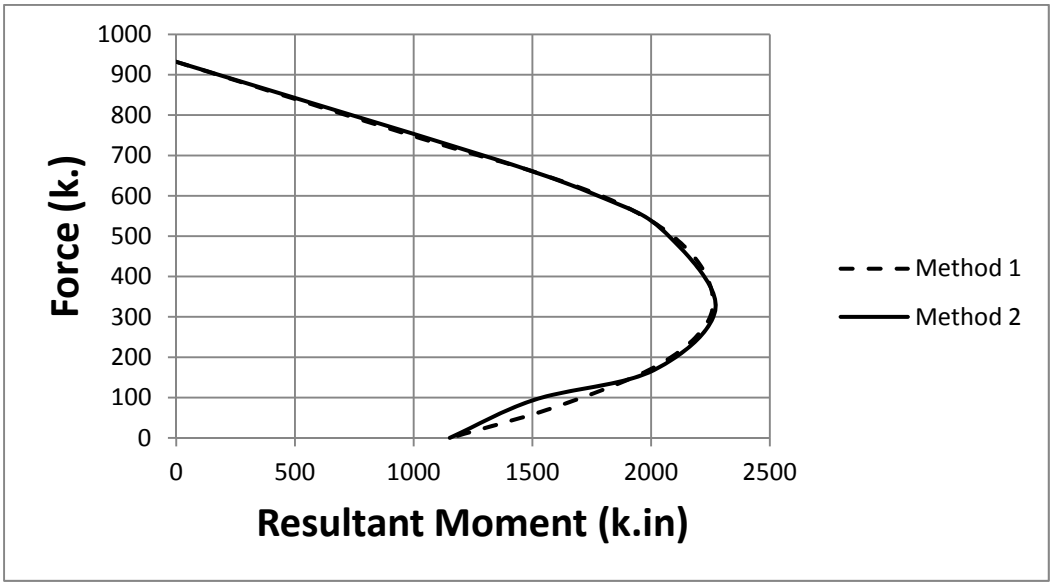

FIGURE 3.14
Comparison of Approach One and Two (α = 4.27)

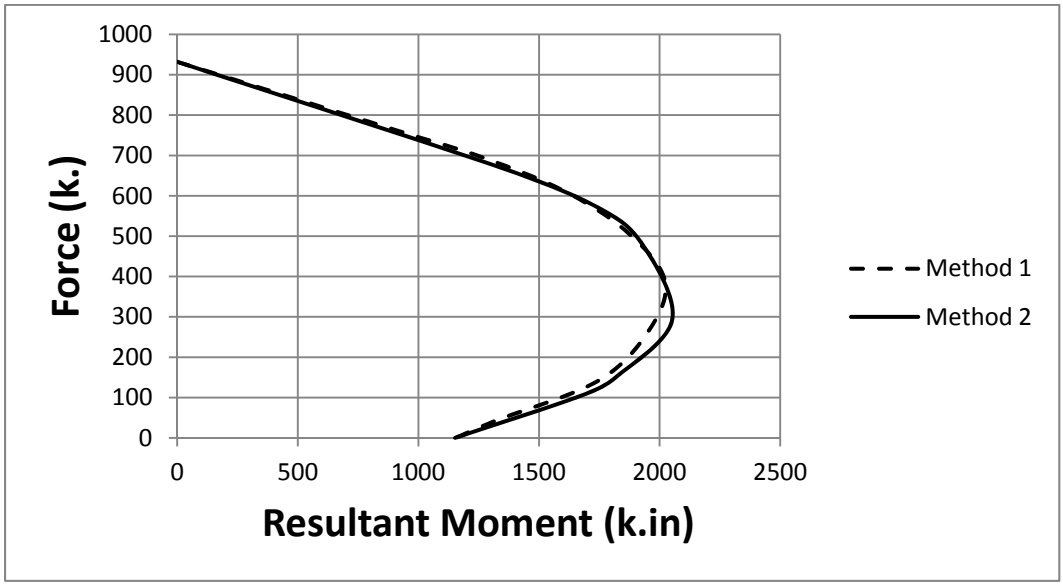

FIGURE 3.15
Comparison of Approach One and Two (α = 10.8)

FIGURE 3.16
Comparison of Approach One and Two (α = 52)

The excellent correlation between the two approaches appears in Figure 3.13 through 3.16. The resultant moment angle is shown below each graph. This is evidence that approach two effectively compared to the well known predefined ultimate strain profile approach. Accordingly, method two can be used in the confined analysis for analyzing the actual capacity of the rectangular columns.

3.2.3.2 Comparison with Existing Commercial Software

KDOT Column Expert is compared with CSI Col 8 of computers and structures Inc. and SP column Software of structure point LLC. The case is selected from Example 11.1 in "Notes on ACI 318-05 Building code Requirements for structural concrete" by PCA. The column details are as follow (Figure 3.17):

Section Height = 24 inches

Section Width = 24 inches

Clear Cover = 1.5 inches

Steel Bars = 16 # 7 evenly distributed

Hoop #3

f'c = 6 *ksi*

fy = 60 ksi.

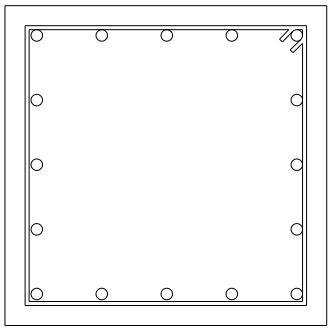

FIGURE 3.17
Column Geometry Used in Software Comparison

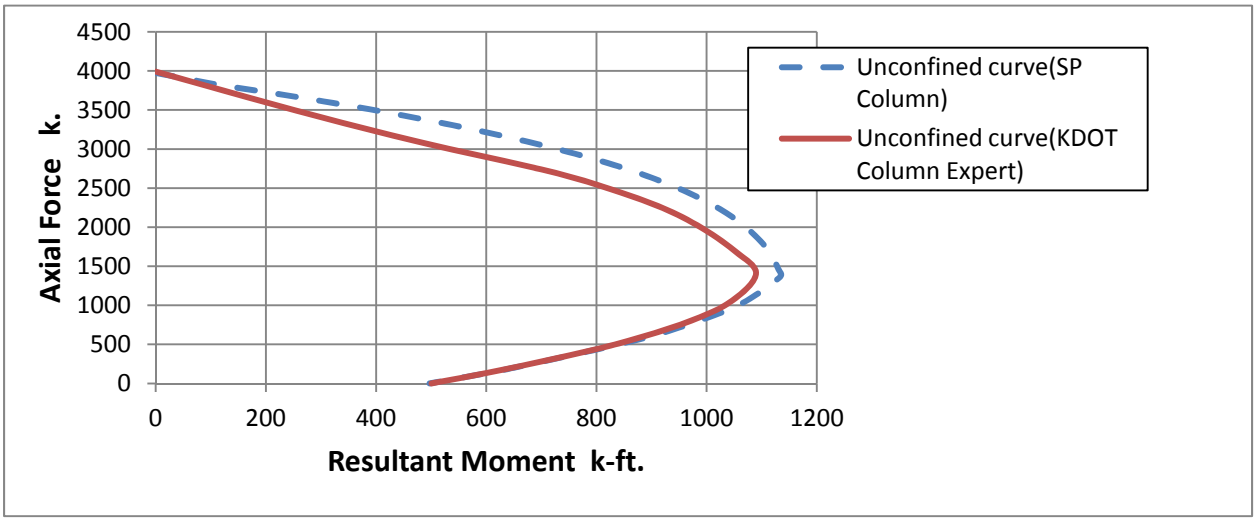

FIGURE 3.18
Unconfined Curve Comparison between KDOT Column Expert and SP Column (α = 0)

Figure 3.18 shows the match between the two programs in axial compression calculations and in tension controlled zone. However KDOT Column Expert shows to be slightly more conservative in compression controlled zone. This might be due to using finite layer approach in calculations that has the advantage of accuracy over other approximations like Whitney stress block.

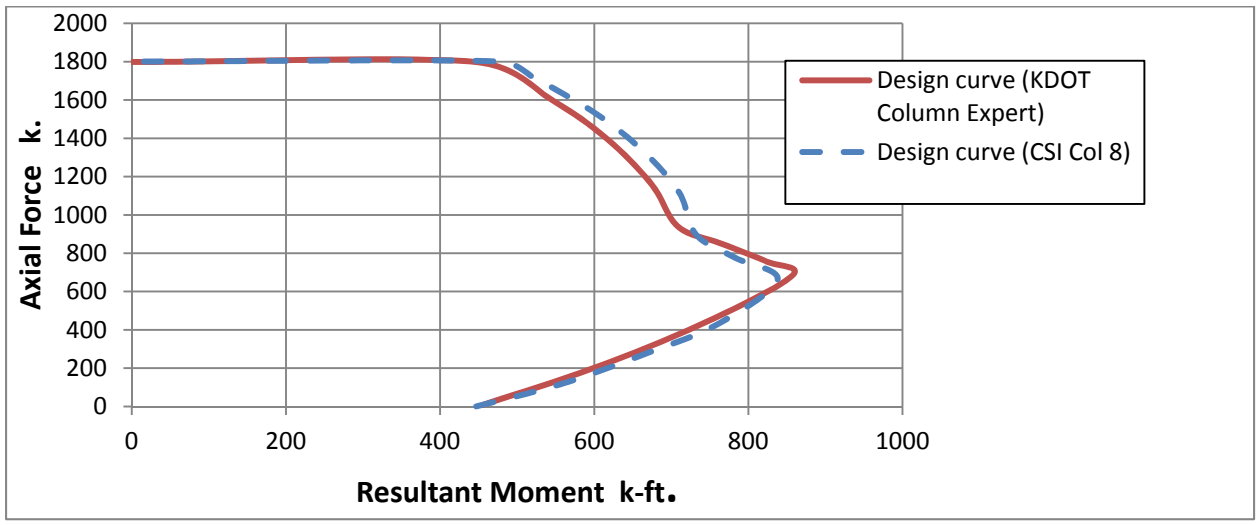

FIGURE 3.19
Design Curve Comparison between KDOT Column Expert and CSI Col 8 Using ACI Reduction Factors

The design curves in Figure 3.19 and Figure 3.20 were plotted using ACI reduction factors that use a reduction factor of 0.65 in compression controlled zone as opposed to 0.75 used by AASHTO. There is a good correlation between the KDOT Column Expert curve and CSI Col 8 and SP Columns curves as shown in Figure 3.19 and Figure 3.20.

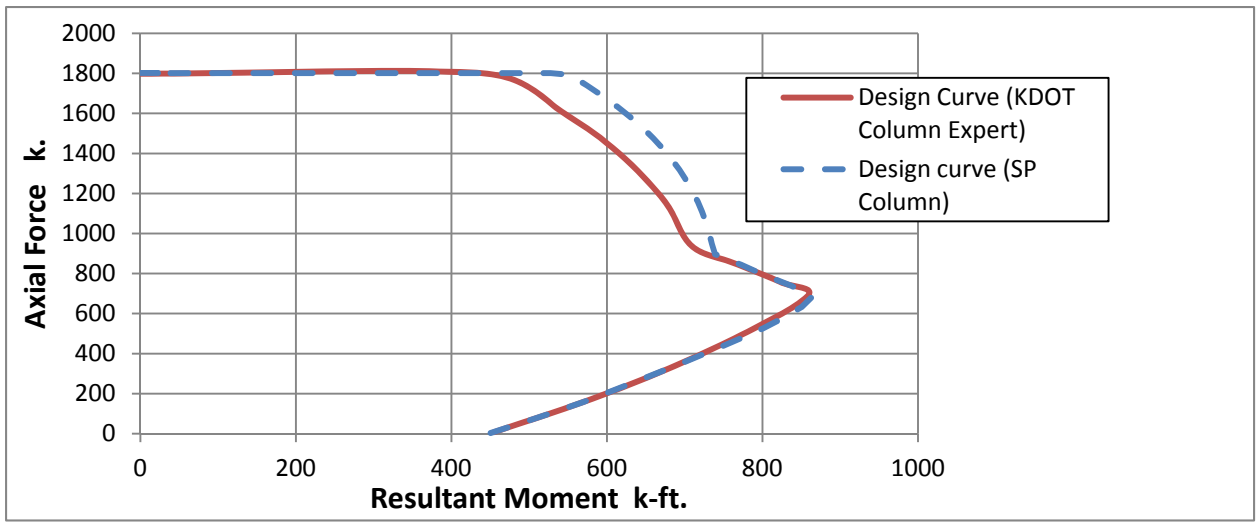

FIGURE 3.20
Design Curve Comparison between KDOT Column Expert and SP Column Using ACI Reduction Factors

3.3 Confined Rectangular Columns Analysis

3.3.1 Formulations

3.3.1.1 Finite Layer Approach (Fiber Method)

The column cross section is divided into finite small-area filaments (Figure 3.21a). The force and moment of each filament is calculated and stored. The rebars are treated as discrete objects in their actual locations. The advantage of that is to avoid inaccuracy generated from using the approximation of the stress block method, as a representative of the compression zone and to well treat cases that have compressive trapezoidal or triangular shapes generated from the neutral axis inclination (Figure 3.21b).

a) b)

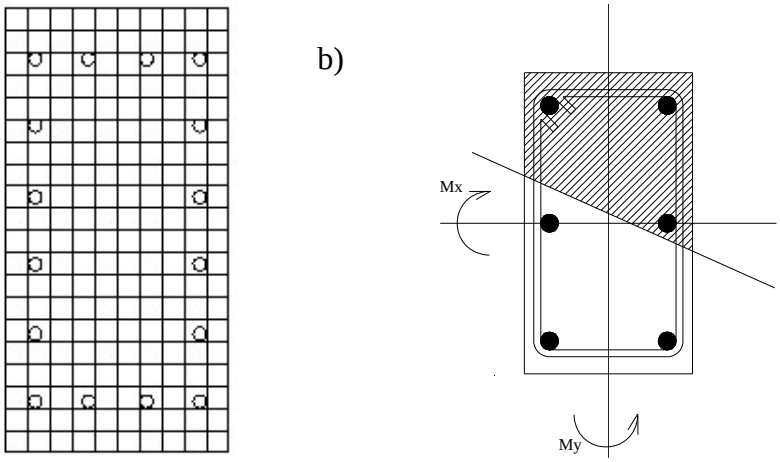

FIGURE 3.21
a) Using Finite Filaments in Analysis b)Trapezoidal Shape of Compression Zone

3.3.1.2 Confinement Model for Concentric Columns

Mander Model for Transversely Reinforced Steel

Mander model (1988) was developed based on the effective lateral confinement pressure, f'_l, and the confinement effective coefficient, k_e which is the same concept found by Sheikh and Uzumeri (1982). The advantage of this procedure is its applicability to any cross section since it defines the lateral pressure based on the section geometry. Mander et al. (1988) showed the adaptability of their model to circular or rectangular sections, under static or dynamic loading, either with monotonically or cyclically applied loads. In order to develop a full stress-strain

curve and to assess ductility, an energy balance approach is used to predict the maximum longitudinal compressive strain in the concrete.

Mander derived the longitudinal compressive concrete stress-strain equation from Popovics model that was originally developed for unconfined concrete (1973):

$$f_c = \frac{f_{cc} x r}{r - 1 + x^r} \qquad \textbf{Equation 3.67}$$

$$x = \frac{\varepsilon_c}{\varepsilon_{cc}} \qquad \textbf{Equation 3.68}$$

$$r = \frac{E_c}{E_c - E_{\sec}} \qquad \textbf{Equation 3.69}$$

$$E_c = 4723\sqrt{f_c^{'}} \quad \text{in } MPa \qquad \textbf{Equation 3.70}$$

$$E_{\sec} = \frac{f_{cc}}{\varepsilon_{cc}} \qquad \textbf{Equation 3.71}$$

and as suggested by Richart et al. (1928) the strain corresponding to the peak confined compressive strength, f'_{cc}, is:

$$\varepsilon_{cc} = \varepsilon_{co}\left[1 + 5\left(\frac{f_{cc}}{f_c^{'}} - 1\right)\right] \qquad \textbf{Equation 3.72}$$

The different parameters of this model are defined in Figure 3.22.

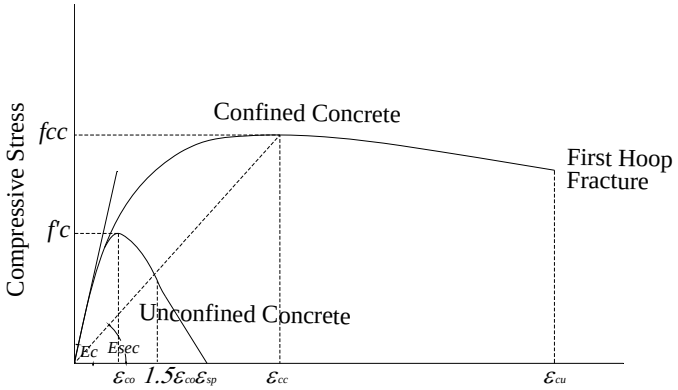

FIGURE 3.22
Axial Stress-Strain Model Proposed by Mander et al. (1988) for Monotonic Loading

As shown in Figure 3.22 Mander et al. (1988) model has two curves; one for unconfined concrete (lower curve) and the other for confined concrete (upper one). The upper one refers to the behavior of confined concrete with concentric loading (no eccentricity). It is shown that it has ascending branch with varying slope starting from E_c decreasing till it reaches the peak confined strength at (f_{cc}, ε_{cc}). Then the slope becomes slightly negative in the descending branch representing ductility till the strain of ε_{cu} where first hoop fractures. The lower curve expresses the unconfined concrete behavior. It has the same ascending branch as the confined concrete curve till it peaks at (f'_c, ε_{co}). Then, the curve descends till 1.5-2$\varepsilon_{co.}$ A straight line is assumed after that till zero strength at spalling strain $\varepsilon_{sp.}$

Mander et al. (1988) utilized an approach similar to that of Sheik and Uzumeri (1982) to determine effective lateral confinement pressure. It was assumed that the area of confined concrete is the area within the centerlines of perimeter of spiral or hoop reinforcement A_{cc} as illustrated in Figure 3.23.

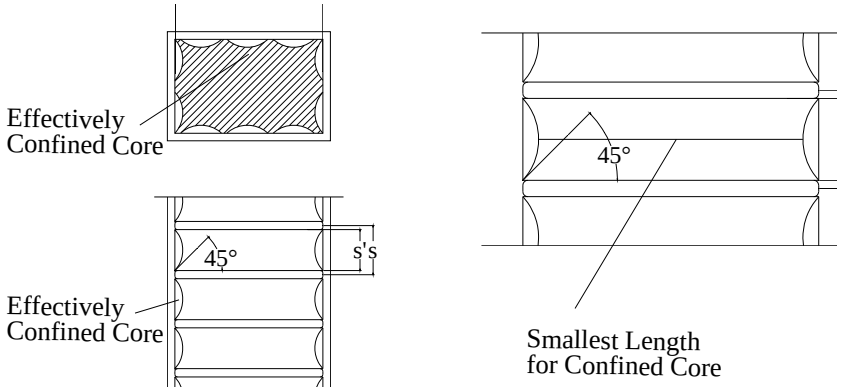

FIGURE 3.23
Effectively Confined Core for Rectangular Hoop Reinforcement (Mander Model)

Figure 3.23 shows that effectively confined concrete core A_e is smaller than the area of core within center lines of perimeter spiral or hoops excluding longitudinal steel area, A_{cc}, and to satisfy that condition the effective lateral confinement pressure f'_l should be a percentage of the lateral pressure f_l:

$$f_l^{'} = k_e f_l \qquad \textbf{Equation 3.73}$$

and the confinement effectiveness coefficient k_e is defined as the ratio of the effective confined area A_e to the area enclosed by centerlines of hoops excluding the longitudinal bars A_{cc}:

$$k_e = \frac{A_e}{A_{cc}} \qquad \textbf{Equation 3.74}$$

$$A_{cc} = A_c - A_{sl} \qquad \textbf{Equation 3.75}$$

$$\frac{A_{cc}}{A_c} = 1 - \frac{A_{sl}}{A_c} \qquad \textbf{Equation 3.76}$$

$$A_{cc} = A_c\left(1 - \rho_{cc}\right) \qquad \textbf{Equation 3.77}$$

where A_c is the area of the section core enclosed by hoops, A_{sl} is the area of longitudinal steel and ρ_{cc} is the ratio of longitudinal steel to the area of the core.

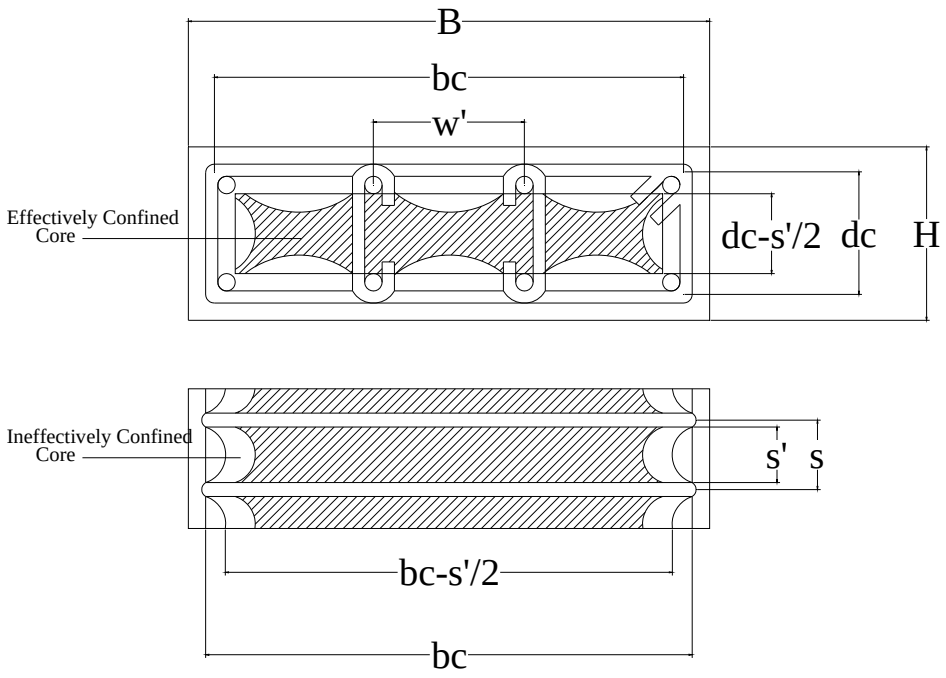

FIGURE 3.24
Effective Lateral Confined Core for Rectangular Cross Section

The total ineffective confined core area in the level of the hoops when there are n bars:

$$A_i = \sum_{i=1}^{n} \frac{\left(w_i^{'}\right)^2}{6} \qquad \textbf{Equation 3.78}$$

Given that the arching formed between two adjacent bars (Figure 3.24) is second degree parabola with an initial tangent slope of 45^o, the ratio of the area of effectively confined concrete to the core area at the tie level:

$$\lambda = \frac{\left(A_{et} - \sum_{i=1}^{n} \frac{\left(w_i^{'}\right)^2}{6} \right)}{A_{et}} \qquad \textbf{Equation 3.79}$$

where $A_c = b_c * d_c$, The area of confined concrete in the midway section between two consecutive ties:

$$A_{emt} = \left(b_c - \frac{s'}{2}\right)\left(d_c - \frac{s'}{2}\right) = b_c d_c \left(1 - \frac{s'}{2b_c}\right)\left(1 - \frac{s'}{2d_c}\right) \quad \textbf{Equation 3.80}$$

Hence, the effective area at midway:

$$A_e = \lambda b_c d_c \left(1 - \frac{s'}{2b_c}\right)\left(1 - \frac{s'}{2d_c}\right) = \frac{1}{b_c d_c}\left(b_c d_c - \sum_{i=1}^{n} \frac{(w_i')^2}{6}\right) b_c d_c \left(1 - \frac{s'}{2b_c}\right)\left(1 - \frac{s'}{2d_c}\right) \quad \textbf{Equation 3.81}$$

$$A_e = \left(b_c d_c - \sum_{i=1}^{n} \frac{(w_i')^2}{6}\right)\left(1 - \frac{s'}{2b_c}\right)\left(1 - \frac{s'}{2d_c}\right) \quad \textbf{Equation 3.82}$$

Using Equation 3.73

$$k_e = \frac{b_c d_c \left(1 - \sum_{i=1}^{n} \frac{(w_i')^2}{6 b_c d_c}\right)\left(1 - \frac{s'}{2b_c}\right)\left(1 - \frac{s'}{2d_c}\right)}{b_c d_c (1 - \rho_{cc})} \quad \textbf{Equation 3.83}$$

$$k_e = \frac{\left(1 - \sum_{i=1}^{n} \frac{(w_i')^2}{6 b_c d_c}\right)\left(1 - \frac{s'}{2b_c}\right)\left(1 - \frac{s'}{2d_c}\right)}{(1 - \rho_{cc})} \quad \textbf{Equation 3.84}$$

and the ratio of the volume of transverse steel in x any y directions to the volume of confined core area ρ_x and ρ_y is defined as:

$$\rho_x = \frac{A_{sx} b_c}{s b_c d_c} = \frac{A_{sx}}{s d_c} \quad \textbf{Equation 3.85}$$

$$\rho_y = \frac{A_{sy} d_c}{s b_c d_c} = \frac{A_{sy}}{s b_c} \quad \textbf{Equation 3.86}$$

A_{sx}, A_{sy} are the total area of lateral steel in x and y direction respectively. The effective lateral confining pressure in x and y directions are given by:

$$f_{lx}^{'} = k_e \rho_x f_{yh}$$ **Equation 3.87**

$$f_{ly}^{'} = k_e \rho_y f_{yh}$$ **Equation 3.88**

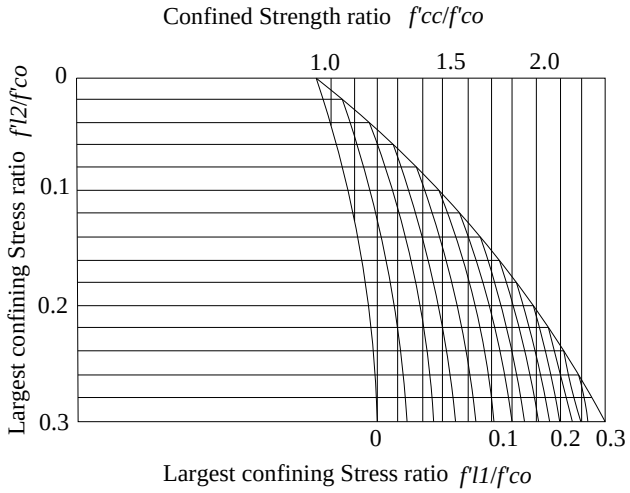

FIGURE 3.25
Confined Strength Determination

Figure 3.25 was developed numerically using multiaxial stress procedure to calculate ultimate confined strength from two given lateral pressures. The numerical procedure is summarized in the following steps:

1. Determining f'_{lx} and f'_{ly} using Equations 3.86 and 3.87
2. Converting the positive sign of f'_{lx} and f'_{ly} from positive to negative to represent the major and intermediate principal stresses (These values are referred to as σ_1 and σ_2 so that $\sigma_1 > \sigma_2$).
3. Estimating the confined strength f_{cc} (σ_3) as the minor principal stress
4. Calculating the octahedral stress σ_{oct}, octahedral shear stress τ_{oct} and lode angle θ as follows:

$$\sigma_{oct} = \frac{1}{3}(\sigma_1 + \sigma_2 + \sigma_3)$$ **Equation 3.89**

$$\tau_{oct} = \frac{1}{3}\left[(\sigma_1 - \sigma_2)^2 + (\sigma_2 - \sigma_3)^2 + (\sigma_3 - \sigma_1)^2\right]^{\frac{1}{2}}$$ **Equation 3.90**

$$\cos\vartheta = \left[\frac{\sigma_1 - \sigma_{oct}}{\sqrt{2}\tau_{oct}}\right]$$ **Equation 3.91**

1. Determining the ultimate strength meridian surfaces T,C (for θ =60^o and 0^o respectively) using the following equations derived by Elwi and Murray (1979) from data by Scickert and Winkler (1977):

$$T = 0.069232 - 0.661091\overline{\sigma_{oct}} - 0.049350\overline{\sigma_{oct}}^2$$ **Equation 3.92**

$$C = 0.122965 - 1.150502\overline{\sigma_{oct}} - 0.315545\overline{\sigma_{oct}}^2$$ **Equation 3.93**

$$\overline{\sigma_{oct}} = \sigma_{oct} / f_c^{'}$$ **Equation 3.94**

2. Determining the octahedral shear stress using the interpolation function found by Willam and Warnke (1975):

$$\overline{\tau_{oct}} = C\frac{0.5D/\cos\theta + (2T - C)\left[D + 5T^2 - 4TC\right]^{\frac{1}{2}}}{D + (2T - C)^2} \qquad \textbf{Equation 3.95}$$

$$D = 4\left(C^2 - T^2\right)\cos^2\theta \qquad \textbf{Equation 3.96}$$

$$\tau_{oct} = \overline{\tau_{oct}} f_c^{'} \qquad \textbf{Equation 3.97}$$

3. Recalculating f_{cc} using the following equation (same as Equation 3.89) but solving for σ_3:

$$\sigma_3 = \frac{\sigma_1 + \sigma_2}{2} - \sqrt{4.5\tau_{oct}^2 - 0.75(\sigma_1 - \sigma_2)^2} \qquad \textbf{Equation 3.98}$$

4. If the value from Equation 3.97 is close to the initial value then there is convergence. Otherwise, the value from Equation 3.97 is reused in steps 4 through 8.

Equations 3.91 and 3.92 that define the tension and compression meridians are compared with different equations for different unconfined compressive strength. The results are shown in section 3.3.3.2.

Mander et al. (1988) proposed an energy balancing theory to predict the ultimate confined strain, which is determined at the first hoop fracture. They stated that the additional ductility for confined concrete results from the additional strain energy stored in the hoops U_{sh}. Therefore from equilibrium:

$$U_{sh} = U_g - U_{co} \qquad \textbf{Equation 3.99}$$

where U_g is the external work done in the concrete to fracture the hoop, and U_{co} is the work done to cause failure to the unconfined concrete. U_{sh} can be represented by the area under the tension stress strain curve for the transverse steel between zero and fracture strain ε_{sf}.

$$U_{sh} = \rho_s A_{cc} \int_0^{\varepsilon_{sf}} f_s d\varepsilon \qquad \textbf{Equation 3.100}$$

while *Ug* is equal to the area under the confined stress strain curve plus the area under the longitudinal steel stress strain curve:

$$U_g = \int_0^{\varepsilon_{scu}} f_c A_{cc} d\varepsilon + \int_0^{\varepsilon_{scu}} f_s A_{sl} d\varepsilon \qquad \textbf{Equation 3.101}$$

similarly, it was proven experimentally that U_{co} is equal to:

$$U_{co} = A_{cc} \int_0^{\varepsilon_{spall}} f_c d\varepsilon = A_{cc} 0.017\sqrt{f_c^{'}} \text{ in } MPa \qquad \textbf{Equation 3.102}$$

and

$$U_{sh} = \rho_s A_{cc} \int_0^{\varepsilon_{sf}} f_s d\varepsilon = 110\rho_s A_{cc} \qquad \textbf{Equation 3.103}$$

Substituting Equations 3.100, 3.101, and 3.102 into Equation 3.98:

$$110\rho_s = \int_0^{\varepsilon_{cu}} f_c d\varepsilon + \int_0^{\varepsilon_{cu}} f_{sl} d\varepsilon - 0.017\sqrt{f_c^{'}} \qquad \textbf{Equation 3.104}$$

where fsl is the stress in the longitudinal steel. Equation 3.103 can be solved numerically for $\varepsilon_{cu.}$

3.3.1.3 Confinement Model for Eccentric Columns

Unlike concentric loading, the eccentric loading generates bending moment in addition to axial loading. Columns subjected to eccentric loading behave differently from those concentrically loaded, as the shape of the stress strain curve for fully confined reinforced concrete (concentric loading) shows higher peak strength and more ductility than the unconfined one (infinite eccentricity). Most of the previous studies were based on the uniform distribution of compressive strain across the column section.

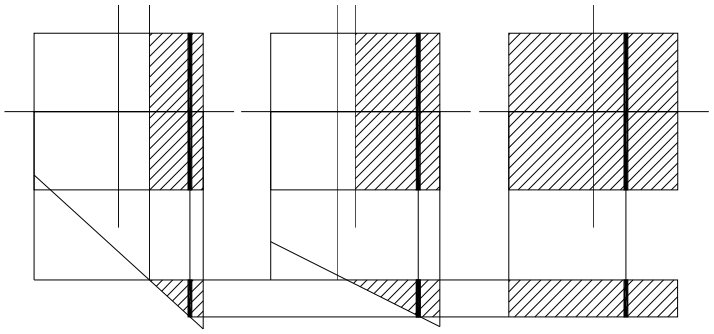

FIGURE 3.26
Effect of Compression Zone Depth on Concrete Stress

Figure 3.26 illustrates three different sections under concentric load, combination of axial load and bending moment and pure bending moment, the highlighted fiber in the three cases has the same strain. Any current confinement model yields the same stress for these three fibers. So the depth or size of compression zone does not have any role in predicting the stress. Hence, it is more realistic to relate the strength and ductility in a new model to the level of confinement utilization and compression zone size.

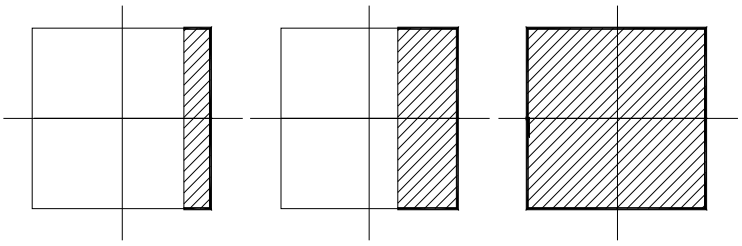

FIGURE 3.27
Amount of Confinement Engaged in Different Cases

By definition, confinement gets engaged only when member is subjected to compression. Compressed members tend to expand in lateral direction, and if confined, confinement will prevent this expansion to different levels based on the degree of compressive force and confinement strength as well. For fully compressed members (Figure 3.27), confinement becomes effective 100% as it all acts to prevent the lateral expansion. Whereas members subjected to compression and tension, when the neutral axis lies inside the section perimeter, only confinement adjacent to the compression zone gets engaged. Accordingly, members become partially confined.

In literature, various models were implemented to assess the ultimate confined capacity of columns under concentric axial load. On the other hand the effect of partial confinement in case of eccentric load (combined axial load and bending moments) is not investigated in any proposed model. Therefore, it is pertinent to relate the strength and ductility of reinforced concrete to the degree of confinement utilization in a new model.

The two curves of fully confined and unconfined concrete in any proposed model are used in the eccentricity-based model as upper and lower bounds. The upper curve refers to concentrically loaded confined concrete (zero eccentricity), while the lower one refers to pure bending applied on concrete (infinite eccentricity). In between the two boundaries, infinite numbers of stress-strain curves can be generated based on the eccentricity. The higher the eccentricity the smaller the confined concrete region in compression. Accordingly, the ultimate confined strength is gradually reduced from the fully confined value f_{cc} to the unconfined value f'_c as a function of eccentricity to diameter ratio. In addition, the ultimate strain is gradually

reduced from the ultimate strain ε_{cu} for fully confined concrete to the ultimate strain for unconfined concrete $1.5\varepsilon_{co}$.

The relation between the compression area to whole area ratio and normalized eccentricity is complicated in case of rectangular cross sections due to the existence of two bending axes. The force location with respect to the two axes causes the compression zone to take a trapezoidal shape sometimes if the force applied is not along one of the axes. Hence the relation between the compression area and the load eccentricity needs more investigation as oppose to the case of circular cross section which was shown to be simpler.

The normalized eccentricity is plotted against the compression area to cross sectional area ratio for rectangular cross sections having different aspect ratio (length to width) at the unconfined failure level. The aspect ratios used are 1:1, 2:1, 3:1, 4:1 as shown in Figures 3.28, 3.29, 3.30, and 3.31. Each curve represents specific α angle (tan α = *My/Mx*) ranging from zero to ninety degrees. It is seen from these figures that there is inversely proportional relation between the normalized eccentricity and compression zone ratio regardless of the α angle followed.

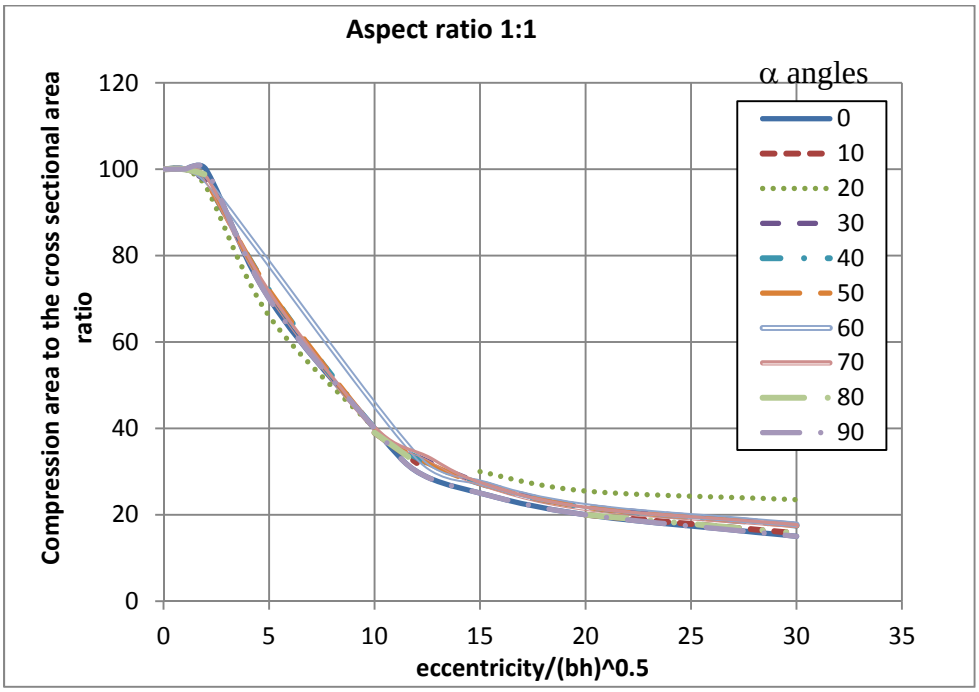

FIGURE 3.28
Normalized Eccentricity versus Compression Zone to Total Area Ratio

(Aspect Ratio 1:1)

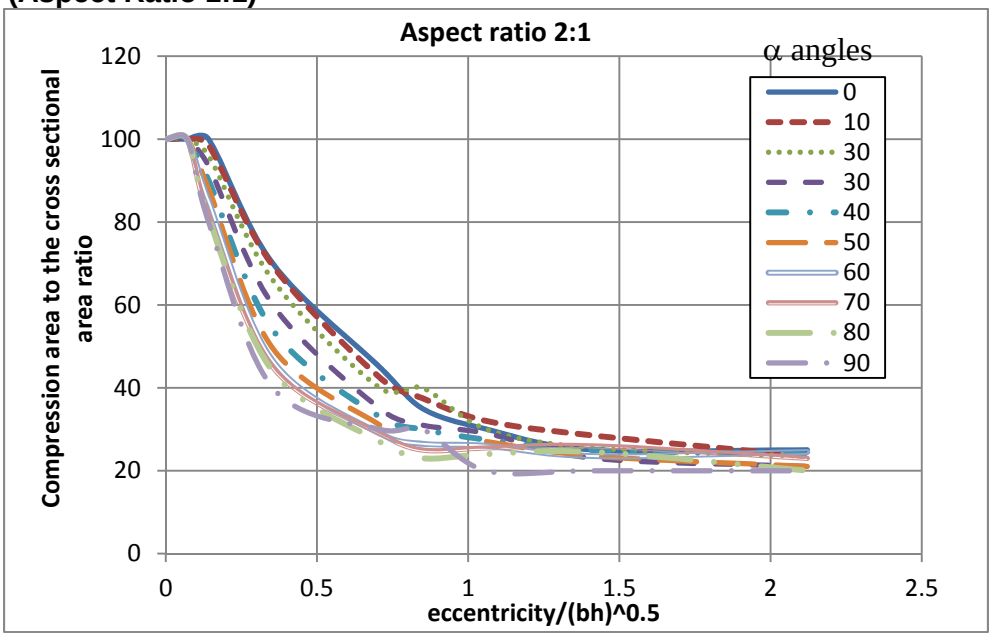

FIGURE 3.29
Normalized Eccentricity versus Compression Zone to Total Area Ratio (Aspect Ratio 2:1)

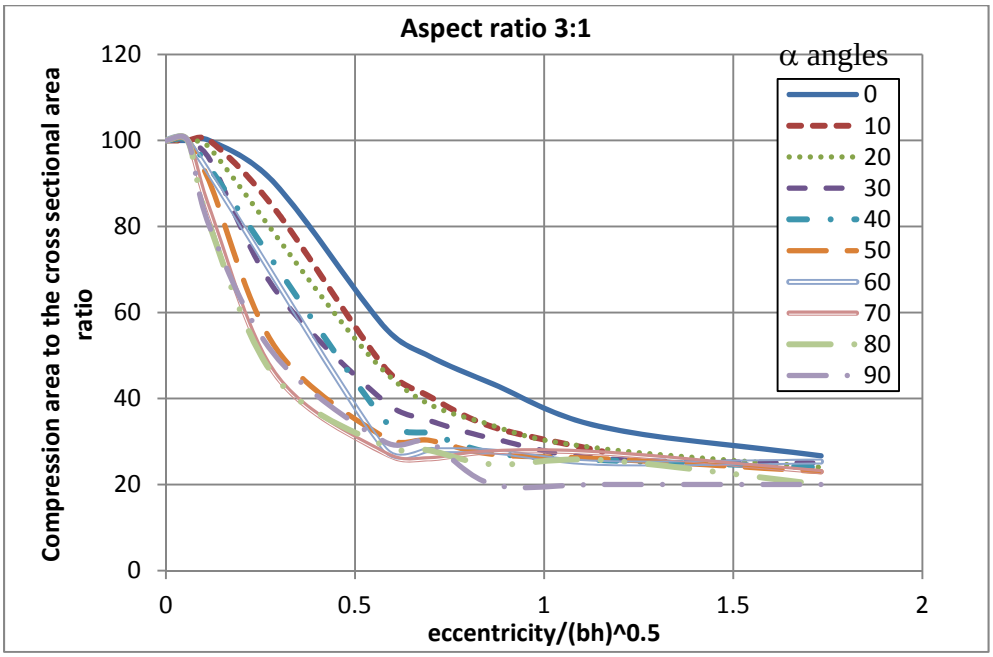

FIGURE 3.30
Normalized Eccentricity versus Compression Zone to Total Area Ratio (Aspect Ratio 3:1)

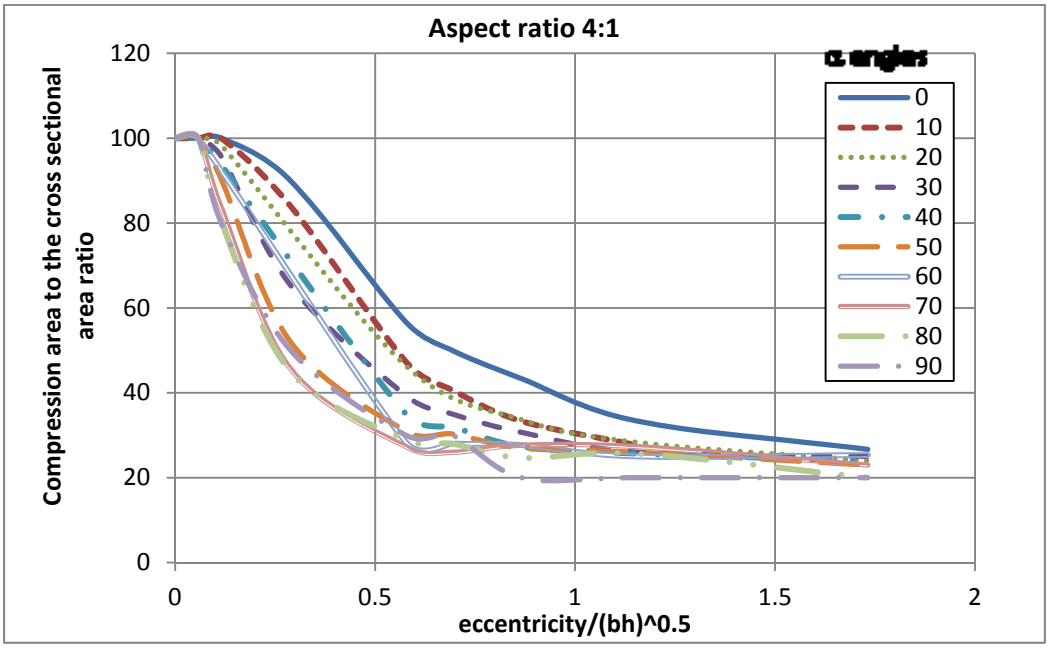

FIGURE 3.31
Normalized Eccentricity versus Compression Zone to Total Area Ratio (Aspect Ratio 4:1)

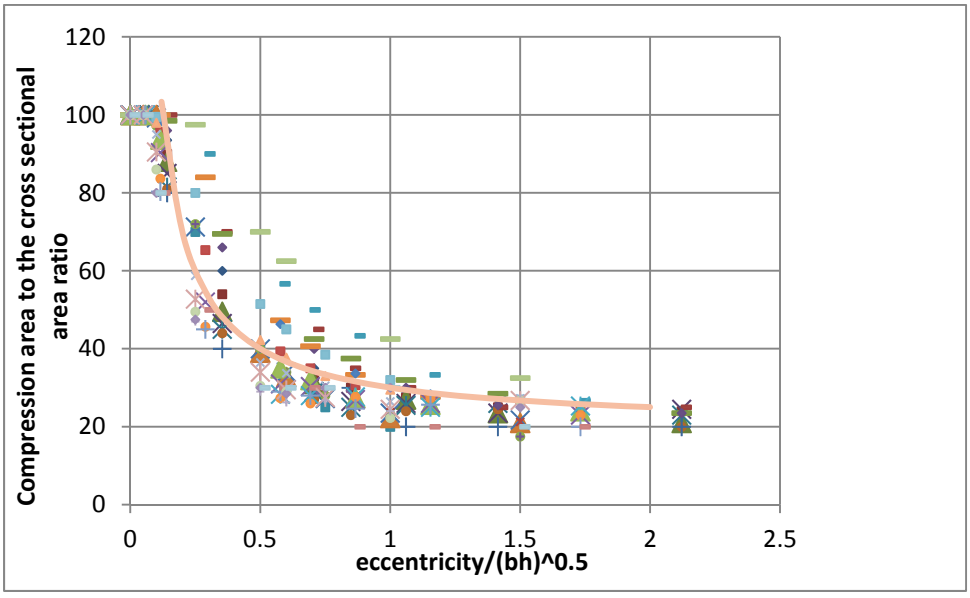

FIGURE 3.32
Cumulative Chart for Normalized Eccentricity against Compression Zone Ratio (All Data Points)

In order to find accurate mathematical expression that relates the compression zone to load eccentricity, the data from Figures 3.28 through 3.31 are replotted as scatter points in Figure 3.32.

The best fitting curve of these points based on the least square method has the following equation:

$$C_R = \frac{0.2 * \frac{e}{\sqrt{bh}} + 0.1}{\frac{e}{\sqrt{bh}}}$$

Equation 3.105

where C_R refers to compression area to cross sectional area ratio.

Eccentric Model based on Mander Equations

The equation that defines the peak strength $\overline{f_{cc}}$ according to the eccentricity is:

$$\overline{f_{cc}} = \frac{1}{1+\frac{1}{C_R}} f_{cc} + \frac{1}{1+C_R} f_c'$$

Equation 3.106

whereas the equation developed for circular cross sections

$$\overline{f_{cc}} = \frac{1}{1+\frac{e}{\sqrt{bh}}} f_{cc} + \frac{1}{1+\frac{\sqrt{bh}}{e}} f_c'$$

Equation 3.107

where e is the eccentricity, b and h is the column dimensions and $\overline{f_{cc}}$ is the peak strength at the eccentricity (e). The corresponding strain $\overline{\varepsilon_{cc}}$ is given by

$$\overline{\varepsilon_{cc}} = \varepsilon_{co}\left[1+5\left(\frac{\overline{f_{cc}}}{f_c'}-1\right)\right]$$

Equation 3.108

and the maximum strain corresponding to the required eccentricity will be a linear function of stress corresponding to maximum strain for confined concrete f_{cu} and the maximum unconfined concrete f_{cuo} at $\varepsilon_{cuo} = 0.003$:

$$\overline{\varepsilon_{cu}} = \overline{\varepsilon_{cc}} \left[\frac{\frac{\overline{E_{\sec}}}{E_{\sec,u}} \bar{r}}{\frac{c}{\overline{\varepsilon_{cu}}} + 1 - \bar{r} + 1} \right]^{\frac{1}{\bar{r}}} \qquad E_{\sec,u} = \frac{f_{cu} - f_{cuo}}{\varepsilon_{cu} - 0.003}$$ **Equation 3.109**

$$c = \frac{f_{cu} - E_{\sec,u} * 0.003}{E_{\sec,u}} \quad \overline{E_{\sec}} = \frac{\overline{f_{cc}}}{\overline{\varepsilon_{cc}}} \qquad \bar{r} = \frac{E_c}{E_c - \overline{E_{\sec}}}$$ **Equation 3.110**

In order to verify the accuracy of the model at the extreme cases, the eccentricity is first set to be zero. The coefficient of f'_c will be zero in Equation 3.105 and Equations 3.105, 3.106 and 3.107 will reduce to be:

$$\overline{f_{cc}} = f_{cc}$$ **Equation 3.111**

$$\overline{\varepsilon_{cc}} = \varepsilon_{cc}$$ **Equation 3.112**

$$\overline{\varepsilon_{cu}} = \varepsilon_{cu}$$ **Equation 3.113**

On the other hand, if the eccentricity is set to be infinity the other coefficient will be zero, and the strength, corresponding strain and ductility equations will be:

$$\overline{f_{cc}} = f_c^{'}$$ **Equation 3.114**

$$\overline{\varepsilon_{cc}} = \varepsilon_{co}$$ **Equation 3.115**

$$\overline{\varepsilon_{cu}} = 0.003$$ **Equation 3.116**

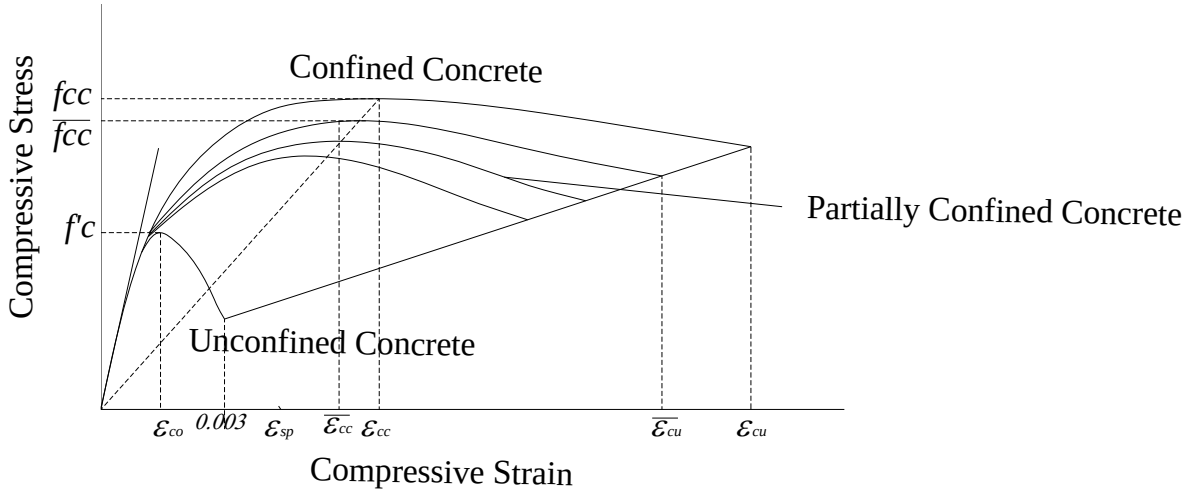

FIGURE 3.33
Eccentricity Based Confined Mander Model

Any point on the generated curves the stress-strain function can be calculated using the following equation:

$$f_c = \frac{\overline{f_{cc}}\,\overline{x}\,\overline{r}}{\overline{r} - 1 + \overline{x}^{\overline{r}}} \qquad \textbf{Equation 3.117}$$

where:

$$\overline{x} = \frac{\varepsilon_c}{\overline{\varepsilon_{cc}}} \qquad \textbf{Equation 3.118}$$

$$\overline{r} = \frac{E_c}{E_c - \overline{E_{\sec}}} \qquad \textbf{Equation 3.119}$$

$$\overline{E_{\sec}} = \frac{\overline{f_{cc}}}{\overline{\varepsilon_{cc}}} \qquad \textbf{Equation 3.120}$$

To show the distinction between the Eccentric model designed for rectangular cross sections, Figure 3.34 and that of circular cross sections, Figure 3.35, Equations 3.105 to 3.107

and 3.114 to 3.117 are used in plotting a set of Stress-Strain curves with eccentricity ranging from 0 inches to ∞. The column cross sectional properties used to plot these curves is 36 in *36 inches, steel bars are 13 #11, spiral bar is # 5, spacing is 4 inches, f'_c is equal to 4 *ksi*, f_y is equal to 60 *ksi* and f_{yh} is equal to 60 *ksi*. This case is used in plotting the Eccentric Stress-Strain curve that are developed for rectangular cross sectional concrete columns; Figure 3.34 while the same case is used in plotting the eccentric Stress-Strain curves that are developed for circular cross section, Figure 3.35. The eccentric stress-Strain curves in Figure 3.35 are almost parallel and equidistant to each other. Whereas, the leap from one curve to the next one in Figure 3.34 is varying. This is due to the effect of the coefficient C_R, that is used in Equation 3.105, which has non linear impact on the compression zone as opposed to the linear relation between the eccentricity and compression zone for circular cross sections (Figure 3.35)

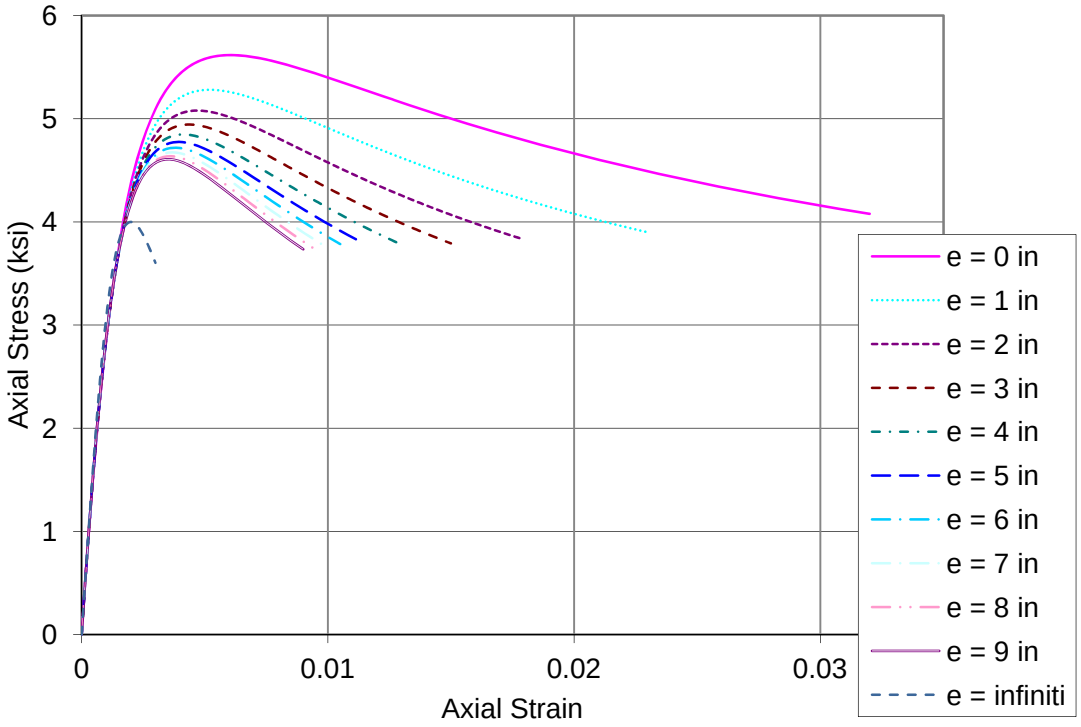

FIGURE 3.34
Eccentric Based Stress-Strain Curves Using Compression Zone Area to Gross Area Ratio

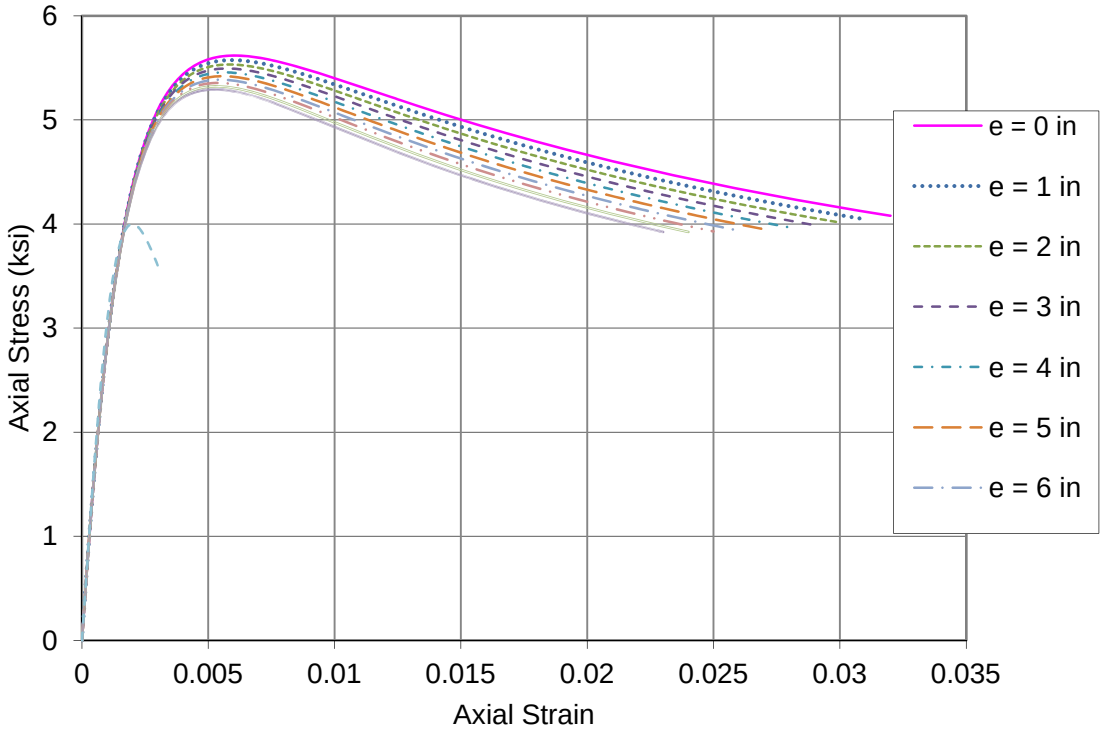

FIGURE 3.35
Eccentric Based Stress-Strain Curves Using Normalized Eccentricity Instead of Compression Zone Ratio

3.3.1.4 Generalized Moment of Area Theorem

The very general axial stress equation in an unsymmetrical section subjected to axial force P and biaxial bending M_x and M_y (Hardy Cross 1930):

$$\sigma_z = \frac{P}{A} + \frac{M_x I_y - M_y I_{xy}}{I_x I_y - I_{xy}^2} y + \frac{M_y I_x - M_x I_{xy}}{I_x I_y - I_{xy}^2} x \qquad \textbf{Equation 3.121}$$

σ_z = normal stress at any point (a) in cross section

P = applied load.

A = cross sectional area.

M_x = bending moment about x-axis

M_y = bending moment about y-axis

x = distance between the point (a) and y-axis

y = distance between the point (a) and x-axis

I_x = moment of inertia about x-axis

I_y = moment of inertia about y-axis

I_{xy} = product moment of inertia in xy plane

Rewriting Equation 3.118 to determine the strain at any point in the cross section:

$$\varepsilon_z = \frac{P}{EA} + \frac{M_x EI_y - M_y EI_{xy}}{EI_x EI_y - EI_{xy}^2} y + \frac{M_y EI_x - M_x EI_{xy}}{EI_x EI_y - EI_{xy}^2} x \qquad \textbf{Equation 3.122}$$

In case of linear elastic analysis, E in EA or EI expressions is constant (E=Ec). However, if the section has linear strain and nonlinear stress profile, it will amount to variable E profile (per filament) in nonlinear analysis. Accordingly, the section parameters must include $\sum_i E_i A_i$, $\sum_i E_i I_i$ for a more generalized theory (Rasheed and Dinno 1994). Note that the linear strain profile of the section from Equation 3.119 yields two distinct constant curvatures:

$$\phi_x = \frac{M_x EI_y - M_y EI_{xy}}{\beta^2} \qquad \textbf{Equation 3.123}$$

$$\phi_y = \frac{M_y EI_x - M_x EI_{xy}}{\beta^2} \qquad \textbf{Equation 3.124}$$

ϕ_x = x- curvature

ϕ_y = y- curvature

$\beta^2 = EI_x EI_y - EI_{xy}^2$

To prove Equations 3.120 and 3.121 above, invoke the coupled equations of moments about the centroid (Bickford 1998).

$$M_x = EI_x \phi_x + EI_{xy} \phi_y \qquad \textbf{Equation 3.125}$$

$$M_y = EI_{xy} \phi_x + EI_y \phi_y \qquad \textbf{Equation 3.126}$$

In a matrix form:

$$\begin{bmatrix} M_x \\ M_y \end{bmatrix} = \begin{bmatrix} EI_x & EI_{xy} \\ EI_{xy} & EI_y \end{bmatrix} \begin{bmatrix} \phi_x \\ \phi_y \end{bmatrix}$$

Equation 3.127

Inverting Equation 3.124

$$\begin{bmatrix} \phi_x \\ \phi_y \end{bmatrix} = \frac{1}{\beta^2} \begin{bmatrix} EI_y & -EI_{xy} \\ -EI_{xy} & EI_x \end{bmatrix} \begin{bmatrix} M_x \\ M_y \end{bmatrix}$$

Equation 3.128

which reproduces Equations 3.120 and 3.121. Rewriting Equation 3.119 in terms of ϕ_x and ϕ_y

$$\varepsilon_z = \frac{P}{EA} + \phi_x y + \phi_y x$$

Equation 3.129

Finding ε_z at the centroid, since $x = y = 0$.

$$\varepsilon_o = P/EA$$

Equation 3.130

Solving for P at the geometric centroid;

$$P = EA\overline{\varepsilon_o} - EA\bar{y}\phi_x - EA\bar{x}\phi_y$$

Equation 3.131

$\overline{\varepsilon_o}$ is the axial strain at the geometric centroid

But

$$EAM_x = EA\bar{y} \qquad \bar{y} = Y_G - Y_c$$

$$EAM_y = EA\bar{x} \qquad \bar{x} = X_G - X_c$$

Y_G is the vertical distance to the geometric centroid measured from bottom, X_G is the distance to the geometric centroid measured from the cross section's left side, Y_c is the vertical distance to the inelastic centroid measured from the bottom and X_c is the horizontal distance to the inelastic centroid measured from the cross section's left side

Thus,

$$P = EA\overline{\varepsilon_o} - EAM_x\phi_x - EAM_y\phi_y \qquad \textbf{Equation 3.132}$$

The general formula of the moments about the geometric x-axis and the geometric y-axis is derived as follows:

when the moment is transferred from the centroid to the geometric centroid (Figure 3.36a)

$$\overline{M_x} = M_x - P\overline{y} \qquad \textbf{Equation 3.133}$$

Substituting Equations 3.122 and 3.129 into 3.130 yields:

$$\overline{M_x} = EI_x\phi_x + EI_{xy}\phi_y - EA\overline{\varepsilon_o}\,\overline{y} + EAM_x\phi_x\overline{y} + EAM_y\phi_y\overline{y} \qquad \textbf{Equation 3.134}$$

$$\overline{M_x} = -EAM_x\overline{\varepsilon_o} + \left(EI_x + EAM_x\overline{y}\right)\phi_x + \left(EI_{xy} + EAM_y\overline{y}\right)\phi_y \qquad \textbf{Equation 3.135}$$

Similarly, Figure 3.36b:

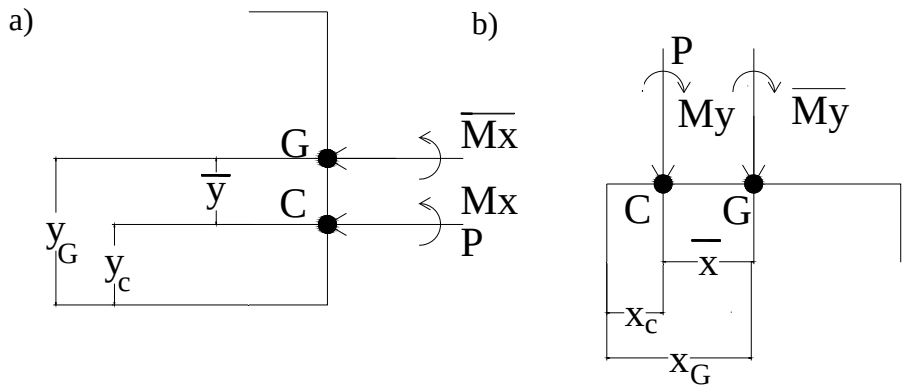

FIGURE 3.36
Transferring Moment from Centroid to the Geometric Centroid

$$\overline{M_y} = M_y - P\bar{x} \qquad \textbf{Equation 3.136}$$

$$\overline{M_y} = EI_{xy}\phi_x + EI_y\phi_y - EA\overline{\varepsilon_o}\,\bar{x} + EAM_x\phi_x\bar{x} + EAM_y\phi_y\bar{x} \qquad \textbf{Equation 3.137}$$

$$\overline{M_y} = -EAM_y\overline{\varepsilon_o} + \left(EI_{xy} + EAM_x\bar{x}\right)\phi_x + \left(EI_y + EAM_y\bar{x}\right)\phi_y \qquad \textbf{Equation 3.138}$$

The terms $EI_x + EAM_x\bar{y}$ and $EI_y + EAM_y\bar{x}$ represent the $\overline{EI_x}$ and $\overline{EI_y}$ about the geometric centroid respectively using the parallel axis theorem. And the terms $EI_{xy} + EAM_x\bar{x}$ and $EI_{xy} + EAM_y\bar{y}$ are equal given that: $EAM_x\bar{x} = EA\bar{y}\bar{x}$ and $EAM_y\bar{y} = EA\bar{y}\bar{x}$. Using Equations 3.129, 3.132 and 3.135 yields the extended general moment of area equation:

$$\begin{bmatrix} P \\ \overline{Mx} \\ \overline{M_y} \end{bmatrix} = \begin{bmatrix} EA & -EAM_x & -EAM_y \\ -EAM_x & \overline{EI_x} & \overline{EI_{xy}} \\ -EAM_y & \overline{EI_{xy}} & \overline{EI_y} \end{bmatrix} \begin{bmatrix} \varepsilon \\ \phi_x \\ \phi_y \end{bmatrix} \qquad \textbf{Equation 3.139}$$

Since the moment of area about the centroid vanishes (Rasheed and Dinno 1994), Equation 3.136 reduces to a partially uncoupled set when it is applied back at the centroid since EAM_x and EAM_y vanish about the centroid.

$$\begin{bmatrix} P \\ M_x \\ M_y \end{bmatrix} = \begin{bmatrix} EA & 0 & 0 \\ 0 & EI_x & EI_{xy} \\ 0 & EI_{xy} & EI_y \end{bmatrix} \begin{bmatrix} \varepsilon_o \\ \phi_x \\ \phi_y \end{bmatrix}$$ **Equation 3.140**

which is simply Equations 3.122, 3.123, and 3.127

3.3.2 Numerical Formulation

This approach simulates the radial loading of the force and moments by keeping the relative proportion between them constant during the loading. Accordingly, all the points will be exactly on the 2D interaction diagram. In addition to the ultimate points, the complete load deformation response is generated. The cross section analyzed is loaded incrementally by maintaining a certain eccentricity between the axial force P and the resultant moment M_R. Since M_R is generated as the resultant of M_x and M_y, the angle $\alpha = \tan^{-1}(M_y/M_x)$ is kept constant for a certain 2D interaction diagram. Since increasing the load and resultant moment cause the neutral axis to vary nonlinearly, the generalized moment of area theorem is devised. This method is based on the general response of rectangular unsymmetrical section subjected to biaxial bending and axial compression. The asymmetry stems from the different behavior of concrete in compression and tension.

The method is developed using the incremental iterative analysis algorithm, secant stiffness approach and proportional or radial loading. It is explained in the following steps Figure 3.40:

1. Calculating the initial section properties:
   - Elastic axial rigidity EA:

$$EA = \sum_i E_c w_i t_i + \sum_i (E_s - E_c) A_{si}$$ **Equation 3.141**

E_c = initial secant modulus of elasticity of the concrete

E_s = initial modulus of elasticity of the steel rebar

- The depth of the elastic centroid position from the bottom fiber of the section Y_c and from the left side of the section $X_{c,}$ Figure 3.37

$$Y_c = \frac{\sum_i E_c w_i t_i (H - Y_i) + \sum_i (E_s - E_c) A_{si} (H - Y_{si})}{EA}$$

Equation 3.142

$$X_c = \frac{\sum_i E_c w_i t_i (B - X_i) + \sum_i (E_s - E_c) A_{si} (B - X_{si})}{EA}$$

Equation 3.143

- Elastic flexural rigidity about the elastic centroid *EI*:

$$EI_x = \sum_i E_c w_i t_i (H - Y_i - Y_c)^2 + \sum_i (E_s - E_c) A_{si} (H - Y_{si} - Y_c)^2$$

Equation 3.144

$$EI_y = \sum_i E_c w_i t_i (B - X_i - X_c)^2 + \sum_i (E_s - E_c) A_{si} (H - X_{si} - X_c)^2$$

Equation 3.145

$$EI_{xy} = \sum_i E_c w_i t_i (H - Y_i - Y_c)(B - X_i - X_c) + \sum_i (E_s - E_c) A_{si} (H - Y_{si} - Y_c)(B - X_i - X_c)$$

Equation 3.146

Typically the initial elastic Yc = *H/2*, X_c = *B/2* and EI_{xy} = 0

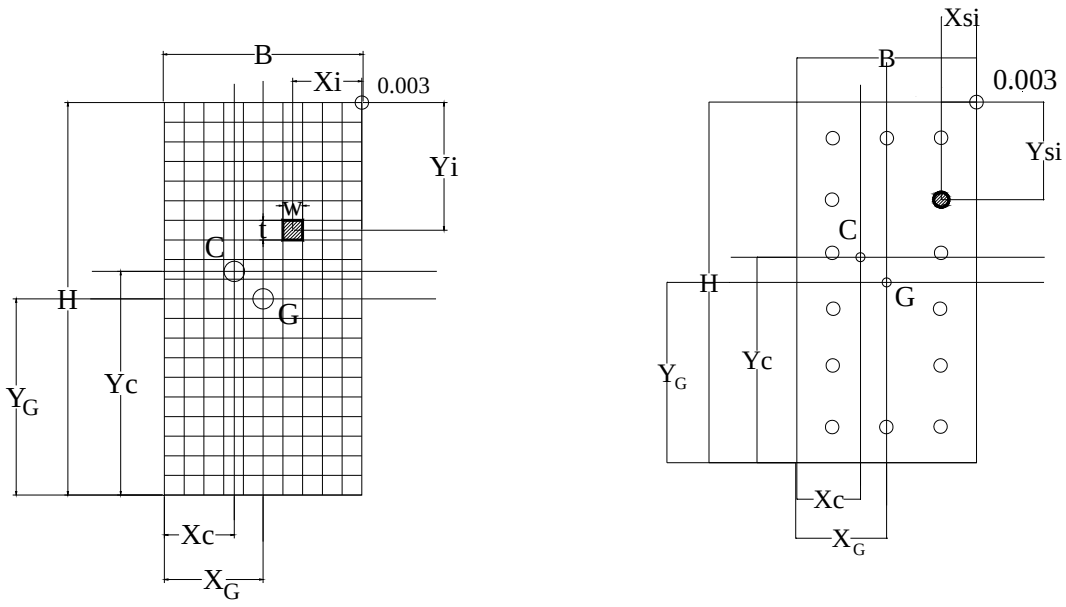

FIGURE 3.37
Geometric Properties of Concrete Filaments and Steel Rebars with Respect to Crushing Strain Point, Geometric Centroid and Inelastic Centroid

The depth of the geometric section centroid position from the bottom and left fibers of the section Y_G, $X_{G,}$ Figure 3.37:

$$Y_G = \frac{H}{2}$$ **Equation 3.147**

$$X_G = \frac{B}{2}$$ **Equation 3.148**

2. Defining eccentricity *e*, which specifies the radial path of loading on the interaction diagram. Also, defining the angle α in between the resultant moment GM_R and GM_X

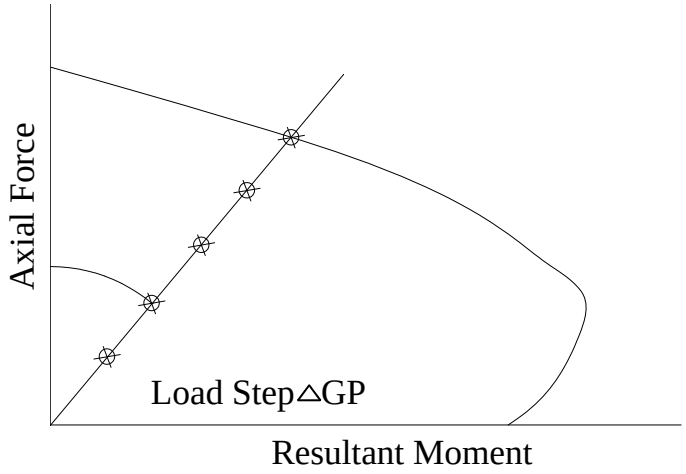

FIGURE 3.38
Radial Loading Concept

3. Defining loading step ΔGP as a small portion of the maximum load, and computing the axial force at the geometric centroid.

$$GP_{new} = GP_{old} + \Delta GP \qquad \textbf{Equation 3.149}$$

4. Calculating moment *GM* about the geometric centroid.

$$e = \frac{GM_R}{GP} \qquad GM_R = e * GP \qquad \textbf{Equation 3.150}$$

$$GM_X = GM_R \cos\alpha \qquad \textbf{Equation 3.151}$$

$$GM_Y = GM_X \tan\alpha \qquad \textbf{Equation 3.152}$$

5. Transferring moment to the current inelastic centroid and calculating the new transferred moment TM_X and TM_Y :

$$TM_X = GM_X + GP(Y_G - Y_c) \qquad \textbf{Equation 3.153}$$

$$TM_Y = GM_Y + GP(X_G - X_c)$$

Equation 3.154

The advantage of transferring the moment to the position of the inelastic centroid is to eliminate the coupling effect between the force and moments, since $EAM_x = EAM_y = 0$ about the inelastic centroid

$$\begin{bmatrix} P \\ TM_x \\ TM_y \end{bmatrix} = \begin{bmatrix} EA & 0 & 0 \\ 0 & EI_x & EI_{xy} \\ 0 & EI_{xy} & EI_y \end{bmatrix} \begin{bmatrix} \varepsilon_o \\ \phi_x \\ \phi_y \end{bmatrix}$$

Equation 3.155

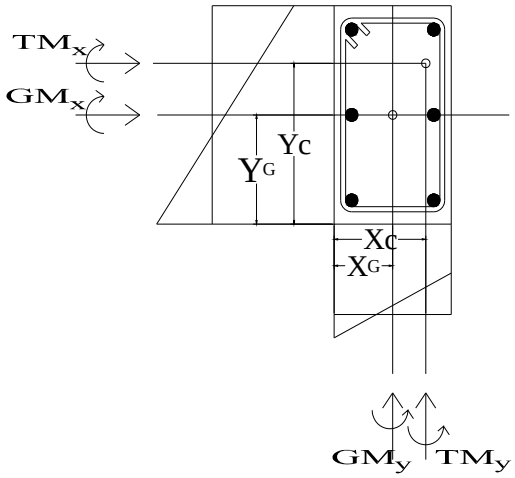

FIGURE 3.39
Moment Transferring from Geometric Centroid to Inelastic Centroid

6. Finding: Curvatures ϕ_X and ϕ_Y

$$\phi_X = \frac{TM_X}{\beta^2} * EI_Y - \frac{TM_Y}{\beta^2} * EI_{XY}$$

Equation 3.156

$$\phi_Y = \frac{TM_Y}{\beta^2} * EI_X - \frac{TM_X}{\beta^2} * EI_{XY}$$

Equation 3.157

$$\beta^2 = EI_X EI_Y - EI_{xy}^2$$

Equation 3.158

Strain at the inelastic centroid ε_o, the extreme compression fiber strain ε_{ec}, and strain at the extreme level of steel in tension ε_{es} are found as follow:

$$\varepsilon_o = \frac{GP}{EA} \qquad \textbf{Equation 3.159}$$

$$\varepsilon_{ec} = \varepsilon_o + \phi_x (H - Y_c) + \phi_y (B - X_c) \qquad \textbf{Equation 3.160}$$

$$\varepsilon_{es} = \varepsilon_o - \phi_x (Y_c - Cover) - \phi_y (X_c - Cover) \qquad \textbf{Equation 3.161}$$

where cover is up to the centers of bars

7. Calculating strain ε_{ci} and corresponding stress f_{ci} in each filament of concrete section by using Eccentric Based Model (Mander Equations)

$$\varepsilon_{ci} = \frac{GP}{EA} + \frac{TM_x (H - Y_c - Y_i)}{\beta^2} EI_y + \frac{TM_y (B - X_c - X_i)}{\beta^2} EI_x - \frac{TM_x (B - X_c - X_i)}{\beta^2} EI_{xy} - \frac{TM_y (H - Y_c - Y_i)}{\beta^2} EI_{xy} \qquad \textbf{Equation 3.162}$$

8. Calculating strain ε_{si} and corresponding stress f_{si} in each bar in the given section by using the steel model shown in Figure 3.2b.

$$\varepsilon_{si} = \frac{GP}{EA} + \frac{TM_x (H - Y_c - Y_{si})}{\beta^2} EI_y + \frac{TM_y (B - X_c - X_{si})}{\beta^2} EI_x - \frac{TM_x (B - X_c - X_{si})}{\beta^2} EI_{xy} - \frac{TM_y (H - Y_c - Y_{si})}{\beta^2} EI_{xy} \qquad \textbf{Equation 3.163}$$

9. Calculating the new section properties: axial rigidity EA, flexural rigidities about the inelastic centroid EI_x, EI_y, EI_{xy} moment of axial rigidity about inelastic

centroid EAM_x, EAM_y, internal axial force F_z, internal bending moments about the inelastic centroid M_{ox} ,M_{oy}:

$$EA = \sum_i E_{ci} w_i t_i + \sum_i (E_{si} - E_{ci}) A_{si}$$ **Equation 3.164**

$$EAM_x = \sum_i E_{ci} w_i t_i (H - Y_c - Y_i) + \sum_i (E_{si} - E_{ci}) A_{si} (H - Y_c - Y_{si})$$ **Equation 3.165**

$$EAM_y = \sum_i E_{ci} w_i t_i (B - X_c - X_i) + \sum_i (E_{si} - E_{ci}) A_{si} (B - X_c - X_{si})$$ **Equation 3.166**

$$F_z = \sum f_{ci} w_i t_i + \sum (f_{si} - f_{ci}) A_{si}$$ **Equation 3.167**

$$EI_x = \sum_i E_{ci} w_i t_i (H - Y_c - Y_i)^2 + \sum_i (E_{si} - E_{ci}) A_{si} (H - Y_c - Y_{si})^2$$ **Equation 3.168**

$$EI_y = \sum_i E_{ci} w_i t_i (B - X_c - X_i)^2 + \sum_i (E_{si} - E_{ci}) A_{si} (H - X_c - X_{si})^2$$ **Equation 3.169**

$$EI_{xy} = \sum_i E_{ci} w_i t_i (H - Y_c - Y_i)(B - X_c - X_i) + \sum_i (E_{si} - E_{ci}) A_{si} (H - Y_c - Y_{si})(B - X_c - X_{si})$$ **Equation 3.170**

$$M_{ox} = \sum f_{ci} w_i t_i (H - Y_c - Y_i) + \sum (f_{si} - f_{ci}) A_{si} (H - Y_c - Y_{si})$$ **Equation 3.171**

$$M_{oy} = \sum f_{ci} w_i t_i (B - X_c - X_i) + \sum (f_{si} - f_{ci}) A_{si} (B - X_c - X_{si})$$ **Equation 3.172**

where E_{ci} = secant modulus of elasticity of the concrete filament $= \frac{f_{ci}}{\varepsilon_{ci}}$.

E_{si} = secant modulus of elasticity of the steel bar $= \frac{f_{si}}{\varepsilon_{si}}$.

10. Transferring back the internal moments about the geometric centroid

$$GM_{ox} = M_{ox} - GP(Y_G - Y_c)$$ **Equation 3.173**

$$GM_{oy} = M_{oy} - GP(Y_G - X_c)$$ **Equation 3.174**

11. Checking the convergence of the inelastic centroid

$$TOL_x = EAM_x / EA / Y_c$$ **Equation 3.175**

$$TOL_y = EAM_y / EA / X_c$$ **Equation 3.176**

12. Comparing the internal force to applied force, internal moments to applied moments, and making sure the moments are calculated about the geometric centroid :

$$\left|GP - F_z\right| \le 1*10^{-5}$$ **Equation 3.177**

$$\left|GM_x - GM_{ox}\right| \le 1*10^{-5} \qquad \left|GM_y - GM_{oy}\right| \le 1*10^{-5}$$ **Equation 3.178**

$$\left|TOL_x\right| \le 1*10^{-5} \qquad \left|TOL_y\right| \le 1*10^{-5}$$ **Equation 3.179**

If Equations 3.174, 3.175 and 3.176 are not satisfied, the location of the inelastic centroid is updated by EAM_x/EA and EAM_y/EA and steps 5 to 11 are repeated till Equations 3.174, 3.175 and 3.176 are satisfied.

$$Y_{c_{new}} = Y_{c_{old}} + \frac{EAM_x}{EA}$$ **Equation 3.180**

$$X_{c_{new}} = X_{c_{old}} + \frac{EAM_y}{EA}$$ **Equation 3.181**

Once equilibrium is reached, the algorithm checks for ultimate strain in concrete ε_{ec} and steel ε_{es} not to exceed $\overline{\varepsilon_{cu}}$ and 0.05 respectively. Then it increases the loading by ΔGP and runs the analysis for the new load level using the latest section properties. Otherwise, if ε_{ec} equals $\overline{\varepsilon_{cu}}$ or ε_{es} equals 0.05, the target force and resultant moment are reached as a point on the failure surface for the amount of eccentricity and angle α used.

This method can be used combined with Approach One in the unconfined analysis, section 3.2.2.1: Predefined Ultimate Strain Profile, for processing time optimization. Initially unconfined analysis is utilized. The sectional properties, EA, EI_x, EI_y, EI_{xy}, EAM_x, EAM_y, Y_c, X_c F_z, M_{ox} *and* M_{oy} are calculated from the unconfined failure point and used as section properties for the following step. So instead of loading the section from the beginning, The equilibrium is sought at unconfined failure point, Then, knowing the internal force capacity of the section, ΔP is added and the cross section is analyzed using the proposed numerical formulation of this section until failure of the confined section.

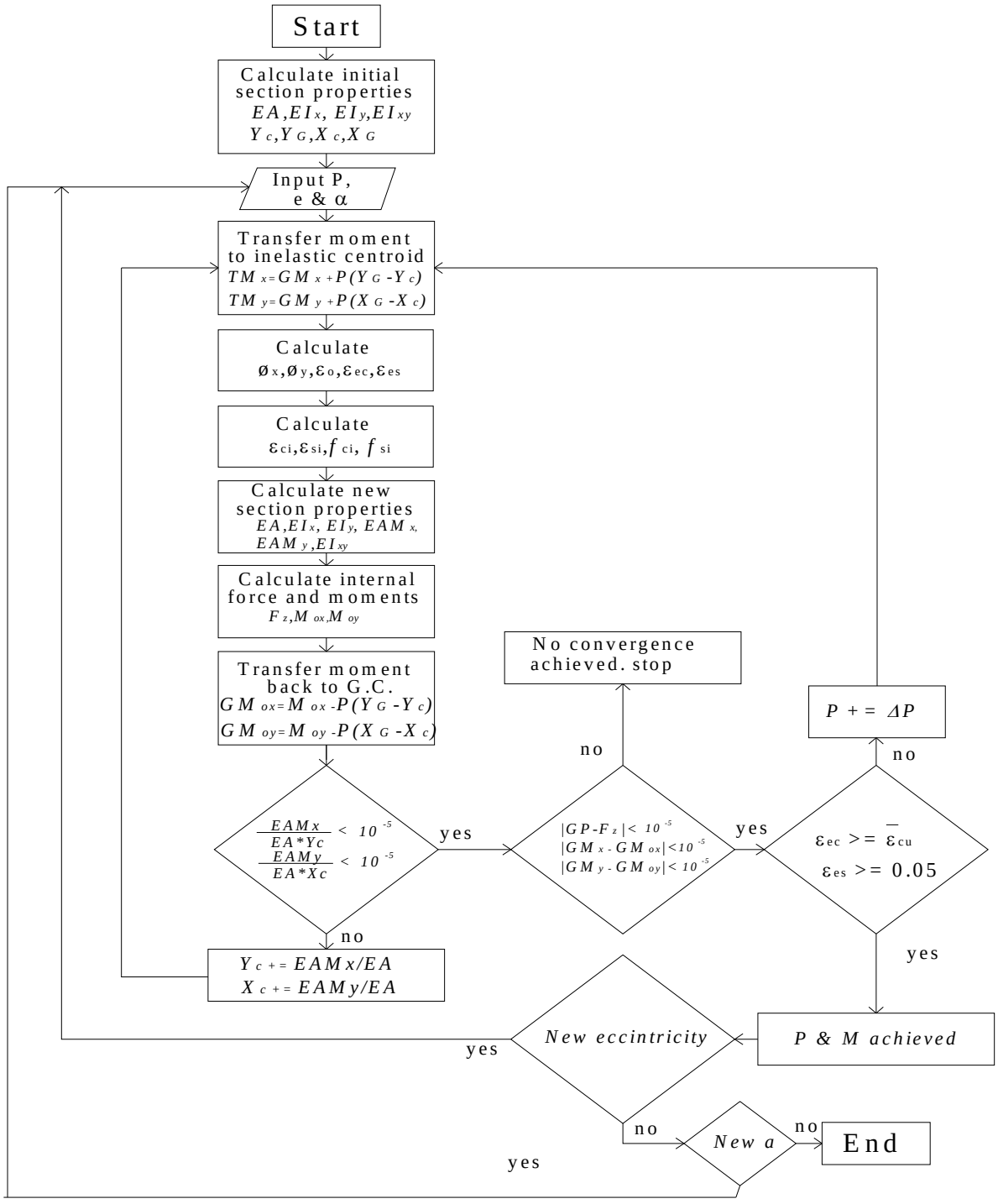

FIGURE 3.40
Flowchart of Generalized Moment of Area Method

3.3.3 Results and Discussion

Interaction diagrams generated by KDOT Column Expert Software are plotted and compared to the corresponding experimental work found in the literature. Interaction diagrams are generated using the numerical formulation described in section 3-3-2.

3.3.3.1 Comparison with Experimental Work Case 1

A Study of combined bending and axial load in reinforced concrete members (Eivind Hogenstad)

Section Height = 10 inches

Section Width = 10 inches

Clear Cover = 0.8575 inches

Steel Bars in x direction = 2

Steel Bars in y direction = 4

Steel Diameter = 0.785 inches

Tie Diameter = 0.25 inches

$f'c$ = 5.1 ksi fy = 60 ksi. f_{yh} = 61.6 ksi. Spacing = 8 inches

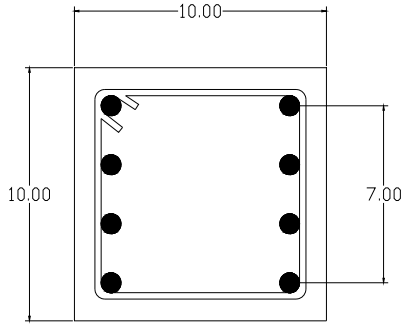

FIGURE 3.41
Hognestad Column

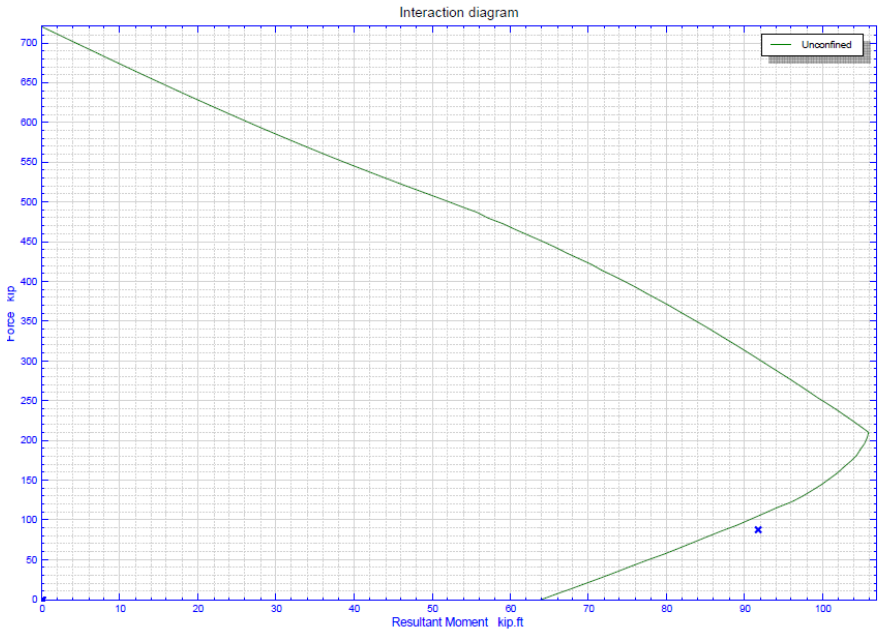

FIGURE 3.42
Comparison between KDOT Column Expert with Hognestad Experiment (α = 0)

3.3.3.2 Comparison with Experimental Work Case 2

Design criteria for reinforced columns under axial load and biaxial bending (Boris Bresler)

Section Height = 8 inches

SectionWidth = 6 inches

Clear Cover = 1.1875 inches

Steel Bars in x direction = 2#5

Steel Bars in y direction = 2#5

Tie Diameter = 0.25 inches

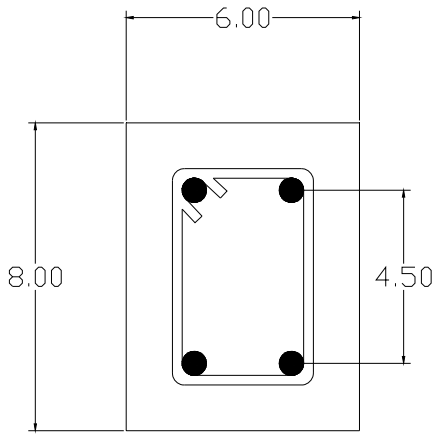

FIGURE 3.43
Bresler Column

$f'c$ = 3.7 ksi fy = 53.5 ksi. f_{yh} = 53.5 ksi. Spacing = 4 in

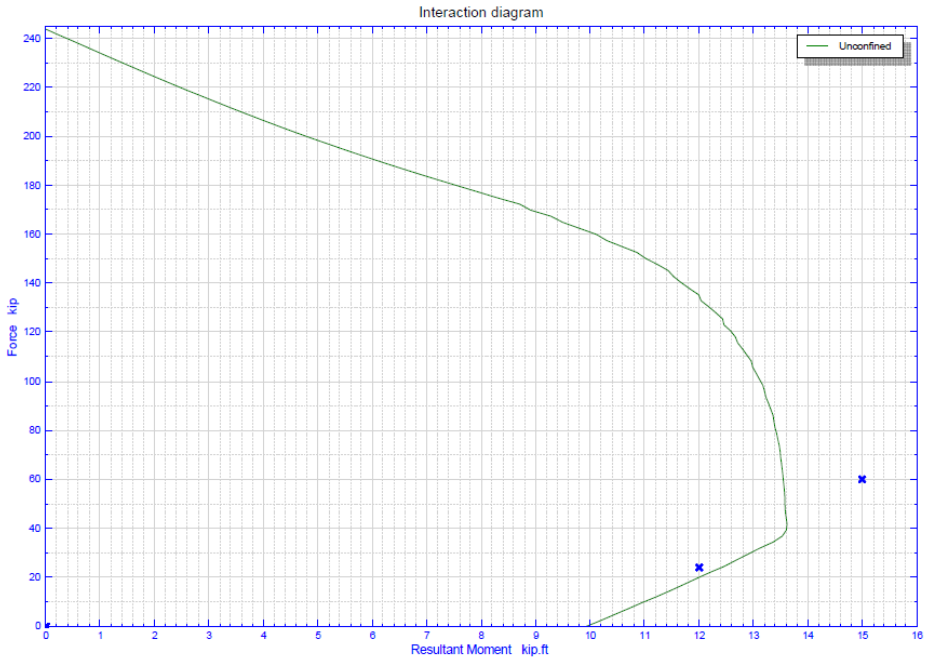

FIGURE 3.44
Comparison between KDOT Column Expert with Bresler Experiment (α = 90)

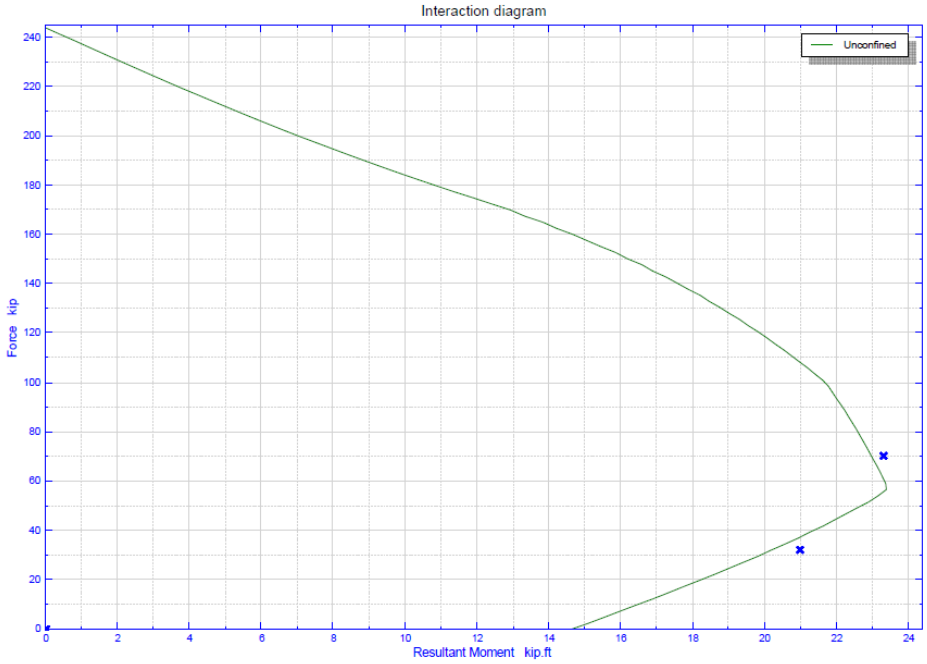

FIGURE 3.45
Comparison between KDOT Column Expert with Bresler Experiment (α = 0)

3.3.3.3 Comparison with Experimental Work Case 3

Investigation of the ultimate strength of square and rectangular columns under biaxially eccentric loads (L.N. Ramamurthy)

Section Height = 12 inches

Section Width = 6 inches

Clear Cover = 1.2375 inches

Steel Bars in x direction = 3#5

Steel Bars in y direction =3#5

Tie Diameter = 0.25 inches

$f'c$ = 3.8 ksi fy = 46.79 ksi f_{yh} = 46.79 ksi. Spacing = 6 inches

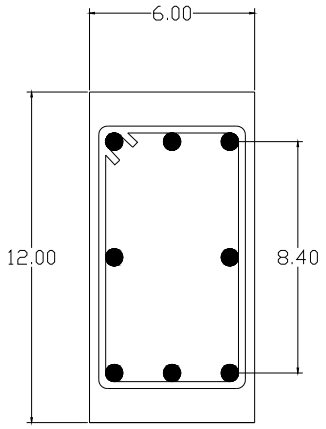

FIGURE 3.46
Ramamurthy Column

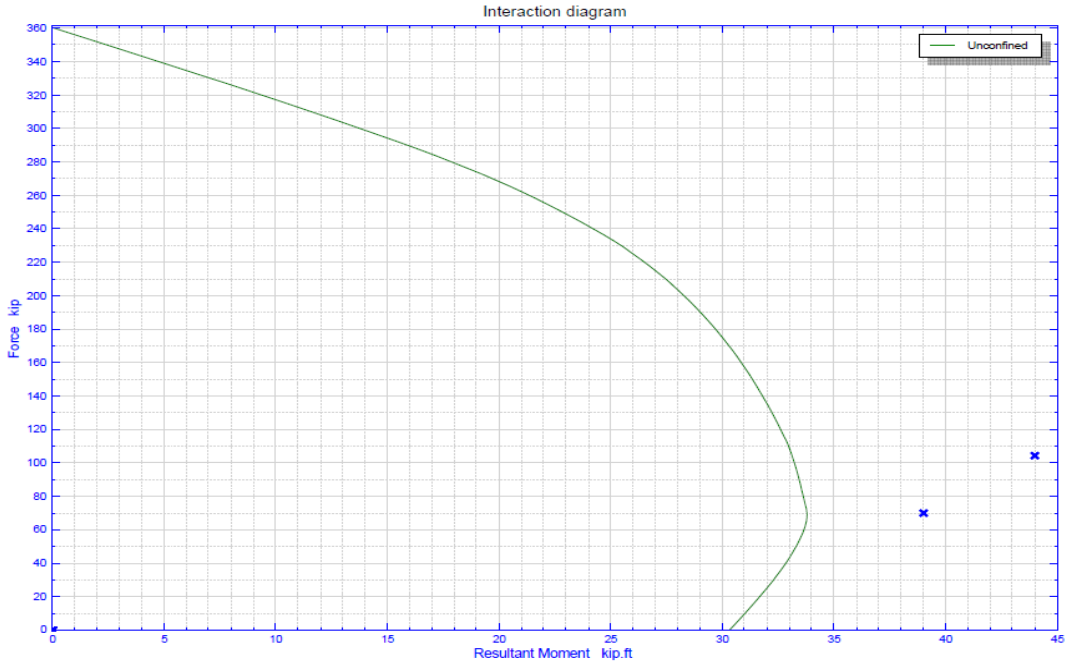

FIGURE 3.47
Comparison between KDOT Column Expert with Ramamurthy Experiment (α = 26.5)

3.3.3.4 Comparison with Experimental Work Case 4

Confined columns under eccentric loading

(Murat Saatcioglu. Amir Salamat and Salim Razvi)

Section Height = 8.27 inches

Section Width =8 .27 inches

Clear Cover = 0. 5 inches

Steel Bars in x direction = 3

Steel Bars in y direction = 3

Steel Area = 0.155 inches^2

Tie Diameter = 0.364 inches

$f'c$ = 5.1 ksi f_y = 75 ksi. f_{yh} = 59.45 ksi. Spacing = 1.97 inches

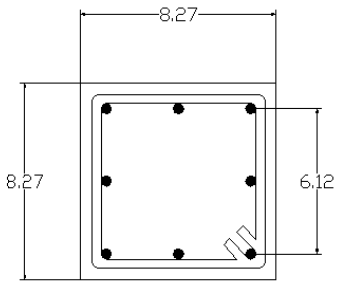

FIGURE 3.48
Saatcioglu Column

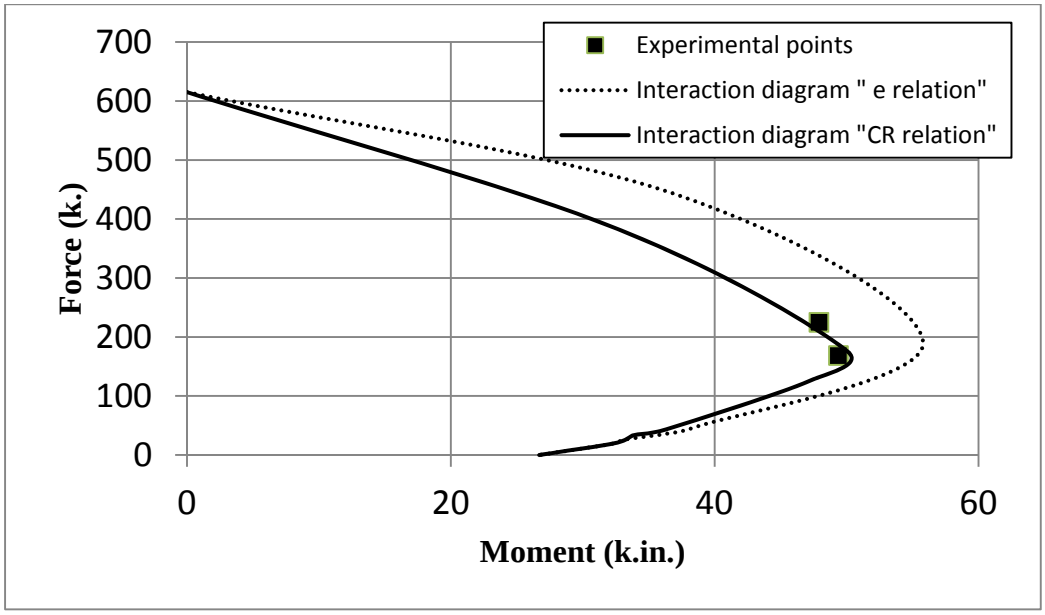

FIGURE 3.49
Comparison between KDOT Column Expert with Saatcioglu et al. Experiment (α = 0)

3.3.3.5 Comparison with Experimental Work Case 5

Confined columns under eccentric loading

(Mural Saatcioglu. Amir Salamat and Salim Razvi)

Section Height = 8.27 inches

Section Width =8 .27 inches

Clear Cover = 0. 5 inches

Steel Bars in x direction = 4

Steel Bars in y direction = 4

Steel Area = 0.155 in^2.

Tie Diameter = 0.364 inches

$f'c$ = 5.1 ksi f_y = 75 ksi. f_{yh} = 59.45 ksi. Spacing = 1.97 inches

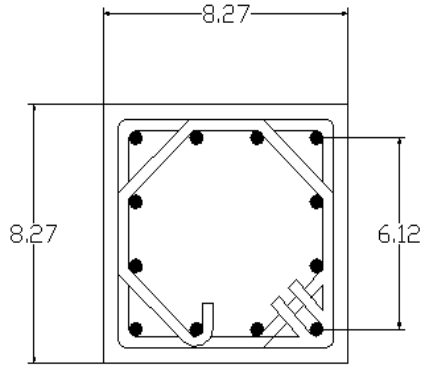

FIGURE 3.50
Saatcioglu Column

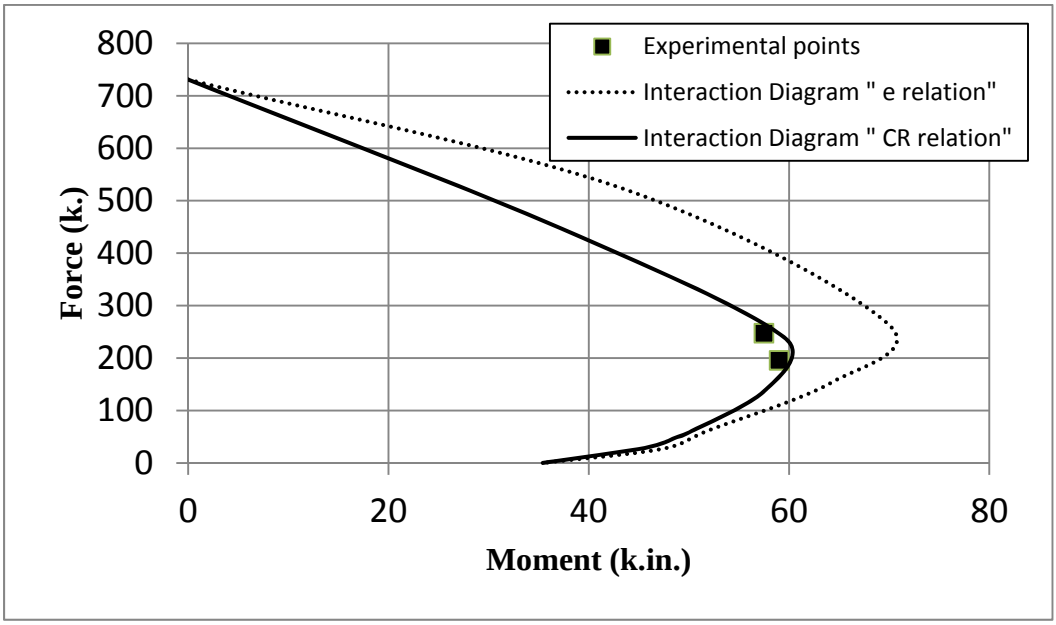

FIGURE 3.51
Comparison between KDOT Column Expert with Saatcioglu et al. Experiment 1 (α = 0)

3.3.3.6 Comparison with Experimental Work Case 6

Stress strain behavior of concrete confined by overlapping hoops at low and high strain rate:

(B. Scott, R Park and M. Priestly)

Section Height = 17.7 inches

Section Width =17 .7 inches

Clear Cover = 0. 787 inches

Steel Bars in x direction = 4

Steel Bars in y direction = 4

Steel Area = 0.49 inches^2

Tie Diameter = 0.394 inches

$f'c$ = 3.67 ksi f_y = 63 ksi. f_{yh} = 44.8 ksi. Spacing = 2.83 inches

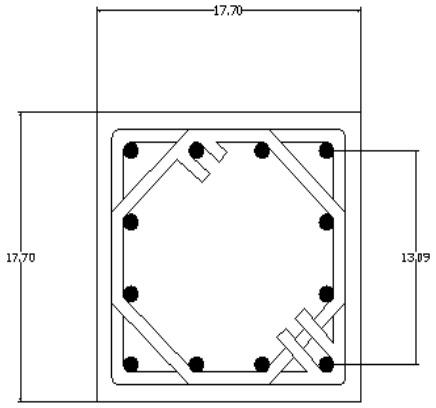

FIGURE 3.52
Scott Column

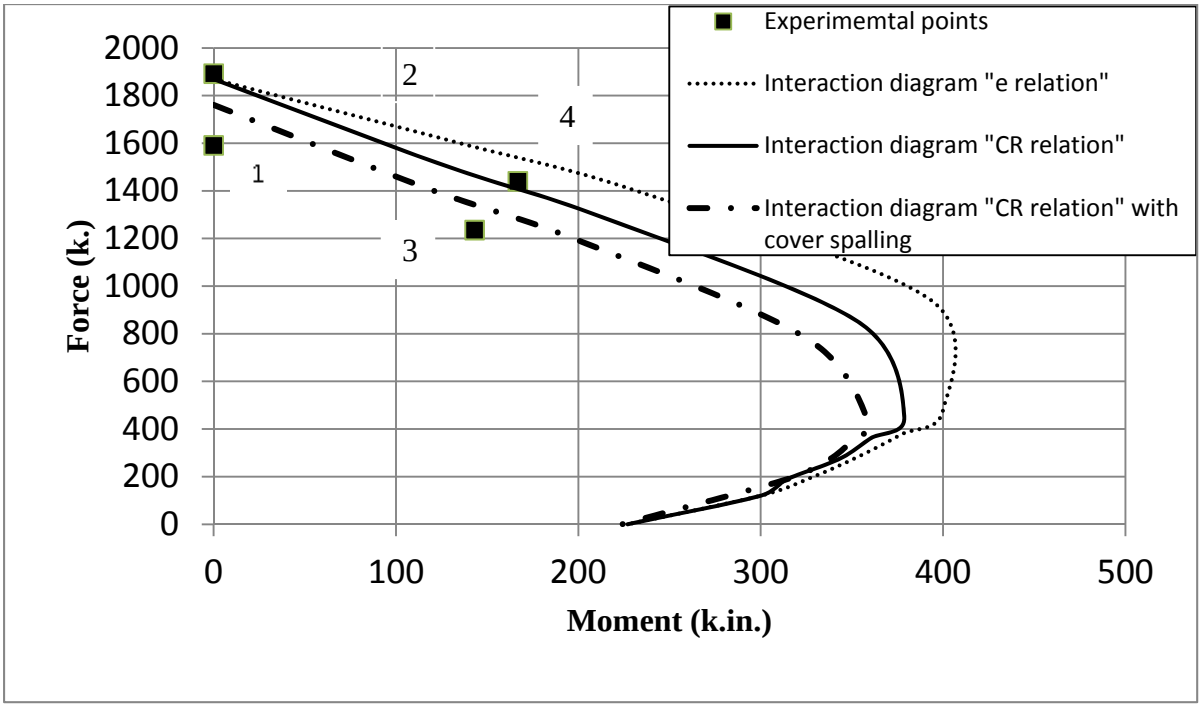

FIGURE 3.53
Comparison between KDOT Column Expert with Scott et al. Experiment (α = 0)

3.3.3.7 Comparison with Experimental Work Case Case 7

Stress strain behavior of concrete confined by overlapping hoops at low and high strain rate

(B. Scott, R Park and M. Priestly)

Section Height = 17.7 inches

Section Width =17 .7 inches

Clear Cover = 0. 787 inches

Steel Bars in x direction = 3

Steel Bars in y direction = 3

Steel Area = 0.7 inches^2.

Spiral Diameter = 0.394 inches

f'c = 3.67 ksi fy = 57.13 ksi. fyh = 44.8 ksi. Spacing = 2.83 inches

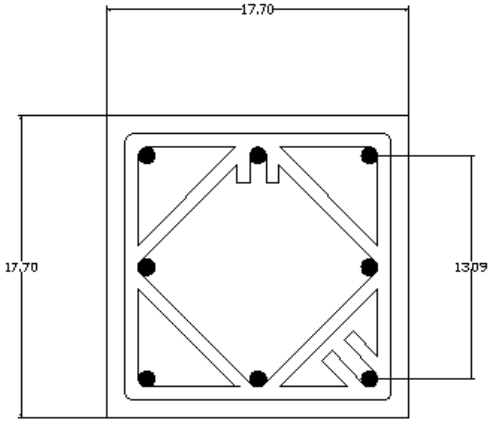

FIGURE 3.54
Scott Column

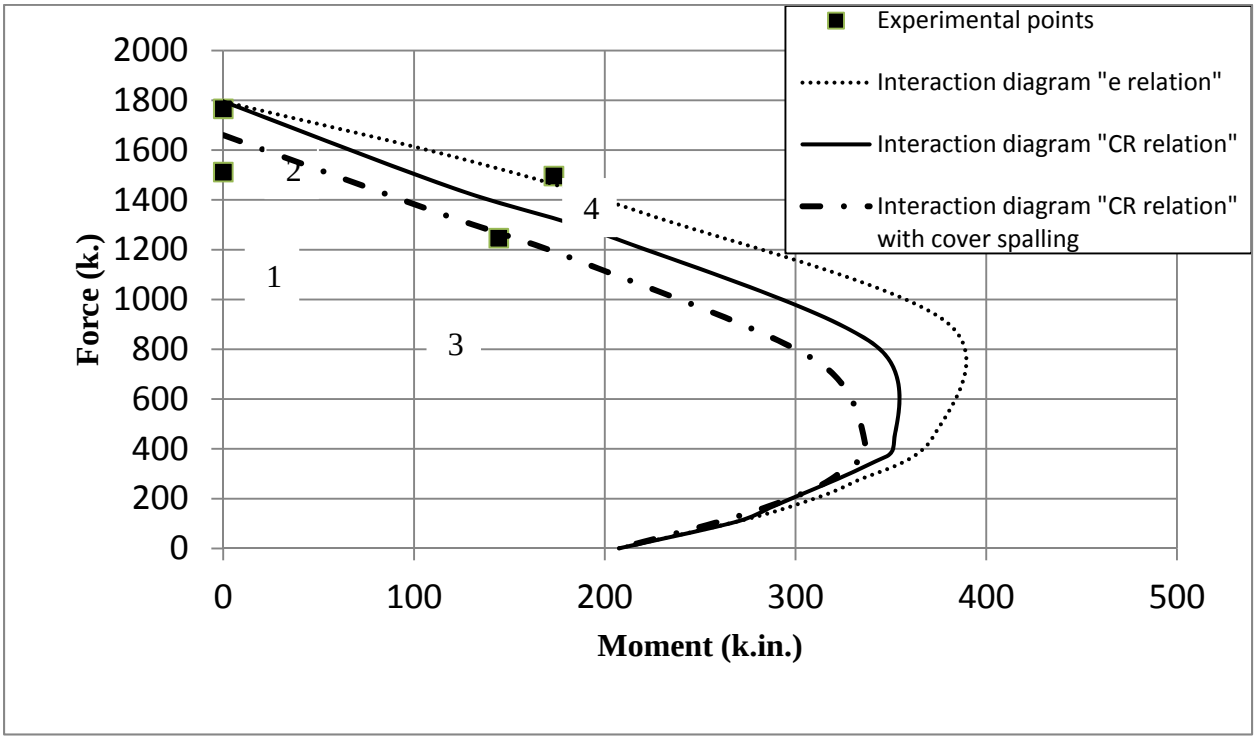

FIGURE 3.55
Comparison between KDOT Column Expert with Scott et al. Experiment (α = 0)

The analyzed seven cases cover the three Interaction diagram zones of; compression controlled, tension controlled and balanced zones. There is good agreement between the theoretical interaction diagram and the corresponding experimental data as shown in Figures 3.42, 3.44, 3.45, 3.47, 3.49, 3.51, 3.53, and 3.55.

It is shown from Figures 3.49, 3.51, 3.53, and 3.55 that interaction diagrams plotted using Equation 3.105 that is representative of the compression zone area are more accurate compared to those plotted using Equation 3.105a that is a function of eccentricity. Also the experimental data correlate well to its associated interaction diagrams.

Figure 3.53 and 3.55 show more accuracy and conservative interaction diagram when the analysis account for the cover spalling when the unconfined crushing strain is considered. This is represented by the most inner curve in Figures 3.53 and 3.55. Also in Figure 3.53 and 3.55 the experimental points 1 and 2 are having the same eccentricity but the loading strain rate is different. The loading strain rate for point 1 is 0.0000033, whereas it is 0.0167 for point 2. Points 3 and 4 also have the same loading strain rate. It is seen that the loading strain rate for points 1

and 3 are extremely small. Hence points 2 and 4 are more realistic and they are captured well by the theoretical interaction diagram. In conclusion, the strain rate is a parameter that needs further investigation.

3.3.3.8 Comparison between the Surface Meridians T&C Used in Mander Model and Experimental Work

The ultimate strength surface meridians equations for compression C and tension T derived by Elwi and Murray (1979) from the data of Scickert and Winkler (1977), that are utilized by Mander et al. (1988) to predict the ultimate confined axial strength using the two lateral confined pressures, are compared herein to some experimental data found from Mills and Zimmerman (1970). The equations used by Mander are developed originally for concrete that has unconfined strength of 4.4 ksi. They have the following formulas

$$T = 0.069232 - 0.661091\overline{\sigma_{oct}} - 0.049350\overline{\sigma_{oct}}^{2} \qquad \textbf{Equation 3.182}$$

$$C = 0.122965 - 1.150502\overline{\sigma_{oct}} - 0.315545\overline{\sigma_{oct}}^{2} \qquad \textbf{Equation 3.183}$$

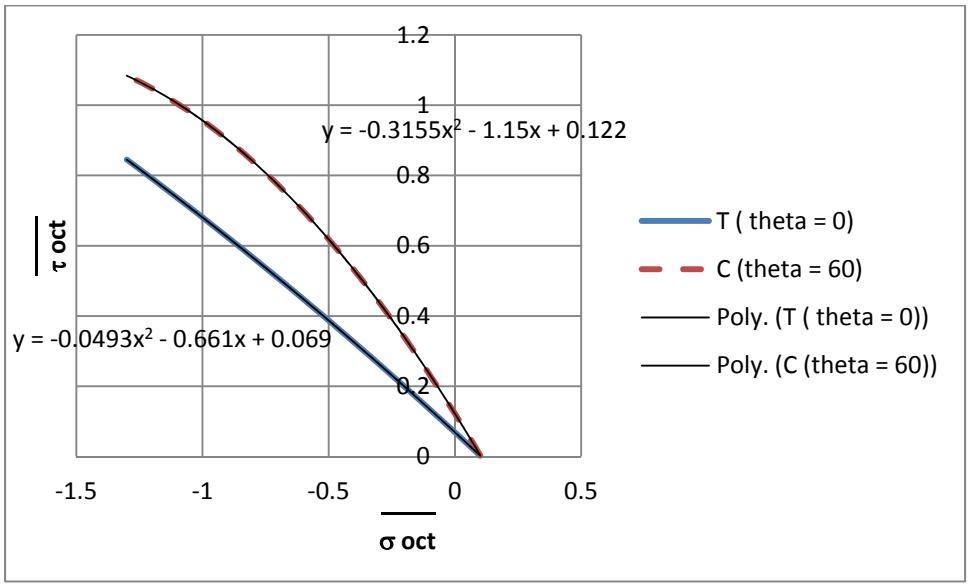

FIGURE 3.56
T and C Meridians Using Equations 3.182 and 3.183 used in Mander Model for f'_c = 4.4 ksi

The T and C meridians adopted by Mander from Elwi and Murray (1979) work are reported on in Figure 3.56. Mills and Zimmerman (1970) developed three sets of multiaxial tests for concrete with unconfined strength of 3.34, 3.9 and 5.2 ksi. For each set, the values of $\overline{\sigma_{oct}}$ and $\overline{\tau_{oct}}$ are extracted at unconfined strength f'_c, the cracking tensile strength f'_t, equibiaxial compressive strength f'_{cb} and two extra points; one on each of the meridians. These five points are used to plot the T and C meridians as shown in Figures 3.57, 3.58 and 3.59.

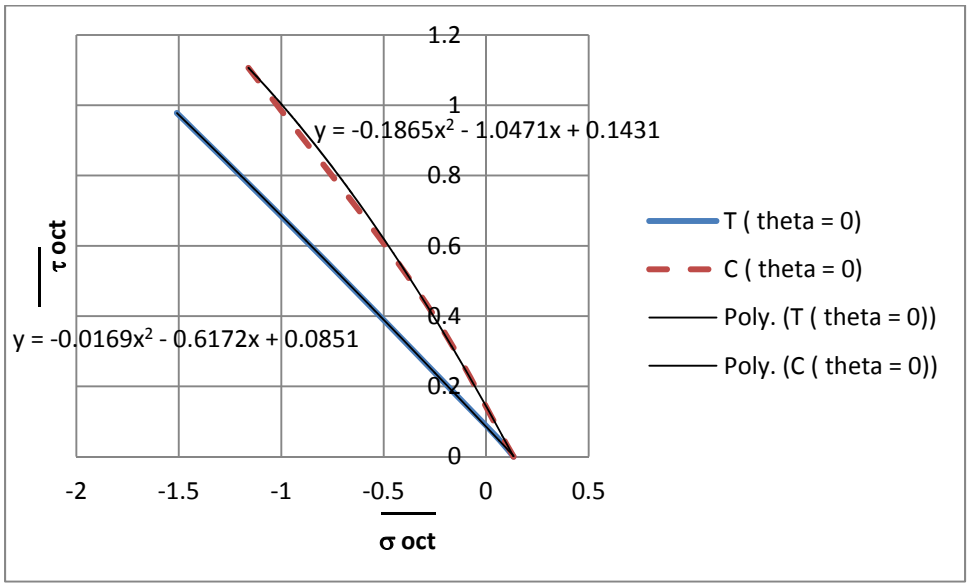

FIGURE 3.57
T and C Meridians for f'_c = 3.34 ksi

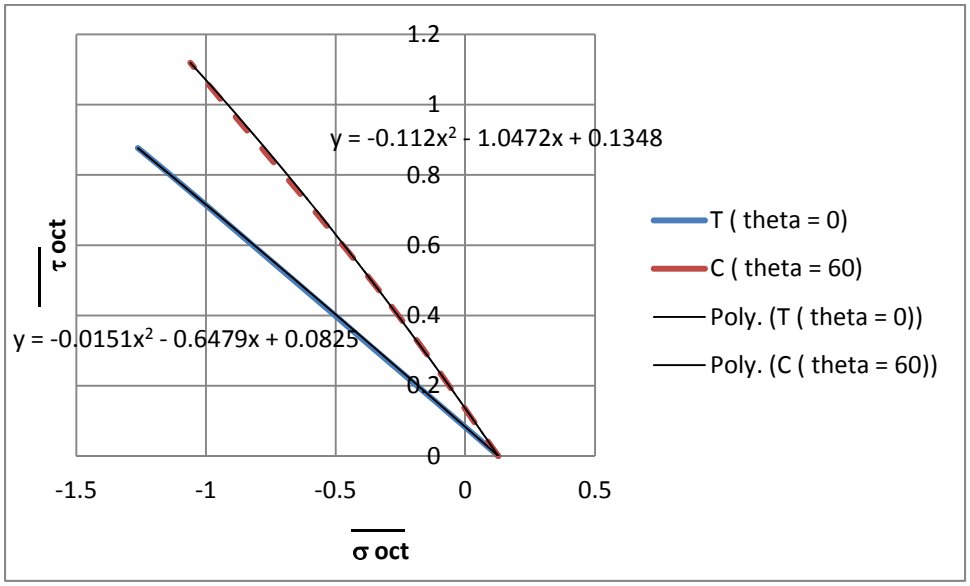

FIGURE 3.58
T and C Meridians for f'_c = 3.9 ksi

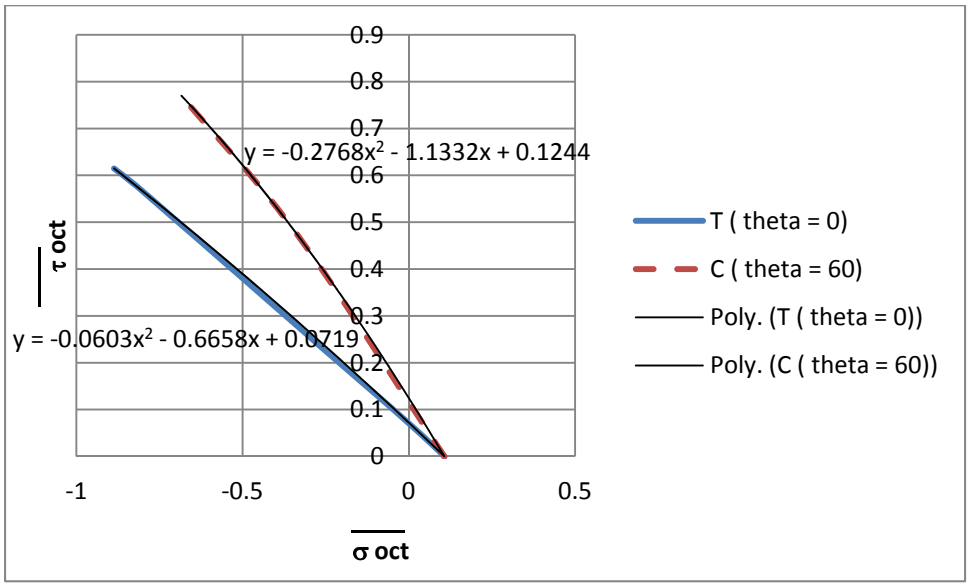

FIGURE 3.59
T and C Meridians for f'_c = 5.2 ksi

The T and C equations for Figures 3.57 through 3.59 are as follow:

for f'_c = 3.34 ksi:

$$T = 0.0851 - 0.6172\overline{\sigma_{oct}} - 0.0169\overline{\sigma_{oct}}^{2} \quad \textbf{Equation 3.184}$$

$$C = 0.1431 - 1.0471\overline{\sigma_{oct}} - 0.1865\overline{\sigma_{oct}}^{2} \quad \textbf{Equation 3.185}$$

for f'_c = 3.9 ksi:

$$T = 0.0825 - 0.6479\overline{\sigma_{oct}} - 0.0151\overline{\sigma_{oct}}^{2} \quad \textbf{Equation 3.186}$$

$$C = 0.1348 - 1.0472\overline{\sigma_{oct}} - 0.112\overline{\sigma_{oct}}^{2} \quad \textbf{Equation 3.187}$$

for f'_c = 5.2 ksi:

$$T = 0.0719 - 0.6658\overline{\sigma_{oct}} - 0.0603\overline{\sigma_{oct}}^{2} \quad \textbf{Equation 3.188}$$

$$C = 0.1244 - 1.1332\overline{\sigma_{oct}} - 0.2768\overline{\sigma_{oct}}^{2} \quad \textbf{Equation 3.189}$$

Equations 3.181 through 3.186 are used in generating confined strength values for different lateral pressures as shown in Appendix A. Equations 3.179 and 3.180 are used also in developing confined strength values for the same lateral pressure values. It is seen from the tables that Equations 3.179 and 3.180 give conservative values compared to Equations 3.181 through 3.186. Accordingly, Equations 3.179 and 3.180 are used herein to predict the ultimate confined axial strength values for any given unconfined strength (f'_c) value.

TABLE 3.1
Data for Constructing T and C Meridian Curves for f'_c Equal to 3.34 ksi

Control Parameter	Oct	Oct
f'c= 3.34 *ksi*	-0.33333	0.471405
f't	0.043258	0.061176
f'cb	-0.81497	0.576271
triaxial on C	-1.15968	1.10653
triaxial on T	-1.50898	0.978094

TABLE 3.2
Data for Constructing T and C Meridian Curves for f'_c Equal to 3.9 ksi

Control Parameter	Oct	Oct
f'c= 3.9 *ksi*	-0.33333	0.471405
f't	0.040006	0.056578
f'cb	-1.0904	0.771027
triaxial on C	-1.06018	1.119058
triaxial on T	-1.26248	0.876414

TABLE 3.3
Data for Constructing T and C Meridian Curves for f'_c Equal to 5.2 ksi

Control Parameter	Oct	Oct
f'c= 5.2 *ksi*	-0.33333	0.471405
f't	0.034553	0.048865
f'cb	-0.80229	0.567306
triaxial on C	-0.68386	0.76993
triaxial on T	-0.88634	0.614725

Chapter 4: Conclusions and Recommendations

4.1 Conclusions

This study accomplished several objectives at the analysis, material modeling, design implications and software development levels. It may be concluded that:

1. Based on the extensive review of the confined model available in the literature, Mander Model is found to be the most suitable concentric loading model expressing the stress-strain behavior of circular and rectangular columns confined with convenient lateral steel and steel tubes as well.
2. The eccentric based stress-strain model developed in this study provides more accuracy compared to the available concentric confined models in the literature as it is shown through comparison with experimental data.
3. For rectangular columns, the ratio of the area of compression zone to the sectional gross area is more representative than the normalized alone eccentricity in correlating eccentric behavior.
4. The non-linear numerical procedure introduced, using the eccentric model and the finite layer approach, successfully predicted the ultimate capacity of rectangular reinforced concrete columns confined with steel.
5. A computer program named “KDOT Column Expert” is developed based on the non-linear approach implemented for analyzing and designing rectangular columns confined with lateral steel hoops.
6. The unconfined concrete analysis carried out by KDOT Column Expert is benchmarked successfully against well-established commercial software for a range of design parameters.
7. The confined concrete analysis implemented by KDOT Column Expert is well correlated to experimental data.

4.2 Recommendations

This work should be extended to address the following areas:

1. Model the effect of FRP wrapping on confinement for rectangular columns.

2. Model corrosion of longitudinal and transverse steel for circular and rectangular columns.
3. Model CFST for circular columns.
4. Model CFST for rectangular columns.
5. Expand the software application to include the CFST columns.

References

Aas-Jakobsen, A. 1964. “Biaxial Eccentricities in Ultimate Load Design.” *ACI Journal* 61 (3): 293–316.

ACI-ASCE Committee 327. 1956. “Ultimate Strength Design.” *ACI Journal*, Proceedings 52: 505–524.

Ahmad, S. H., and Shah, S. P. 1982. “Complete Triaxial Stress-Strain Curves for Concrete.” *ASCE Journal* 108 (ST4): 728–743.

Ahmad, S. H., and Shah, S. P. 1982. “Stress-Strain Curves of Concrete Confined by Spiral Reinforcement.” *ACI Journal* 79 (6): 484–490.

Andersen, Paul. 1941. “Design Diagrams for Square Concrete Columns Eccentrically Loaded in Two Directions.” *ACI Journal*, Proceedings 38: 149.

Ang, Cho-Lim Charles. 1961. “Square Column with Double Eccentricities Solved by Numerical Method.” *ACI Journal*, Proceedings 57: 977.

Assa B., Nishiyama, M., and Watanabe, F. 2001. “New Approach for Modeling Confined Concrete. I: Circular Columns.” *Journal of Structural Engineering*, ASCE 127 (7): 743–750.

Attard, M. M., and Setunge, S. 1996. “Stress-Strain Relationship of Confined and Unconfined Concrete.” *ACI Materials Journal* 93 (5): 432–442.

Au, Tung. 1957. “Ultimate Strength Design Charts for Columns Controlled by Tension.” *ACI Journal*, Proceedings 54: 471.

Au, Tung. 1958. “Ultimate Strength Design of Rectangular Concrete Members Subjected to Unsymmetrical Bending.” *ACI Journal*, Proceedings 54: 657.

Bajaj, S., and Mendis, P. 2005. “New Method to Evaluate the Biaxial Interaction Exponent for RC Columns.” *Journal of Structural Engineering*, ASCE 131 (12): 1926–1930.

Bakhoum, Michel. 1948. “Analysis of Normal Stresses in Reinforced Concrete Sections under Symmetrical Bending.” *ACI Journal*, Proceedings 44: 457.

Bazant, Z. P., and Bhat, P. D. 1976. “Endochronic Theory of Inelasticity and Failure of Concrete.” *Journal of the Engineering Mechanics Division*, ASCE 102 (4): 701–722.

Bazant, Z. P., and Bhat, P. D. 1977. “Prediction of Hysteresis of Reinforced Concrete Members.” *Journal of the Structural Division*, ASCE 103 (1): 153–167.

Binici, B. 2005. “An Analytical Model for Stress–Strain Behavior of Confined Concrete.” *Engineering Structures* 27 (7): 1040–1051.

Blume, J. A, Newmark, N. M., and Corning L. H. 1961. “Design of Multi Storey Reinforced Concrete Building for Earthquake Motions.” Chicago. Portland Cement Association.

Bonet, J. L., Barros, F. M., Romero, M. L. 2006. “Comparative Study of Analytical and Numerical Algorithms for Designing Reinforced Concrete Section under Biaxial Bending.” *Computers and Structures* 8:31–2.

Bonet, J. L., Miguel, P. F., Fernandez, M. A., and Romero, M. L. 2004. “Analytical Approach to Failure Surfaces in Reinforced Concrete Sections Subjected to Axial Loads and Biaxial Bending.” *Journal of Structural Engineering* 130 (12): 2006–2015.

Building Code Requirements for Reinforced Concrete. 1956. ACI 318-56. American Concrete Institute (ACI). Detroit, Michigan.

Braga, F., Gigliotti, R., Laterza, M. 2006. “Analytical Stress–Strain Relationship for Concrete Confined by Steel Stirrups and/or FRP Jackets.” *Journal of Structural Engineering* ASCE 132 (9): 1402–1416.

Breen, J. E. 1962. “The Restrained Long Concrete Column as a Part of A Rectangular Frame.” Ph. D. Thesis Presented to the University of Texas, Austin, TX.

Bresler, B. 1960. ‘‘Design, Criteria for Reinforced Columns under Axial Load Bi-Axial Bending.’’ *ACI Journal* Nov.: 481–491.

Bresler, B., and Gilberg, P. H. 1961. ‘‘Tie Requirements for Reinforced Concrete Columns.’’ *ACI Journal* 58 (5): 555–570.

Brettle, H. J.; Taylor, J. M. 1969. “Comparison of Experimental Results with Ultimate Strength Theory for Reinforced Concrete Columns in Biaxial Bending.” Transactions of the Institution of Engineers, Australia, Civil Engineering April 11 (1): 63–74.

Candappa, D. 2000. “The Constitutive Behavior of High Strength Concrete under Lateral Confinement.” PhD Thesis, Monash University, Clayton, VIC, Australia.

Candappa, D. P., Sanjayan, J. G., and Setunge, S. 2001. “Complete Triaxial Stress-Strain Curves of High-Strength Concrete.” *Journal of Materials in Civil Engineering* 13 (3): 209–215.

Candappa, D. P., Setunge, S., and Sanjayan, J. G. 1999. “Stress Versus Strain Relationship of High Strength Concrete under High Lateral Confinement.” *Cement and Concrete Research* 29 (12): 1977–1982.

Carreira, D J., and Chu, K. H. 1985. “Stress-Strain Relationship for Plain Concrete in Compression.” *ACI Journal* 83 (6): 797–804.

Cedolin, L.; Cusatis, G.; Eccheli, S.; Roveda, M. 2006. “Biaxial Bending of Concrete Columns: an Analytical Solution.” *Studies and Researches* 26. http://www.inti.gov.ar/cirsoc/

Cedolin L, Cusatis G, Ecchelli S, Roveda M. 2008. “Capacity of Rectangular Crosssections under Biaxially Eccentric Loads.” *ACI Structural Journal* 105 (2): 215–24.

Cervin, D. R. 1948. “Design of Rectangular Tied Columns Subjected to Bending with Steel in All Faces.” *ACI Journal* 19: 401–412.

Chan, W. W. L. 2002. “The Ultimate Strength and Deformation of Plastic Hinges in Reinforcement Concrete Frameworks.” *Magazine of Concrete Research* (London) 128 (12): 1551–1564.

Chu, Kuang-Han and Pabarcius, A. 1958. “Biaxially Loaded Reinforced Concrete Columns.” *ASCE Proceedings* 84 (ST 8): Paper 1865.

Cross, H. 1930. “The Column Analogy: Analysis of Elastic Arches and Frames.” Urbana, IL: University of Illinois.

Cusson, D. and Paultre, P. 1995. “Stress-Strain Model for Confined High-Strength Concrete.” *ASCE Journal of Structural Engineering* 121 (3): 468–477.

Czerniak. E. 1962. “Analytical Approach to Biaxial Eccentricity.” Proceedings of the ASCE *Journal the Structural Division* 88: 105–158.

Davister, M. D. 1986. “A Computer Program for Exact Analysis.” *Concrete International: Design and Construction* 8 (7): 56–61.

Demagh, K. Chabil, H.; Hamzaoui, L. 2005. “Analysis of Reinforced Concrete Columns Subjected to Biaxial Loads.” *Proceedings of the International Conference on Concrete for Transportation Infrastructure* 433–440.

Ehsani, Mohammad R. 1986. “CAD for Columns.” *Concrete International: Design and Construction* 8 (9): 43–47.

El-Dash, K. M., and Ahmad, S. H. 1995. “A Model for Stress- Strain Relationship of Spirally Confined Normal and High-Strength Concrete Columns.” *Magazine of Concrete Research* 47 (171): 177–184.

Elwi, A., and Murray, D. W. 1979. “A 3D Hypoelastic Concrete Constitutive Relationship.” *Journal of Engineering Mechanics* 105: 623–641.

Esmaily, A., and Xiao, Y. 2004. “Behavior of Reinforced Concrete Columns under Variable Axial Load.” *ACI Structural Journal* 101 (1): 124–132.

Everand, Noel J., and Cohen, Edward. 1964. “Ultimate Strength Design of Reinforced Concrete Columns.” *ACI Special Publication* SP-7: 182.

Everand, Noel J. 1997. “Axial Load Moment Interaction for Cross Sections Having Longitudinal Reinforcement Arranged in a Circle.” *ACI Journal* 94 (6).

Fafitis, A., and Shah, S.P. 1985. “Lateral Reinforcement for High-Strength Concrete Columns.” *ACI Special Publication* SP 87 (12): 213–232.

Fleming, J. F., and Werner, S. D. 1965. “Design of Columns Subjected to Biaxial Bending.” *ACI Journal*, Proceedings 62 (3): 327–342.

Fujii, M., Kobayashi, K., Miyagawa, T., Inoue, S., and Matsumoto, T. 1988. “A Study on the Application of a Stress-Strain Relation of Confined Concrete.” Proceedings, *JCA Cement and Concrete* 42, Japan Cement.

Furlong. R. W. 1961. “Ultimate Strength of Square Columns under Biaxially Eccentric Loads.” *Journal of the American Concrete Institute* 57 (53): 1129–1140.

Furlong, R. W., Hsu, C. T. T, Mirza, S. A. 2004. “Analysis and Design of Concrete Columns for Biaxial Bending-Overview.” *ACI Structural Journal* 101 (3): 413–23.

Giakoumelis, G., Lam, D. 2004. “Axial Capacity of Circular Concrete-Filled Tube Columns.” *Journal of Constructional Steel Research* 60 (7): 1049–1068.

Gouwens, Albert J. 1975. “Biaxial Bending Simplified,” *Reinforced Concrete Columns*, SP-50, American Concrete Institute, Detroit, 233–261.

Gunnin, B. L., Rad, F. N., and Furlong, R. W. 1979. “A General Nonlinear Analysis of Concrete Structures and Comparison with Frame Tests.” *Computers and Structures* 105 (2): 297–315.

Helgason, V. 2010. “Development of a Computer Program to Design Concrete Columns for Biaxial Moments and Normal Force.” M.S. Thesis. Lunds Institute of Technology, Lund University, Lund, Sweden.

Hartley, G.A. 1985. “Radial Contour Methods of Biaxial Short Column Design.” *ACI Journal* 82 (62): 693–700.

Hognestad, E. 1930. “A Study of Combined Bending and Axial Load in Reinforced Concrete Members.” University of Illinois, Urbana.

Hong, H. P. 2000. ‘‘Short RC Column Capacity under Biaxial Bending and Axial Load.’’ *Canadian Journal of Civil Engineering* 27 (6): 1173–1182.

Horowitz, B. 1989. “Design of Columns Subjected to Biaxial Bending.” *ACI Structural Journal* 86 (6): 717–722.

Hoshikuma, J., Kawashima, K., Nagaya, K., and Taylor, A. W. 1997. “Stress-Strain Model for Confined Reinforced Concrete in Bridge Piers.” *Journal of Structural Engineering* 123 (5): 624–633.

Hsu, C. T. T. 1988. “Analysis and Design of Square and Rectangular Columns by Equation of Failure Surface.” *ACI Structural Journal* 85 (2): 167–179.

Hsu, L. S., and Hsu, C. T. T. 1994. “Complete Stress-Strain Behavior of High-Strength Concrete under Compression.” *Magazine of Concrete Research* 46 (169): 301–312.

Hu, Lu-Shien. 1955. “Eccentric Bending in Tow Directions of Rectangular Concrete Columns.” *ACI Journal* 51: 921.

Karabinis, A. I., and Kiousis, P. D. 1994. “Effects of Confinement on Concrete Columns: Plasticity Approach.” ASCE *Journal of Structural Engineering* 12099: 2747–2767.

Kent, D., and Park, R. 1971. “Flexural Members with Confined Concrete.” *Journal of Structural Division*, Proceedings of the American Society of Civil Engineers 97 (ST7): 1969–1990.

Kroenke, W. C., Gutzwiller, M. J., and Lee, R. H. 1973. “Finite Element for Reinforced Concrete Frame Study.” *Journal of Structural Division*, ASCE 99 (ST7): 1371–1390.

Lazaro, A. L., and Richards, Jr., R. 1974. “Full Range Analysis of Concrete Frames.” *Journal of Structural Division*, ASCE 100 (ST12): 2419–2432.

Lejano, B., A. 2007. “Investigation of Biaxial Bending of Reinforced Concrete Columns through Fiber Method Modeling.” Journal of Research of Science and Computer Engineering 4 (3): 61–73.

Li, G. 2006. “Experimental Study of FRP Confined Concrete Cylinders.” *Journal Engineering Structures* 28: 1001–1008.

Lokuge, W. P., Sanjayan, J. G., and Setunge S. 2005. “Stress Strain Model for Laterally Confined Concrete.” *Journal of Materials in Civil Engineering*, ASCE 17 (6): 607–616.

Lucio, K. 2004. “Analytical Performance of Reinforced Concrete Sections using Various Confinement Models.” Master’s Thesis, Kansas State University.

Mander, J. B., Priestley, M. J. N., and Park, R. 1988. “Theoretical Stress-Strain Model for Confined Concrete.” *Journal of Structural Engineering*, ASCE 114 (8): 1827–1849.

Mander, J. B., Priestley, M. J. N., and Park, R. 1988. “Observed Stress Strain Behavior of Confined Concrete.” *Journal of Structural Engineering*, ASCE 114 (8): 1804–1825.

Mander, J. B. 1983. “Seismic Design of Bridge Piers.” Ph.D. thesis. University of Canterbury, New Zealand.

Mansur, M. A., Chin, M. S., and Wee, T. H. 1997. “Stress-Strain Relationship of Confined High Strength Plain and Fiber Reinforcement.” *Journal of Materials in Civil Engineering* 9 (4): 171–179.

Mattock, Allan H., and Kritz, Ladislav, B. 1961. “Rectangular Concrete Stress Distribution in Ultimate Strength Design.” *ACI Journal* Proceedings 57: 875. Discussion by P. W. Abeles, Homer M. Hadley, K. Hanjnal-Konyi, J. L. Meek, Luis Saenz, Ignacio Martin, Rafael Tamargo, *ACI Journal*, September, 1961, p 1763.

Martinez, S., Nilson, A. H., and Slate, F. O. 1984. “Spirally Reinforced High-Strength Concrete Columns.” *ACI Journal* 81 (5): 431–442.

Mazzotti, C., and M. Savoia. 2002. “Nonlinear Creep, Possion’s Ratio and Creep-Damage Interaction of Concrete in Compression.” *ACI Materials Journal* 99 (5): 450–457.

Medland, I. C., and Taylor, D. A. 1971. “Flexural Rigidity of Concrete Column Sections.” *Journal of Structural Division*, ASCE 97 (ST2): 573–586.

Meek, J. M. 1963. “Ultimate Strength of Columns with Biaxially Eccentric Loads.” *ACI Journal* 60 (August): 1053–1064.

Mendis, P., Pendyala, R. and Setunge, S. 2000. “Stress Strain Model to Predict the Full Range Moment Curvature Behavior of High Strength Concrete Section.” *Magazine of Concrete Research* 52 (4): 227–234.

Mikhalkin, B. 1952. “The Strength of Reinforced Concrete Members Subjected to Compression and Unsymmetrical Bending.” M.S. Thesis, University of California.

Mills, L. L., and Zimmerman, R. M. 1970. “Compressive Strength of Plain Concrete under Multiaxial Loading Conditions.” *ACI Materials Journal* 67 (101): 802–807.

Moran, D. A., Pantelides, C. P. 2002. “Stress–Strain Model for Fiber-Reinforced 665 Polymer-Confined Concrete.” *Journal of Computing in Construction*, ASCE 6 (4): 233–40.

Mylonas, G. A. 1967. “Working Stress Column Design Using Interaction Diagrams.” Volume 64, August 1.

Najami, A., and Tayem, A. 1996. “Design of Round Reinforced Concrete Columns.” Journal of Structural Engineering, ASCE 122 (9): 1062–1071.

Pantazopoulou, S. J., Mills, R., H. 1995. “Microstructural Aspects of the Mechanical Response of Plain Concrete.” *ACI Materials Journal* 92 (6): 605–616.

Pannel, F. N. 1963. “Failure Surfaces for Members in Compression and Biaxial Bending.” *ACI Journal*, Proceedings 60 (1): 129–140.

Park, R., Priestley, M. J. N., and Gill, W. D. 1982. “Ductility of Square Confined Concrete Columns.” *Proceedings of ASCE* 108 (ST4): 929–950.

Parker, L. G., and Scanton, J. J. 1940. “A Simple Analysis for Eccentrically Loaded Concrete Sections.” *Civil Engineering* 10 (10): 656.

Parme, A. L., Nieves, J. M., and Gouwens, A. 1966. “Capacity of Reinforced Rectangular Columns Subject to Biaxial Bending.” *Journal of the American Concrete Institute* 63 (9): 911–923.

Popovics, S. 1973. “A Numerical Approach to the Complete Stress-Strain Curves of Concrete.” *Cement and Concrete Research* 3 (5): 583-59.

Ramamurthy, L. N. 1966. “Investigation of the Ultimate Strength of Square and Rectangular Columns under Biaxially Eccentric Loads.” Symposium on Reinforced Concrete Columns, Detroit, ACI-SP-13, Paper No. 12, 263–298.

Rasheed, H. A., and Dinno, K. S. 1994. “An Efficient Nonlinear Analysis of RC Sections.” *Computers and Structures* 53 (3): 613–623

Razvi, S., and Saatcioglu, M. 1999. “Confinement Model for High-Strength Concrete.” Journal of Structural Engineering 125 (3): 281–289.

Richart. F. E., Brandtzaeg, A., and Brown R. L. 1929. “The Failure of Plain and Spirally Reinforced Concrete in Compression.” Bulletin No. 190, Engineering Station, University of Illinois, Urbana.

Rodriguez, J. A., and Ochoa, J. D. A. 1999. “Biaxial Interaction Diagrams for Short RC Columns of Any Cross Section.” *Journal Structural Engineering* ASCE 125 (6): 672–83.

Row, D. G., and Paulay, T. E. 1973. “Biaxial Flexure and Axial Load Interaction in Short Rectangular Columns.” *Bulletin of the New Zealand Society for Earthquake Engineering* 6 (3): 110–12.

Roy, H. E. H., and Sozen, M. A. 1965. “Ductility of Concrete.” *Flexural Mechanics of Reinforced Concrete* SP-12, American Concrete Institute/American Society of Civil Engineers, Detroit, 213–224.

Saatcioglu, M., and Razvi, S. R. 1992. “Strength and Ductility of Confined Concrete.” *Journal of Structural Engineering* 118 (6): 1590–1607.

Saatcioglu, M., Salamt, A. H., and Razvi, S. R. 1995. “Confined Columns under Eccentric Loading.” *Journal of Structural Engineering* 121 (11): 1547–1556.

Sacks, R., Buyukozturk, O. 1987. “Expert Interactive Design of R\C Columns under Biaxial Bending.” *ASCE Journal of Computers in Civil Engineering* 1 (2).

Saenz, L. P. 1964. “Equation for the Stress-Strain Curve of Concrete.” *ACI Journal* 61(9): 1229–1235.

Sallah, A. Y. 1983. “Analysis of Short Rectangular Reinforced Concrete Columns Subjected to Biaxial Moments.” Master of Engineering thesis, Department of Civil Engineering, Carleton University, Ottawa, 124 pp.

Sargin, M. 1971. “Stress-Strain Relationships for Concrete and the Analysis of Structural Concrete Sections.” Solid Mechanics Division, University of Waterloo, Study No. 4.

Scott, B. D., Park, R., and Priestley, N. 1982. “Stress-Strain Behavior of Concrete Confined by Overlapping Hoops at Law and High Strain Rates.” *ACI Journal* 79 (1): 13–27.

Sheikh, S. A. 1982. “A Comparative Study of Confinement Models.” 1982. *ACI Journal* 79 (4): 296–306.

Sheikh, S. A., and Uzumeri, S. M. 1982. “Analytical Model for Concrete Confinement in Tied Columns.” *Journal of Structural Engineering*, ASCE 108 (ST12): 2703–2722.

Sheikh, S. A., and Toklucu, M. T. 1993. “Reinforced Concrete Columns Confined by Circular Spirals and Hoops.” *ACI Journal* 90 (5): 542–553.

Soliman, M. T. M., and Yu, C. W. 1967. “The Flexural Stress-Strain Relationship of Concrete Confined by Rectangular Transverse Reinforcement.” *Magazine of Concrete Research* 19 (61): 223–28.

Taylor, M. A., and Ho, S. W. 1984. “Design Contour Charts for Biaxial Bending of Rectangular Reinforced Concrete Columns Using Bresler Method.” *Structural Engineering Practice* 2 (4): 301–317.

Troxel, G. E. 1941. “Reinforced Concrete Columns Subjected to Bending about Both Principal Axes.” *Civil Engineering* 11 (4): 237.

Vallenas, J., Bertero, V. and Popov, E. 1977. ”Concrete Confined by Rectangular Hoops and Subjected to Axial Loads.” Research Center Report UCB/EERC-77-13, University of California at Berkeley.

Wang, W., and Hong, H. 2002. “Reliability of Reinforced Concrete Columns under Axial Load and Biaxial Bending.” Proceedings, Annual Conference - Canadian Society for Civil Engineering 2161–2169.

Wang, G. G., and Hsu, C. T. 1992. “Complete Biaxial Load-Deformation Behavior of RC Columns.” *Journal of Structural Engineering*, ASCE 118 (9): 2590–2609.

Wang, P. T., Shah, S. P., and Naaman, A. E. 1978. “Stress-Strain Curves of Normal and Lightweight Concrete in Compression.” *ACI Journal* 75 (11): 603–611.

Weber, D.C. 1966. Ultimate Strength Design Charts for Columns with Biaxial Bending. *ACI Journal* 63(11), 1205–1230, (1966).

Wee, T. H., Chin, M. S., and Mansur, M. A. 1996. “Stress-Strain Relationship of High Strength Concrete in Compression.” *Journal of Materials in Civil Engineering* 8 (2): 70–6.

Wessman, Harold E. 1946. “Reinforced Concrete Columns under Combined Compression and Bendind.” *ACI Journal*, Proceedings 43: 1.

Whitney, C. S. and Cohen, E. 1956. “Guide for the Ultimate Strength Design of Reinforced Concrete.” *ACI Journal*, Proceedings 53 (November), 455–475.

Wiesinger, Frederick P. T. “Design of Symmetrical Columns with Small Eccentricities in One or Tow Directions.” *ACI Journal*, Proceedings 55 (August): 273.

Yong, Y.-K., Nour, M. G., and Nawy, E. G. 1998. “Behavior of Laterally Confined High-Strength Concrete under Axial Loads.” *Journal of Structural Engineering* 114 (2): 332–351.

Yoo, S. H., Shin, S. W. 2007. “Variation of Ultimate Concrete Strain at RC Columns Subjected to Axial Loads with Bi-Directional Eccentricities.” *Key Engineering Materials* 348-349: 617–620.

Zak, M. 1993. “Computer Analysis of Reinforced Concrete Sections under Biaxial Bending and Longitudinal Load.” *ACI Structural Journal* 90 (2):163–169.

Appendix A: Ultimate Confined Strength Tables

Table A.1 is developed for f'c of 3.3 using Equations 3.181 and 3.182. Table A.2 is for f'c of 3.9 using Equations 3.183 and 3.184. Table A.3 is developed using Mander procedure that utilizes Scickert and Winkler (1977) formulas. Table A.4 is for f'c of 5.2 using Equations 3.185 and 3.186. Tables A.5 through A.7 show the confined values for the same lateral pressure using Scickert and Winkler (1977) equations. Tables A.5 through A.7 give conservative values compared to table A.1, A.2 and A.4. This indicates that Equations 3.179 and 3.180 found by Scickert and Winkler (1977) and utilized by Mander et al. (1988) are conservative enough to be used in the analysis

$$\sigma_1 *= \frac{f_{lx}}{f_c'}$$

$$\sigma_2 *= \frac{f_{ly}}{f_c'}$$

TABLE A.1
Ultimate Confined Strength to Unconfined Strength Ratio for f'_c = 3.3 ksi

σ_{1*} / σ_{2*}	0.02	0.04	0.06	0.08	0.1	0.12	0.14	0.16	0.18	0.2	0.22	0.24	0.26	0.28	0.3
0.02	3.7260	3.9001	4.0336	4.1442	4.2396	4.3238	4.3994	4.4680	4.5309	4.5888	4.6424	4.6924	4.7389	4.7825	4.8233
0.04	3.9001	4.1298	4.2988	4.4318	4.5436	4.6408	4.7273	4.8054	4.8768	4.9424	5.0032	5.0598	5.1128	5.1624	5.2091
0.06	4.0336	4.2988	4.5141	4.6779	4.8098	4.9220	5.0205	5.1086	5.1887	5.2621	5.3299	5.3930	5.4520	5.5074	5.5596
0.08	4.1442	4.4318	4.6779	4.8808	5.0396	5.1700	5.2821	5.3812	5.4705	5.5519	5.6269	5.6965	5.7614	5.8223	5.8797
0.1	4.2396	4.5436	4.8098	5.0396	5.2316	5.3855	5.5140	5.6257	5.7250	5.8150	5.8974	5.9736	6.0445	6.1109	6.1734
0.12	4.3238	4.6408	4.9220	5.1700	5.3855	5.5679	5.7172	5.8436	5.9544	6.0537	6.1440	6.2271	6.3041	6.3761	6.4436
0.14	4.3994	4.7273	5.0205	5.2821	5.5140	5.7172	5.8910	6.0358	6.1600	6.2698	6.3687	6.4591	6.5425	6.6201	6.6928
0.16	4.4680	4.8054	5.1086	5.3812	5.6257	5.8436	6.0358	6.2019	6.3424	6.4643	6.5728	6.6712	6.7614	6.8450	6.9230
0.18	4.5309	4.8768	5.1887	5.4705	5.7250	5.9544	6.1600	6.3424	6.5015	6.6380	6.7575	6.8647	6.9623	7.0522	7.1357
0.2	4.5888	4.9424	5.2621	5.5519	5.8150	6.0537	6.2698	6.4643	6.6380	6.7907	6.9233	7.0405	7.1462	7.2428	7.3322
0.22	4.6424	5.0032	5.3299	5.6269	5.8974	6.1440	6.3687	6.5728	6.7575	6.9233	7.0703	7.1991	7.3139	7.4180	7.5137
0.24	4.6924	5.0598	5.3930	5.6965	5.9736	6.2271	6.4591	6.6712	6.8647	7.0405	7.1991	7.3407	7.4660	7.5784	7.6810
0.26	4.7389	5.1128	5.4520	5.7614	6.0445	6.3041	6.5425	6.7614	6.9623	7.1462	7.3139	7.4660	7.6026	7.7245	7.8347
0.28	4.7825	5.1624	5.5074	5.8223	6.1109	6.3761	6.6201	6.8450	7.0522	7.2428	7.4180	7.5784	7.7245	7.8566	7.9753
0.3	4.8233	5.2091	5.5596	5.8797	6.1734	6.4436	6.6928	6.9230	7.1357	7.3322	7.5137	7.6810	7.8347	7.9753	8.1031

TABLE A.2
Ultimate Confined Strength to Unconfined Strength Ratio for f'_c = 3.9 ksi

σ_{1*} / σ_{2*}	0.02	0.04	0.06	0.08	0.1	0.12	0.14	0.16	0.18	0.2	0.22	0.24	0.26	0.28	0.3
0.02	4.4819	4.7318	4.9351	5.1101	5.2656	5.4063	5.5355	5.6552	5.7670	5.8721	5.9712	6.0651	6.1544	6.2394	6.3206
0.04	4.7318	5.0412	5.2854	5.4880	5.6642	5.8217	5.9649	6.0969	6.2196	6.3345	6.4427	6.5450	6.6422	6.7347	6.8230
0.06	4.9351	5.2854	5.5802	5.8187	6.0197	6.1962	6.3548	6.4998	6.6337	6.7587	6.8759	6.9865	7.0914	7.1911	7.2862
0.08	5.1101	5.4880	5.8187	6.1005	6.3333	6.5323	6.7083	6.8674	7.0134	7.1488	7.2753	7.3943	7.5068	7.6136	7.7154
0.1	5.2656	5.6642	6.0197	6.3333	6.6037	6.8308	7.0273	7.2024	7.3616	7.5081	7.6443	7.7720	7.8923	8.0062	8.1145
0.12	5.4063	5.8217	6.1962	6.5323	6.8308	7.0908	7.3125	7.5063	7.6802	7.8389	7.9855	8.1222	8.2506	8.3718	8.4868
0.14	5.5355	5.9649	6.3548	6.7083	7.0273	7.3125	7.5631	7.7795	7.9704	8.1427	8.3007	8.4471	8.5840	8.7128	8.8346
0.16	5.6552	6.0969	6.4998	6.8674	7.2024	7.5063	7.7795	8.0215	8.2328	8.4208	8.5913	8.7483	8.8942	9.0310	9.1599
0.18	5.7670	6.2196	6.6337	7.0134	7.3616	7.6802	7.9704	8.2328	8.4670	8.6733	8.8582	9.0269	9.1827	9.3279	9.4644
0.2	5.8721	6.3345	6.7587	7.1488	7.5081	7.8389	8.1427	8.4208	8.6733	8.9002	9.1018	9.2837	9.4503	9.6048	9.7492
0.22	5.9712	6.4427	6.8759	7.2753	7.6443	7.9855	8.3007	8.5913	8.8582	9.1018	9.3219	9.5190	9.6978	9.8624	10.0154
0.24	6.0651	6.5450	6.9865	7.3943	7.7720	8.1222	8.4471	8.7483	9.0269	9.2837	9.5190	9.7328	9.9255	10.1014	10.2638
0.26	6.1544	6.6422	7.0914	7.5068	7.8923	8.2506	8.5840	8.8942	9.1827	9.4503	9.6978	9.9255	10.1334	10.3220	10.4948
0.28	6.2394	6.7347	7.1911	7.6136	8.0062	8.3718	8.7128	9.0310	9.3279	9.6048	9.8624	10.1014	10.3220	10.5243	10.7080
0.3	6.3206	6.8230	7.2862	7.7154	8.1145	8.4868	8.8346	9.1599	9.4644	9.7492	10.0154	10.2638	10.4948	10.7080	10.9060

TABLE A.3
Ultimate Confined Strength to Unconfined Strength Ratio for f'_c = 4.4 ksi (used by Mander et al. (1988))

σ_{2^*} \ σ_{1^*}	0.02	0.04	0.06	0.08	0.1	0.12	0.14	0.16	0.18	0.2	0.22	0.24	0.26	0.28	0.3
0.02	5.0255	5.2550	5.4259	5.5656	5.6849	5.7895	5.8829	5.9674	6.0444	6.1152	6.1806	6.2412	6.2976	6.3502	6.3993
0.04	5.2550	5.5622	5.7791	5.9460	6.0845	6.2040	6.3096	6.4044	6.4906	6.5695	6.6423	6.7098	6.7728	6.8315	6.8866
0.06	5.4259	5.7791	6.0569	6.2623	6.4247	6.5613	6.6803	6.7860	6.8815	6.9686	7.0487	7.1230	7.1920	7.2566	7.3171
0.08	5.5656	5.9460	6.2623	6.5164	6.7112	6.8688	7.0030	7.1209	7.2263	7.3218	7.4094	7.4903	7.5654	7.6355	7.7012
0.1	5.6849	6.0845	6.4247	6.7112	6.9456	7.1307	7.2834	7.4150	7.5313	7.6359	7.7312	7.8188	7.9000	7.9756	8.0464
0.12	5.7895	6.2040	6.5613	6.8688	7.1307	7.3486	7.5248	7.6726	7.8012	7.9157	8.0193	8.1140	8.2013	8.2825	8.3582
0.14	5.8829	6.3096	6.6803	7.0030	7.2834	7.5248	7.7283	7.8964	8.0394	8.1650	8.2775	8.3797	8.4735	8.5604	8.6413
0.16	5.9674	6.4044	6.7860	7.1209	7.4150	7.6726	7.8964	8.0875	8.2480	8.3864	8.5089	8.6193	8.7200	8.8127	8.8989
0.18	6.0444	6.4906	6.8815	7.2263	7.5313	7.8012	8.0394	8.2480	8.4282	8.5818	8.7156	8.8350	8.9431	9.0422	9.1338
0.2	6.1152	6.5695	6.9686	7.3218	7.6359	7.9157	8.1650	8.3864	8.5818	8.7522	8.8994	9.0289	9.1451	9.2510	9.3483
0.22	6.1806	6.6423	7.0487	7.4094	7.7312	8.0193	8.2775	8.5089	8.7156	8.8994	9.0610	9.2022	9.3276	9.4408	9.5443
0.24	6.2412	6.7098	7.1230	7.4903	7.8188	8.1140	8.3797	8.6193	8.8350	9.0289	9.2022	9.3560	9.4916	9.6130	9.7231
0.26	6.2976	6.7728	7.1920	7.5654	7.9000	8.2013	8.4735	8.7200	8.9431	9.1451	9.3276	9.4916	9.6383	9.7687	9.8861
0.28	6.3502	6.8315	7.2566	7.6355	7.9756	8.2825	8.5604	8.8127	9.0422	9.2510	9.4408	9.6130	9.7687	9.9087	10.0343
0.3	6.3993	6.8866	7.3171	7.7012	8.0464	8.3582	8.6413	8.8989	9.1338	9.3483	9.5443	9.7231	9.8861	10.0343	10.1683

TABLE A.4
Ultimate Confined Strength to Unconfined Strength Ratio for f'_c = 5.2 ksi

σ_2^* \ σ_1^*	0.02	0.04	0.06	0.08	0.1	0.12	0.14	0.16	0.18	0.2	0.22	0.24	0.26	0.28	0.3
0.02	5.9070	6.1647	6.3409	6.4785	6.5923	6.6891	6.7730	6.8467	6.9120	6.9700	7.0217	7.0679	7.1091	7.1458	7.1783
0.04	6.1647	6.5586	6.8072	6.9847	7.1258	7.2436	7.3448	7.4332	7.5113	7.5810	7.6435	7.6996	7.7502	7.7959	7.8370
0.06	6.3409	6.8072	7.1633	7.4023	7.5789	7.7215	7.8417	7.9458	8.0373	8.1187	8.1917	8.2574	8.3170	8.3710	8.4201
0.08	6.4785	6.9847	7.4023	7.7279	7.9573	8.1317	8.2746	8.3962	8.5020	8.5957	8.6794	8.7548	8.8231	8.8853	8.9420
0.1	6.5923	7.1258	7.5789	7.9573	8.2579	8.4780	8.6495	8.7917	8.9137	9.0206	9.1157	9.2010	9.2782	9.3485	9.4126
0.12	6.6891	7.2436	7.7215	8.1317	8.4780	8.7576	8.9688	9.1369	9.2778	9.3996	9.5070	9.6028	9.6893	9.7678	9.8395
0.14	6.7730	7.3448	7.8417	8.2746	8.6495	8.9688	9.2303	9.4332	9.5975	9.7367	9.8579	9.9652	10.0615	10.1486	10.2280
0.16	6.8467	7.4332	7.9458	8.3962	8.7917	9.1369	9.4332	9.6790	9.8740	10.0344	10.1716	10.2917	10.3987	10.4951	10.5826
0.18	6.9120	7.5113	8.0373	8.5020	8.9137	9.2778	9.5975	9.8740	10.1061	10.2937	10.4501	10.5850	10.7039	10.8102	10.9063
0.2	6.9700	7.5810	8.1187	8.5957	9.0206	9.3996	9.7367	10.0344	10.2937	10.5135	10.6941	10.8465	10.9790	11.0964	11.2019
0.22	7.0217	7.6435	8.1917	8.6794	9.1157	9.5070	9.8579	10.1716	10.4501	10.6941	10.9029	11.0770	11.2255	11.3555	11.4713
0.24	7.0679	7.6996	8.2574	8.7548	9.2010	9.6028	9.9652	10.2917	10.5850	10.8465	11.0770	11.2759	11.4438	11.5885	11.7159
0.26	7.1091	7.7502	8.3170	8.8231	9.2782	9.6893	10.0615	10.3987	10.7039	10.9790	11.2255	11.4438	11.6338	11.7959	11.9367
0.28	7.1458	7.7959	8.3710	8.8853	9.3485	9.7678	10.1486	10.4951	10.8102	11.0964	11.3555	11.5885	11.7959	11.9776	12.1342
0.3	7.1783	7.8370	8.4201	8.9420	9.4126	9.8395	10.2280	10.5826	10.9063	11.2019	11.4713	11.7159	11.9367	12.1342	12.3084

TABLE A.5
Ultimate Confined Strength to Unconfined Strength Ratio for f'_c = 3.3 ksi (using Scickert and Winkler (1977))

σ_{2*} \ σ_{1*}	0.02	0.04	0.06	0.08	0.1	0.12	0.14	0.16	0.18	0.2	0.22	0.24	0.26	0.28	0.3
0.02	3.7369	3.9076	4.0347	4.1385	4.2272	4.3050	4.3745	4.4373	4.4946	4.5472	4.5958	4.6408	4.6827	4.7218	4.7584
0.04	3.9076	4.1360	4.2973	4.4214	4.5244	4.6133	4.6918	4.7623	4.8263	4.8850	4.9391	4.9894	5.0361	5.0799	5.1208
0.06	4.0347	4.2973	4.5039	4.6566	4.7773	4.8789	4.9674	5.0460	5.1170	5.1818	5.2414	5.2966	5.3479	5.3959	5.4410
0.08	4.1385	4.4214	4.6566	4.8456	4.9904	5.1076	5.2074	5.2950	5.3734	5.4445	5.5096	5.5697	5.6255	5.6777	5.7266
0.1	4.2272	4.5244	4.7773	4.9904	5.1647	5.3023	5.4159	5.5137	5.6002	5.6780	5.7489	5.8140	5.8744	5.9306	5.9832
0.12	4.3050	4.6133	4.8789	5.1076	5.3023	5.4643	5.5954	5.7053	5.8009	5.8861	5.9631	6.0335	6.0984	6.1588	6.2151
0.14	4.3745	4.6918	4.9674	5.2074	5.4159	5.5954	5.7467	5.8717	5.9780	6.0714	6.1551	6.2311	6.3009	6.3654	6.4256
0.16	4.4373	4.7623	5.0460	5.2950	5.5137	5.7053	5.8717	6.0138	6.1332	6.2361	6.3271	6.4092	6.4841	6.5531	6.6171
0.18	4.4946	4.8263	5.1170	5.3734	5.6002	5.8009	5.9780	6.1332	6.2671	6.3813	6.4809	6.5696	6.6500	6.7237	6.7918
0.2	4.5472	4.8850	5.1818	5.4445	5.6780	5.8861	6.0714	6.2361	6.3813	6.5081	6.6175	6.7138	6.8003	6.8789	6.9513
0.22	4.5958	4.9391	5.2414	5.5096	5.7489	5.9631	6.1551	6.3271	6.4809	6.6175	6.7377	6.8427	6.9359	7.0201	7.0970
0.24	4.6408	4.9894	5.2966	5.5697	5.8140	6.0335	6.2311	6.4092	6.5696	6.7138	6.8427	6.9571	7.0579	7.1481	7.2300
0.26	4.6827	5.0361	5.3479	5.6255	5.8744	6.0984	6.3009	6.4841	6.6500	6.8003	6.9359	7.0579	7.1669	7.2639	7.3512
0.28	4.7218	5.0799	5.3959	5.6777	5.9306	6.1588	6.3654	6.5531	6.7237	6.8789	7.0201	7.1481	7.2639	7.3681	7.4614
0.3	4.7584	5.1208	5.4410	5.7266	5.9832	6.2151	6.4256	6.6171	6.7918	6.9513	7.0970	7.2300	7.3512	7.4614	7.5611

TABLE A.6
Ultimate Confined Strength to Unconfined Strength Ratio for f'_c = 3.9 ksi (Using Scickert and Winkler (1977))

σ_2^* \ σ_1^*	0.02	0.04	0.06	0.08	0.1	0.12	0.14	0.16	0.18	0.2	0.22	0.24	0.26	0.28	0.3
0.02	4.4163	4.6181	4.7683	4.8909	4.9958	5.0877	5.1698	5.2441	5.3118	5.3740	5.4314	5.4846	5.5342	5.5804	5.6236
0.04	4.6181	4.8880	5.0786	5.2253	5.3470	5.4520	5.5448	5.6281	5.7038	5.7732	5.8372	5.8965	5.9518	6.0035	6.0519
0.06	4.7683	5.0786	5.3228	5.5032	5.6460	5.7660	5.8705	5.9635	6.0474	6.1239	6.1944	6.2596	6.3203	6.3770	6.4302
0.08	4.8909	5.2253	5.5032	5.7266	5.8977	6.0362	6.1542	6.2577	6.3504	6.4344	6.5113	6.5824	6.6484	6.7100	6.7677
0.1	4.9958	5.3470	5.6460	5.8977	6.1038	6.2664	6.4006	6.5162	6.6184	6.7104	6.7941	6.8711	6.9424	7.0089	7.0711
0.12	5.0877	5.4520	5.7660	6.0362	6.2664	6.4578	6.6127	6.7426	6.8557	6.9563	7.0473	7.1305	7.2072	7.2785	7.3452
0.14	5.1698	5.5448	5.8705	6.1542	6.4006	6.6127	6.7916	6.9392	7.0650	7.1753	7.2742	7.3640	7.4465	7.5228	7.5939
0.16	5.2441	5.6281	5.9635	6.2577	6.5162	6.7426	6.9392	7.1072	7.2483	7.3699	7.4775	7.5745	7.6630	7.7445	7.8202
0.18	5.3118	5.7038	6.0474	6.3504	6.6184	6.8557	7.0650	7.2483	7.4066	7.5416	7.6592	7.7641	7.8591	7.9462	8.0267
0.2	5.3740	5.7732	6.1239	6.4344	6.7104	6.9563	7.1753	7.3699	7.5416	7.6913	7.8207	7.9345	8.0367	8.1297	8.2152
0.22	5.4314	5.8372	6.1944	6.5113	6.7941	7.0473	7.2742	7.4775	7.6592	7.8207	7.9628	8.0868	8.1970	8.2964	8.3874
0.24	5.4846	5.8965	6.2596	6.5824	6.8711	7.1305	7.3640	7.5745	7.7641	7.9345	8.0868	8.2220	8.3412	8.4478	8.5446
0.26	5.5342	5.9518	6.3203	6.6484	6.9424	7.2072	7.4465	7.6630	7.8591	8.0367	8.1970	8.3412	8.4700	8.5846	8.6878
0.28	5.5804	6.0035	6.3770	6.7100	7.0089	7.2785	7.5228	7.7445	7.9462	8.1297	8.2964	8.4478	8.5846	8.7077	8.8175
0.3	5.6236	6.0519	6.4302	6.7677	7.0711	7.3452	7.5939	7.8202	8.0267	8.2152	8.3874	8.5446	8.6878	8.8175	8.9358

Table A.7
Ultimate Confined Strength to Unconfined Strength Ratio for f'_c = 5.2 ksi (Using Scickert and Winkler (1977))

σ_{2^*} \ σ_{1^*}	0.02	0.04	0.06	0.08	0.1	0.12	0.14	0.16	0.18	0.2	0.22	0.24	0.26	0.28	0.3
0.02	5.8885	6.1574	6.3577	6.5213	6.6610	6.7836	6.8931	6.9921	7.0823	7.1652	7.2418	7.3128	7.3788	7.4405	7.4980
0.04	6.1574	6.5173	6.7715	6.9671	7.1294	7.2694	7.3931	7.5042	7.6051	7.6976	7.7829	7.8620	7.9357	8.0046	8.0692
0.06	6.3577	6.7715	7.0970	7.3376	7.5279	7.6880	7.8274	7.9513	8.0632	8.1652	8.2592	8.3461	8.4270	8.5027	8.5736
0.08	6.5213	6.9671	7.3376	7.6354	7.8636	8.0483	8.2056	8.3437	8.4672	8.5792	8.6818	8.7765	8.8645	8.9467	9.0237
0.1	6.6610	7.1294	7.5279	7.8636	8.1384	8.3552	8.5342	8.6883	8.8246	8.9472	9.0588	9.1615	9.2566	9.3452	9.4281
0.12	6.7836	7.2694	7.6880	8.0483	8.3552	8.6105	8.8169	8.9902	9.1409	9.2750	9.3963	9.5073	9.6096	9.7047	9.7935
0.14	6.8931	7.3931	7.8274	8.2056	8.5342	8.8169	9.0554	9.2523	9.4200	9.5671	9.6989	9.8187	9.9286	10.0304	10.1251
0.16	6.9921	7.5042	7.9513	8.3437	8.6883	8.9902	9.2523	9.4763	9.6644	9.8265	9.9700	10.0994	10.2174	10.3261	10.4270
0.18	7.0823	7.6051	8.0632	8.4672	8.8246	9.1409	9.4200	9.6644	9.8755	10.0554	10.2123	10.3522	10.4789	10.5949	10.7023
0.2	7.1652	7.6976	8.1652	8.5792	8.9472	9.2750	9.5671	9.8265	10.0554	10.2551	10.4276	10.5793	10.7155	10.8396	10.9536
0.22	7.2418	7.7829	8.2592	8.6818	9.0588	9.3963	9.6989	9.9700	10.2123	10.4276	10.6170	10.7824	10.9293	11.0619	11.1832
0.24	7.3128	7.8620	8.3461	8.7765	9.1615	9.5073	9.8187	10.0994	10.3522	10.5793	10.7824	10.9627	11.1216	11.2637	11.3928
0.26	7.3788	7.9357	8.4270	8.8645	9.2566	9.6096	9.9286	10.2174	10.4789	10.7155	10.9293	11.1216	11.2934	11.4462	11.5838
0.28	7.4405	8.0046	8.5027	8.9467	9.3452	9.7047	10.0304	10.3261	10.5949	10.8396	11.0619	11.2637	11.4462	11.6103	11.7574
0.3	7.4980	8.0692	8.5736	9.0237	9.4281	9.7935	10.1251	10.4270	10.7023	10.9536	11.1832	11.3928	11.5838	11.7574	11.9144

K-TRAN

KANSAS TRANSPORTATION RESEARCH AND NEW-DEVELOPMENT PROGRAM

AD ASTRA PER ASPERA

Kansas

Department of Transportation